Comparative evaluation of diagnostic efficacy of laser Raman spectroscopy and histopathology in an animal model of oral carcinogenesis

By

PIYUSH KUMAR

[LIFE09201004022]

Tata Memorial Centre

Mumbai

A thesis submitted to the

Board of Studies in Life Sciences

In partial fulfillment of requirements

for the Degree of

DOCTOR OF PHILOSOPHY

of

HOMI BHABHA NATIONAL INSTITUTE

January, 2017

Homi Bhabha National Institute

Recommendations of the Viva Voce Committee

As members of the Viva Voce Committee, we certify that we have read the dissertation prepared by Mr. Piyush Kumar entitled "Comparative evaluation of diagnostic efficacy of laser Raman spectroscopy and histopathology in an animal model of oral carcinogenesis" and recommend that it may be accepted as fulfilling the thesis requirement for the award of Degree of Doctor of Philosophy.

Chairman – Dr. Neelam Shirsat	Date: 16.01.2017
Guide/Convener – Dr. C. Murali Krishna	Date: 16.01.2017
Member 1 – Dr. Tanuja Teni	Date: 16.01.2017
Member-2 – Dr. Sanjay Gupta	Date: 16.01.2017
Technical Advisor – Dr. Arvind Ingle	Date: 16.01.2017
External Examiner – Dr. Santosh Noronha	Date: 16.01.2017

Final approval and acceptance of this thesis is contingent upon the candidate's submission of the final copies of the thesis to HBNI.
I hereby certify that I have read this thesis prepared under my direction and recommend that it may be accepted as fulfilling the thesis requirement.

Date: 16.01.2017
Place: Navi Mumbai

Dr. C. Murali Krishna
Guide

STATEMENT BY AUTHOR

This dissertation has been submitted in partial fulfillment of requirements for an advanced degree at Homi Bhabha National Institute (HBNI) and is deposited in the Library to be made available to borrowers under rules of the HBNI.

Brief quotations from this dissertation are allowable without special permission, provided that accurate acknowledgement of source is made. Requests for permission for extended quotation from or reproduction of this manuscript in whole or in part may be granted by the Competent Authority of HBNI when in his or her judgment the proposed use of the material is in the interests of scholarship. In all other instances, however, permission must be obtained from the author.

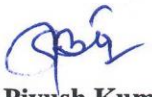

Piyush Kumar

DECLARATION

I, hereby declare that the investigation presented in the thesis has been carried out by me. The work is original and has not been submitted earlier as a whole or in part for a degree / diploma at this or any other Institution / University.

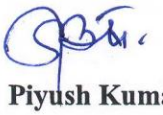

Piyush Kumar

List of Publications arising from the thesis

Journal

1. "Raman spectroscopy in experimental oral carcinogenesis: investigation of abnormal changes in control tissues", **P. Kumar**, T. Bhattacharjee, M. Pandey, A. Hole, A. Ingle, C. Murali Krishna, Journal of Raman Spectroscopy, **2016**.
2. "Raman spectroscopy of experimental oral carcinogenesis: Study on sequential cancer progression in hamster buccal pouch model", **P. Kumar**, T. Bhattacharjee, A. Ingle, G.B. Maru, C. Murali Krishna, Technology in Cancer Research and Treatment, **2015**.
3. "Animal models in disease diagnosis: Exploration using Raman spectroscopy", **P. Kumar**, C. Murali Krishna Asian Journal of Physics, **2015.**
4. "Multimodal spectroscopic applications in cancer diagnosis: Combined Raman spectroscopy and Optical coherence tomography", **P. Kumar** and C. Murali Krishna, Asian Journal of Physics, **2015**.

Chapters in books and lectures notes

1. "Optical techniques: investigations in oral cancers" In Oral Cancer Detection: Novel Strategies and Clinical Impact, Ed. Dr. P. Panth, Springer, **2017** (In Press).

Conferences

1. "Raman spectroscopy of experimental oral carcinogenesis: investigating precancer changes due to confounding factors in controls", presented at **International Conference on Perspectives in Vibrational Spectroscopy (ICOPVS),** Lucknow, 2016
2. "Raman spectroscopy of experimental carcinogenesis: investigating suitability of *ex vivo* models to evaluate *in vivo* spectra", **A Conference of New Ideas in Cancer-Challenging Dogmas,** Mumbai in February 2016 (European Journal of Cancer, 2016)
3. "Stages in experimental oral carcinogenesis: Raman spectroscopic and immunohistochemical evaluation", **SPEC Shedding New Light on Diseases 2014,** Krakow, Poland in August 2014.
4. "Tracking DMBA-induced biochemical and morphological changes in Syrian Hamsters: Raman and OCT Study", **National Laser Symposium NLS 22**, Manipal Academy of Higher Education, Manipal in January 2014 (Proceedings of NLS, 2014)

5. "Experimental Oral Carcinogenesis: Sequential progression study through Raman Spectroscopy", **23rd International Conference on Raman Spectroscopy (ICORS)**, Bangalore in August 2012.
6. "Experimental Oral Carcinogenesis: A preliminary diagnostic efficacy of Raman spectroscopy", American Association of Cancer Research **(AACR) New Horizons in Cancer Research**, Gurgaon, Delhi-NCR in December 2011.

Others

1. "Evaluation of Raman spectroscopy for prediction of antitumor response to silibinin and its nanoparticulates in DMBA - induced oral carcinogenesis", M. Gohulkumar, **P. Kumar**, C. Murali Krishna, N. Krishnakumar, Journal of Raman Spectroscopy, **2016**.
2. "Raman spectroscopy detects biomolecular changes associated with nanoencapsulated hesperetin: treatment in experimental oral carcinogenesis", K. Gurushankar, M. Gohulkumar, **P. Kumar**, C. Murali Krishna, N. Krishnakumar, Laser Physics Letters, **2016**.
3. "Disease Diagnosis by optical spectroscopy: Role of multivariate analysis", N. Tayal, **P. Kumar**, C. Murali Krishna, Asian Journal of Physics, **2015**.
4. "Raman spectroscopy of serum: A study on 'pre' and 'post' breast adenocarcinoma resection in rat models", T. Bhattacharjee, **P. Kumar**, A. Ingle, G. Maru, C. Murali Krishna, , Journal of Biophotonics, **2015**.
5. "Swiss bare mice: a suitable model for transcutaneous in vivo Raman spectroscopic studies of breast cancer", T. Bhattacharjee, **P. Kumar** (Equal Contribution), A. Ingle, G. Maru, C. Murali Krishna, Lasers in Medical Sciences, **2014**.
6. "Optical, spectroscopic, and doppler evaluation of "normal" and "abnormal" reflexology areas in lumbar vertebral pathology: a case study", Krishna Dalal, D. Elanchezhiyan, V. B. Maran, R. K. Das, **P. Kumar**, S. P. Singh, C. Murali Krishna, J. Chatterjee, Case Reports in Medicine, **2012**.

Piyush Kumar

DEDICATION

The thesis is dedicated to my parents

(Late) Mrs. Rekha Rani

and

Mr. Bindeshwar Prasad Singh

ACKNOWLEDGEMENT

I would start by thanking Dr. C. Murali Krishna, my research guide and mentor. He gave me the opportunity to work with him, constantly provided with important inputs and arranged for any infrastructure whenever needed. He always shared his life experiences to enrich my scientific knowledge as well as general understanding of life. On the personal front, he provided an unconditional support during a personal crisis, when my mother was undergoing treatment for cancer at ACTREC; and when I have not been in good physical or mental condition. He has even driven me to doctor during my time of illness.

Next I would like to thank Dr G. B. Maru who has been a wonderful co-guide and also my ex doctoral committee (DC) member. He always believed in my capabilities and made sure that I am never short of any motivation. Likewise, Dr. S. Zingde, my ex DC chairperson as well as ex Deputy Director, ACTREC, has been another source of motivation and inspiration. Both Dr. Maru and Dr. Zingde have taken keen interest in my research project and have an important role in completion of this work.

I would like to thank Dr. S. Chiplunkar, Director, ACTREC and Dr. S. Gupta, Deputy Director, ACTREC, for providing an opportunity to work and for easy access to the excellent ACTREC facilities. Sincere thanks to Dr. R. Sarin, ex Director ACTREC for being a wonderful Director-cum-doctor. I am indebted to him for his immense help during my mother's treatment. I also thank the Council of Scientific and Industrial Research (CSIR) for my fellowship.

I am thankful to all my current DC members, Dr. N. Shirsat (Chairperson), Dr. T. Teni, Dr. S. Gupta and Dr. A. Ingle for their expert comments and deliberations which helped in a logical conclusion of the project. Dr. M. Mahimkar deserves special thanks. Though not an official DC member, he gave his time and energy to my project and also provided his laboratory facilities for several experiments.

I thank Chilakapati lab members for their continuous support as wonderful labmates and friends. Dr. S. P. Singh, my senior in lab, taught me the technicalities and basic concepts of Raman spectroscopy and data analysis. He would often sit with me during analysis and make sure that I learn the nuances. Dr. R. Shaikh also taught me several things in lab and often took care of my mother. Dr. T. Bhattacharjee and Dr. A. Sahu helped with experimental work and also provided with several ideas and suggestions in times of experimental failiures. Mr. P. Tawde, my technical assistant deserves a special praise for his complete dedication to my experiments and being there whenever I needed him. Mrs A. Adhav has been a wonderful lab member and has been like a guardian. She has done many thankless jobs right from indenting to animal handling and tissue sectioning whenever needed. Aditi deserves a special mention.

She has been the best labmate and friend I could ask for. She has been a pillar of support and inspiration and played an important role in the successful completion of this PhD. I would like to thank other members who spent time in lab and taught me one thing or other- Sneha, Sandeep and Mahazabeen.

I would like to thank my wonderful batchmates who made life comfortable at ACTREC. Rajan , Ram and Raja have been 'best buddies' who would literally be there for me, even at midnight. I would like to thank them on behalf of my parents as well. I also thank Crismita, Shyam, Poonam, Asif, Rushikesh, Indrajit, Yasser, Richa, Nikhat for their help. Several people from ACTREC need to be thanked- Gaurav taught me everything about animal experiments, Sushmita, Ajit Sharma, Kedar, Subhoshree, Dilip Badgujar, Mr. Rajkumar Gaikwad (Security), all nursing and day care staff, Dr. Sumati (blood bank), Dr. Deepan and Dr. Anand (Residents), Dr. Thorat, Mr. Ravi, Mr. Chavan, and several other members of Laboratory Animal Facility, ACTREC imaging facility, and ACTREC administration staff, especially Mrs Seema and Mrs Anuradha. Special thanks to Ms Isha Behl and Mrs Sarita Behl. I may have missed several names but this doesn't make them less important.

I express my gratitude to my friends who have been with me since time immemorial- Kundan, Moquit, Vinay, Vikky, Debangana, Sachin, Sonia, Ami, Rajiv, Amit and Satya. I thank my amazing siblings- Kavita and Kislay.

Last but not the least; I thank my parents, to who I dedicate this thesis and the Almighty for everything.

Piyush Kumar

CONTENTS

PREFACE

Cancers are yet to be tamed menace to the human kind, inflicting scars on world health and socio-economics, in spite of scavenging funds worth multi-million dollars and scientific manpower. Oral cancer is the most common cancer among males in the South Asian nations such as India, with a poor 5-year survival rate, ascribed to late detection of the disease and recurrences. Various reports suggest that early detection of oral cancers is important for better prognosis and increased 5-year survival rate. However, currently practiced screening/diagnostic tools suffer from several limitations such as tedious sample preparation, long output time and inter-observer variances. Biopsy followed by histopathology, the current gold-standard, is not only invasive but also depends on selection of appropriate region. Thus it requires expert personnel. Further, it may not be very convenient for screening and therapeutic monitoring which require repeated sampling. Rapid, objective and preferably non-invasive alternatives as screening /diagnostic techniques are hence being extensively explored.

Raman spectroscopy (RS) is one such candidate tool which has found applicability in discriminating many diseases from healthy conditions. RS, which can provide chemical fingerprint/biochemical profile, has shown promising results in diagnosis of several cancers, including oral cancers. In this thesis, RS based evaluation of sequential progression of oral cancers, compared with gold standard, was carried out. As such studies are not feasible in humans due to ethical/practical considerations, the widely used hamster buccal pouch (HBP) model was employed to achieve the aim. HBP model shows cancer progression through stages similar to human oral carcinogenesis, with tumour formation by 14 weeks on application of 7, 12-dimethylbenz[a]anthracene (DMBA) on buccal pouches.

Chapter 1 (Introduction) provides the background information pertaining to oral cancers, various candidate diagnostic techniques, optical/spectroscopic techniques and developments in RS based exploration of oral cancers which steered the aim of the work - “Comparative evaluation of diagnostic efficacy of Raman spectroscopy and histopathology using a sequential animal model study”.

Chapter 2 (Materials and Methods) describes the methodologies, materials and protocols employed to achieve the objectives.

Chapter 3 (Results and Discussion) describes the results of the experiments for each objective along with discussion on the importance of the observations.

Chapter 4 (Conclusion and Outlook) provides concluding remarks for the thesis and gives and outlook of the work done.

SYNOPSIS

Prelude

This section provides the synopsis of the thesis, submitted to the university on 25th April, 2016.

Homi Bhabha National Institute

Synopsis of Ph. D. Thesis

1. Name of the Student: **Piyush Kumar**
2. **Name of the Constituent Institution:** Tata Memorial Centre, ACTREC
3. **Enrolment No.:** LIFE09201004022
4. **Title of the Thesis:** Comparative evaluation of diagnostic efficacy of laser Raman spectroscopy and histopathology in an animal model of oral carcinogenesis.
5. **Board of Studies**: Life Sciences

1. Introduction

Oral cancer is the most common cancer among Indian men [1]. Despite advancements in treatment modalities, 5-year survival rate remains a meager 50%. The poor prognosis has been attributed to late detection. Studies have shown that early detection improves prognosis and 5-year survival rate [2, 3]. The currently practiced gold-standard, biopsy followed by histopathology, is invasive (and painful), prone to subjective errors and not convenient for screening and therapeutic monitoring. Hence, rapid, objective, non-invasive techniques which are sensitive to tissue biochemistry could be more effective in early diagnosis as biochemical changes precede visible morphological alterations. The change in biochemical properties is also reflected in the optical properties and thus spectroscopic techniques such as Raman spectroscopy [4] (RS) can also be explored as a diagnostic adjunct. RS is a rapid, non-invasive and label-free technique being extensively explored in disease diagnosis and has shown promising results in the diagnosis of several cancers [5] including oral cancers [6-11]. RS studies in oral cancers have

shown classification of pathological conditions and detection of factors such as cancer field effects, demonstrating efficiency of the technique. These studies have relied on clinical examination and histopathology for pathological status. However, as mentioned earlier, histopathology suffers from limitations and is available only for cancerous and premalignant conditions which present morphological changes in mucosa. It would be imperative that biochemical changes preceding tumor conditions be identified. Thus, studies exploring sequential changes in oral carcinogenesis from absolutely healthy condition to tumor with proper age matched controls are warranted. As such studies cannot be undertaken on human beings due to ethical and practical considerations, animal models can be used. Hamster buccal pouch (HBP) is a widely used model for experimental oral carcinogenesis [12, 13], owing to attributes such as architectural similarities to human buccal mucosa, cancer progression through stages similar to human oral carcinogenesis and almost 100% incidence of tumors in 14 weeks on treatment with 7, 12-Dimethylbenz(a)anthracene (DMBA). Thus HBP model was employed in this study to carry out comparative evaluation of RS in oral carcinogenesis.

2. Aim and objectives:

Aim: Comparative evaluation of diagnostic efficacy of Raman spectroscopy and histopathology using a sequential animal model study.

Objective 1: Sequential and Comparative evaluation of Raman Spectral changes in DMBA-induced HBP carcinogenesis at various time periods.

Objective 2: Comparison with histopathology and specific biomarkers to determine whether RS can be developed as a sensitive diagnostic tool.

To address the first objective, sequential progression of oral carcinogenesis was followed using both ex vivo and in vivo approaches while for second objective, RS models based on gold standards (histopathology and immunohistochemistry) was employed. Study was also carried out to look into the contribution of physico-mechanical factors in carcinogenesis, using suitable controls. To further explore the findings two additional experiments were performed:

- Optical coherence tomography study of buccal pouches.
- Effect of discontinuation of DMBA application on cancer progression.

3. Objective 1: Sequential and comparative evaluation of Raman Spectral changes in DMBA-induced HBP carcinogenesis at various time periods.

To monitor sequential progression during oral carcinogenesis, three approaches were explored. First was ex vivo while the next two were in vivo in nature.

(a) Ex-vivo study: In this approach, the spectra were recorded ex vivo from (n=115) excised out buccal pouches of DMBA treated and control animals, after animal sacrifice. Golden Syrian hamsters (male, 6-8 weeks) were obtained from Laboratory Animal Facility, ACTREC. Topical application of 0.5% DMBA (Sigma-Aldrich, purity 95%) dissolved in groundnut oil (Dhara, India) was carried out for 14 weeks, 3 times a week, on right buccal pouch of the test animals using a paint brush (Camel, no. 4, India) and thus the process is referred to as painting. These pouches are referred to as DMBA treated pouches. The left buccal pouches of these animals served as and are referred to as DMBA contralateral controls. The right buccal pouch of control animals (age matched) were painted with the vehicle oil (groundnut oil, Dhara) for the same duration. In this report, these pouches have been addressed as vehicle controls while the left

pouches addressed as vehicle contralateral pouches. 5 test and 3 control animals were sacrificed every week over the 14-week duration of carcinogen/oil treatment. HBPs were then excised out, snap frozen in liquid nitrogen and stored at -80^{o}C till spectra recording. Spectra were recorded from these tissues after thawing on ice, and spreading over aluminium grids (3X3) using fiber optic probe (InPhotonics, USA) coupled HE-785 commercial Raman spectrometer (Jobin-Yvon-Horiba, France), employing 785 nm wavelength laser (Process Instruments, USA). One spectrum was recorded from the tissue region present in the center of each grid. The spectra from DMBA treated and control pouches have been referred to as Tx and Cx, respectively (x= 1 to 14, referring to weeks of treatment). Tissues were cut along gridlines and processed for histopathology. The raw spectra were preprocessed and subjected to multivariate analysis methods such as unsupervised Principal Component Analysis (PCA) and supervised Principal Component based Linear Discriminant Analysis (PC-LDA) followed by Leave One Out Cross Validation (LOOCV) through MATLAB based algorithms[14] to analyze classification.

Progressive visual and histopathological changes were observed during the 14-week carcinogenesis period, consistent with literature: normal/healthy (controls and week 1 of DMBA treated), hyperplasia/inflammatory (week 2 onwards), dysplasia (week 7 onwards) followed by squamous cell carcinoma (SCC) (week 12 onwards).

Mean spectral features: C0 and T0 spectra show dominance of lipid features- 1303 cm^{-1}, δCH_2 (1448 cm^{-1}), Amide I (1655 cm^{-1}), and ester bands (1750 cm^{-1}) whereas T14 (tumors) spectra show dominance of proteins and nucleic acids with changes in 1200-1400 cm^{-1} regions, Amide III, CH_2 (1454 cm^{-1}), 1583 cm^{-1}, and Amide I (1651 cm^{-1}). T2 to T13 spectra showed sequential

changes in Amide III and Amide I regions, suggesting progressively increasing protein dominance. These spectral features correlated well with human buccal mucosa spectra.

Multivariate analysis: 3 group classification involving week 0 controls (C0), DMBA-treated HBP (Tx) and vehicle controls (Cx) were used (e.g. C0 vs C2 vs T2, for week 2)

PCA: PCA scatter plots exhibited overlapping clusters for all the three groups in weeks 1 to 4. Tendency of classification was observed from week 5 onwards, attributable to DMBA induced changes. Exclusive cluster of Tx spectra were seen from week 12. Poor classification tendency was observed between C0 and Cx, suggesting lack of appreciable age-related changes.

PC-LDA: On basis of classification efficiency, Tx spectra from the 14 weeks can be divided into three phases. (a) T0-T7: progressive increase in classification, up to 70%. (b) T8-T11: showed plateauing phase, classification efficiency of 70-80% and (c) T12-T14: classification up to 100%.

Thus the ex vivo study demonstrated feasibility of studying sequential changes during oral carcinogenesis. As this approach is invasive, in vivo analysis were carried out to ascertain above described findings.

(b) In vivo sequential study: In this approach, spectra were recorded from buccal pouch of alive, but, anaesthetized animals. 2 test and 2 control animals were used each week and thus a total of 56 animals were used. Post spectra acquisition, the animals were sacrificed. In vivo Raman spectral features and trends of multivariate analysis were similar to ex vivo study. PC-LDA based classification for Tx increased till week 8, plateaued between weeks 8-11 and then increased beyond 90% by week 14.

(c) In vivo follow up study: This approach was also in vivo, with an objective to monitor sequential progression from the same set of animals during the entire period of 14 weeks. Such approaches overcome inter-animal variations and require fewer animals. In vivo Raman spectra were acquired from buccal pouch (3 test and 3 controls) post anaesthetization, each week for the entire duration of 14 weeks, without sacrificing them. Findings were in agreement with ex vivo and in vivo sequential study. *(Technology in Cancer Research and Treatment, 2015)*

Misclassification between spectra from DMBA treated and control HBP: Repeated observations of misclassifications of Tx and Cx spectra were observed in the later weeks; the origin of such misclassifications was explored. Histopathological analysis of such control tissues revealed abnormal changes in some vehicle controls attributable to injuries due to repeated pulling out of HBP by forceps. These changes in the control tissues were further explored in the next objective.

4. Objective 2: Comparison with histopathology and specific biomarkers to determine whether RS can be developed as a sensitive diagnostic tool.

In this objective, spectra were evaluated against models based on standard diagnostic approaches like histopathology and specific biomarkers, employing test (n=70) and control animals (n=45). As mentioned in the ex vivo study, 5 test and 3 control animals were sacrificed each week and spectra acquired after spreading HBP tissues on 3X3 grids. To facilitate RS, histopathology and immunohistochemical analysis (IHC) of the same region, after spectra acquisition, the laser probed region on HBP tissues were marked in waterproof ink (Camel, India), tissues cut along gridlines and each tissue piece was immersed in separate tubes with 10% neutral buffered formalin for 24-hour fixation. The fixed tissue pieces were embedded in paraffin blocks and

three 5 micron sections from the ink-marked spots were taken on glass slides for histopathology while two successive 5 micron sections were taken on poly-L-Lysine (Sigma) coated glass slides for IHC. Spectra with histopathological consensus among pathologists have been referred to as 'histopathology certified spectra' in this report. IHC was carried out for cell proliferation marker Cyclin D1. In the next step, PC-LDA models were built using the spectra certified on basis of histopathology and Cyclin D1 expression. LOOCV of models was followed by evaluation with independent spectra from DMBA treated as well as control animals.

(a) Spectral model based on histopathology: 2 factors contributing 78% classification were used to build PC-LDA models from spectra corresponding to the histopathological stages- control (healthy), hyperplasia, dysplasia and SCC. Spectral features showed lipid dominance in control while increasing protein/lipid ratio was observed with increasing severity of pathology. PCA suggested tendency of classification for all stages.

Evaluation using independent data set of DMBA treated spectra: 3/100, 29/164, 87/151 and 86/101 spectra were predicted as higher pathologies for weeks 1-3, 4-7, 8-11 and 12-14, respectively. Thus incidence of higher pathologies (dysplasia and SCC) increased with duration of DMBA application.

(b) Spectral model based on Cyclin D1 expression: Cyclin D1, which has a major regulatory role at G1/S checkpoint, is an important cell proliferation biomarker as deregulation of G1 to S phase progression of cell cycle, is a common target in carcinogenesis[15]. Many studies have reported overexpression of Cyclin D1 in oral cancers [16, 17]. Hence IHC was carried out for cyclin D1 markers and spectra corresponding to pathologist certified grading of 0, 1, 2 and +3 (represented as G0, G1 G2 and G3) on basis of Cyclin D1 expression were used for multivariate

analysis. G0 and G1 grades show zero or minimum expression of the biomarker, G2 shows intermediate expression while G3 involves expression in maximum/entire region in a section. 2 factors contributing 78% classification were used to build PC-LDA models for G0, G1, G2 and G3.

Evaluation using independent data set of DMBA treated spectra: Findings were similar to histopathology based model. 9/98, 37/171, 70/167 and 89/102 spectra were predicted as higher pathologies (G2,G3) for weeks 1-3, 4-7, 8-11 and 12-14, respectively, suggesting increased incidence.

(c) Investigation of abnormal changes in control pouches: To explore abnormal changes in controls, three different types of controls were employed: (a) vehicle controls (n=335): spectra from right pouch of vehicle control animals; (b) vehicle contralateral (n=77): spectra from the untreated left pouches of vehicle controls and (c) DMBA contralateral (n=375): spectra from the untreated left pouch of DMBA treated animals.

Evaluation of control spectra against the models: In case of histopathology based model, 4, 36 and 65 vehicle contralateral, vehicle control and DMBA contralateral, were predicted as dysplastic/SCC spectra, respectively. In case of IHC based model 3, 37 and 68 vehicle contralateral, vehicle control and DMBA contralateral were predicted as G2/G3, respectively. Thus incidence of higher pathologies (dysplasia/SCC/G2/G3) was least in case of vehicle contralateral and highest for DMBA contralateral controls. A probable reason for this observation could be minimal damage to the vehicle contralateral pouch due to lack of repeated handling. DMBA contralaterals showed more abnormal changes, probably due to leaching and mixing of DMBA in saliva. Thus increased incidence for weeks 11 to 14 indicated higher

duration of handling and associated injuries/indirect exposure to DMBA may be a probable cause. Such observations of higher pathologies has not been reported in control animals although, isolated cases of tumor development in pet hamsters [18] and in contralateral HBP [19] are reported.

In the present study, though small in number, some control spectra were predicted as higher pathologies. In our previous in vivo studies on oral cancers [9-11], similar misclassifications observed between normal (control) and tumors were attributed mainly to tumor heterogeneity. No histopathological confirmation of normal tissues could be made due to ethical considerations. In the present study, presence of abnormalities in vehicle control may be attributed to repeated mechanical irritation similar to those observed in non-tobacco habitués, especially women. A probable cause in such cases is chronic physico-mechanical irritations in the oral cavity due to irregular/sharp teeth and improperly fit dentures [20, 21]. *(Journal of Raman Spectroscopy, 2016).*

5. Optical coherence tomography (OCT) to study abnormal changes in control pouches.

To explore the observed abnormalities in control tissues using another complementary technique, OCT was selected to carry out this small scale study. OCT uses low-coherence interferometry to produce two-dimensional images of optical backscattering from internal tissue microstructures analogous to ultrasonic pulse-echo imaging [22]. OCT was carried out using an in-house instrument at Bhabha Atomic Research Centre, Vishakhapatnam on 6 DMBA treated and 8 control tissues of early and late weeks. While OCT images suggested intact epithelial architecture for 6 controls and 4 DMBA treated pouches of early weeks, the entire layer was

disrupted in case of tumors from week 13 (n=2). In 2 vehicle control tissues (week 12 and 13), epithelial architecture was disrupted in OCT images suggesting damage to the epithelium of such tissues and in concordance with Raman findings. *(Asian Journal of Physics, 2015).*

6. Effect of discontinuation of DMBA application in cancer progression.

As mentioned in Objective 1, plateauing of classification of Tx spectra from 8 to 11 weeks of carcinogenesis was observed. A reason for this observation is accumulation of dysplastic changes across the HBP. However, continuous application of DMBA, beyond 8 weeks results into development of tumors (histopathologically SCC) by 13 weeks. In the present study, the effect of discontinuation of DMBA after 8 weeks was studied to find out if progression to SCC is observed. Following groups of animals were taken: (a) DMBA application for 14 weeks (n =5) and then spectra acquired (T14, 34 spectra). (b) DMBA application only for 8 weeks and then discontinued (n =5). Spectra were recorded from these animals at the end of 8 weeks (T8, 55 spectra) and 14 weeks (T14dc, 46 spectra). (c) Vehicle oil was applied (n =5) for 8 weeks and then discontinued. Spectra were acquired at week 0 (C0, 37 spectra), week 8 (C8dc, 42 spectra) and week 14 (C14dc, 57 spectra).

PCA scatter plot suggested 3 exclusive clusters: 1^{st} for T14 spectra, 2^{nd} for T8 spectra and 3^{rd} consisting of all the vehicle controls (C0, C8dc, C14dc). The spectra of interest, T14dc, were spread across these clusters. Findings suggest most T14dc spectra overlapped with controls or T8 cluster. Some T8dc spectra (~13; 28%) overlapped with the T14 spectra indicating that some area in mucosa can progress to higher pathologies even after withdrawal of the carcinogenic agents. Thus people who quit tobacco habits at lesser risk than those who continue with the habit.

Still, as a preventive measure, it would be prudent for them to visit preventive oncology departments.

7. Summary

Sequential spectral changes were monitored over a 14-week period of carcinogenesis in the hamster buccal pouch model ex vivo. Spectral changes showed decreasing lipid and increasing protein dominance while multivariate analysis indicated increasing efficiency of classification with the duration of carcinogen application. Sensitivity was 70% by week 8, 70 to 80% for week 9 to 11 and 80 to 100% for week 12 to 14. Further, spectral models were trained on basis of histopathological stages (control, hyperplasia, dysplasia and SCC) and Cyclin D1 expression (G0, G1, G2 and G3) employing 2 factors contributing 78 and 87% classification, respectively. Evaluation of DMBA treated spectra showed increasing incidence of higher pathologies with progression of weeks (3% for week 1-3 to 89% for week 12-14). It should be noted that histopathology was carried out from three 5 µm sections from the laser probed region which were of 200 µm diameter in this study, posing a technical limitation. Heterogeneity within the laser probed region cannot be ruled out and thus, despite best efforts, pure models for intermediate stages such as hyperplasia and dysplasia is difficult. Optical coherence tomography study on limited samples indicated abnormal changes in 2 control pouches of week 12 and 13 which undergo more handling than hamsters from early weeks. These pouches, further investigated using RS and histopathology, confirmed small regions of abnormalities. Such changes appear similar to those observed in non-tobacco habitués who develop cancers as a result of chronic physico-mechanical irritations in oral cavity. In another study, effect of discontinuation of DMBA was investigated. DMBA application was carried out for 8 weeks only but spectra were recorded at the end of 14^{th} week. Evaluation of these spectra suggested that 72% and

28% spectra getting classified as control/week 8 and tumors, respectively. Findings suggested reduced risk in case of tobacco habitués who have quit, than those who continue with the habit.

Notwithstanding the limitations, findings suggest ability of RS in monitoring changes during carcinogenesis and in identifying abnormal changes and microheterogenity in buccal mucosa which may often go unnoticed in clinical examinations and conventional studies wherein tissue extracts/homogenates are employed. Over all, results provide further proof of RS being a potential adjunct for prospective non-invasive, label-free, online applications for screening purposes.

8. References for Synopsis

1. Jemal A, Siegel R, Xu J, Ward E: **Cancer statistics, 2010**. *CA Cancer J Clin* 2010, **60**(5):277-300.
2. Mehrotra R, Gupta DK: **Exciting new advances in oral cancer diagnosis: avenues to early detection**. *Head Neck Oncol* 2011, **3**(1):33.
3. Sankaranarayanan R, Ramadas K, Thomas G, Muwonge R, Thara S, Mathew B, Rajan B, Trivandrum Oral Cancer Screening Study G: **Effect of screening on oral cancer mortality in Kerala, India: a cluster-randomised controlled trial**. *Lancet* 2005, **365**(9475):1927-1933.
4. Raman CV, Krishnan KS: **A new type of secondary radiation**. *Nature* 1928, **121**(3048):501-502.
5. Pence I, Mahadevan-Jansen A: **Clinical instrumentation and applications of Raman spectroscopy**. *Chemical Society Reviews* 2016, **45**(7):1958-1979.
6. Venkatakrishna K, Kurien J, Pai KM, Valiathan M, Kumar NN, Murali Krishna C, Ullas G, Kartha V: **Optical pathology of oral tissue: a Raman spectroscopy diagnostic method**. *Current science* 2001, **80**(5):665-669.
7. Guze K, Short M, Sonis S, Karimbux N, Chan J, Zeng H: **Parameters defining the potential applicability of Raman spectroscopy as a diagnostic tool for oral disease**. *Journal of biomedical optics* 2009, **14**(1):014016-014016-014019.
8. Bergholt MS, Zheng W, Huang Z: **Characterizing variability in in vivo Raman spectroscopic properties of different anatomical sites of normal tissue in the oral cavity**. *Journal of Raman Spectroscopy* 2012, **43**(2):255-262.
9. Singh SP, Deshmukh A, Chaturvedi P, Murali Krishna C: **In vivo Raman spectroscopic identification of premalignant lesions in oral buccal mucosa**. *J Biomed Opt* 2012, **17**(10):105002.
10. Singh S, Sahu A, Deshmukh A, Chaturvedi P, Krishna CM: **In vivo Raman spectroscopy of oral buccal mucosa: a study on malignancy associated changes (MAC)/cancer field effects (CFE)**. *Analyst* 2013, **138**(14):4175-4182.

11. Sahu A, Deshmukh A, Hole AR, Chaturvedi P, Krishna CM: **In vivo subsite classification and diagnosis of oral cancers using Raman spectroscopy**. *Journal of Innovative Optical Health Sciences* 2016:1650017.
12. Salley JJ: **Experimental carcinogenesis in the cheek pouch of the Syrian hamster**. *J Dent Res* 1954, **33**(2):253-262.
13. Gimenez-Conti IB, Slaga TJ: **The hamster cheek pouch carcinogenesis model**. *Journal of Cellular Biochemistry* 1993, **53**(S17F):83-90.
14. Ghanate AD, Kothiwale S, Singh SP, Bertrand D, Krishna CM: **Comparative evaluation of spectroscopic models using different multivariate statistical tools in a multicancer scenario**. *J Biomed Opt* 2011, **16**(2):025003.
15. Hall M, Peters G: **Genetic alterations of cyclins, cyclin-dependent kinases, and Cdk inhibitors in human cancer**. *Adv Cancer Res* 1996, **68**:67-108.
16. Staibano S, Lo Muzio L, Pannone G, Mezza E, Argenziano G, Vetrani A, Lucariello A, Franco R, Errico ME, De Rosa G *et al*: **DNA ploidy and cyclin D1 expression in basal cell carcinoma of the head and neck**. *Am J Clin Pathol* 2001, **115**(6):805-813.
17. Xu J, Gimenez-Conti IB, Cunningham JE, Collet AM, Luna MA, Lanfranchi HE, Spitz MR, Conti CJ: **Alterations of p53, cyclin D1, rb, and H-ras in human oral carcinomas related to tobacco use**. *Cancer* 1998, **83**(2):204-212.
18. Selk Ghaffari M, Moayer F, Dezfoulian O: **Spontaneous differentiated squamous cell carcinoma of cheek pouch in a Syrian hamster**. *Iranian Journal of Veterinary Research* 2009, **10**(1):84-86.
19. Dachi SF, Sanders JE, Urie EM: **Effects of dimethyl sulfoxide on dimethylbenzanthracene-induced carcinogenesis in the hamster cheek pouch**. *Cancer research* 1967, **27**(7):1183-1185.
20. Piemonte ED, Lazos JP, Brunotto M: **Relationship between chronic trauma of the oral mucosa, oral potentially malignant disorders and oral cancer**. *Journal of oral pathology & medicine* 2010, **39**(7):513-517.
21. Preston-Martin S, Pike MC, Ross RK, Jones PA, Henderson BE: **Increased cell division as a cause of human cancer**. *Cancer Research* 1990, **50**(23):7415-7421.
22. Huang D, Swanson EA, Lin CP, Schuman JS, Stinson WG, Chang W, Hee MR, Flotte T, Gregory K, Puliafito CA *et al*: **Optical coherence tomography**. *Science* 1991, **254**(5035):1178-1181.

Publications in Refereed Journals

a. Published

1. **P. Kumar**, T. Bhattacharjee, A. Ingle, G.B. Maru, C. Murali Krishna, Raman spectroscopy of experimental oral carcinogenesis: Study on sequential cancer progression in hamster buccal pouch model, Technology in Cancer Research and Treatment, 2015.
2. **P. Kumar** and C. Murali Krishna, Animal models in disease diagnosis: Exploration using Raman spectroscopy, Asian Journal of Physics, 2015.

3. **P. Kumar** and C. Murali Krishna, Multimodal spectroscopic applications in cancer diagnosis: Combined Raman spectroscopy and Optical coherence tomography, Asian Journal of Physics, 2015.
4. N. Tayal, **P. Kumar**, C. Murali Krishna Disease Diagnosis by optical spectroscopy: Role of multivariate analysis, Asian Journal of Physics, 2015.

b. <u>Accepted</u>

c. <u>Communicated</u>

1. **P. Kumar**, T. Bhattacharjee, M. Pandey, A. Hole, A. Ingle, C. Murali Krishna, Raman spectroscopy in experimental oral carcinogenesis: investigation of abnormal changes in control tissues, J Raman Spectroscopy, (under review).

d. <u>Other Publications</u>

1. M. Gohulkumar, **P. Kumar**, C. Murali Krishna, N. Krishnakumar, Evaluation of Raman spectroscopy for prediction of antitumor response to silibinin and its nanoparticulates in DMBA - induced oral carcinogenesis, Journal of Raman Spectroscopy, 2016.
2. K. Gurushankar, M. Gohulkumar, **P. Kumar**, C. Murali Krishna, N. Krishnakumar, Raman spectroscopy detects biomolecular changes associated with nanoencapsulated hesperetin: treatment in experimental oral carcinogenesis, Laser Physics Letters, 2016.
3. T. Bhattacharjee, **P. Kumar**, A. Ingle, G. Maru, C. Murali Krishna, Raman spectroscopy of serum: A study on 'pre' and 'post' breast adenocarcinoma resection in rat models, Journal of Biophotonics, 2015.
4. T. Bhattacharjee, **P. Kumar** (Equal Contribution), A. Ingle, G. Maru, C. Murali Krishna, Swiss bare mice: a suitable model for transcutaneous in vivo Raman spectroscopic studies of breast cancer, Lasers in Medical Sciences, 2014.
5. Krishna Dalal, D. Elanchezhiyan, V. B. Maran, R. K. Das, **P. Kumar**, S. P. Singh, C. Murali Krishna, J. Chatterjee, Optical, spectroscopic, and doppler evaluation of "normal" and "abnormal" reflexology areas in lumbar vertebral pathology: a case study, Case Reports in Medicine, 2012.

Refereed Conference Proceedings

6. Raman spectroscopy of experimental carcinogenesis: investigating suitability of *ex vivo* models to evaluate *in vivo* spectra, **A Conference of New Ideas in Cancer-Challenging Dogmas,** Mumbai in February 2016 (European Journal of Cancer, 2016).

7. Stages in experimental oral carcinogenesis: Raman spectroscopic and immunohistochemical evaluation, **SPEC Shedding New Light on Diseases 2014,** Krakow, Poland in August 2014.
8. Tracking DMBA-induced biochemical and morphological changes in Syrian Hamsters: Raman and OCT Study, **National Laser Symposium NLS 22**, Manipal Academy of Higher Education, Manipal in January 2014 (Proceedings of NLS, 2014)
9. Experimental Oral Carcinogenesis: Sequential progression study through Raman Spectroscopy, **23rd International Conference on Raman Spectroscopy (ICORS)**, Bangalore in August 2012.
10. Experimental Oral Carcinogenesis: A preliminary diagnostic efficacy of Raman spectroscopy, American Association of Cancer Research (**AACR) New Horizons in Cancer Research**, Gurgaon, Delhi-NCR in December 2011.

Signature of Student:

Date: 18/04/2016

Doctoral Committee

S. No.	Name	Designation	Signature	Date
1.	Dr. N. Shirsat	Chairman		15-4-16
2.	Dr. C. Murali Krishna	Guide & Convener		18.4.16
3.	Dr. T. Teni	Member		18.04.16
4.	Dr. S. Gupta	Member		20/04/16
5.	Dr. A. Ingle	Technical Advisor		20-04-16

Forwarded through:

S. Chiplunkar 21/4/16

Dr. S.V. Chiplunkar
Director ACTREC
Chairperson,
Academic & Training Programme

Dr. S. V. Chiplunkar
Director
Advanced Centre for Treatment, Research & Education in Cancer (ACTREC)
Tata Memorial Centre
Kharghar, Navi Mumbai 410210.

Dr. K. Sharma
Director, Academics
T.M.C.

PROF. K. S. SHARMA
DIRECTOR (ACADEMICS)
TATA MEMORIAL CENTRE,
PAREL, MUMBAI

List of Figures

List of Tables

Contents in detail

1 Chapter 1: Introduction

Prelude

This chapter starts with the basic definition of cancers and a brief history to suggest cancer has been affecting the living beings since ancient times. As the focus of this thesis is oral cancers, etiology and epidemiology related to oral cancers has been presented. The conventional methods of clinical diagnosis and their limitations have propelled the research towards tools and technologies which may serve as possible adjuncts to the existing gold standards. In this respect, various biomarkers and optic based techniques have been mentioned. Next, Raman spectroscopy, being explored as a potential diagnostic adjunct, has been described along with the basic principles and its selective advantages in oral cancer diagnosis. Developments in the field of Raman based diagnosis in oral cancers have been categorized as invasive/ex vivo, minimally invasive and non-invasive/in vivo approaches. Finally, animal models based explorations of RS has been highlighted. Subsequently, the aim and objectives of the study has been presented.

1.1 Cancer

Cancer is a genetic condition characterized by unregulated cell proliferation due to loss/gain of several gene functions. To quote Weinberg, “The hallmarks of cancer comprise six biological capabilities acquired during the multistep development of human tumours. The hallmarks constitute an organizing principle for rationalizing the complexities of neoplastic disease. They include sustaining proliferative signaling, evading growth suppressors, resisting cell death, enabling replicative immortality, inducing angiogenesis, and activating invasion and metastasis” [23].

1.1.1 Brief history of cancer

Paleopathological evidences suggest that tumours have existed as long as the human beings have, if not less. Brain tumour has been observed in a 72 million years old dinosaur (Gargosaurus) fossil, on display at the Children’s Museum of Indianapolis [24]. Nasopharyngeal carcinomas and osteosarcomas have been observed in Egyptian mummies [25]. Ancient Greeks and Romans had their own notions and philosophies regarding cancer-like conditions [26, 27] . Hippocrates is supposed to have coined the term carcinos for a non-ulcerating tumour while carcinoma was used for an ulcerating tumour. The Greek word for tumour is ‘oncos’. Claudius Galenus, popularly known as Galen, was a famous physician of the Roman period. He called tumours as ‘cancer’ and also introduced the term sarcoma. The basic understanding of cancers has majorly emerged from the research in the last 2 centuries [28], with the most significant discoveries made post revolution in the field of molecular and cell biology. Table 1.1 summarizes the major events in the field of oncology.

Year	Discovery/Event
1863	Cellular origin of cancer (Virchow)
1914	Chromosomal mutations in cancer (Boveri)
1944	Transmission of information by DNA (Avery)
1950	Availability of cancer drugs (Cancer Chemotherapy National Service Service Center)
1953	Structure of DNA (Watson and Crick)
1961	Genetic code
1970	Reverse Transcriptase
1971	Restriction Enzymes
1975	Hybridomas and Monoclonal Antibodies
1976	Cellular origin of retroviral oncogene
1979	EGFR
1981	p53
1984	G proteins
1986	Retinoblastoma gene
1991	APC gene mutation and colorectal cancers
1994	BRCA1
2000	Human Genome Sequencing
2002	Epigenetics/MicroRNAs in cancer
2006	Tumor stromal Interaction

Table 1.1: Major events which have broadened the understanding of cancers.

1.1.2 Cancer: a leading cause of death

Cancers have already surpassed heart diseases as the leading cause of death [29, 30] in the United States. Nearly ten million new cancer cases are diagnosed annually in the world and out of these about half of the cases are reported from developing nations. It is predicted that by 2020, annually, over 10 million people would die of cancer globally, with 70% deaths from the developing nations [31]. According to Global Adult Tobacco Survey–GATS (2010), an initiative of World Health Organization (WHO), more than one-third (35%) of adults in India use tobacco in some form or the other [32], which poses a great health risk.

1.2 Oral cancers

Oral cancers have emerged as a major hazard, with epidemic like status in the South Asian and several developing nations, ascribed to rampant tobacco and alcohol abuse. In case of the Indian subcontinent, oral cancer is the major killer in males, ranking third among both sexes, with a poor five-year survival rate.

1.2.1 Epidemiology

India has the ninth highest incidence of oral cancer in the world (age-adjusted incidence in some areas is as high as 17·1 per 100 000 men and 7·6 per 100 000 women. A poor 5-year survival rate, between 54·3% and 60·2% for localized cancers of the mouth, can distressingly be as low as 3·1–3·3% in advanced stages of oral cancer [33, 34].

1.2.2 Etiological factors

The major etiological factors for oral cancers include tobacco, betel quid (paan, betel leaf, areca nut, sweeteners), alcohol, human papillomavirus (HPV) and poor hygiene/dietary habits [35-38].

Tobacco is a known risk factor for oral cancers. Tobacco is known to contain several compounds including tobacco specific nitrosamines and poly aromatic hydrocarbons such as benzo[a]pyrene and benz[a]anthracene which can be potential carcinogens [3][39]. It is estimated that around 75% patients above the age of fifty and diagnosed with oral cancer have used tobacco in one form or the other. In fact, tobacco use, alcohol consumption and poor oral hygiene account for over 90% of all cases of oral cancers [40]. All forms of smoke (cigarettes, pipes, cigars, bidis) and smokeless tobacco (chewing tobacco, snuff, and betel quid) are known to play a role in oral cancer development. Cigarette smoking is associated with an increased risk factor of 1·9–3·6 [35, 41] while chewing tobacco is associated with an even greater risk (relative risk 4·7–12·8) [42, 43]. According to WHO, if serious measures are not taken, annual tobacco related deaths are projected to increase to 8 million by 2030 (10% of all deaths) [44]. In case of betel quid chewing, risks of oral cancer with simultaneous usage of tobacco are 1·5–5·4 times greater than chewing without tobacco [36, 45].

Alcohol has been observed to play a synergistic role with tobacco in oral carcinogenesis [36, 46]. Alcohol possesses a risk of about 18% when taken alone. Combined exposure to alcohol and tobacco poses an estimated risk from 35% to 80% [47, 48]. Some studies have suggested that cohort of patients with both smoking and drinking habits can have hundred times greater risk [49-55].

Infectious agents such as viruses have been shown to be associated with oral and oropharyngeal cancers. HPV infection-related risk is apparently specific to cancers of the oropharynx (base of tongue, soft palate, lingual tonsil, tonsil, uvula, oropharyngeal region) [36, 56], particularly in case of non-tobacco habitué females below 40 years of age. Other than high-risk HPVs such as

HPV-16 and HPV-18 [57], herpes simplex virus (HSV) and Epstein-Barr virus (EBV) may also play a role in oral carcinogenesis [58-61].

Additional factors such as nutritional deficiencies, genetic predisposition, occupational risks, poor oral hygiene and irregular dentition can also lead to oral cancer [38, 62-67]. With increasing incidence of cancers around the globe, it is necessary to understand events in cancer initiation and progression in order to explore avenues to combat cancer. Cancer results from a series of changes at cellular levels through the process of carcinogenesis which has been described in the next section.

1.3 Carcinogenesis

Carcinogenesis is a multistage, multifactorial and long evolving process involving genetic alterations in the cell cycle and signaling pathways. The combined effects of several factors, such as stimulatory (e.g. cytokines and hormones), stress mediators (oxygen radicals) and exogenous aggressions (radiation, viruses, carcinogens and xenobiotic compounds) can affect cell cycle regulation, cellular proliferation and lead to tissue transformation.

1.3.1 Multistage process

Carcinogenesis majorly involves three major steps: initiation, promotion and progression [68]. The first stage of carcinogenesis, initiation, results from an irreversible genetic alteration, most likely through one or more mutations, which may include transversions, translocations and/or small deletions in DNA. The reversible stage of promotion does not involve changes in the structure of DNA but rather in the expression of the genome mediated through promoter-receptor interactions. It involves selective clonal expansion of initiated cells upon stimulation/promotion.

The final stage of progression is characterized by karyotypic instability, increased proliferative capacity and metastatic potential, leading to malignant growth. Critical molecular targets during the stages of carcinogenesis include proto-oncogenes, cellular oncogenes, and tumour suppressor genes. Although many such critical target genes and associated pathways have been identified, the ultimate number and characteristics of molecular alterations that result into cancer still eludes us.

1.3.2 Experimental carcinogenesis

Ethical considerations allow only selected clinical trials on human subjects. Animal models can be employed to carry out research in a regulated environment. Research on animal models range from prevention to treatment and cure of diseases. Animal models find applications in various fields including vaccines to chemoprevention, diabetes to neurological disorders, patterns in social behavior to preferences of mating partners; and have led to major medical breakthroughs. Animal models can belong to (but are not limited to) one of the following categories: (1) induced (experimental) models, (2) spontaneous (genetic, mutant) models, (3) genetically modified models, (4) negative models, and (5) orphan models [69]. Rodents such as mice, rats and hamsters are among the most commonly employed animals. Rabbits, guinea pigs and primates are used, depending on the hypothesis and the experiments designed. The commonly employed animal models for oral cancers have been described below:

1.3.2.1 Rats and mice

Water-soluble 4-nitroquinoline 1-oxide (4NQO) induced palatal carcinomas are observed in these animals by seven months. 4NQO has been used in several studies to induce squamous cell carcinomas (SCC) in the palatal mucosa of rats and mice [70, 71]. A close similarity was

observed between the histologic features of 4NQO-induced dysplasia in the rat/mouse palatal mucosa and human oral epithelial dysplasia. Repeated application of 4NQO on tongue can also produce SCC of the tongue in rats. The sequential histopathological changes in the lingual epithelium carcinogenesis progress from mild to moderate and then severe atypia before development of SCC. Initiation, with its putative irreversible cellular changes, occurs within 4 weeks [72]. Systemic administrations of 4NQO via the drinking water has also been used to induce massive tumours on the tongues of both CBA and C57Bl/6 female mice. Pathological analyses indicated that these were flat squamous dysplasia, exophytic papillary squamous tumours (papillomas), and invasive SCC [73]. Cancer initiation and progression were correlated with abnormal expression of H-ras, Bcl-2 and Bax, P53, and, E- and P-cadherin [74, 75].

1.3.2.2 Rabbits

Rabbit as an oral cancer model involves implantation, often through intraoral injection, of VX2 tumour cell lines [76-78]. It is not produced in situ, consequently, its behavior relies on the location of transplantation. Moreover, it is not considered suitable to monitor sequential progression of oral cancers [76].

1.3.2.3 Hamsters

Since the 1950s, the Syrian Golden hamster cheek/buccal pouch (HBP) has been widely used on account of its anatomical and physiological features [79]. A pouch on each side of the oral cavity, under the cheek muscles, opens into the anterior part of the oral cavity and is associated with small salivary glands that produce both serous and mucous secretions. The pouches extend backwards along the oral cavity and are used for storage of food. Histologically, the buccal cavity is lined with keratinizing squamous epithelium. Chemical induced carcinogenesis in HBP

are extensively explored. The first successful production of tumours at this site was achieved by Salley [12], who investigated the effects of the carcinogen DMBA, dissolved either in acetone or benzene. Each solution was painted onto the pouch three times a week for 16 weeks. The first 2 weeks showed an inflammatory phase with necrosis and sloughing of the distal part of the pouch, followed by healing and shrinkage. The mucosa subsequently passed through four histologically recognizable stages: hyperplasia, papilloma, carcinoma in situ and SCC. This experimental technique was further standardized by Morris [80]. He demonstrated that five week-old animals were better suited for the commencement of experimental carcinogenesis. He also observed that a 0.5% solution of DMBA in acetone applied three times a week, produced the maximum tumour yield with minimum latency and no morbidity.

The hamster model reflects many aspects of human oral cancer development [13, 81-84]. The common features include changes in oncogenic expression, such as p53 and/or ras [85-87], expression of proliferation markers, early expression of c-glutamyl transpeptidase [88, 89], downregulation of Keratin 76 expression [84], the requirement for neovascularization during oral carcinogenesis [90, 91] and the response to retinoids, tocopherols and carotenoids that inhibit or prevent the development of premalignant or invasive carcinoma [92, 93].

A common criticism against the hamster model is that the human oral cavity, of course, is devoid of a similar pouch. Another objection to this model is that the HBP tissue is considerably thinner [94-96]. However, in spite of these differences, based on its several similarities with human buccal mucosa and stage wise development of oral cancers, the HBP model has been widely employed in research as shown in a number of reports.

1.4 Role of prevention and early diagnosis

A cancer subject expects a certainty in cure rather than a promising treatment module. Notwithstanding the advancements in the field of biomedical research, the fact remains that a perfect cure still eludes us and we can't offer our patients a promising hope. The only assurance presented is that *early diagnosis can be the key to a better survival rate*. International cancer burden is expected to increase due to the growth and ageing of the population, besides the adoption of unhealthy lifestyles in general. Economically less developed nations, with historically low rates, are now experiencing an increased frequency of cancers of breast, cervix, lung, and colorectum. Cancer burden can be substantially reduced through preventive measures, employing widespread application of existing cancer control knowledge, including tobacco control, vaccination (for liver and cervical cancers), early detection, and the promotion of physical activity and healthy dietary patterns. Additional suffering and premature death could be alleviated through appropriate treatment modules and palliative care. However, in spite of advancements in the treatment modalities, including chemotherapy, radiotherapy and chemo-radiotherapy, survival rates are disappointingly low, especially in case of oral cancers. Often, this is attributed to delayed diagnosis as well as lack of mechanisms to predict recurrences.

1.5 Diagnostics in oral cancers

Clinical oral examination followed by histopathology is still the gold standard for confirmatory diagnosis since decades. In case of oral cancers, several methodologies such as staining techniques and exfoliated cells are often employed additionally, for diagnosis [97, 98]. They are discussed as follows:

1.5.1 Conventional diagnosis

Conventionally, diagnosis includes a clinical oral examination followed by biopsy of the suspected regions in the oral cavity. The biopsied sections are subjected to histopathology to confirm the stage/grade of cancer.

1.5.1.1 Standard screening test

This involves visual inspection/ clinical oral examination (COE) of the oral cavity. The criteria for identifying an oral premalignant disorder (OPMD) or oral SCC include changes in surface texture, color, size, loss of surface integrity, contour deviation or mobility of intraoral or extra oral structures [99]. A meta-analysis employing criteria such as sensitivity, specificity, positive predictive value, negative predictive value and diagnostic odds ratio of available literature reported 93% of sensitivity for the COE, but specificity was only 31% [100]. COE has fared poorly overall as a diagnostic method for predicting dysplasia and oral SCC (OSCC) and has been shown to be effective as a preventive measure in early detection only in high risk groups, reported by Sankaranarayanan *et al* [3]. Comparatively better prognosis is reported with early diagnosis though definite evidences are still needed to conclude that organized and systematic, population-based oral screening using COE can reduce mortality [3]. Often, COE also cannot reliably differentiate between benign and dysplastic lesions [101].

1.5.1.2 Histopathology

Histopathology involves microscopic examination of tissue sections from biopsied samples of the order of microns, by pathologists, after staining of the sections with dyes such as hematoxylin and eosin.

1.5.1.3 Limitations

Existing methodologies present several limitations in terms of scope and applications.

a) COE demands experienced medical practitioners. Clinical risk stratification often lacks accuracy and reproducibility. Studies have shown that conventional visual screening was effective mainly in the high-risk groups i.e. tobacco/alcohol habitués [102]. Thus, better tools are needed for screening the general population.

b) Histopathology is prone to subjectivity, is time consuming and most importantly, is invasive, which makes it inconvenient as a screening methodology of choice. Additionally, it has practical limitations in the hugely populated nations such as India where oral cancers are almost epidemic.

c) It is often difficult to recognize subtle clinical changes which are indicative of early neoplastic transformation in pre-cancers. This can also lead to the dilemma of '*when and where to biopsy*'. Thus, histological risk stratification requires highly trained pathologists and clinicians.

1.5.2 Common diagnostic adjuncts

1.5.2.1 Oral cytology

Oral brush biopsy involves collection of trans-epithelial cell samples from oral cavity. Cells from superficial, intermediate and parabasal/basal layers of the epithelium are usually studied [103]. Cells are fixed onto a glass slide, stained with a modified Papanicolaou test and observed under a microscope. 'Positive/atypical' cellular morphology needs to be confirmed by tissue biopsy. Several studies have evaluated sensitivity and specificity of brush biopsy in detecting dysplasia

or OSCC. However, bias in such studies has been reported by different groups [104-107]. OralCDx® based approach has been observed to have high sensitivity and specificity in detecting dysplastic changes in high-risk mucosal lesions. However, reduced accuracy and increased rate of false-positive findings are observed in low-risk populations with benign-appearing oral epithelial lesions [97].

1.5.2.2 Vital staining or dye based screening

These techniques employ a range of pigments to focus on cells with high reproductive rate, such as neoplastic cells, to identify suitable areas to perform biopsies. Toluidine blue and methylene blue are commonly used dyes for oral screening, Some other dyes reported in literature include Lugol's iodine [108] and Rose Bengal [109].

Toluidine blue is the most commonly used vital dye which can selectively bind to free anionic groups such as phosphate, sulphate, and carboxylate radicals of large molecules. It can bind to the phosphate groups of the nucleic acids and be retained in the intercellular spaces of dysplastic epithelium [101]. It has been exploited in clinical identification and demarcation of oral premalignant disorders (OPMD) prior to excision [110-112]. Methylene blue dyes cells with acidophilic characteristic and may penetrate into cells with abnormal increase in nucleic acid, resulting into a differential uptake between normal and dysplastic/malignant cells. A study by Chen *et al* (2007) revealed sensitivity, specificity, positive predictive value (PPV) and negative predictive value (NPV) of 90%, 69%, 74% and 87%, respectively [113]. Some studies have explored efficiency of the combined use of more than one dye to overcome limitations of individual dyes. The simultaneous use of Lugol's iodine and toluidine blue resulted in higher specificity as reported by Epstein *et al* [108]. Peng *et al* [114] evaluated double staining with

Lugol's Iodine and methylene blue and they obtained sensitivity, specificity, PPV and NPV of 97.7%, 100%, 97.8% and 100%, respectively.

Several studies on toluidine blue present significant limitations and methodological bias [115, 116]. Reviewed in detail by Lingen *et al*, these limitations include (i) absence of randomized controlled trials, (ii) absence of histological diagnosis as a gold standard, (iii) and variability in methods of application [115]. Toluidine blue, though good at detecting carcinomas, suffers from poor sensitivity in detecting dysplasia [115]. Moreover, a high percentage of false positives impair its application in primary care settings as a reliable screening tool [115, 116]. Additionally, interpretation of mucosal staining is subjective while criteria for positive results (e.g. dark royal blue versus pale blue staining) lacks unanimity [115]. Studies using other dyes need further evaluation with larger sample size.

1.5.2.3 Chemiluminescence based techniques

Clinical inspection of oral mucosa in presence of chemiluminescent blue/white light is shown to improve identification of mucosal abnormalities with respect to the regular incandescent light [115-120]. Commercially available technologies based on chemiluminescence include ViziLite™ Plus and Microlux™ DL.

ViziLite Plus: The technology (Zila Pharmaceuticals, USA) involves the use of an oral rinse with 1% acetic acid solution for a minute prior to the examination of the oral mucosa under diffuse chemiluminescent blue/white light (wavelength: 490 to 510 nm). Acetic acid overcomes the glycoprotein barrier and mildly desiccates the oral mucosa. The absorption/reflection of blue/white light by abnormal mucosal cells is different compared to normal cells [115-120]. Thus, normal mucosa appears blue, while abnormal mucosal areas reflect the light (attributed to

higher nuclear/cytoplasmic ratio) and appear more aceto-white with fairly distinct margins [117-121].

MicroLux DL**:** MicroLux DL (AdDent Inc., USA) is a modification upon the ViziLite system and includes the application of Toluidine blue. The Microlux DL and Orascoptic DK use a reusable, battery-powered light-emitting diode (LED) light source that provides a similar blue-white (440 nm range) illumination [121].

In many such studies, subjects with only visible lesions were included. The utility of enhanced visual findings in low-risk populations is not known. Well-controlled clinical trials are needed that specifically investigate the ability of those devices to detect OPMD that are invisible by COE alone.

1.5.2.4 Biomarker present in body fluids

Blood/Serum: Blood and serum have been used to study the immunological/biochemical perturbations for early diagnosis of oral cancers [122]. Lower serum iron and selenium levels while higher copper levels were observed in patients with OSCC or precancerous lesions [122]. However, serum tumour markers for OSCC have not shown promising sensitivity in early diagnosis. The serum concentrations of carcinoembryonic antigen (CEA), SCC associated antigen (SCCAA), inhibitor of apoptosis (IAP), and cytokeratin fragments (CYFRA) have been shown to have a sensitivity of 81% for the detection of OSCC [123]. Annexin A1 (ANXA1) is identified in peripheral blood and can serve as a potential diagnostic biomarker for OSCC [124].

Saliva: Saliva analysis could be a proficient, non-invasive tool for the diagnosis of OSCC [125]. The diagnostic potential may arise from the intimacy with the site of cancer. Salivary levels of

total sugar, protein-bound and free sialic acid, sodium, calcium, immunoglobulin G, albumin, and lactate dehydrogenase have been observed to be higher in cancer subjects than the healthy individuals [126, 127]. Significant surge in the concentrations of specific cancer related cytokines, insulin-like growth factor (IGF), and matrix metalloproteinases (MMP-2 and MMP-9) in saliva are reported [125]. Significant alterations of epithelial tumour markers CYFRA 21-1, tissue polypeptide specific (TPS) antigen, several oxidative stress-related parameters, and RNA transcripts of interleukin (IL) 8, IL-1B, dual specificity phosphatase (DUSP1) (regulator of cell proliferation), HA3 (oncogene), OAZ1 (regulator of polyamine synthesis), S100P (calcium binding protein), and the spermidine N1-acetyltransferase (SAT, involved in polyamine metabolism) are also reported. Hypermethylation of some promoters as well as salivary micro-RNA (miRNA) has been found to be an efficient tool for the detection of oral cancer [128].

Biomarkers with good sensitivity and specificity for oral cancers are still debatable. Moreover, results may be affected by the storage and transportation conditions. Other methodologies mentioned in the previous section still need the scrutiny over large clinical samples. Present studies have revealed reduced accuracy and increased false-positive findings in low-risk populations with apparent benign lesions [97].

It is a fortunate development that there has been an increase in the number of potential oral cancer screening methods/tools recently. Unfortunately, definitive evidence of significantly improved sensitivity or specificity of oral cancer screening beyond COE alone has not been observed. Moreover, many of the studies had flawed designs while certain others were employed in a “case-finding” fashion, rather than as true screening tools [97]. Currently, large scale mass screening based studies to support the contention that these technologies can help the clinician to

identify premalignant lesions before they are detectable by COE alone are lacking. Reliable biomarkers with good sensitivity/specificity in for oral cancers are still under exploration. Moreover, the storage and transportation conditions can influence results. Other methodologies based on vital dyes and transcriptomics still need the scrutiny over large clinical samples as studies have revealed reduced accuracy and increased false-positive findings in low-risk populations [97]. Thus, search for an efficient diagnostic tool is still not over. In the recent decades, optical techniques have been widely explored as diagnostic tools and the findings have been discussed in the next section.

1.5.3 Optical techniques

Rapid, objective and non-invasive technologies which are sensitive to tissue biochemistry could be more effective for early diagnosis and screening, as biochemical changes often precede visible morphological alterations. These changes in biochemical properties are also reflected in the optical properties. The electromagnetic spectrum provides an array to explore potential tools to probe and exploit the optical changes in biological systems. Often, such optical techniques utilize ultraviolet (UV), visible, near infrared (NIR) and infrared (IR) regions to measure absorption, scattering and/or fluorescence in biological samples. Optical techniques, being widely explored, as will be discussed, have shown great promise in discrimination of diseased and healthy tissues and organs. Multimodal methodologies involving two or more techniques to gain additional and complementary information simultaneously are also being explored. The following Jablonski diagram, first proposed by Professor Alexander Jablonski (1935), summarizes some optical phenomena in response to interaction of light and matter, in terms of energy exchange.

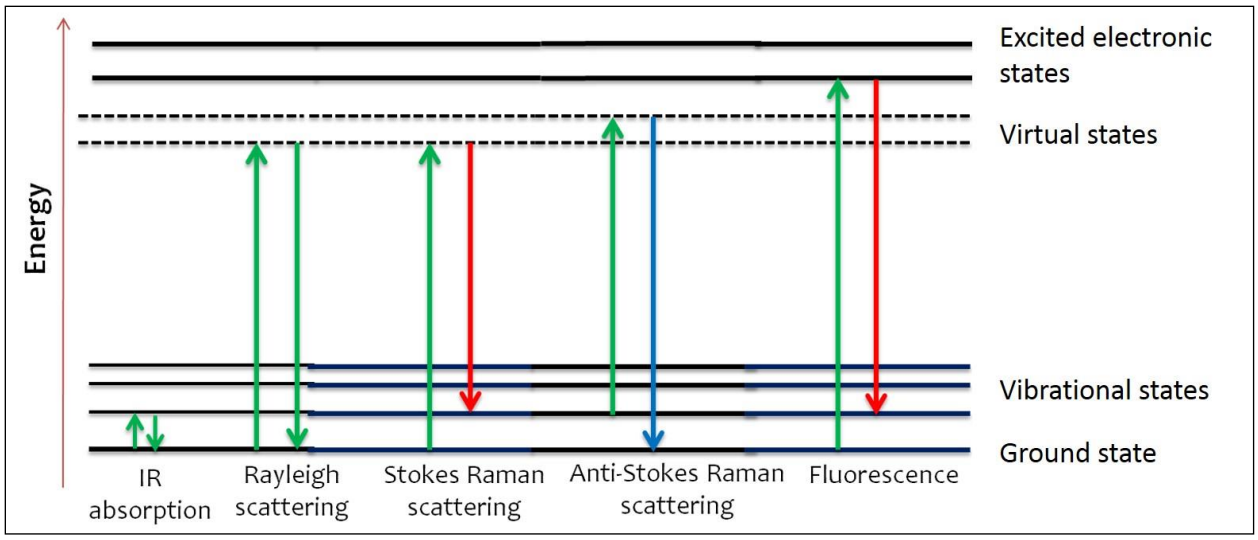

Figure 1.1: Jablonski diagram depicting phenomena of IR, Raleigh and Raman scattering, and fluorescence.

Though fluorescence spectroscopy gained an early momentum due to requirement of simple instrumentation, of late, Raman spectroscopy (RS) has been taking rapid strides in the field of optical biopsy, accentuated by rapid developments in the field of lasers and detection system. Moreover, RS can give a global biochemical profile and is also not affected by the presence of water. A summary of major developments in some optical techniques have been provided before describing RS and its applications in oral cancer diagnosis.

1.5.3.1 Fluorescence spectroscopy

Sir David Brewster reported several observations related to fluorescence, a term which was coined by Sir George Gabriel Stokes in 1840's [129]. Explained as Stoke's law, fluorescence is often characterized by the wavelength of the emitted light, longer than that used for excitation [130]. Fluorescence spectroscopy can exploit endogenous fluorophores present in the tissues (autofluorescence) or exogenous fluorophores (light-sensitive chemicals/photosensitizers) which can be introduced in the biological system to induce fluorescence (induced fluorescence). Typically, this technique involves irradiation of organs/tissues at some specific wavelength (mostly near-ultraviolet or visible) to excite fluorophores. The selection of wavelength depends on the fluorophore being targeted. The fluorescent emission is represented as an emission spectrum (fluorescence emission intensity vs. wavelength).

Induced fluorescence: Photosensitizers or precursors to photosensitizers are introduced in subjects, which leads to a differential accumulation of fluorophores in healthy and tumour tissues. Some examples of photosensitizers include hematoporphyrin derivative (HpD), meso-tetra-(hydroxyphenyl)-chlorin (MTHPC), benzoporphyrin derivative (BPD), and pthalocyanine [131]. One of the most commonly used fluorophore in oral cancers is 5-aminolaevulinic acid

(ALA) which is a precursor of protoporphyrin IX (PpIX), a fluorescent photosensitizer. ALA can be applied topically to the oral mucosa/facial skin [132]. Subsequent irradiation of the ALA applied area with visible light, to excite the main absorption peak of PpIX (405 nm), leads to red fluorescence emission at 635 nm [132]. Non photosensitizers such as Nile blue derivatives and caretenoporphyrins have also been explored as exogenous fluorophores [133].

Autofluorescence: Few biomolecules, such as amino acids (tyrosine and tryptophan), proteins (collagen), coenzymes (flavin adenine dinucleotide (FAD)), nicotinamide adenine dinucleotide (NAD)), vitamins and porphyrins, can fluoresce and thus contribute to autofluorescence when excited with suitable wavelengths. For the endogenous fluorophores, excitation maxima often lie in the 250–450 nm range (spanning the UV/visible spectral range), whereas their emission maxima fall in the 280–700 nm range (spanning the UV/visible/NIR spectral range) [134]. Various pathological changes can alter endogenous fluorophore distribution. The changes may be in the structure (e.g., hyperkeratosis, hyperchromatin and increased cellular/nuclear pleomorphism) and metabolism (e.g. FAD [135] and NAD concentration) in the epithelium; and sub-epithelial stroma (e.g. composition of collagen matrix and elastin) [115, 136].

Many studies have explored utility of fluorescence spectroscopy in oral cancers [115, 116, 136-145]. Initial studies using 300 nm excitation on hamster buccal pouch (HBP) tissues showed discrimination of healthy, premalignant and tumour tissues [138, 139]. In vivo autofluorescence spectra from oral mucosa have explored various wavelengths for excitation, such as using 337, 365, and 410 and 635 nm using healthy volunteers as well as patients. Gillenwater *et al* studied 8 healthy volunteers and 15 patients and reported that the ratio of red region (635 nm) to blue region (455 to 490 nm) intensities was greater in abnormal areas on basis of NADH and

porphyrin, with best discrimination provided by 410 nm [141]. Ebenezar *et al* used 635 nm to characterize variation in porphyrin excitation between normal volunteers and oral cancer patients [143]. Heintzelman *et al* reported in their study that optimal excitation wavelengths for detection of oral neoplasia were 350, 380 and 400 nm [140]. Autofluorescence spectroscopy can also differentiate potentially malignant conditions such as oral submucous fibrosis (OSMF), leukoplakia [145], erythroplakia and lichen planus from normal oral sites. Haris *et al* differentiated oral mucosa of healthy volunteers and patients with OSMF using 320 nm [146]. Venugopal *et al* using 410 nm excitation wavelength, reported a sensitivity of 96 and 100% and overall specificity of 100% in differentiating between normal area and leukoplakia [145]. Autofluorescence spectroscopy could discriminate between oral cavity cancers with varying pathological grading using porphyrin emission peaks [147]. Early perturbations in oral cavity owing to tobacco/areca nut habit have been reported by Shaizu *et al*. Their findings suggest a variation in collagen and flavin levels (areca nut-habitues) and hemoglobin and porphyrin levels (tobacco-habitues) with respect to non-habitues [148, 149]. LED Medical Diagnostics Inc. in partnership with the British Columbia Cancer Agency, has been using tissues fluorescence applications in cancer diagnostics, marketed as VELscope system [115, 116, 136].

1.5.3.2 Elastic scattering spectroscopy (ESS)

The process of scattering may be classified as elastic and inelastic scattering. When photons interact with matter, the energy of the scattered photons may remain the same or undergo a change. The former process is called elastic while the latter is referred to as inelastic scattering. Elastic scattering is also called Rayleigh scattering. Inelastic scattering is being described under the heading Raman scattering.

ESS is wavelength dependent and provides information about the structural and morphological changes in tissues, being sensitive to size and shape of dense sub-cellular organelles like nucleus, nucleolus; chromatin content and nuclear: cytoplasmic ratio. ESS is an attractive technique as it provides information about the sub-cellular morphology of the tissue as well as the chromophore content [150]. ESS is distinguished from a similar technique, diffuse-reflectance spectroscopy (described in the next section) in that the source-detector separation is very small in comparison to the scattering mean free path in case of ESS [150]. The tissue is subjected to short pulses of white light, while the elastically scattered light is collected to gain information.

In one of the first studies, a trimodal spectroscopic approach which included intrinsic fluorescence, diffuse reflectance and elastic scattering was used to study 91 tissue sites from 15 patients and 8 healthy volunteers in vivo [144]. Cancerous sites could be distinguished from normal sites. Jerjes *et al* explored feasibility of identifying metastasis in 130 cervical lymph node sites from 13 patients who underwent neck dissection [151]. The nodes (formalin fixed, bivalve) were subjected to ESS and processed for histopathology yielding a sensitivity of 98% and a specificity of 68%. In another study by Jerjes *et al*, bony resection margins from formalin fixed samples were assessed by ESS and correlated with the histopathological diagnosis [152]. 231 spectra (21 patients) were acquired from histologically positive sites while 110 spectra were acquired from normal tissues. A sensitivity of 87% and a specificity of 80% was obtained using linear discriminant analysis (LDA). In another study, investigation of premalignant and malignant oral lesions was carried out along with a corresponding histopathological analysis on 25 oral sites from 25 patients with oral leukoplakia. LDA yielded a sensitivity of 72% and a specificity of 75% [153]. These results suggest potential of ESS to identify oral dysplasia.

1.5.3.3 Diffuse reflectance spectroscopy (DRS)

DRS measures tissue scattering/absorption properties, to provide information like nuclear size, distribution, collagen content, and the oxy/deoxy status of haemoglobin, utilizing UV-visible-NIR excitation (300 to 800 nm). DR is generated from single and multiple backscattering of the excitation light and is sensitive to the absorption and scattering properties of epithelial tissues. The relationship between reflectance, absorbance, and light scattering is given by the Kubelka–Munk equation [154]. A simplified form of the equation is as follows:

$$f_{(R)} = \frac{(1-R)^2}{2R} = \frac{K}{S}$$

(R = absolute reflectance; K = molar absorbance coefficient; S = scattering coefficient of the specimen)

In biological samples, heamoglobin (both oxygenated, HbO_2, and deoxygenated, Hb), in blood vessels/stroma are dominant absorbers while light scattering is caused mainly by cell nuclei and other organelles in epithelium and stroma, collagen and cross-links in stroma. During neoplastic transformation, stromal layer absorption increases due to angiogenesis while scattering in stroma decreases due to degradation of extracellular matrix. On the contrary, epithelial scattering increases due to hyperplasia, increase in nuclear size and DNA content. DRS is a cost-effective, rapid and sensitive technique with portable modifications available.

DRS has been explored to identify malignant changes in oral and cervical epithelium. De Veld *et al* have employed bimodal autofluorescence and DR spectra and shown classification of normal, benign, premalignant and malignant lesions [155]. Spectral ratio R540/R575 of oxygenated hemoglobin bands can distinguish normal oral mucosal areas from hyperplastic and dysplastic

sites on basis of angiogenesis [156, 157]. Reflectance spectral intensity from malignant lesions is observed to be greater than that from normal mucosa [158]. Tungsten-halogen lamp is often employed as an excitation source on biopsy specimens (tongue, buccal mucosa, and alveolus) to measure diffusely reflected light. Advancements such as multi-spectral imaging camera system that records diffuse reflectance (DR) images of the oral lesion at 545 and 575 nm with white light illumination can scan entire oral lesions [159]. DRS study on HBP model showed encouraging results, employing 500–800 nm spectral range [160, 161]. Changes in the DR ratio have been observed according to the stage of oral malignancy. The potential of DRS has also been explored for tongue cancer detection. Under in vivo conditions (carried out by Jayanthi *et al*) spectra from the buccal mucosa of healthy controls, precancerous, and cancerous subjects using a fiber-optic probe coupled system in the 400 to 700 nm regions, compared against the gold standard, histopathology, DR spectra of healthy and pathological conditions show a significant dip around 545 and 575 nm, assigned to oxygenated hemoglobin [157]. The ratio (R545/R575) increases significantly with the severity in pathology, i.e., from healthy to cancerous lesions through hyperplasic and dysplastic stages. Sensitivities and specificities ranging from 95% to 100% have been observed for different groups. Additionally, methemoglobin and melanin absorption by tissues can also be exploited alongside and enhancements can be achieved using Monte Carlo method and inverse algorithms to simulate the tissue diffuse reflectance of normal and oral cancer tissues [162] .

1.5.3.4 Optical coherence tomography

OCT uses low-coherence interferometry to produce two-dimensional images of optical backscattering from internal tissue microstructures analogous to ultrasonic pulse-echo imaging

[22]. One can term OCT as an optical analog of ultrasound imaging wherein backscattered intensity of light is measured instead of sound. OCT enables *in vivo*, non-invasive imaging of the macroscopic characteristics of epithelial and subepithelial structures. OCT images can also be used to obtain functional information to detect the presence of embedded blood vessels. Such measures can preclude bleeding or stroke-related complications during surgery [163] .

OCT imaging in biomedical field was originally introduced in 1991 for noninvasive imaging of retina [22]. In the last two decades, OCT underwent rapid and dramatic developments with major applications in ophthalmology [164, 165], oncology [166-168], cardiology [169], and developmental biology [170]. OCT has been used ex vivo for 2D imaging as well as 3D *en face* imaging [171, 172]. OCT has been explored in several cancer conditions including skin, larynx, esophagus, cervix, brain and oral cancers [171-184]. Preliminary studies by Wilder Smith *et al* have demonstrated the capability of OCT to detect and diagnose oral premalignant lesions in vivo on 50 patients [185]. Prestin *et al* measured epithelial thickness within the oral cavity using OCT [184] while Tsai *et al* reported discrimination of oral lesions in different carcinogenesis stages. HBP model of oral carcinogenesis has also been employed in OCT studies [185-190]. Mathney *et al* showed for the first time feasibility of OCT in detecting malignancy in HBP model [185]. As a part of this thesis, OCT was carried out on carcinogen (DMBA) treated and normal HBP tissues using protocol mentioned elsewhere [191]. Tissues corresponding to intermediate stages of DMBA-induced carcinogenesis were employed.

1.5.3.5 Fourier transform infrared (FTIR) spectroscopy

An infrared spectrum represents a fingerprint of a sample with absorption peaks corresponding to the frequencies of vibrations between the bonds of the atoms that make up the material being

probed and can provide rapid information. The energy of the absorbed infrared radiation by a molecule is equal to the difference between two energy levels of the molecule's vibration. Thus, the absorption occurs on the basis of transition between the energy levels of molecular vibration, leading to a vibrational spectrum of a molecule. A schematic is shown in Figure 1.1. The advent of Fourier transformed spectrometers, around 1970, revolutionized the field of FTIR spectroscopy, permitting simultaneous measurement of spectra in the entire wavenumber region with higher accuracy and resolution.

Vibrational spectroscopic techniques such as FTIR and Raman spectroscopy (RS) are relatively simple, nondestructive to the tissue and require a very small amount of sample with minimum sample preparation. In addition, these techniques also provide molecular-level information allowing investigation of functional groups, bonding types, and molecular conformations. Spectral bands in vibrational spectra are molecule specific and provide direct information about the biochemical composition, leading to a 'molecular fingerprint'. As biochemical composition is affected during pathogenesis, spectral features are altered, which can be exploited for disease detection. The bands are relatively narrow, easy to resolve, and sensitive to molecular structure, conformation, and environment. Both RS and FTIR exploit changes in vibrational modes of biological tissues/organs with respect to the changing tissue biochemistry in response to pathological changes. Raman and FTIR are complementary techniques. However, while FTIR is based on the principle of absorption, RS is based on inelastic scattering. RS is described in Section 1.6.

Spectral differences between normal and malignant tissues suggest applicability of FTIR to a range of biological and medical problems [192]. Collagen presence in tissues is especially useful

in disease diagnosis by infrared spectroscopic method, with particular reference to cancer [193]. FTIR spectral differences have been studied by Fukuyama *et al* using samples such as OSCC (n =15) and normal gingival epithelium (NGE) or normal subgingival tissue (NST) (n =10) [194]. Paraffin-embedded tissue sections were employed by Banerjee *et al* from 47 human subjects (8 normal, 16 OLK, and 23 OSCC) [195]. Linear and quadratic support vector machine (SVM) at 10-fold cross-validation was used for classification, using different combinations of spectral features. They could classify OLK and OSCC with 81.3 % sensitivity, 95.7 % specificity, and 89.7 % overall accuracy.

1.6 Raman spectroscopy (RS)

1.6.1 Basic Principle

RS, based on the principle of inelastic or Raman scattering, was experimentally verified by Nobel Laureate Sir C. V. Raman [4]. Depending on changes in energy or frequency, the scattered photons may be classified as inelastic (change in energy) and elastic (no change in energy). Inelastic scattering constitutes Raman scattering, further classified as anti-Stokes (the scattered photon gains energy) or Stokes (the scattered photon loses energy). The different types of scattering are illustrated in Figure 1.1. The energy difference between the incident and scattered photon (Raman shift) is usually represented as wavenumber (cm^{-1}) and is plotted against the intensity of scattered light to obtain a Raman spectrum. The principles of RS are well explained in several books [196-201]. As mentioned in Section 1.5, RS is a vibrational spectroscopic technique which can detect biochemical perturbations in an organ or tissue. Further, due to negligible interference of water, a major constituent of living cells and organs, Raman can serve as a promising tool for in vivo biomedical investigations. Since RS is a weak phenomenon, its applications were initially very much limited in biological systems. Development of powerful lasers, Raleigh rejection filters and better detection systems, such as CCDs, gave an impetus to biological applications of RS Many portable/transportable instruments are now available at reduced costs. Further, various adaptations of the conventional RS have also been reported over the last decade. A schematic of a typical Raman spectrometer is shown in Figure 1.2. The components of a typical Raman spectrometer have been explained in chapter 2 (Materials and Methods).

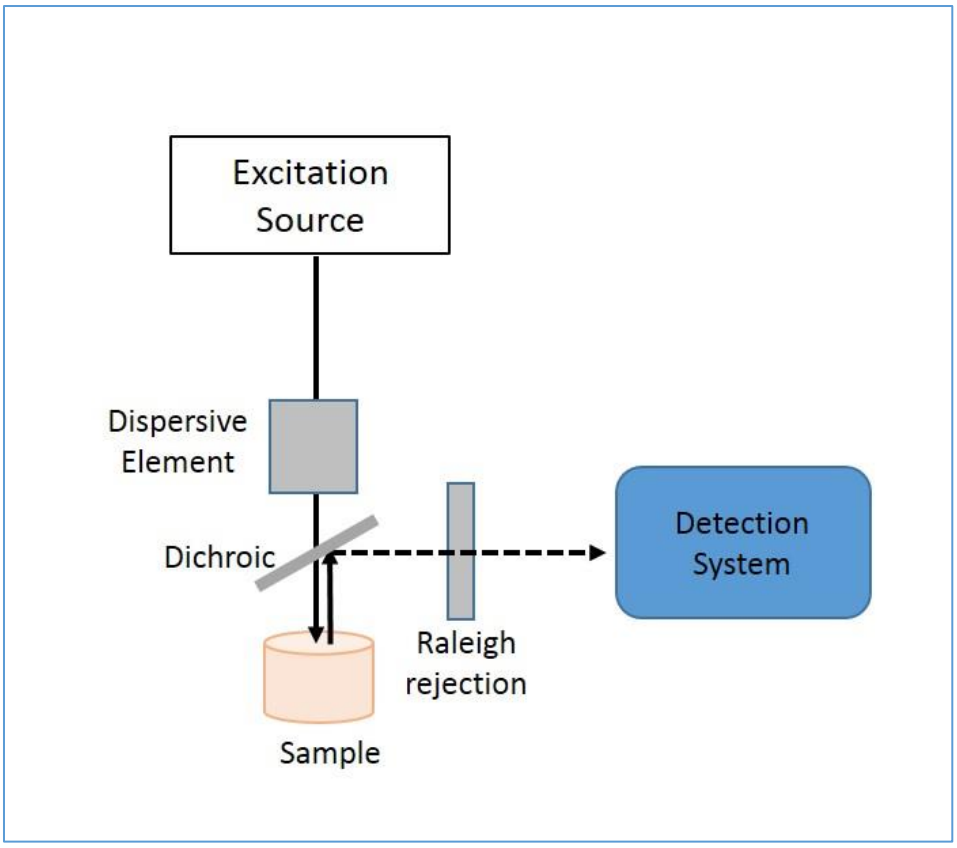

Figure 1.2: Schematic of a typical Raman spectrometer

1.6.2 Advantages of RS

RS, with features like non-destructiveness, minimal sample preparation needs, rapidity, objectivity and negligible interference with water, is better suited for biological applications compared to other optical techniques. The Raman spectra provide global information and thus a single wavelength of light can be used to obtain a unique molecular fingerprint, allowing chemical identity of a sample. The contribution of molecules in the Raman spectrum is proportional to their relative abundance in the sample, which is the basis for determining the quantity of a sample. Such features facilitate spectral interpretation, creation of spectral libraries, sample molecular quantitation and application of chemometric tools [202-204].

1.6.3 Adaptations for enhancement of Raman signal

RS being an inherently weak process (1 in 10 million photons are Raman scattered), several modifications to the conventional Raman methodology have enhanced the overall efficiency and the range of applications. Spectrometer can be coupled to a microscope to design a Raman microscope for analysis of samples using smaller spot-size and desired magnification; facilitating bio-fluids and cells/organelles-based experiments. Various improvisations have led to development of techniques such as surface-enhanced Raman spectroscopy (SERS) [205, 206], coherent anti-Stokes Raman spectroscopy (CARS) [207, 208], stimulated Raman spectroscopy (SRS) [209-211], drop coating deposition Raman (DCDR) spectroscopy [212-214], spatially offset Raman spectroscopy (SORS) [215], and surface-enhanced spatially offset Raman spectroscopy (SESORS) [216, 217].

1.6.4 Raman applications

The unique attributes of RS have enabled extensive application in fields such as chemistry, forensics, geology, biology, pharmacology, pharmaceuticals, archaeology and material sciences. Some specific applications include process monitoring, detection of pollutants (environmental science), gunpowder residues, blood and semen (forensics), identification of possibly hazardous chemicals (security); identification of paintings and materials found during excavations (art and archaeology), microbial identification, food adulterations and authentications [218-224]. As pathology is associated with biochemical changes, RS has been explored as a biomedical diagnostic tool in several conditions such as bladder dysfunction, atherosclerotic plaques, Parkinson's and Alzheimer's disease, rheumatoid arthritis and osteogenesis imperfecta along with several clinico-oncological applications [225-235]. RS is now finding applications in almost all disciplines of life sciences, including microbiology, immunology, biophysics, regenerative medicine and oncology [236-243].

1.6.5 RS based explorations in cancers

1.6.5.1 Invasive/Ex vivo approach

This approach involves RS of tissue biopsies. One of the first study on human oral cancers biopsies was reported by Venkatakrishna *et al* (2001). One hundred forty spectra from 49 biopsies were acquired using 785 nm excitation and SpeX Triax 320 spectrometer. Using PCA based multivariate analysis, sensitivity and specificity of 85% and 90% was observed [6]. A successive study by the same group (2004) demonstrated the suitability of formalin-fixed tissues for Raman spectroscopy [230]. Malini *et al* (2006), using 785 nm excitation and 30 s integration time, reported classification of normal, cancerous, precancerous and inflammatory conditions.

Lipid rich features in normal conditions and predominant protein features were observed in the pathological conditions, including tumours. Classification between different groups was explored using PCA coupled with multi-parametric 'limit test' to achieve high sensitivity and specificity [244]. In the same year, Oliveira *et al* explored the feasibility of differentiating normal, dysplastic and SCC tissues in the HBP model of oral carcinogenesis. The FT-RS study, using 1064-nm Nd:YAG laser line, reported distinct properties of DMBA induced cancer tissues from the healthy buccal pouch of hamsters. Major differences between normal and malignant spectra were attributed to composition, conformational, and structural changes of proteins, and possible increase in their content in the malignant epithelia yielding 91% and 69% sensitivity and specificity [245]. Hu *et al* acquired spectra of 66 human oral mucosa tissues (43 normal and 23 malignant) using confocal Raman micro-spectroscopy in 2008. After preprocessing spectra using wavelet-based analysis, PCA along with calculation of areas under bands 1004, 1156, 1360 1587 and 1660 cm^{-1} were used as a classification method [246]. Another study by Sunder *et al* in 2011 was carried out to evaluate the applicability of near infrared (NIR) Raman spectroscopy in differentiating normal epithelium and different grades of oral cancer. Findings demonstrated that oral carcinomas of different pathological grades can also be identified with Raman spectroscopy. On the basis of protein and lipid conformations, authors have noted changes in the relative intensities of bands at 1656, 1440 and 1450 cm^{-1} [231]. Singh *et al* conducted a study to correlate spectral and biochemical markers [247].

1.6.5.2 Minimally invasive approaches

Minimally invasive approaches involve samples such as blood, other body fluids and exfoliated cells which can be obtained with minimal discomfort to patients or healthy volunteers.

Serum: Serum, obtained from blood, is often employed in a range of biochemical tests for disease diagnosis. Serum Raman spectroscopy has been investigated for detection of pre-eclampsia [232], sepsis and systemic immune response syndrome (SIRS) [225], Hepatitis C [226], Alzheimer's [227, 248] and Parkinson's disease [228], dengue fever [229, 233], sickle cell anemia [234, 235, 249] and asthma [250]. Diagnosis of several cancers has been investigated using serum Raman spectroscopy. One of the first studies on cancer diagnosis was carried out by Li *et al* [251]. Breast cancers were explored by Pichardo *et al* [252] who analyzed ratio of band intensities corresponding to proteins, phospholipids, and polysaccharides. Recently, Bhattacharjee *et al* [253] in an animal model of breast cancer has shown that serum from tumour-bearing Sprague-Dawley rats is different before and after surgical excision, and both groups are also different from healthy controls. Colorectal cancer was explored by Lin *et al* [254, 255]. Serum RS has also been reported in case of pancreatic cancers [256], cervical cancers [257] and ovarian cancers [258]. Prospects of biofluids vibrational spectroscopy has been recently reviewed by Baker *et al* [259]

Serum RS in oral cancer diagnosis: In a study by Harris *et al* [260], potential of a peripheral blood sample to achieve diagnosis of head and neck cancers was evaluated using 20 head and neck cancer patients and 20 patients with respiratory diseases. Conventional LDA approaches showed an accuracy of around 65% while genetic evolutionary algorithm obtained an accuracy of 83%. Feng *et al* [261] carried out a study for SERS-based specific identification of nasopharyngeal cancers. ATR (attenuated total reflectance)-FTIR and RS were simultaneously explored. Diagnosis of oral cancers using both resonance and conventional Raman spectroscopy was explored by Sahu *et al* with an efficiency of 78% and 70%, respectively, between normal and oral cancer groups [262, 263]. These studies were followed up with a large cohort of 328

subjects belonging to healthy controls, premalignant, disease controls, and oral cancer groups. A sensitivity and specificity rates of 64 and 80%, respectively was obtained which is comparable to standard screening approaches [264]. Recurrence in oral cancers was identified by serum RS of post-surgery samples with ~80% efficiency [265]. Serum was collected from 22 oral cancer subjects [with recurrence (n = 10) and no-recurrence (n = 12)] before and after surgery. PC-LDA suggest that recurrent and non-recurrent cases cannot be classified in before surgery serum samples while an average classification efficiency of ~78% was obtained in after-surgery samples [265].

Other body fluids: Blood, saliva and urine have also been explored for oral cancer diagnosis. SERS studies on 10 saliva samples were carried out by Kho *et al* in 2005 on gold particle films and spectra were acquired with He-Ne laser excitation. Additional peaks at 1097 and 1627 cm^{-1}, as compared to conventional Raman, were observed in cancer saliva samples [266]. Blood plasma was explored for oral cancer diagnosis by Rekha *et al* in 2013 using 28 plasma samples. Spectra were acquired from Labram HR 800 in the spectral range 800-1800 cm^{-1}. Marked spectral differences were observed between plasma from cancer patients and healthy people, corresponding to protein, amino acid, glucose and lipids [267]. A recent study for oral cancer diagnosis using urine was carried out by Elumalai *et al* where characterization of the metabolites of human urine of normal subjects and oral cancer patients in the finger print region (500–1800 cm^{-1}) was explored. PC-LDA findings yield sensitivity and specificity of 98.6% and 87.1%, respectively to discriminate healthy and cancer patients [268].

Oral exfoliated cells: The feasibility of Raman oral exfoliative cytology along with cytopathology for oral cancer diagnosis was evaluated by Sahu *et al* in 70 specimens. Exfoliated

cells were obtained from 15 healthy volunteers (HV), 15 healthy tobacco users (HT), and 20 contralateral or disease control (DC) and 20 tumour (T) sites of same oral-cancer patients. Pap staining was carried out post Raman spectral acquisition. Spectral findings demonstrate that with increase in severity of pathology from HV to T, higher DNA and changes in secondary structure of proteins were encountered. PC-LDA findings indicate that HV and HT are distinct from cancer groups DC and T. Misclassifications were also observed between HT and DC. The findings were relatable with cytopathological observations [269].

1.6.5.3 Non-invasive/In vivo Raman spectroscopy

Even though Raman based optical diagnosis of tissues has shown efficiency in detection of potentially pre-cancerous tissues and real-time tissue evaluation, biopsy is an inherently invasive procedure. In most cases, this procedure has some associated morbidity and in some cases poses a high risk when involvement of vital anatomy is encountered. The actual promise of optical techniques such as RS lies in non-invasive or in vivo diagnosis, without disruption of native conformation of the organs.

Developments in in vivo RS: After successful classification of normal, benign and cancer breast tissues, in vivo Raman studies were undertaken for intraoperative tumour margin assessment in 9 patients undergoing partial mastectomy procedure in 2006 [270]. Even though data set were small, 100% sensitivity and specificity was observed. Interestingly, Raman spectra from one margin correlated to a cancerous lesion which was grossly invisible, and upon postoperative pathological findings the margin was deemed positive, leading to further surgery for excision of the lesion. These findings provided evidence about sensitivity of Raman spectroscopy in identification of pathological conditions. Lieber *et al* (2008) developed a portable confocal

Raman device along with a hand-held probe and demonstrated feasibility of in vivo spectra acquisition on 19 patients. Successful discrimination between normal, inflamed, basal cell carcinoma (BCC) and SCC with efficiency of 95% was achieved [271]. In the same year, Bitar *et al* (2008) demonstrated feasibility of transcutaneous spectral acquisition from the DMBA induced tumours and their margins in Sprague-Dawley rats [272]. Application of RS in brain cancer diagnosis is widely reported. In vivo studies have been conducted in animal models by Kirsch *et al* [273] and Beljebbar *et al* [274]. Several studies coupled RS with endoscopy and white light imaging to assess internal organs such as stomach [275-281]. Several in vivo studies have been carried out in the last decade with a portable fiber-probe based Raman spectroscopic system for diagnosis of cervical abnormalities [282-287]. In one study, Duraipandian *et al* explored the combined Raman /Autofluorescence spectroscopy modality for improving early diagnosis of cervical precancers [288]. Buckley *et al* (2014) demonstrated that SORS can noninvasively detect a known compositional, genetic bone abnormality, osteogenesis imperfecta [289]. A study conducted by Rubina *et al* (2014) [290] also confirmed utility of in vivo RS in detection of cervical cancers. Recent studies by Bergholt *et al* reported in vivo RS of normal colorectal tissues and adenomatous polyps [291, 292]. Significant progress in detection of brain cancer in vivo using Raman spectroscopy has been made. Studies by Jerymn *et al* [293] first demonstrated intra-operative acquisition of Raman spectra from normal and cancerous areas of the brain, followed by resection of glioma affected region. Findings indicate successful distinguishing of necrosis from tumour and normal brain tissue with an accuracy of 87% [294].

In vivo Raman spectroscopy in oral cancers:

The first in vivo Raman spectroscopic applications in oral cancers were investigated by Schut *et al* in 2000 in a rat model. Raman spectra of normal and dysplastic tissues were obtained with 100 s integration time and sensitivity and specificity of 100% for detecting high-grade dysplasia/ CIS were observed[295]. Successful ex vivo studies on human biopsies paved the way for in vivo oral cancer studies, with the first report by Guze *et al* (2009) identifying site wise variations in the human oral cavity. In this study, reproducibility of Raman spectra from normal oral mucosa among anatomic oral sites (buccal mucosa, tongue, floor of mouth, lip and hard palate) in subjects across races and gender were explored, employing 51 subjects (25 Caucasian and 26 Asian). The authors reported that subject ethnicity and gender do not influence spectra. Further, different oral cavity sites can be discriminated based on degree of keratinization[7]. Bergholt *et al* (2011) characterized in vivo spectra of different anatomical regions (inner lip, attached gingiva, floor, dorsal tongue, ventral tongue, hard palate, soft palate, and buccal) in the oral cavity in the fingerprint region (800-1800 cm^{-1}). Findings suggested that anatomical characteristics of different sites have influence on spectra and these sites can be grouped together based on anatomical and spectral similarity to develop diagnostic algorithms [8]. Singh *et al* (2012) reported the first in vivo spectral acquisition from oral cancer subjects in clinically implementable time [296, 297]. Subsequently studies suggested that premalignant conditions can be objectively discriminated against normal and tumour conditions [9]. In an another study, the origin of Raman signals in tissues was also investigated by the same group [298]. Singh *et al* conducted further studies to detect malignancy-associated-changes (MAC) or cancer-field-effects (CFE) in oral cancer subjects [10]. Studies by Krishna *et al* investigated spectral differences among oral cavity subsites. Their findings suggested clustering of sub-sites into 4 major anatomical clusters- a) outer lip, and lip vermillion, b) buccal mucosa c) hard palate d) dorsal,

lateral and ventral tongue and soft palate. Further, the authors also suggested the use of anatomy-matched algorithms to increase discrimination between healthy and abnormal conditions [299, 300]. Anatomical differences between subsites and their possible influence on healthy vs pathological classification were evaluated on 85 oral cancer and 72 healthy subjects by Sahu *et al*. Spectra were acquired from buccal mucosa, lip and tongue in healthy, contralateral (internal healthy control), premalignant and cancer conditions using fiber-optic Raman spectrometer. Mean spectra indicate predominance of lipids in healthy buccal mucosa, contribution of both lipids and proteins in lip while major dominance of protein in tongue spectra. Findings indicated buccal mucosa and tongue are distinct entities, while lip misclassifies with both these subsites [301].

Animal models of oral cancers: scope of application

Most of the in vivo studies described above have explored differences between frank tumours and healthy tissues only. Some studies have also explored classification between clinically visible premalignant patches like leukoplakia and the buccal mucosa of apparently healthy contralateral mucosa and healthy volunteers. For translation of RS to clinics as a non-invasive tool, in vivo clinical studies involving sequential progression of carcinogenesis from a healthy till development of tumours, along with proper age matched controls are required. This cannot be undertaken on human beings due to ethical and practical considerations. Moreover, the patients coming to hospitals belong to a range of socio economic strata with different genetic susceptibilities; many patients are presented with late stages of cancers and thus maintaining uniform experimental conditions may not be easy.

To circumvent this problem, animal models can be used. Genetically similar strains of animal models can be maintained under controlled environmental (temperature, pressure and humidity) and dietary conditions. Rodents are one of the most commonly employed models in experimental carcinogenesis. They can be exposed to carcinogen and spectra can be acquired at regular intervals post carcinogen treatment till tumour appearance. Moreover, further corroboration with the existing diagnostic gold standard of histopathology can be carried out for not only the carcinogen treated animals but also for the healthy age matched control animals, which cannot be done in case of human subjects.

1.6.5.4 Raman spectroscopy of animal models

There are several major reviews focusing on utility of RS in biomedical applications [242, 302] and diagnostics [303-305] using both ex vivo and in vivo approaches on human subjects. However, as already mentioned, due to ethical and practical considerations, several experiments need to be performed on animal models. The earliest application of RS on animal model dates back to late 80s with diabetic cataract model [306-309]. Further, studies were carried out in rat models for mineralization in 1995 [310, 311]. Classification between tumour and normal conditions has been demonstrated in many cancers. One of the first cancers to be studied in an animal model was palate cancer by Schut *et al* (2000) [312]. This study was also the first in vivo Raman study in oral cancers. RS has been explored in several other animal models of cancers such as esophagus [313-315], breast [316-322], brain [273, 274, 323-325], skin [326], pancreas [327], cervix [328], liver [329] and colon [330].

Raman applications in animal models of oral cancer

Rodents have been commonly employed in oral cancer research [331]. Schut *et al* used the carcinogen 4-nitroquinoline 1-oxide to develop palate cancers in rats, through topical application. They obtained specificity as well as sensitivity of 1 for detecting high-grade dysplasia/ carcinoma in situ [312]. The next major study in experimental oral carcinogenesis was reported by Oliveira *et al* in 1996 in HBP model [332]. They used DMBA induced HBP model [12, 13] for their study. Employing 1064 nm as excitation, they used FT-Raman followed by Principal Component Analysis (PCA) to achieve 100% sensitivity and 55% specificity. Another ex vivo study on DMBA treated HBP tissues for 0, 2, 4 , 8 and 12 weeks demonstrated feasibility of identifying early changes [333]. The spectra reported for normal buccal pouch and tumours in these studies were found to have features similar to those reported later on in human studies [9, 334-337].

1.7 Aims and Objectives

The information presented in this chapter suggests that despite advancements in treatment modalities, oral cancers still suffer from a poor 5-year survival rate of ~50%. Studies have shown that early detection improves prognosis and 5-year survival rate [2, 3]. However, the currently practiced diagnostic gold-standard, biopsy followed by histopathology, is invasive (and painful), prone to subjective errors and not convenient for repeated samplings during screening and therapeutic monitoring. Hence, rapid, objective, non-invasive techniques which are sensitive to tissue biochemistry could be more effective in early diagnosis as biochemical changes precede visible morphological alterations. As the change in biochemical properties is also reflected in the optical properties, spectroscopic techniques such as RS [4] has been explored as a rapid, non-invasive and label-free diagnostic adjunct. RS has shown promising results in the diagnosis of several cancers [5] including oral cancers [6-11]. RS studies in oral cancers have shown classification of pathological conditions and detection of factors such as cancer field effects, demonstrating efficiency of the technique. These studies have relied on clinical examination and histopathology for pathological status. However, as mentioned earlier, biopsies are performed only when cancerous/premalignant conditions present clinical changes in oral mucosa. It would be imperative that biochemical changes preceding visible tumour conditions be explored and confirmed with gold standard. As such studies cannot be undertaken on human beings due to ethical and practical considerations, HBP model was employed to carry out RS based evaluation of oral carcinogenesis.

Aim: Comparative evaluation of diagnostic efficacy of Raman spectroscopy and histopathology using a sequential animal model study.

The work was majorly carried out as following objectives:

Objective 1: Sequential and comparative evaluation of Raman spectral changes in DMBA-induced HBP carcinogenesis at various time periods.

Objective 2: Comparison with histopathology and specific biomarkers to determine whether RS can be developed as a sensitive diagnostic tool.

To address the first objective, sequential progression of oral carcinogenesis was followed using both ex vivo and in vivo approaches while for second objective, RS models based on gold standards (histopathology and immunohistochemistry) was employed. Studies were also carried out to look into the contribution of physico-mechanical factors in carcinogenesis, using suitable controls. All these experiments included age matched controls.

Following additional experiments were also performed:

- Optical coherence tomography study of buccal pouches.
- Raman based investigation of discontinuation of DMBA application and its effect on cancer progression in hamster buccal pouch model.

The materials and methods employed to achieve the objectives have been described in Chapter 2 while the findings have been described in Chapter 3.

2 Chapter 2: Materials and Methods

Prelude

This chapter presents materials and methodologies used in the experiments for better understanding of the results. The chapter includes details related to animals, animal handling, carcinogenesis, instrumentation and multivariate analysis; and protocols related to carcinogen application, Raman spectroscopy, histopathology, immunohistochemical evaluations, spectral acquisition, preprocessing and analysis.

2.1 Ethics Approval

The study was approved by the Institutional Animal Ethics Committee of Advanced Centre for Treatment, Research and Education in Cancer (ACTREC), Navi Mumbai, which is endorsed by the Committee for the Purpose of Control and Supervision of Experiments on Animals (CPCSEA), Government of India: Approval no. 12/2009, ACTREC.

2.2 Animal model:

Hamsters [338], as mentioned in Chapter 1, have two buccal pouches in their oral cavity. Owing to similarities to human buccal mucosa, the hamster buccal pouch (HBP) model is commonly employed in experimental oral carcinogenesis. Golden Syrian hamsters are one of the most commonly employed species in oral experimental carcinogenesis. Table 2.1 gives the scientific classification for Syrian hamsters. Figure 2.1 shows HBP pulled out using a pair of forceps.

The animals used in the experiment were obtained from Laboratory Animal Facility (LAF) of ACTREC, where they were bred as well as maintained during the period of the study. All the hamsters employed in the study were males and were obtained at the age of 6 to 7 weeks.

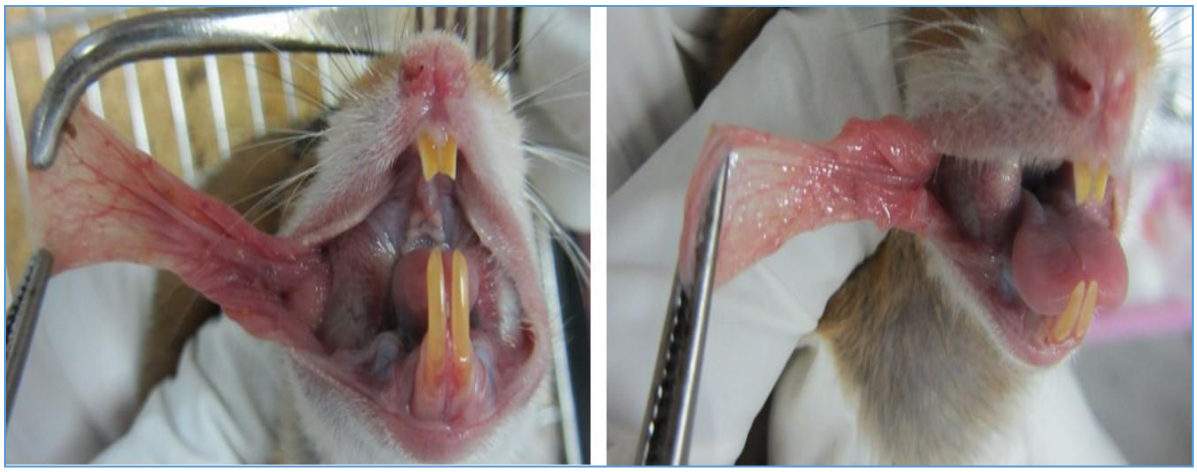

Figure 2.1: Hamster buccal pouch pulled out using a pair of forceps. Each hamster has two buccal pouches in their oral cavity which is used for temporary storage of food.

Kingdom	Animalia
Phylum	Chordata
Class	Mammalia
Order	Rodentia
Family	Cricetidae
Scientific name:	*Mesocricetus auratus*
Common name in English	Golden Syrian hamster
Natural distribution	Aleppinian plateau in Syria [339]

Table 2.1: Classification of Golden Syrian hamsters

2.3 Experimental animals

The experimental animals were randomly distributed into various groups, housed in polypropylene cages (4-5 animals per cage) and maintained under standard conditions of temperature: 22 ± 2 °C, relative humidity: 40 ± 5 % and 12 h light/dark cycles in the LAF, ACTREC. Corncob bedding material was provided for comfort of animals and a well labeled tag was used for identification of animals, as shown in Figure 2.2. The hamsters were transferred to cages with fresh bedding material twice a week to maintain hygiene. All animals were fed a diet of in-house-prepared pellets and provided with water *ad libitum*. Drinking water was provided from a UV based water purifier.

Sacrificing animals: Hamsters were sacrificed using standard guidelines of the CPCSEA, employing CO_2 as a euthanasia agent. Hamsters were placed in a CO_2 chamber and kept there till they stopped breathing.

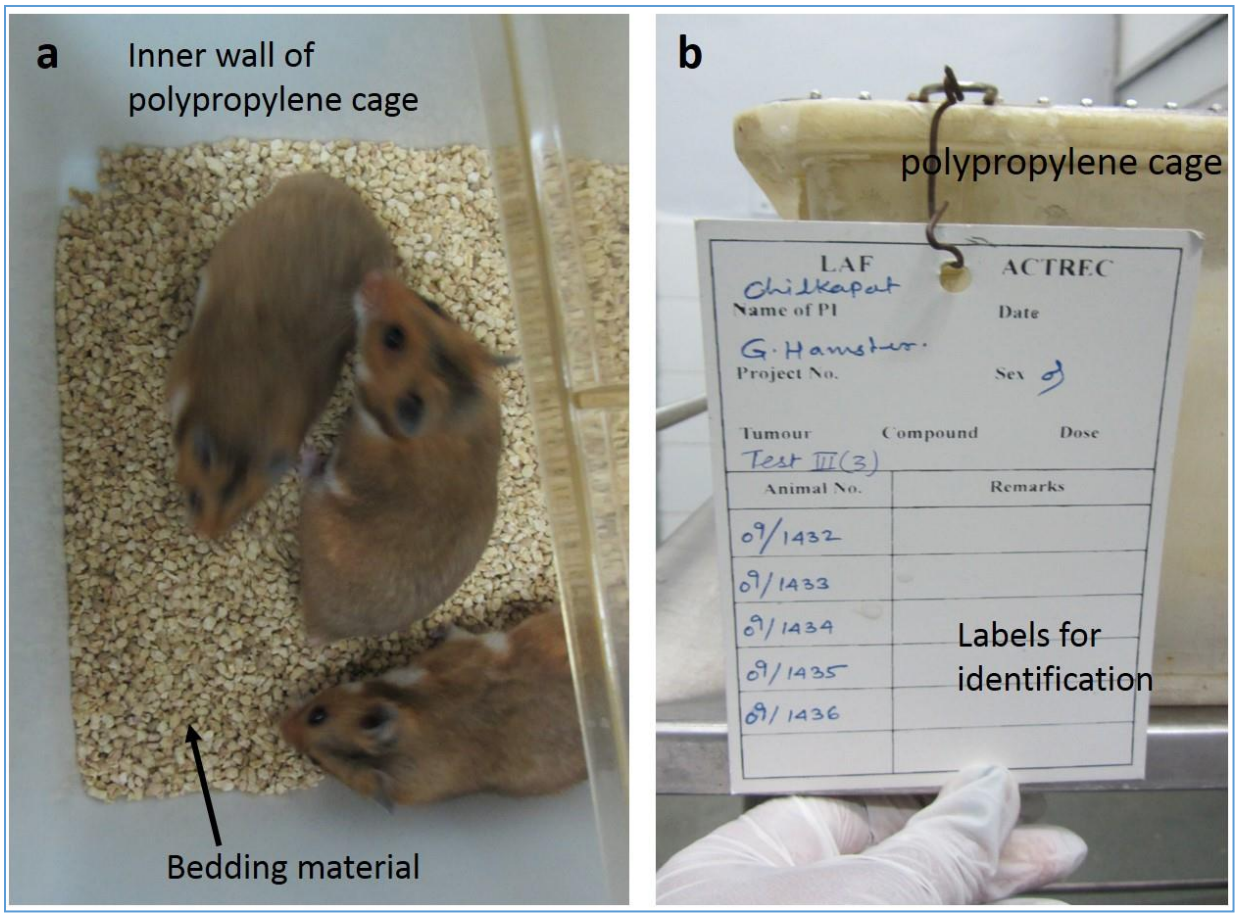

Figure 2.2: Maintenance of hamsters. (a) Hamsters inside the polypropylene cages, on the corncob bedding material. (b) Label hooked outside a cage for identification of animals.

2.4 Test and control animals

Test animals: Test animals were treated with the carcinogen DMBA dissolved in vegetable oil (Groundnut oil, Dhara) on their right buccal pouch. These pouches are referred to as DMBA treated pouches (T). The left buccal pouches of these animals served as contralateral control and are referred as *DMBA contralateral controls*.

Vehicle control animals: The right buccal pouches of these animals were treated with the vehicle oil (Groundnut oil, Dhara). In the thesis, these pouches have been addressed as vehicle controls. The left buccal pouches of these animals have been addressed as *vehicle contralateral* pouches.

Carcinogen: 7,12-Dimethylbenz[a]anthracene (DMBA; SID 24893738) [340]

DMBA is a potent carcinogen used for experimental carcinogenesis. The ring structure is shown in Figure 2.3. Most of the experiments involving HBP oral carcinogenesis employ DMBA as the carcinogen of choice. DMBA has also been observed in high concentration in the tar fraction of cigarette smoke [341]. DMBA can induce oxidative stress as well as modification of DNA in vivo. Further, it leads to formation of oxidized DNA bases as observed in response to ionizing radiation. Multiple/repeated applications of DMBA to mucosal surface leads to both "initiation" and "promotion", the steps in carcinogenesis [342].

PubChem CID:	6001
Chemical Names:	DMBA; 7,12-dimethylbenz[a]anthracene; 7,12-dimethylbenzanthracene; 7,12-dimethylbenzo[a]phenanthrene (IUPAC)
Molecular Formula:	$C_{20}H_{16}$
Molecular Weight:	256.34104 g/mol
Source	Sigma Aldrich, USA
Purity	95%
Storage	4^0C, in dark

Table 2.2: Details of DMBA

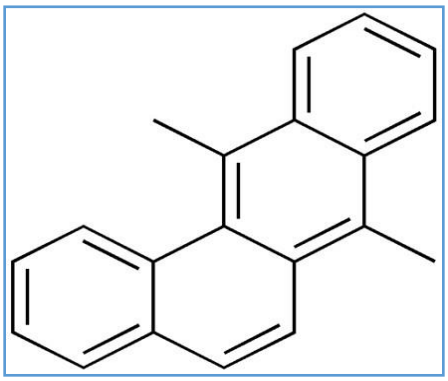

Figure 2.3: Structure of DMBA

Carcinogen application

0.5% DMBA (Sigma-Aldrich, SID 24893738, purity 95%) dissolved in groundnut oil (Dhara, India) was topically applied using a paint-brush (Camlin, no. 4) on the right buccal pouch of test animals thrice a week for 14 weeks; this process will be referred to as 'painting' in the thesis. Vehicle control animals were painted with only oil (Dhara, India) on their right buccal pouch. It is estimated that application of oil/DMBA leads to transfer of approximately 0.1 ml oil/DMBA on the HBP. Schematics of carcinogenesis regime has been shown in Figure 2.4.

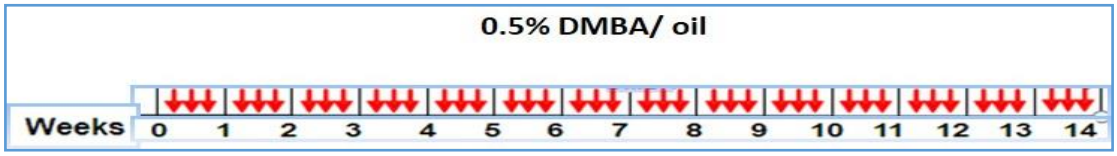

Figure 2.4: Painting or application of DMBA (on test HBP) or oil (on vehicle control HBP) over 14 weeks using a paint brush. Before painting a pouch, paint brush was dipped in a tube containing DMBA solution, wrapped in aluminium foil, and excess solution was drained at the rim of the tube. Similar protocol was followed for vehicle control animals using a different brush. Each arrow indicates one application using paint brush. Thus there were three applications each week over the period of 14 weeks. The animals were 8 weeks old when painting started.

2.5 Raman spectroscopy

Commercially available HE 785 Raman spectrometer (Jobin Yvon Horiba, France) was used in this study, the components of which are shown in

Figure 2.5.

2.5.1 Components of Raman spectrometer

The advent of powerful lasers and better and sensitive detector systems like charge coupled device (CCD), along with development of miniature and endoscope coupled fiber optic probes have revolutionized Raman spectroscopy mediated diagnostics and therapeutics research. Increasing avenues of research and development have reduced the cost of Raman instruments and many portable/transportable instruments are now available. Further, several improved multivariate analysis algorithms have greatly reduced the time of analysis. Typically, Raman spectroscopic studies involve spectral acquisition, preprocessing and multivariate analysis to explore spectral features, differences and classifications among the groups of specimens being studied.

Excitation: While Sir Raman used sunlight for his experiments, now lasers have become an integral part of Raman experiments since their discovery. Near Infrared (NIR) lasers are commonly used for biomedical application and 785 nm is one of the most commonly employed wavelengths. 1064 nm is often employed to minimize fluorescence in Fourier Transformed (FT) Raman experiments. The experiments mentioned in this thesis have employed 785 nm laser for excitation (Process Instruments, USA).

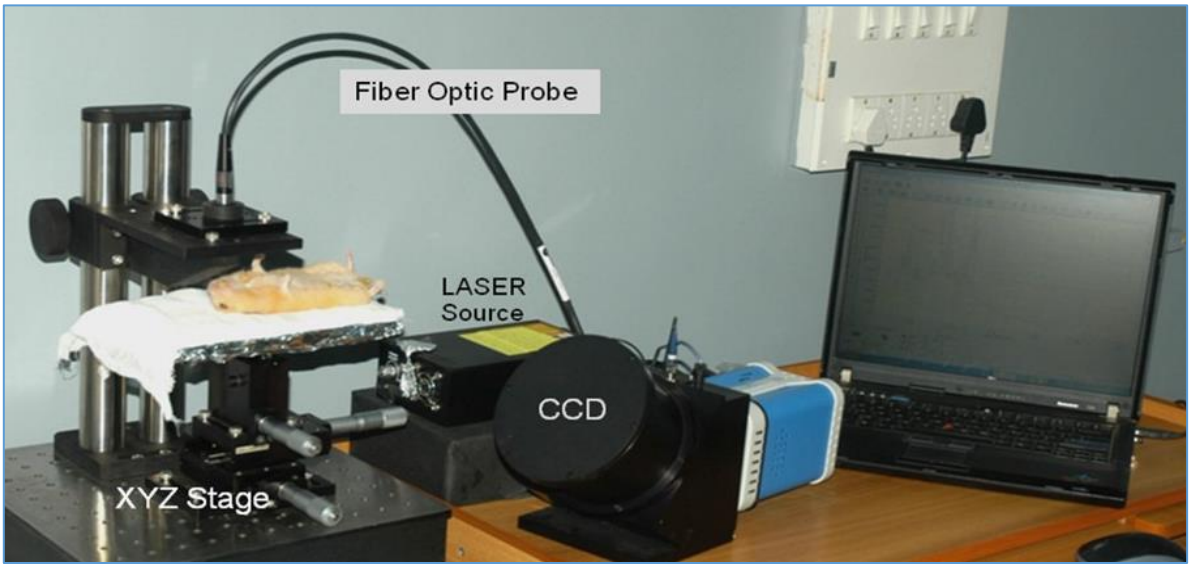

Figure 2.5: Raman spectrometer used in the study. It is a commercially available from Jobin Yvon Horiba, France. The detection system and laser source (Process Instruments, USA; 785 nm) are coupled with InPhotonics (USA) fiber optic probe. The XYZ stage is used to place the samples. The figure shows a hamster kept on the sample stage.

Sample illumination: RS, being an inherently weak phenomenon, requires proper focusing of laser beam onto the sample as well as efficient collection of the scattered photons for higher efficiency. Excitation and collection can be achieved by combinations of lenses through optical configurations like 90 and 180 degree scattering geometry. Lenses play a very important role in both excitation and collection. The ratio of the focal length of the lens (f) and the diameter of lens (D) is called F number, which determines the gathering power of a lens. The light gathering power of a lens is inversely proportional to F number. To obtain maximum light throughput, F number should be in accordance with the wavelength selector. The instrument room must be kept as dark as possible during spectroscopy.

Spectral Acquisition: Nowadays, microprobes (microscope objectives) and fiber-optic probes are used to expose samples to laser and channel the scattered photons to the spectrometer. Compact and highly efficient fiber optic probes are commercially available. In the studies mentioned in this thesis, a fiber optic probe (InPhotonics Inc, USA), which can be fixed on a sample stage with movable axes, was used for sample illumination as well as collection of scattered photons, as shown in Figure 2.6 and Figure 2.7. The probe consists of 105 µm excitation fiber and 200 µm collection fiber. Back scattering geometry is employed for collection of scattered photons. As per manufacturer's specifications, theoretical spot size and depth of penetration of the Raman probe are 105 µm and 1 mm, respectively. Typically, laser power of ~70 mW was used for excitation.

Figure 2.6: Fiber optic probe from InPhotonics Inc. The probe consists of 105 µm excitation fiber and 200 µm collection fiber. The probe uses back scattering geometry for collection of scattered photons.

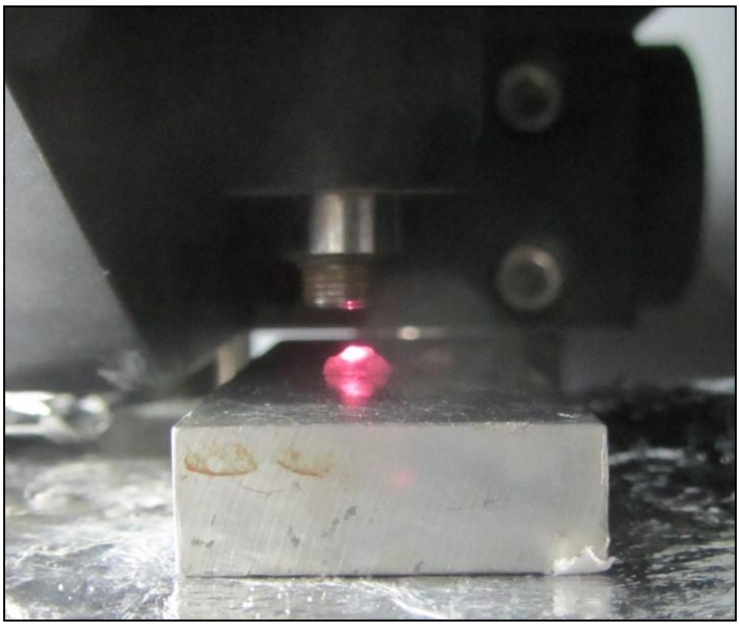

Figure 2.7: Acquisition of Raman spectra from an ex vivo tissue sample kept on aluminium substrate, placed under fiber optic probe, being excited with 785 nm laser.

*Spectrometer***:** It may include a simple device like an interference filter and prism to grating monochromators and spectrographs. The resolution of an instrument is greatly dependent on gratings. With higher number of grooves, better dispersion and thus greater resolution can be obtained. The spectrograph in the present experiment is equipped with a fixed 950 gr/mm grating.

*Detection***:** The inherently weak Raman signals require sensitive detection techniques. This is a major reason for poor development of Raman spectroscopy in spite of the discovery of Raman effect, way back in 1928. Most of the early works involved photographic plates exposed over a long time. Various detection devices developed with time include photon counting, photodiode array and CCD.

CCDs: CCDs are commonly used detectors in at present. By definition, a CCD is a silicon-based semiconductor, arranged as an array of photosensitive elements with each capable of generating photoelectrons and storing them as a small charge. The charge stored on each pixel is a function of number of photons hitting that pixel. Charges are shifted to next higher row from left to right and finally read by an analogue to digital converter. The CCD (Synapse) containing 1024 X 256 pixels employed in the study is available from Horiba, France. Specifications of the Synapse CCD are available at the following web link (date of access: January 19, 2017:

(http://www.horiba.com/fileadmin/uploads/Scientific/Documents/OSD/OSD0061256BIUV.pdf)

2.5.2 Raman spectral acquisition in in vivo studies

In vivo Raman spectra were acquired from test and control HBP of anaesthetized animals (Figure 2.8). The following anaesthetic agents were administered simultaneously:

- Ketamine hydrochloride: 150 mg per kg body weight of hamsters.
- Xylazine hydrochloride: 10 mg per kg body weight of hamsters.

Ketamine and Xylazine are commonly employed for anaesthetizing pets/domesticated animals for veterinary purposes. The anaesthetic agents were administered intraperitoneally. At the mentioned dosage, the hamsters lost consciousness within 10 minutes of injection and remained unconscious for about 30 minutes. The unconscious hamsters were placed on the sample stage, buccal pouches were pulled out using forceps and spectra were acquired from 10 to 15 different regions on the buccal pouch, depending on how soon the hamsters revived.

Typically, laser power-70 mW was used for excitation. Spectra were integrated for 15 seconds and averaged over 3 accumulations.

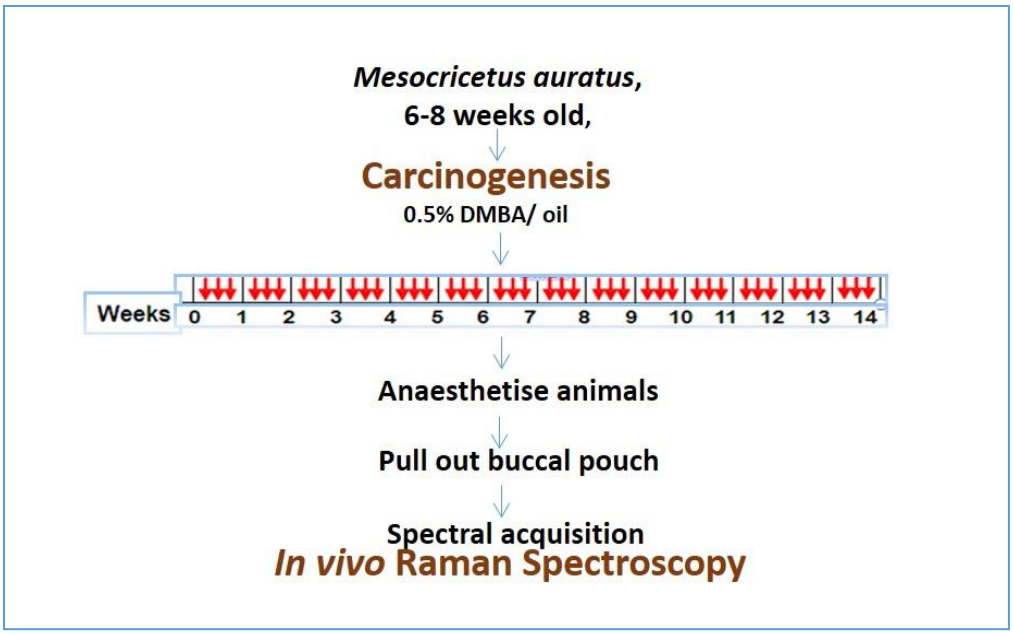

Figure 2.8: Schematic for in vivo spectroscopy.

2.5.3 Raman spectral acquisition in ex vivo studies

Test and controls animals, as per protocol, were sacrificed every week after due carcinogen application for 14 weeks. Buccal pouches were then excised out of the sacrificed hamsters, snap frozen in liquid nitrogen and stored at -80^{o}C till spectra recording. Spectra were recorded from these tissues after passive thawing on ice. After tissues thawed, they were washed in normal saline once to get rid of any food particle or blood and spread on an aluminium plate with grids (3X3) etched on surface . The grid was placed on a sample holder attached with an XYZ stage, with the fiber optic probe fixed within the apparatus as shown in Figure 2.9. After spectra acquisition, the sites of laser irradiation were marked in ink for identification during preparation of tissue sections for histopathology. Spectral acquisition parameters were same as those in the in vivo studies. Typically, laser power-70 mW was used for excitation. Spectra were integrated for 15 seconds and averaged over 3 accumulations. Approximately 9 spectra were recorded from each pouch, with one spectrum acquired from each grid. After spectral acquisition, tissues sections were cut along gridlines, fixed in neutral buffered formalin (NBF) for 24 hours, paraffin embedded and processed for further histopathological or histochemical analysis.

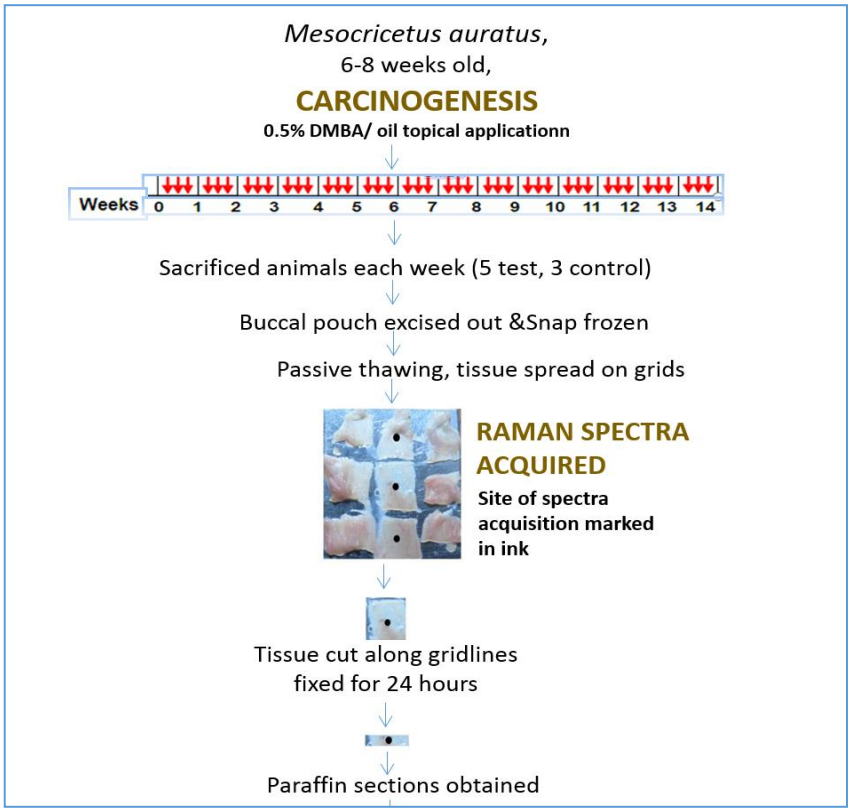

Figure 2.9: Schematic for the ex vivo study. After spectral acquisition, tissues were fixed in 10% neutral buffered formalin and then embedded in paraffin wax blocks were prepared. The paraffin sections obtained were used for corroboration with histopathology and immunohistochemical analysis.

2.6 Histopathology

To identify sites of spectral acquisition on buccal pouches, they were marked in waterproof India ink, the tissues were then cut along gridlines and immersed in formalin for 24 hours for fixation (Figure 2.10).

The formalin fixed tissues were embedded in paraffin blocks. To obtain a precise histopathological evaluation for the laser probed area, three parallel sections of 5 micron each were taken from the paraffin embedded tissues at the sites marked in ink. These sections were stained with Hematoxylin and Eosin dyes (H&E) and were evaluated by trained pathologists, blinded to Raman findings. Based on the histopathological assessment of all the parallel sections by the pathologists, the corresponding spectra were labeled as per their pathological status- healthy, hyperplasia, dysplasia or SCC; which are the major stages observed in oral carcinogenesis. The spectra corresponding to the evaluated tissue sections have been referred to as ‘histopathologically certified spectra’ in the thesis.

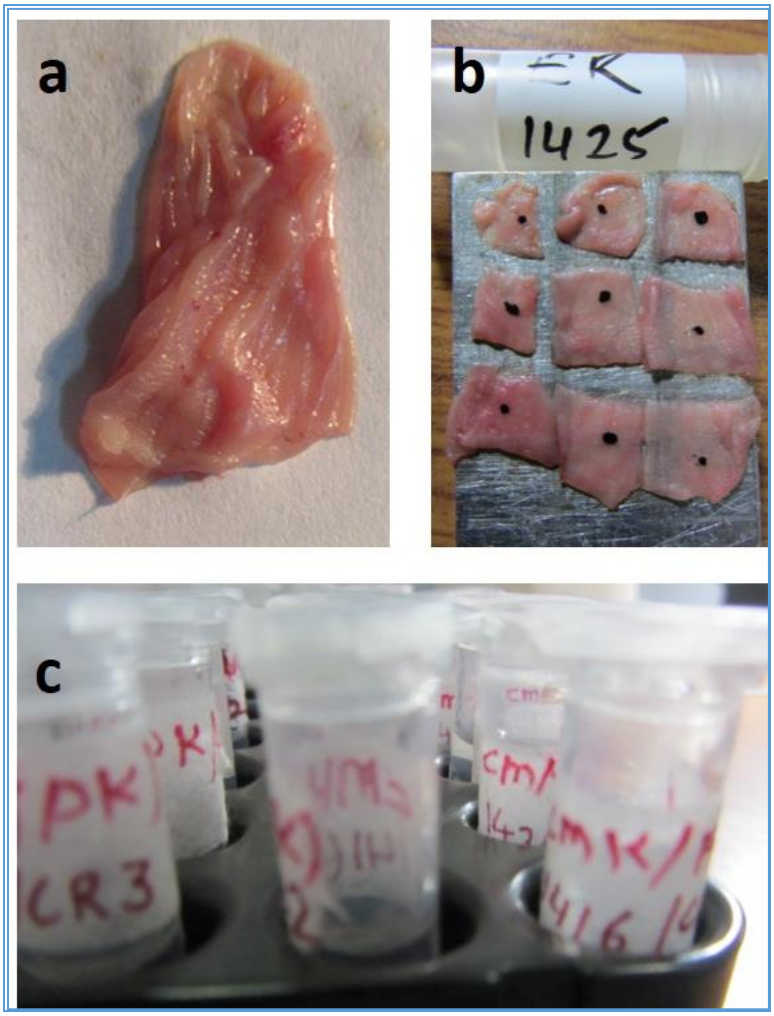

Figure 2.10: Preparatory steps for histopathology. (a) The tissue stored at -80^{0}C was thawed over ice and rinsed with normal saline. (b) The rinsed tissue was spread over aluminium plate with grids etched. After spectral acquisition, the site of spectral acquisition was marked in ink and the tissues were cut along gridlines. (c) The tissues were immersed for 24 hours in separate well labeled tubes containing neutral buffered formalin for fixation.

2.7 IHC

Immunohistochemical evaluation (IHC) for cyclin D1 expression was also employed in the present study. IHC based spectral models were built after evaluation of sections on the basis of cyclin D1 expression on a commonly employed scale of 0 to +3. An expression of 0 grade signified minimum/baseline level of expression.. +1, +2 and +3 signified low, medium and high amount of expression of cyclin D1, respectively in the tissue sections being investigated. In this thesis, grade 0, +1, +2 and +3 have been denoted as G0, G1, G2 and G3 respectively.

The major steps followed are shown in Figure 2.11. For IHC, two 5 µm tissue sections were taken on poly-L-lysine (Sigma-Aldrich, USA) coated glass slides. These slides were kept at 60^0C in an incubator for one hour and were deparaffinized with xylene and rehydrated with sequential ethanol washes. To quench the endogenous peroxidase activity, sections were incubated with 2% hydrogen peroxide (Sigma-Aldrich, USA) in methanol for 30 minutes in dark. After heat based antigen retrieval with sodium citrate buffer (pH = 5.8), sections were incubated with normal horse serum (Vector laboratories, USA) at room temperature. Next, the sections were incubated overnight with rabbit polyclonal anti-human cyclin D1 antibody (1:100, Santa Cruz Biotechnology, USA) at 4°C for sixteen hours. Sections were then incubated with biotinylated Universal® secondary antibody solution (Vector Laboratories, USA) for 30 minutes followed by incubation with Vectastain Universal® ABC (Vector Laboratories, USA) reagent for the same time. The immunoreaction in tissue sections was visualized using 3,3′–diaminobenzidine tetrahydrochloridehydrate (Sigma-Aldrich, USA). The slides were finally counterstained with hematoxylin and evaluated by pathologists and assigned with grades corresponding to Cyclin D1 expression.

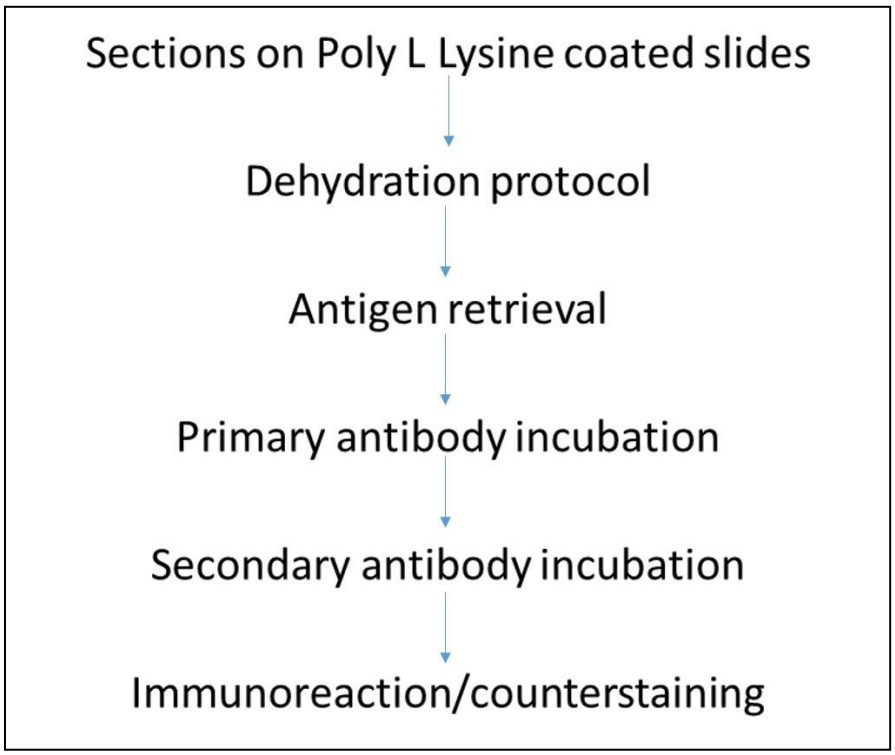

Figure 2.11: Major steps in immunohistochemical analysis.

2.8 Optical Coherence Tomography (OCT)

Typically, OCT components would consist of a Michelson-type interferometer with a focused sample arm beam and a lateral-scanning mechanism. OCT has evolved from the field of optical coherence-domain reflectometry, a 1-D distance mapping technique originally developed to localize reflections from faults in fiber optic networks and was quickly adapted for biological applications [343]. The spatial resolution of modern OCT systems is ~1-15 μm, and the imaging depth in scattering tissues is around 1-3 mm [344, 345]. In recent years, OCT has emerged as a powerful tool striving to bring together microscopy and ultrasound. The combination of coherence gating of OCT and confocal gating of microscopy has led to development of optical coherence microscope (OCM) that provides tomographic images with cellular resolution due to better rejection of unwanted photons. A schematic of the instrument used in the experiment is shown in Figure 2.12. The instrument is installed at Bhabha Atomic Research Centre (BARC), Vishakhapatnam.

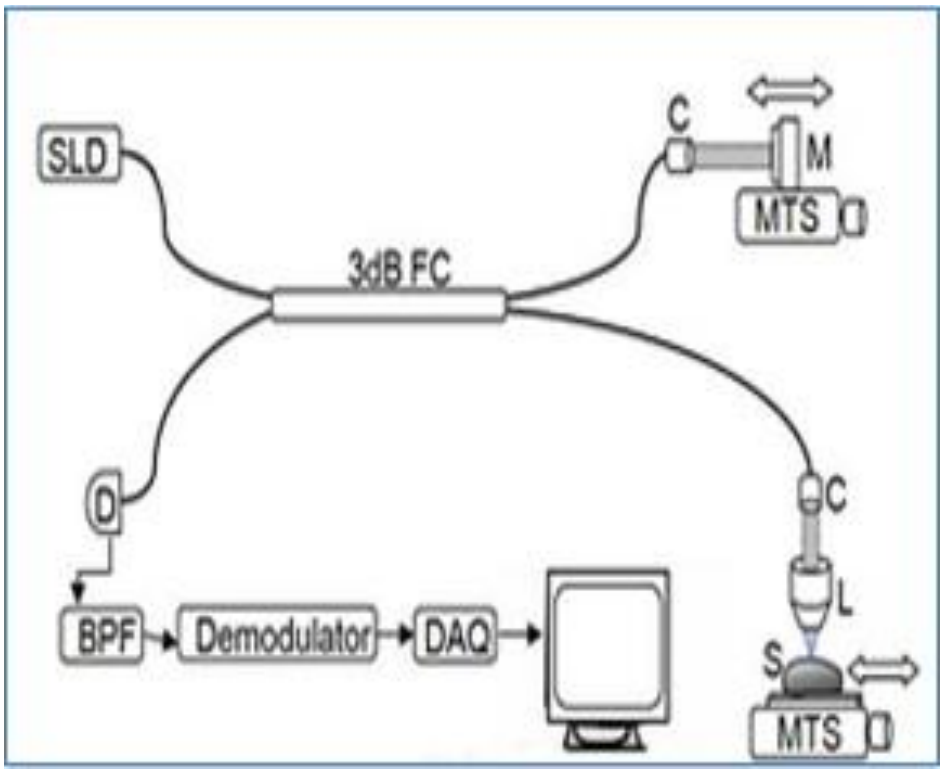

Figure 2.12: Schematic of OCT system; BPF- Bandpass filter; C- collimator; D- Photodetector; FC- Fiber coupler; L –lens; M-Mirror; MTS- motorized translation stage; S- Sample; SLD- superluminescent diode.

2.9 Data analysis

Raw Raman spectra may be contaminated with contributions from background elements, fibers and optical components. Data pre-processing is carried out to remove contaminating spectral contributions for improved signal to noise ratio before subjecting spectra to data analysis. Calibration based on standard reference material available from National Institute of Standards and Technology (NIST) or white light correction to compare spectra acquired from different instruments may be carried out. The environmental background noise may be subtracted from the acquired spectra. Further, spectral interpolation in defined regions (fingerprint region or high wave number regions) may improve the final analysis. Normalization of the spectra is carried out before multivariate analysis to remove intensity related changes.

Spectral preprocessing: Raw spectra were corrected for CCD response using a NIST certified SRM 2241 material followed by subtraction of spectral contribution from optical elements[346]. To remove interference of slow moving background, first derivatives of spectra were computed [347]. Spectra were interpolated in the 1200-1800 cm^{-1} region as previous studies on oral cancer have already demonstrated the efficacy of this region in classification [296, 297, 337]. Moreover, this region is free from interference of fiber signals which are generated due to fused silica fibers [347]. Interpolated spectra were vector normalized to remove intensity related variations and subjected to multivariate analysis. A summary of steps followed during spectral preprocessing is shown in Figure 2.13.

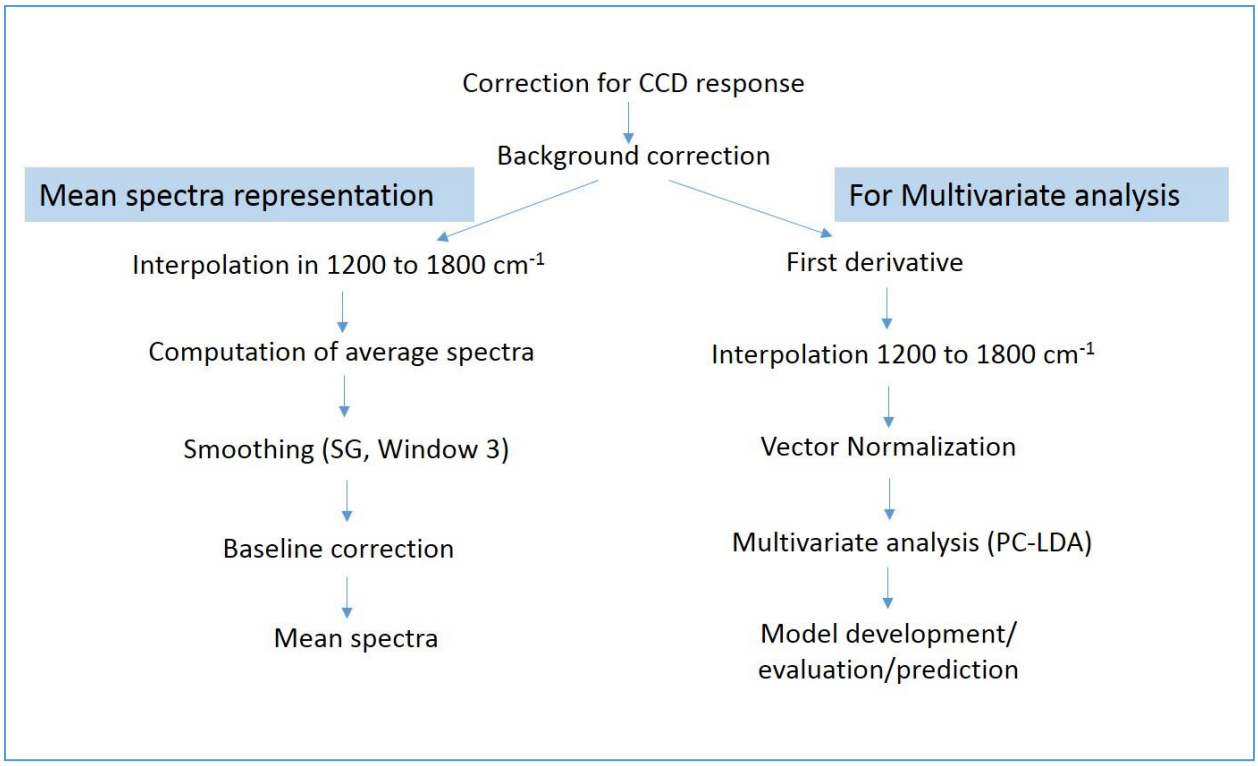

Figure 2.13: Steps followed during spectral preprocessing in the studies mentioned. Mean spectra were used for identifying major spectral features and for spectral comparison across various groups of specimens while multivariate analysis was used to explore classification among the groups.

Computation of mean spectra: Average or mean spectra were computed from the background corrected spectra for each class and baseline corrected by fitting a 5^{th} order polynomial function using LabSpec 4.18 (Horiba Jobin Yvon, France). These baseline corrected spectra followed by vector normalization were used for obtaining an average for spectral comparison across different groups.

Sometimes a difference spectrum is also used to identify subtle differences across groups. Usually, it is computed by subtracting normalized mean spectra of one group from another. The positive bands indicate contribution from the first group while the negative bands indicate contributions from the second group.

Data analysis

Spectroscopic techniques in conjunction with proper chemometric tools can distinguish subtle but significant changes in the complex biological environment. However, it is important to know the limits and assumptions employed in each analysis method for a reliable and reproducible diagnosis. Both univariate and multivariate analyses can be carried out for spectroscopic data. However, in view of levels of complexity in living organisms, multivariate analysis may be a suitable approach.

2.9.1 Multivariate analysis

The aim of multivariate analysis is to train models that distinguish seemingly similar patterns in certain conditions and identify independent samples. Multivariate analysis can be unsupervised where no prior information is given and the method tries to establish relationships or trends in

classification de novo. In the absence of preliminary information, non-supervised methods provide a first-hand estimate about the nature of data. Supervised learning methods are used to predict the association of new variables to one of the pre-existing groups. In this case, model is trained using available information and evaluated with an independent data set.

A flowchart explaining the commonly employed methods of analysis is shown in Figure 2.14.

2.9.1.1 Unsupervised analysis

The analysis is called ‘unsupervised’ since no prior knowledge of the sample class or group is provided. Principal Component Analysis (PCA) is one of the most popular unsupervised multivariate analysis methods. PCA [348, 349] explores the variation in the data, extracts spectral features contributing to the variation (eigenvectors) and arranges them in the order of importance based on their contribution to the variation (eigenvalues) - such that eigenvectors affecting maximum variation is placed first and so on. The data set is then transformed with the highest eigenvectors forming the x and y axes (and z axis in 3D plots) of the new system, displaying variation in the data. PCA is usually used to reveal patterns in unknown data as well as to remove noise. It can be used in conjunction with supervised techniques such as LDA where PCA supplies non-redundant spectral features for further analysis. Another commonly used methods, Hierarchical Clustering Analysis (HCA), also does not need prior knowledge of groups and is an excellent exploratory method [350].

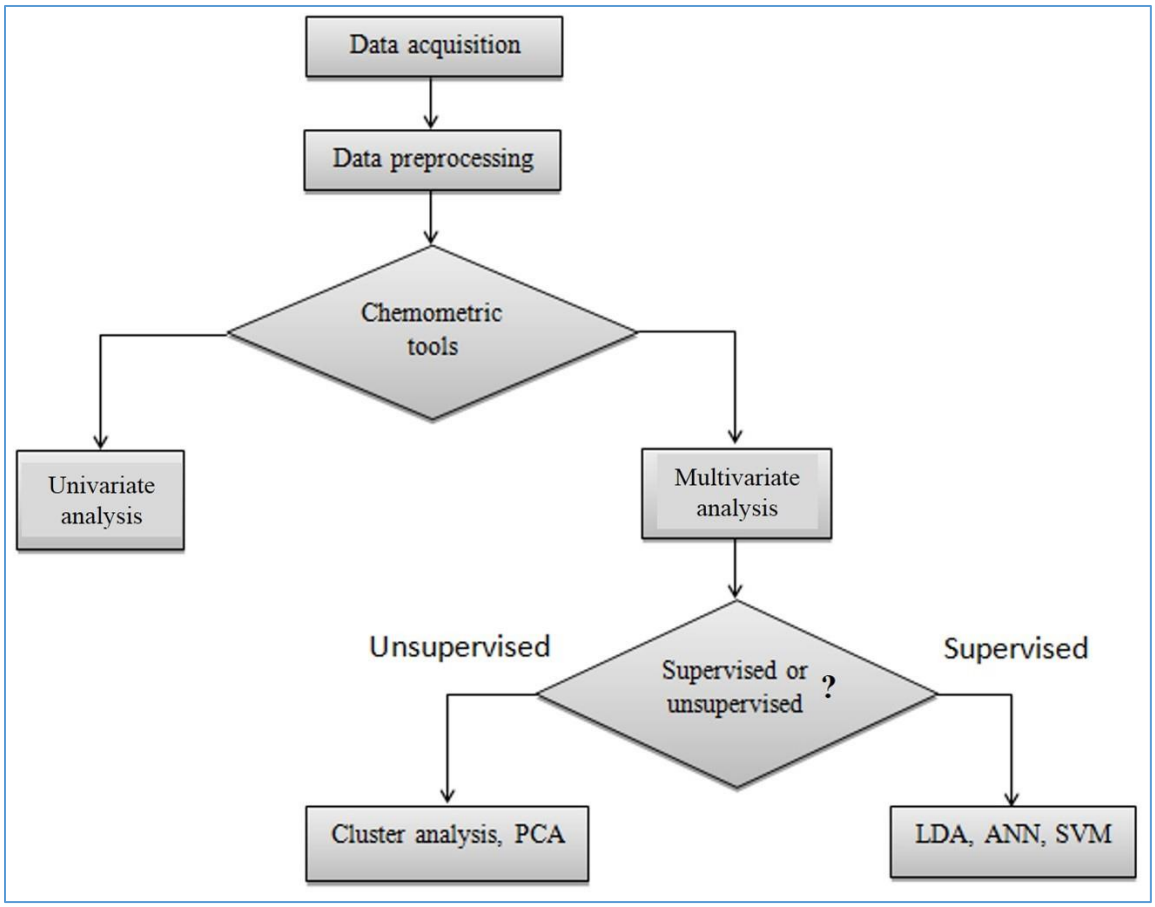

Figure 2.14: Flowchart for data analysis.

Method	**Attributes**
Univariate analysis	Corresponding p values are measure of significance. Prone to false positive unless corrected significance limit is used.
Cluster analysis	Classification scheme to divide data in clusters. Hierarchical clustering provides relationships between clusters.
Partial Least Square Regression	To predict a set of dependent variables from a (very) large set of independent variables.
Principal Component Analysis	Provides an overview for large data sets. Identify outliers, clusters and trends in dataset.
Bayes Classifier	Leads to classification but a large training set is needed.
Linear Discriminant Analysis	Discrimination method related to multiple linear regressions. Number of variables must be smaller than number of observations.
Neural Networks	High flexibility in modelling non-linear data but prone to overfitting.
Support Vector Machines	High flexibility in modelling non linearities. Careful model selection reduces possibility of overfitting.

Table 2.3: Summary of some commonly employed analysis methods.

2.9.1.2 Supervised analysis

Supervised methods involve training an algorithm to discriminate between two groups so as to allow classification of unknown sample. Evaluation is usually carried out by independent data set. Methods such as Artificial neural networks (ANN), Support vector machines (SVM) and Linear Discriminant Analysis (LDA) are commonly employed for classification of biological samples ANN use several layers (input, intermediate and output) to select spectral features that will force classification into designated classes. The method is prone to overfitting or under fitting resulting in poor outcome during validation. SVM use classifying hyperplane coupled with margins, support vectors, to achieve best separation between classes. SVM also suffers from the problem of overfitting if precautions are not taken. LDA increases inter class variance and reduce intra class variance and classifies different groups. This method has been used widely for biological data. In cases where linear function cannot distinguish the groups, non-linear functions such as factorial (Factorial Discriminant Analysis), quadratic (Quadratic Discriminant Analysis) and partial least square (Partial Least Square Discriminant analysis) can be explored for classification [351-356].

2.10 Multivariate analysis employed in thesis

Preprocessed spectra were subjected to unsupervised Principal Component Analysis (PCA), as well as supervised Principal Component based Linear Discriminant Analysis (PC-LDA) using algorithms implemented in MATLAB-based in-house software [357].

PCA: As already mentioned, PCA is the most frequently applied method for computing linear latent variables which allows visual inspection of clustering of objects or variables through unsupervised classification. The main aim of PCA is dimension reduction by which it explains maximum variability with few Principal Components (PCs)/factors [349]. Most variance is often captured by the first 10 PCs [358, 359].

PC-LDA: Linear Discriminant Analysis (LDA), as mentioned earlier, maximizes inter-class separation and reduces intra-class separation to bring out discrimination [360]. For data with high-dimensionality, dimension reduction may be achieved by application of PC-LDA: PCA followed by LDA, using PCA scores, instead of original variables. Further, for classification methods like LDA the first few factors/PCs often account for more than 90% classification when PC-LDA is carried out [359]. Classification efficiency of standard models was evaluated by Leave-one-out cross-validation (LOOCV) which is based on a hypothetical validation set used in absence of an explicit validation set. Leave-one-out involves using a single observation from the original sample as the validation data, and the remaining observations as training data. This is repeated such that each observation in the sample is used once as the validation data and averaged over the rounds. The flowchart for preprocessing and data analysis employed in the present study is presented in Figure 2.15.

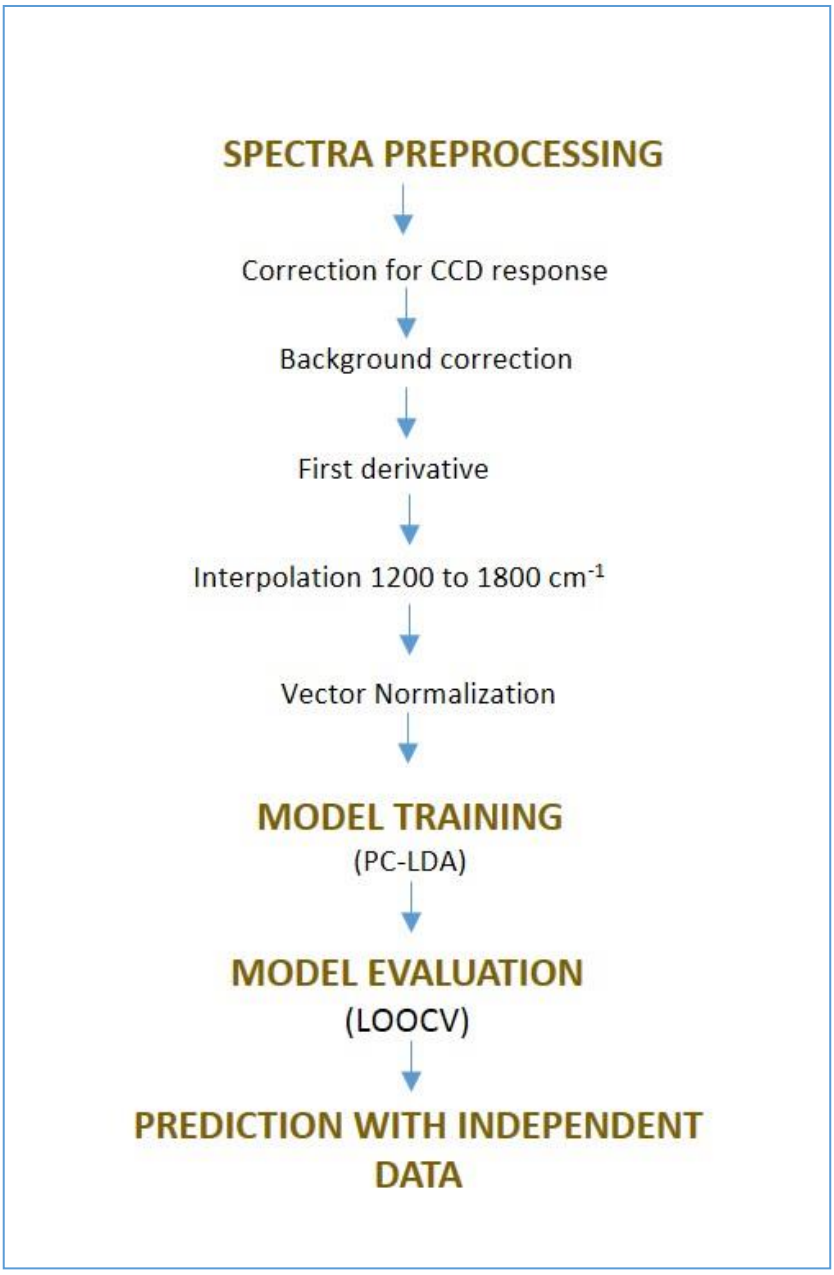

Figure 2.15: Steps in spectral data analysis followed in the experiments.

3 Chapter 3: Results and Discussion

Prelude

Chapter 3 provides the detailed findings and the discussion based on the results of the studies carried out. Entire work has been described under four sub chapters 3.1 to 3.4. Chapter 3.1 explains the findings of the first objective: sequential and comparative evaluation of Raman spectral changes in DMBA-induced HBP carcinogenesis at various time periods. Chapter 3.2 describes Raman spectroscopy vis-a-vis histopathology and cyclin D1 expression to build spectral models and investigation of abnormal changes in control tissues based on these models. Next, the combined Raman and OCT study on limited samples were carried out to verify abnormal changes in control tissues and have been discussed in section 3.3. Finally, in vivo Raman based investigation of discontinuation of carcinogen on the process of carcinogenesis has been debated in Section 3.4.

3.1 Sequential and comparative evaluation of Raman spectral changes in DMBA-induced HBP carcinogenesis at various time periods

The present section describes sequential Raman spectroscopic evaluation of buccal pouch carcinogenesis with respect to vehicle treated age-matched controls using three approaches: i) ex-vivo ii) in-vivo sequential and iii) in vivo follow-up, described below:

a) Ex-vivo study: In this approach, animals were sacrificed and the spectra were recorded from ex vivo buccal pouch tissues of test and control animals. 5 test and 3 control animals were sacrificed every week over the 14 week duration as mentioned in Chapter 2.5.3.

b) In vivo sequential study: Spectra were recorded from buccal pouch of alive, anaesthetized animals. Each week Raman spectra were recorded from buccal pouch of 2 test and 2 control animals. After spectra acquisition, the animals were sacrificed, pouches excised out and processed for histopathology. Thus a total of 60 animals were used over the period of 14 weeks.

c) In vivo follow up study: This approach was also an in vivo approach, with an objective to follow sequential progression in same animals. In vivo Raman spectra were acquired from buccal pouch of these hamsters (3 test and 3 controls) post anaesthetization each week for the entire duration of 14 weeks. The animals were sacrificed at the end of 14 weeks.

A total of 181 six to eight weeks old Golden Syrian male hamsters were used in the study. Oral carcinogenesis was induced in 103 HBP (treated group) using DMBA carcinogenesis protocol [84]. 78 HBP were painted with only oil (vehicle control group) using paint brush. A schematic of experimental approach is shown in Figure 3.1.

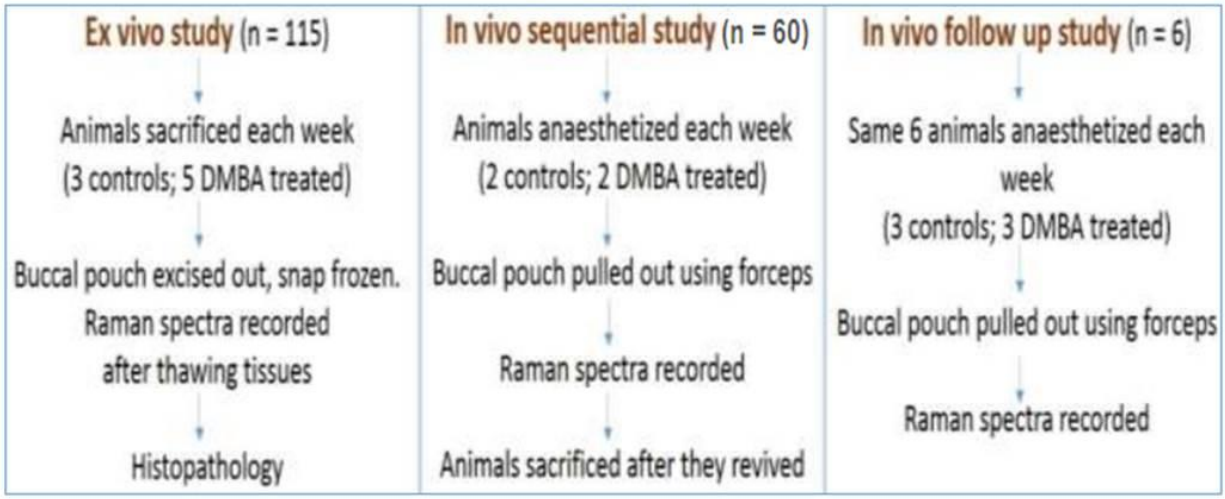

Figure 3.1: Schematic of experimental approach followed for ex vivo, in vivo sequential and in vivo follow up study. In ex vivo study, animals were first sacrificed and then spectra were recorded from ex vivo tissues. In in vivo sequential study, spectra were recorded in vivo from different animals in different weeks and then animals were sacrificed. In case of follow up study, same six animals were followed up in vivo for the period of 14 weeks.

3.1.1 Spectral acquisition

Spectra were integrated for 15 s and averaged over 3 accumulations. Approximately 9 spectra were recorded from each pouch in ex vivo study, 1 spectrum from each aluminium grid, as shown in Figure 2.9. In case of in vivo sequential study, 15 spectra were recorded from selected sites and 10–15 spectra were recorded from each pouch for in vivo follow up study.

In this and subsequent sections, control and DMBA-painted groups have been designated as C and T respectively while the number succeeding C (Cx) or T (Tx) denotes the number of weeks of DMBA or oil application/painting. Thus, C0, C1 and C14 indicate control of 0, 1 and 14 weeks of oil painting and T0, T1 and T14 indicate DMBA painting for 0, 1 and 14 weeks, respectively.

3.1.2 Findings

In all the approaches, a 3-group classification system involving week 0 controls (C0) along with DMBA-treated HBP (Tx) and age-matched controls (Cx) was used (e.g. C0 vs C1 vs T1, C0 vs C2 vs T2, C0 vs C3 vs T3 and so on up to C0 vs C14 vs T14) for data analysis. This is expected to make the spectral model more robust, compared to a two group classification system involving only DMBA painted and age-matched controls (e.g. C1 vs T1). RS studies on human oral mucosa have already demonstrated that despite feasibility of classifying early and late physiological age groups of healthy volunteers, it has no bearing on classification of normal and abnormal conditions [337]. No age-related physiological changes have been reported hitherto in hamsters. A 3-group classification system (C0 vs Cx vs Tx) can also highlight any possible age-related changes.

3.1.2.1 Ex vivo study:

Spectral features: Spectral features of week 0 control (C0) and DMBA-painted buccal pouches (T1 to T14) have been shown in Figure 3.2. C0 and T0 spectra were similar and show dominance of lipid features- 1303 cm^{-1}, δCH_2 (1448 cm^{-1}), Amide I (1655 cm^{-1}), and ester bands (1750 cm^{-1}), whereas T14 (frank tumours) spectra show dominance of proteins and nucleic acids with change in features in 1200-1400 cm^{-1} regions corresponding to Amide III, CH_2 (1454 cm^{-1}), 1583 cm^{-1}, and broad Amide I (1651 cm^{-1}). The spectra from T2 to T13 also show changes in Amide III and Amide I regions which progressively indicate increasing protein dominance. These spectral features correlate well with human buccal mucosa, featuring similar bands [6, 244]. A probable reason for loss of lipids and increased dominance of proteins in tumours or other pathological conditions could be the changes in the architectural arrangement of epithelial layers, leading to loss of lipid features. Moreover, cells under pathological conditions undergo changes in the amounts of surface and receptor proteins, enzymes, antigens, and antibodies which can give rise to a protein dominated spectrum [7]. These findings further corroborate earlier reports of ex vivo and in vivo RS studies on human subjects [8, 246, 361]. The 1583 cm^{-1} band, attributed to heme proteins and prominently observed in DMBA-treated pouches of later weeks could be due to angiogenesis- a well-known hallmark of carcinogenesis.

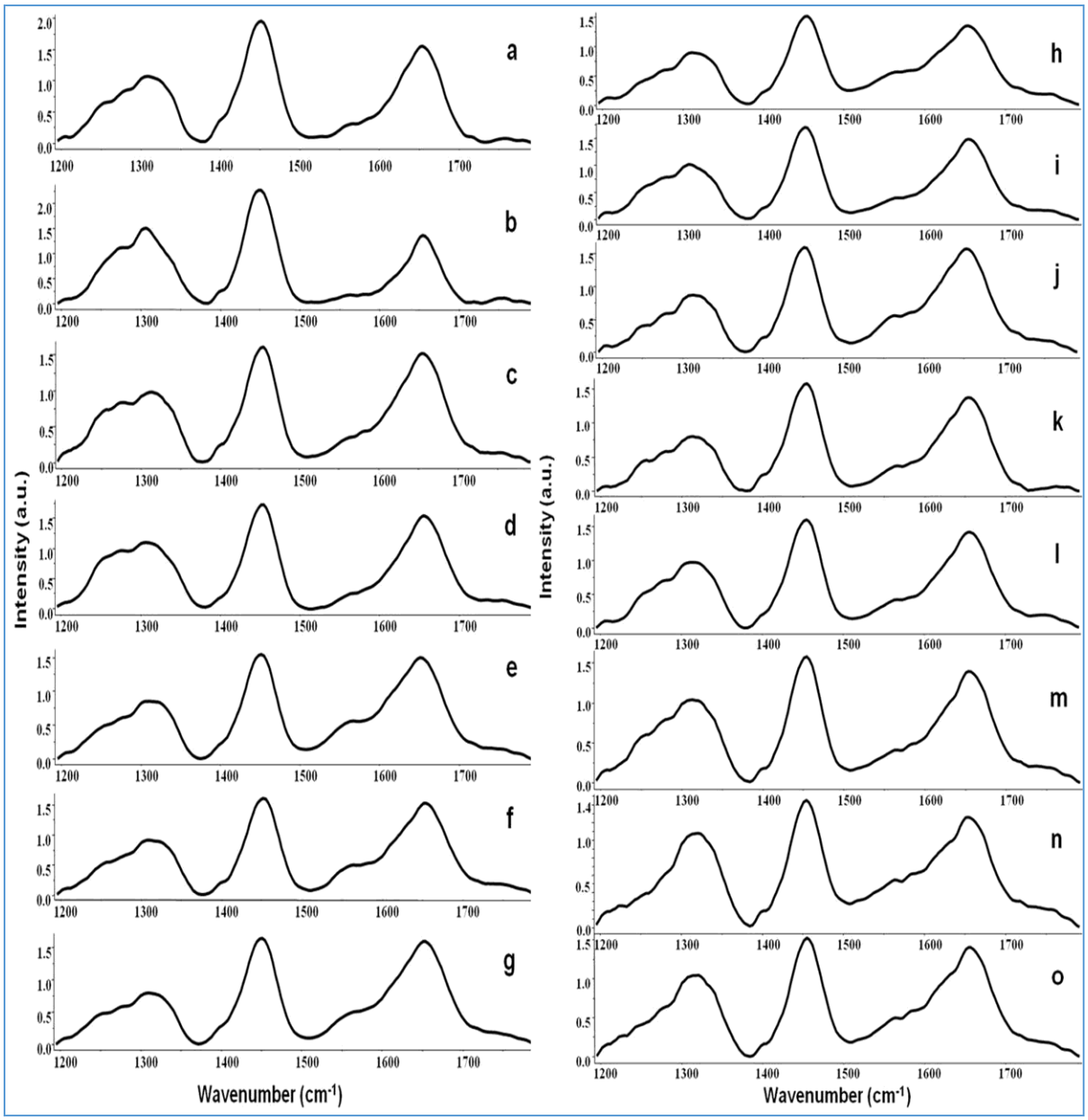

Figure 3.2: Mean spectra of DMBA treated hamster buccal pouch. a- week 0, b- week 1, c-week2, d-week 3, e-week 4, f-week 5, g-week 6, h-week 7, i-week 8, j-week 9, k-week 10, l-week 11, m-week 12, n-week 13, o-week 14. The spectra are shown in the 1200 to 1800 cm^{-1} range and show decreasing lipid dominance and increasing protein/nucleic acid dominance with progression of carcinogenesis.

Multivariate analysis: PCA scatter plots for all 14 weeks using scores of factor 1 vs 2 are shown in Figure 3.3. These plots exhibit overlapping clusters for all the three groups in the initial weeks, i.e. from 0 to 4 weeks. An increased classification of treated pouch spectra was observed from 5^{th} week onwards, attributable to DMBA induced changes. Plateauing of classification was observed for week 8-11 while exclusive clusters were observed from 12^{th} week onwards showing the best classification between treated and control spectra during these later weeks. Poor classification was observed between C0 and age-matched controls suggesting lack of appreciable age-related changes in the 14 week period of carcinogenesis.

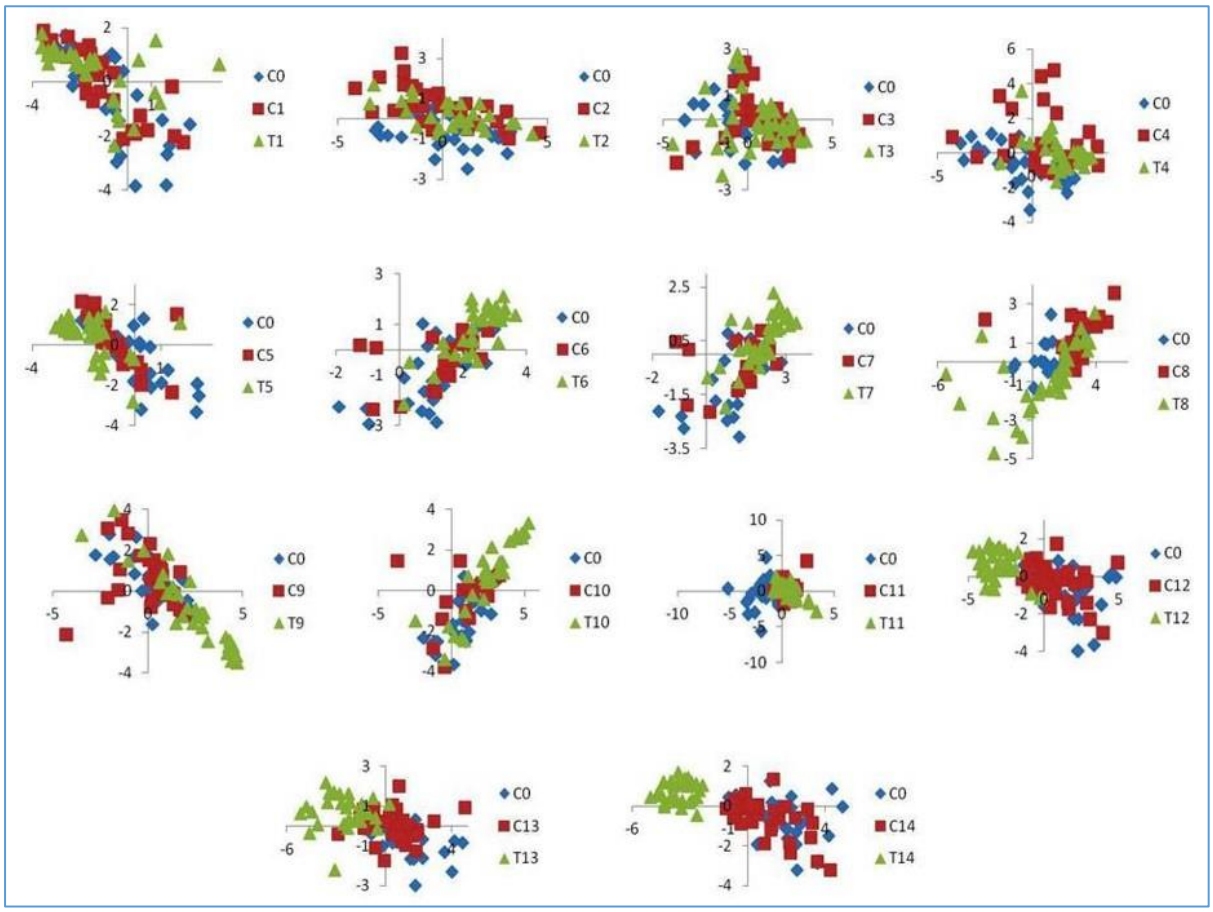

Figure 3.3: Scatter plots of PCA over the period of 14 weeks of DMBA treatment of Hamster buccal pouch; Segregation of spectra from DMBA treated pouches (triangles) can be observed from 6 weeks onwards while exclusive cluster can be observed in the 14 week spectra. (X-axis: Score of factor 1, Y-axis: Score of factor 2; C0- week 0 control spectra, Cx- age-matched control spectra for a given week; Tx- spectra from DMBA-treated pouch for a given week).

PC-LDA: As PCA is an overview tool used to visualize trends in the data and not a classification tool, PC-LDA was carried out to explore feasibility of classification through supervised analysis between C0, Cx and Tx. 2-4 factors were used. The confusion matrix for PC-LDA is shown in Table 3.1 Efficiency of models was evaluated by LOOCV. Week-wise LOOCV findings are presented in the form of confusion matrices in Table 3.2. On the basis of PC-LDA findings, the 14 weeks can be sub-divided into three phases: week 0-7 (T0-T7), week 8-11 (T8-T11) and week 12-14 (T12-T14). T0-T7 showed progressive increase in classification, up to 70%. T8 - T11 showed a plateauing phase where classification efficiency remained around 70% while T12 – T14 showed classification up to 100%. Thus an overall sequential increase in classification efficiency was observed from 0 to 14 weeks of DMBA application.

	WEEK 1				WEEK 2				WEEK 3				WEEK 4				WEEK 5				WEEK 6				WEEK 7			
	C0	CX	TX	TOT	C0	CX	TX	TOT	C0	CX	TX	TOT	C0	CX	TX	TOT	C0	CX	TX	TOT	C0	CX	TX	TOT	C0	CX	TX	TOT
C0	22	7	2	31	19	6	6	31	26	2	3	31	26	3	2	31	25	5	1	31	21	4	6	31	24	3	4	31
CX	5	12	16	33	5	17	10	32	4	15	14	33	2	14	11	27	2	29	5	36	1	25	4	30	1	14	15	30
TX	2	12	19	33	3	6	24	33	0	13	27	40	4	11	21	36	0	7	25	32	4	4	24	32	0	11	31	42

	WEEK 8				WEEK 9				WEEK 10				WEEK 11				WEEK 12				WEEK 13				WEEK 14			
	C0	CX	TX	TOT	C0	CX	TX	TOT	C0	CX	TX	TOT	C0	CX	TX	TOT	C0	CX	TX	TOT	C0	CX	TX	TOT	C0	CX	TX	TOT
C0	24	4	3	31	21	8	2	31	25	3	3	31	25	3	3	31	29	2	0	31	24	6	1	31	26	5	0	31
CX	7	9	11	27	5	22	4	31	1	21	8	30	5	48	15	68	3	31	0	34	4	27	3	34	5	29	0	34
TX	2	3	33	38	2	5	26	33	0	8	23	31	3	13	27	43	0	7	25	32	1	5	25	31	0	0	33	33

Table 3.1: PC-LDA for ex vivo study, C0: week 0 control spectra, CX- age-matched control spectra for a given week; TX- spectra from DMBA-treated pouch for a given week, TOT- total (Diagonal elements are true positive predictions while non-diagonal elements represent misclassifications)

	WEEK 1				WEEK 2				WEEK 3				WEEK 4				WEEK 5				WEEK 6				WEEK 7			
	C0	CX	TX	TOT	C0	CX	TX	TOT	C0	CX	TX	TOT	C0	CX	TX	TOT	C0	CX	TX	TOT	C0	CX	TX	TOT	C0	CX	TX	TOT
C0	23	6	2	31	19	6	6	31	27	2	2	31	26	3	2	31	25	5	1	31	21	4	6	31	24	3	4	31
CX	5	12	16	33	5	17	10	32	3	16	14	33	1	14	12	27	2	29	5	36	1	25	4	30	0	17	13	30
TX	2	14	17	33	3	6	24	33	0	13	27	40	3	10	23	36	0	7	25	32	4	4	24	32	0	11	31	42

	WEEK 8				WEEK 9				WEEK 10				WEEK 11				WEEK 12				WEEK 13				WEEK 14			
	C0	CX	TX	TOT	C0	CX	TX	TOT	C0	CX	TX	TOT	C0	CX	TX	TOT	C0	CX	TX	TOT	C0	CX	TX	TOT	C0	CX	TX	TOT
C0	24	4	3	31	21	8	2	31	25	3	3	31	25	3	3	31	29	2	0	31	24	6	1	31	26	5	0	31
CX	7	9	11	27	5	22	4	31	1	21	8	30	5	48	15	68	3	31	0	34	4	27	3	34	5	29	0	34
TX	2	3	33	38	2	5	26	33	0	8	23	31	3	13	27	43	0	7	25	32	1	5	25	31	0	0	33	33

Table 3.2: LOOCV confusion matrix for ex vivo study, C0: week 0 control spectra, CX- age-matched control spectra for a given week; TX- spectra from DMBA-treated pouch for a given week, TOT- total (Diagonal elements are true positive predictions while non-diagonal elements represent misclassifications).

For additional insights, the LOOCV confusion matrices are also presented graphically in Figure 3.4. It is noteworthy that true classification is indicative of differences between the groups while misclassifications between groups suggest homogeneity and similarity in biochemical properties [321, 362, 363]. First, to understand true classification of Tx over 14 weeks, percentage of correct classification for treated group (Tx) was plotted against each week (Figure 3.4a). As continuous application of DMBA leads to development of tumours, the classification between spectra from DMBA treated pouch and vehicle control should increase with time. Percentage of correct classification for Tx (Figure 3.4a) increases from about 50% in week 1 to ~70% by the 7^{th} week, remains similar between 8-11 weeks, then increases to >90% by 14^{th} week.

Second, to understand trends of misclassification over 14 weeks during carcinogenesis, misclassifications were plotted- percentage of misclassification of Cx with C0; Tx with C0 and Tx with Cx; and are shown in Figure 3.4b.

Misclassifications between Cx vs C0 would suggest age related changes: if there is lack of significant age related changes, the misclassifications would remain almost same throughout 14 weeks and there should not be increase in classification efficiency. Graph suggests lack of age related changes.

Misclassifications in case of Tx vs C0 and Tx vs Cx: This should decrease with time due to increasing biochemical changes in DMBA painted pouches. In the initial weeks, all the pouches are healthy and thus misclassifications are expected. With time, due to DMBA application, HBP would change biochemically and similarities of C0 and Cx with Tx would decrease leading to decreasing percentage misclassification with respect to the controls. Thus Tx vs Cx/C0 would be indicative of changes due to DMBA induced carcinogenesis. As per the graph, misclassification

plot of Tx vs Cx/C0 suggests decreasing classification efficiency, which indirectly states that differences in DMBA treated pouches with respect to the two controls increased over the 14 week period of carcinogenesis.

Thus the ex vivo study demonstrates feasibility of studying sequential changes during DMBA induced carcinogenesis. However, this approach is invasive. It is known that non-invasive, in vivo approach is always desirable in a clinical set-up, especially for screening and therapeutic monitoring. Hence in vivo studies were carried out to ascertain above described findings of the ex vivo study.

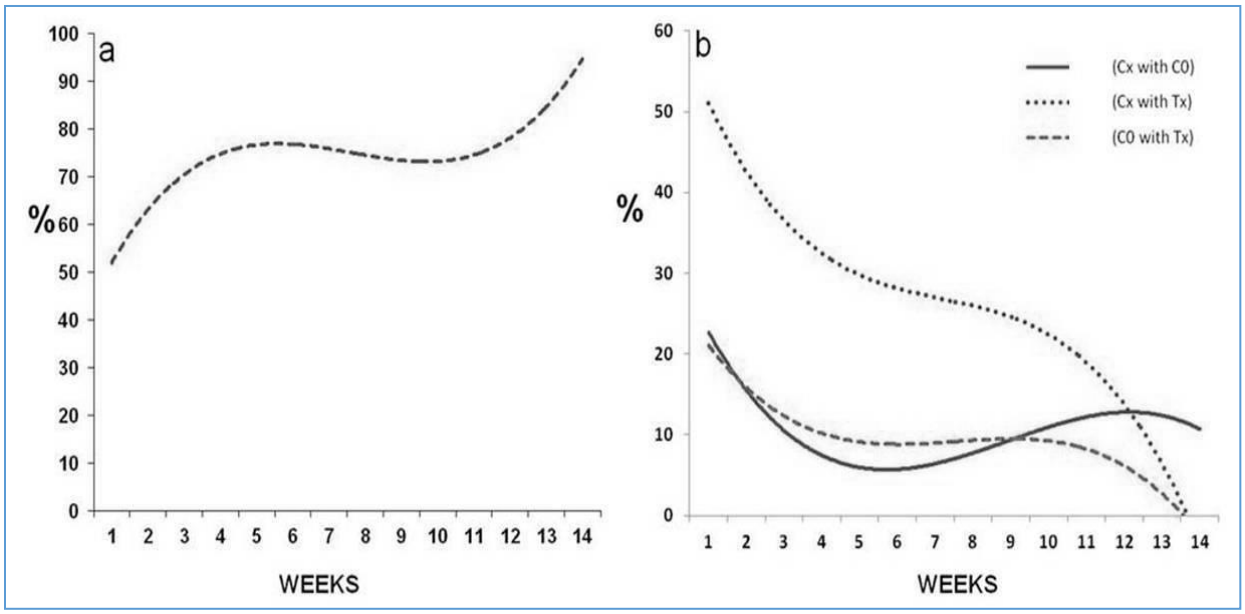

Figure 3.4: (a) Week wise true percentage classification of Tx for the ex vivo study (b) Week wise percentage misclassification of Cx with C0, Cx with Tx and C0 with Tx for the ex vivo study for the period of 14 weeks. Cx vs C0 suggests lack of significant age related changes as misclassifications are within a range throughout 14 weeks. Decreasing Tx vs C0 and Tx vs Cx suggests that over 14 weeks, misclassification decreased to 0 due to cancerous changes in DMBA painted pouches (X axis- Weeks; Y axis- percentage).

3.1.2.2 *In-vivo* sequential study:

In vivo study also exhibits changes similar to ex vivo study. Spectral features (Figure 3.5) and trends of PCA classification similar to the ex vivo study were observed in this approach. PCA plots are shown in Figure 3.6. To demonstrate these similarities PC-LDA and LOOCV data are shown as confusion matrices in Table 3.3 and Table 3.4, respectively and graphically presented in Figure 3.7. Percentage of correct classification for Tx (Figure 3.7a) increased from about 50% in week 1 to more than 60% by the 7^{th} week, remained similar between 8-11 weeks, then increased to more than 90% by 14^{th} week. Misclassification (Figure 3.7b) between C0 and Cx (continuous line) remained constant while C0 vs Tx (broken line) and Cx vs Tx (dotted line) decreased over the period of 14 weeks. Thus, trends were similar in ex vivo and in vivo sequential studies.

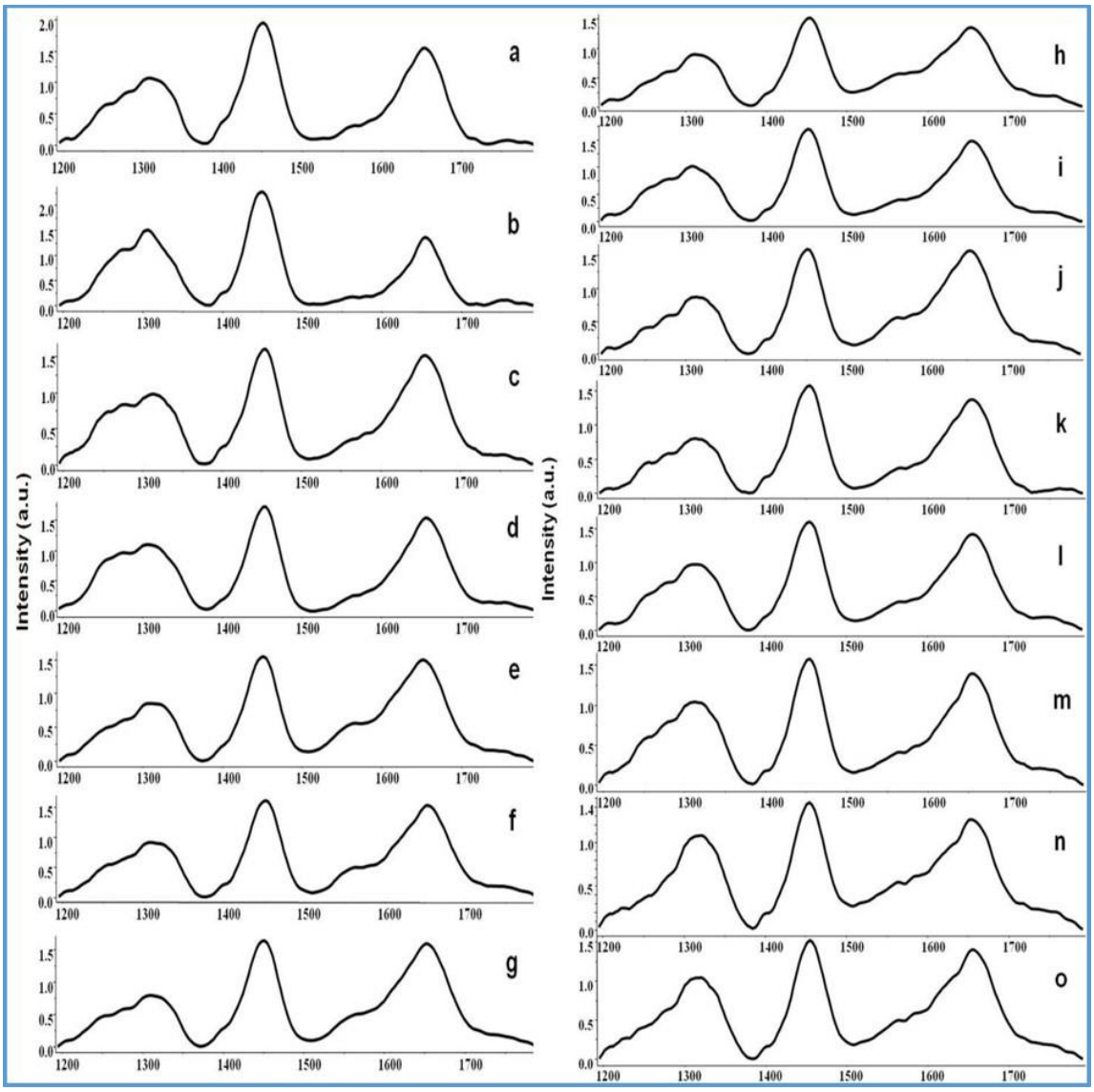

Figure 3.5: Mean spectra of DMBA treated hamster buccal pouch for in vivo sequential study. a-week 0, b- week 1, c-week2, d-week 3, e-week 4, f-week 5, g-week 6, h-week 7, i-week 8, j-week 9, k-week 10, l-week 11, m-week 12, n-week 13, o-week 14. The spectra are shown in the 1200 to 1800 cm^{-1} range and show decreasing lipid dominance and increasing protein/nucleic acid dominance with progression of carcinogenesis as in case of ex vivo study.

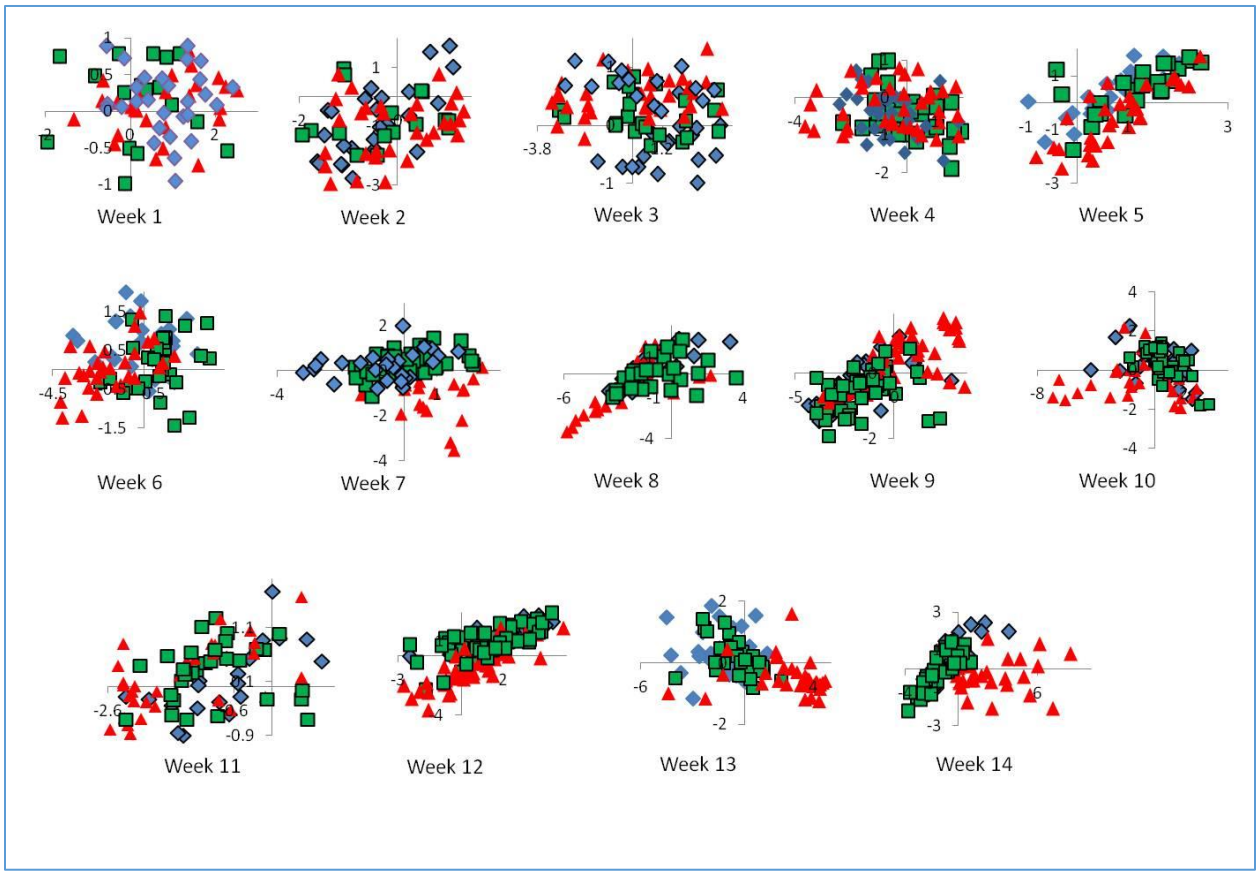

Figure 3.6: Scatter plots of PCA over the period of 14 weeks of DMBA treatment of Hamster buccal pouch; Segregation of spectra from DMBA treated pouches (triangles) can be observed from 6 weeks onwards while exclusive cluster can be observed in the 14 week spectra. (X-axis: Score of factor 1, Y-axis: Score of factor 2; C0- week 0 control spectra ♦), Cx- age-matched control spectra for a given week (■); Tx- spectra from DMBA-treated pouch (▲) for a given week).

	WEEK 1				WEEK 2				WEEK 3				WEEK 4				WEEK 5				WEEK 6				WEEK 7			
	C0	CX	TX	TOT	C0	CX	TX	TOT	C0	CX	TX	TOT	C0	CX	TX	TOT	C0	CX	TX	TOT	C0	CX	TX	TOT	C0	CX	TX	TOT
C0	19	5	5	29	18	10	1	29	22	5	2	29	26	2	1	29	19	6	4	29	6	13	10	29	23	4	2	29
CX	3	17	8	28	4	19	2	25	4	26	2	32	4	33	12	49	4	17	7	28	13	16	4	33	1	24	9	34
TX	5	7	20	32	5	9	10	24	1	6	17	24	0	10	20	30	5	7	20	32	9	1	20	30	2	3	22	27

	WEEK 8				WEEK 9				WEEK 10				WEEK 11				WEEK 12				WEEK 13				WEEK 14			
	C0	CX	TX	TOT	C0	CX	TX	TOT	C0	CX	TX	TOT	C0	CX	TX	TOT	C0	CX	TX	TOT	C0	CX	TX	TOT	C0	CX	TX	TOT
C0	19	8	4	29	21	8	2	31	16	1	12	29	15	11	3	29	26	5	1	29	21	5	3	29	24	5	0	29
CX	1	27	19	47	5	22	4	31	5	26	2	33	7	28	3	38	5	30	19	54	8	17	5	30	7	25	0	32
TX	0	19	35	54	2	5	26	33	19	3	24	36	6	4	22	32	3	7	45	55	6	1	23	30	1	3	26	30

Table 3.3: PC-LDA Confusion matrix for in vivo sequential study, C0: week 0 control spectra, C_X- age-matched control spectra for a given week; T_X- spectra from DMBA-treated pouch for a given week, TOT- total (Diagonal elements are true positive predictions while non-diagonal elements represent misclassifications).

	WEEK 1				WEEK 2				WEEK 3				WEEK 4				WEEK 5				WEEK 6				WEEK 7			
	C0	CX	TX	TOT	C0	CX	TX	TOT	C0	CX	TX	TOT	C0	CX	TX	TOT	C0	CX	TX	TOT	C0	CX	TX	TOT	C0	CX	TX	TOT
C0	19	5	5	29	19	9	1	29	20	7	2	29	26	2	1	29	19	5	5	29	6	13	10	29	23	4	2	29
CX	3	17	8	28	4	18	3	25	4	26	2	32	4	33	12	49	3	17	8	28	13	16	4	33	2	24	8	34
TX	5	7	20	32	5	9	10	24	2	5	17	24	0	10	20	30	5	7	20	32	9	1	20	30	3	3	21	27

	WEEK 8				WEEK 9				WEEK 10				WEEK 11				WEEK 12				WEEK 13				WEEK 14			
	C0	CX	TX	TOT	C0	CX	TX	TOT	C0	CX	TX	TOT	C0	CX	TX	TOT	C0	CX	TX	TOT	C0	CX	TX	TOT	C0	CX	TX	TOT
C0	19	7	3	29	21	8	2	31	17	1	11	29	15	12	2	29	24	4	1	29	22	5	2	29	24	5	0	29
CX	1	29	17	47	5	22	4	31	5	26	2	33	7	29	2	38	5	30	19	54	9	16	5	30	7	25	0	32
TX	0	19	35	54	2	5	26	33	10	2	24	36	6	4	22	32	3	5	47	55	6	1	23	30	1	3	26	30

Table 3.4: LOOCV Confusion matrix for in vivo sequential study, C0: week 0 control spectra, C_X- age-matched control spectra for a given week; T_X- spectra from DMBA-treated pouch for a given week, TOT- total (Diagonal elements are true positive predictions while non-diagonal elements represent misclassifications).

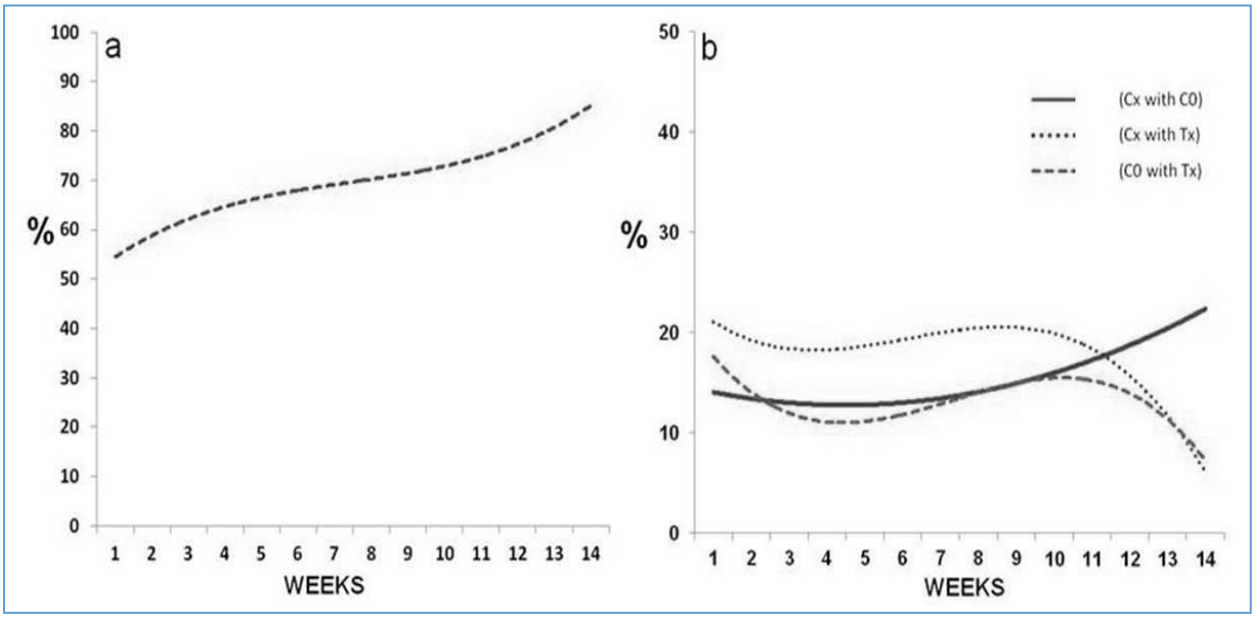

Figure 3.7: (a) Week wise true percentage classification of Tx; (b) Week wise percentage misclassification of Cx with C0, Cx with Tx and C0 with Tx for in vivo sequential study for the period of 14 weeks. Cx vs C0 suggests lack of significant age related changes as misclassifications are within a range throughout 14 weeks. Decreasing Tx vs C0 and Tx vs Cx suggests that over 14 weeks, misclassification approaches to 0 due to cancerous changes in DMBA painted pouches (X axis- Weeks; Y axis- percentage).

3.1.2.3 *In-vivo* follow-up study

Follow up studies allow monitoring of changes in vivo in the same animals, avoiding inter-animal variations and also require fewer animals. Thus in vivo follow up approach was also employed. Spectral features and PCA trends were observed to be similar to ex-vivo and sequential in vivo studies as shown in Figure 3.8 and Figure 3.9, respectively. PC-LDA and LOOCV results show similarities to the previous approaches, as shown as confusion matrices in Table 3.5 and Table 3.6, respectively and graphically presented in Figure 3.10. True classification as shown in Figure 3.10 a increased from 0-7 weeks, plateaued around 8-11 weeks and then increased beyond 80% by 14^{th} week, whereas misclassifications between C0 and Tx, Cx and Tx decreased while C0 and Cx remained almost similar (Figure 3.10b).

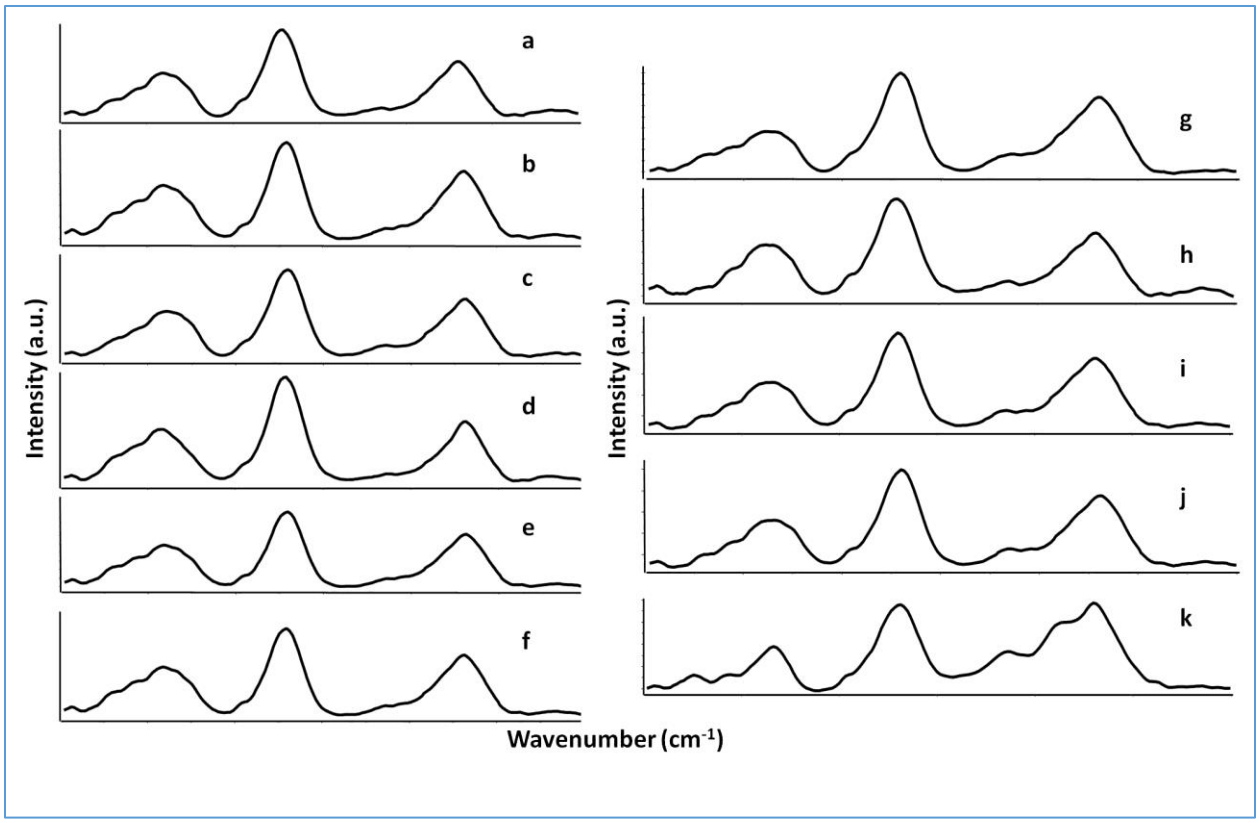

Figure 3.8: Mean spectra of DMBA treated hamster buccal pouch for in vivo follow up study. a-week 1, b- week 2, c-week 4, d-week 5, e-week 6, f-week 8, g-week 9, h-week 10, i-week 12, j-week 13, k-week 14. The spectra are shown in the 1200 to 1800 cm^{-1} range and show decreasing lipid dominance and increasing protein/nucleic acid dominance with progression of carcinogenesis as in case of ex vivo study. Some data points are missing (Week 3,7,11) as spectra could not be acquired due to reasons such as bleeding from buccal pouch (week 3 and 11) or early revival of hamsters in spite of anaesthetization (week 7).

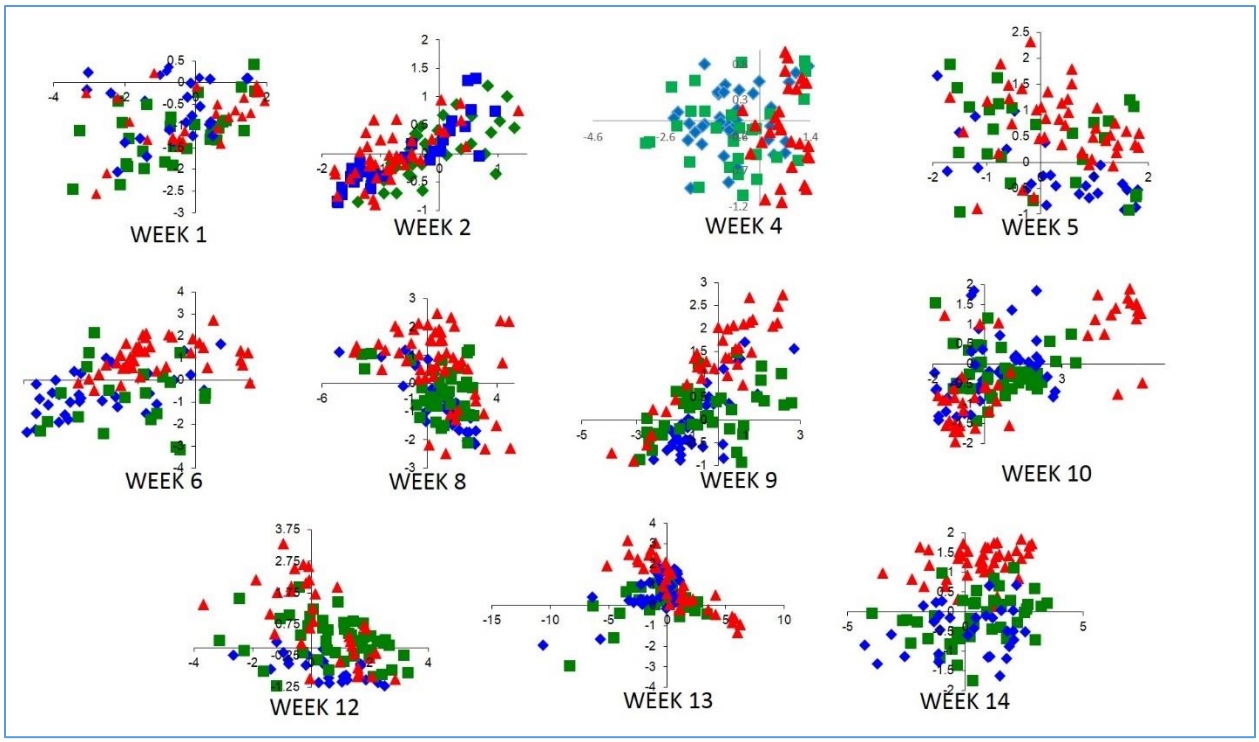

Figure 3.9: Scatter plots of PCA for in vivo follow up study; Segregation of spectra from DMBA treated pouches (triangles) can be observed from 6 weeks onwards while exclusive cluster can be observed in the 14 week spectra. (X-axis: Score of factor 1, Y-axis: Score of factor 2; C0- week 0 control spectra ( ), Cx- age-matched control spectra for a given week ( ); Tx- spectra from DMBA-treated pouch ( ) for a given week). Some data points are missing (Week 3,7,11) as spectra could not be acquired due to reasons such as bleeding from buccal pouch (week 3 and 11) or early revival of hamsters in spite of anaesthetization (week 7).

	WEEK 1				WEEK 2				WEEK 4				WEEK 5				WEEK 6				WEEK 8			
	C0	CX	TX	TOT	C0	CX	TX	TOT	C0	CX	TX	TOT	C0	CX	TX	TOT	C0	CX	TX	TOT	C0	CX	TX	TOT
C0	19	5	5	29	19	5	5	29	25	13	7	45	38	2	5	45	28	12	5	45	35	7	3	45
CX	10	21	8	39	6	20	4	30	5	22	4	31	1	23	8	32	9	10	14	33	8	18	11	37
TX	7	8	26	41	4	5	16	25	1	8	19	28	5	9	21	35	2	10	35	47	4	8	43	55

	WEEK 9				WEEK 10				WEEK 12				WEEK 13				WEEK 14			
	C0	CX	TX	TOT	C0	CX	TX	TOT	C0	CX	TX	TOT	C0	CX	TX	TOT	C0	CX	TX	TOT
C0	25	11	8	44	33	10	2	45	39	6	0	45	43	2	0	45	34	3	8	45
CX	7	28	4	39	10	25	8	43	8	29	10	47	1	25	8	34	5	32	10	47
TX	6	8	37	51	5	10	26	41	4	7	36	47	0	8	28	36	1	3	38	42

Table 3.5: PC-LDA Confusion matrix for in vivo follow up study, C0: week 0 control spectra, C_X- age-matched control spectra for a given week; T_X- spectra from DMBA-treated pouch for a given week, TOT- total (Diagonal elements are true positive predictions while non-diagonal elements represent misclassifications). Some data points are missing (Week 3,7,11) as spectra could not be acquired due to reasons such as bleeding from buccal pouch (week 3 and 11) or early revival of hamsters in spite of anaesthetization (week 7).

	WEEK 1				WEEK 2				WEEK 4				WEEK 5				WEEK 6				WEEK 8			
	C0	CX	TX	TOT	C0	CX	TX	TOT	C0	CX	TX	TOT	C0	CX	TX	TOT	C0	CX	TX	TOT	C0	CX	TX	TOT
C0	19	5	5	29	19	5	5	29	25	13	7	45	38	2	5	45	28	11	6	45	35	7	3	45
CX	10	21	8	39	6	21	3	30	5	22	4	31	1	23	8	32	9	10	14	33	8	18	11	37
TX	8	7	26	41	4	5	16	25	1	8	19	28	5	9	21	35	1	10	36	47	4	9	42	55

	WEEK 9				WEEK 10				WEEK 12				WEEK 13				WEEK 14			
	C0	CX	TX	TOT	C0	CX	TX	TOT	C0	CX	TX	TOT	C0	CX	TX	TOT	C0	CX	TX	TOT
C0	25	11	8	44	33	10	2	45	39	6	0	45	43	2	0	45	35	3	7	45
CX	8	27	4	39	10	25	8	43	8	29	10	47	1	25	8	34	5	32	10	47
TX	5	9	37	51	5	10	26	41	4	7	36	47	0	8	28	36	0	4	38	42

Table 3.6: LOOCV Confusion matrix for in vivo follow up study, C0: week 0 control spectra, C_X- age-matched control spectra for a given week; T_X- spectra from DMBA-treated pouch for a given week, TOT- total (Diagonal elements are true positive predictions while non-diagonal elements represent misclassifications). Some data points are missing (Week 3,7,11) as spectra could not be acquired due to reasons such as bleeding from buccal pouch (week 3 and 11) or early revival of hamsters in spite of anaesthetization (week 7).

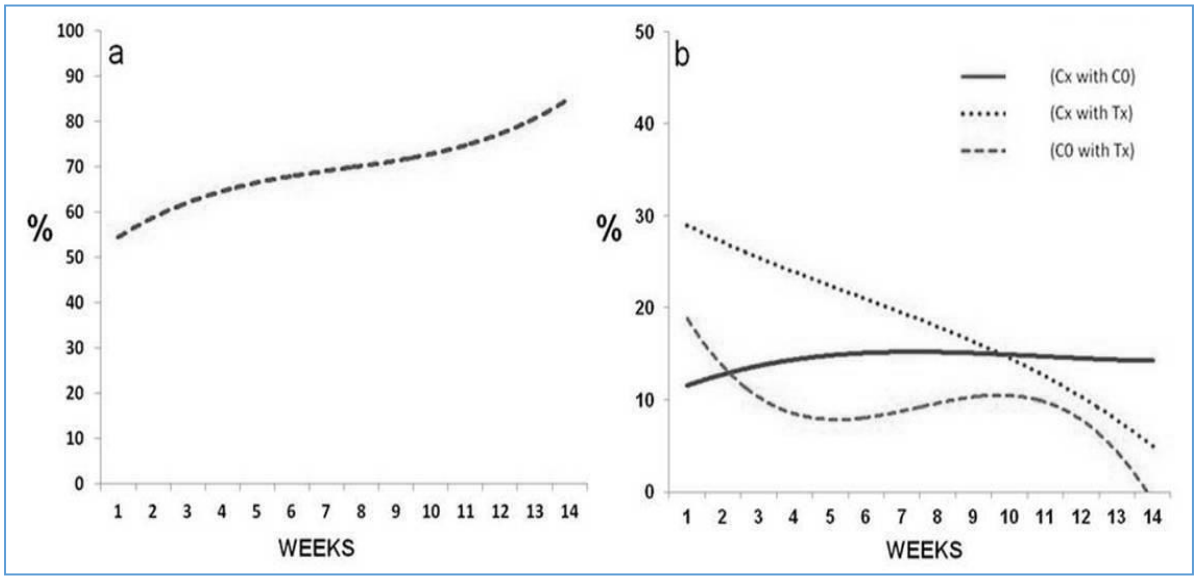

Figure 3.10: a) Week wise true percentage classification of Tx; (b) Week wise percentage misclassification of Cx with C0, Cx with Tx and C0 with Tx for in vivo follow-up study for the period of 14 weeks. Cx vs C0 suggests lack of significant age related changes as misclassifications are within a range throughout 14 weeks. Decreasing Tx vs C0 and Tx vs Cx suggests that over 14 weeks, misclassification approaches to 0 due to cancerous changes in DMBA painted pouches (X axis- Weeks; Y axis- percentage).

3.1.2.4 A note on classifications and misclassification

True classification is indicative of differences between the groups while misclassifications between groups suggest homogeneity and similarity in biochemical properties. Hence, both true classifications and misclassifications have been used to draw inference in this study. In case of the DMBA painted pouches (Figure 3.4a-Figure 3.10a), true classification trend shows progressive increase from ~50% in week 1 to ~100% in week 14, indicating potential of RS in identifying sequential changes. But, sometimes, true classification may not represent the complete picture in case of biochemically similar groups. For example, as C0 and age matched controls are of similar nature, they are expected to misclassify, leading to poorer classifications. Had there been a significant age-related difference over 14 weeks, misclassifications between C0 and age-matched controls should have decreased by 14 weeks leading to better classification. No change in misclassification between C0 and Cx over 14 weeks suggest homogeneity owing to possible lack of appreciable age-related changes. On similar lines, higher misclassifications between Tx and Cx/C0 during the early weeks indicate similarity. The similarities decrease with progression of carcinogenesis, leading to decreased misclassification which, as expected, reaches to a minimum by 14 weeks of DMBA application.

3.1.2.5 Visual and histopathological support

The animals were inspected for visual changes thrice a week and photograph was taken weekly. As shown in Figure 3.11 and Figure 3.12, following changes were observed in buccal pouches of hamsters:

a) visibly and histopathologically normal – Vehicle controls; pouches with 0, 1 week post carcinogen application.

b) inflammatory and ulcerative changes in response to DMBA toxicity are observed after 2 and 3 weeks of carcinogen application (histopathologically hyperplastic).

c) visually normal/ ablation of inflammation (attributable to mucosal recovery), are observed from 3 to 6/7 week; histopathologically these tissues show hyperplasia and a few low grade dysplasia (LGD) regions.

d) visible reddening of mucosa (erythema) appear after 7 weeks; histopathologically these tissues present hyperplasia, LGD and high grade dysplasia (HGD).

e) mucosal roughening and small papillomas are observed 9^{th} week onwards while, f) frank tumours which are pathologically SCC are seen 12 to 14 weeks post carcinogen application. Majority of vehicle-treated HBPs were visibly and histopathologically normal throughout the duration of the study.

Representative H&E stained images for weeks 1 to 14 for the DMBA treated HBP has been shown in Figure 3.13.

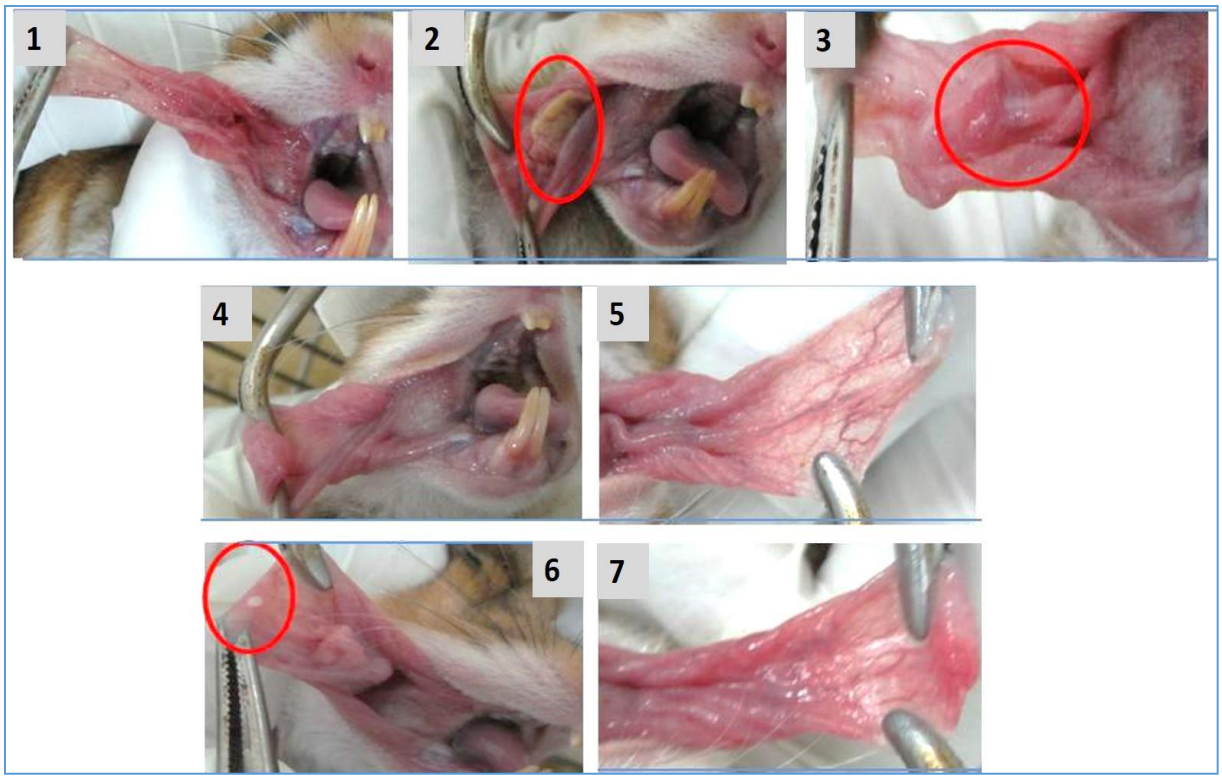

Figure 3.11: Representative photographs showing visual changes in hamster buccal pouch over weeks 1 to 7 in response to application of DMBA. Most of the pouches were visually normal, except for week 2/3 pouches which show inflammatory and ulcerative changes in response to DMBA toxicity, and week 6 where the circled region shows a leukoplakia like patch.

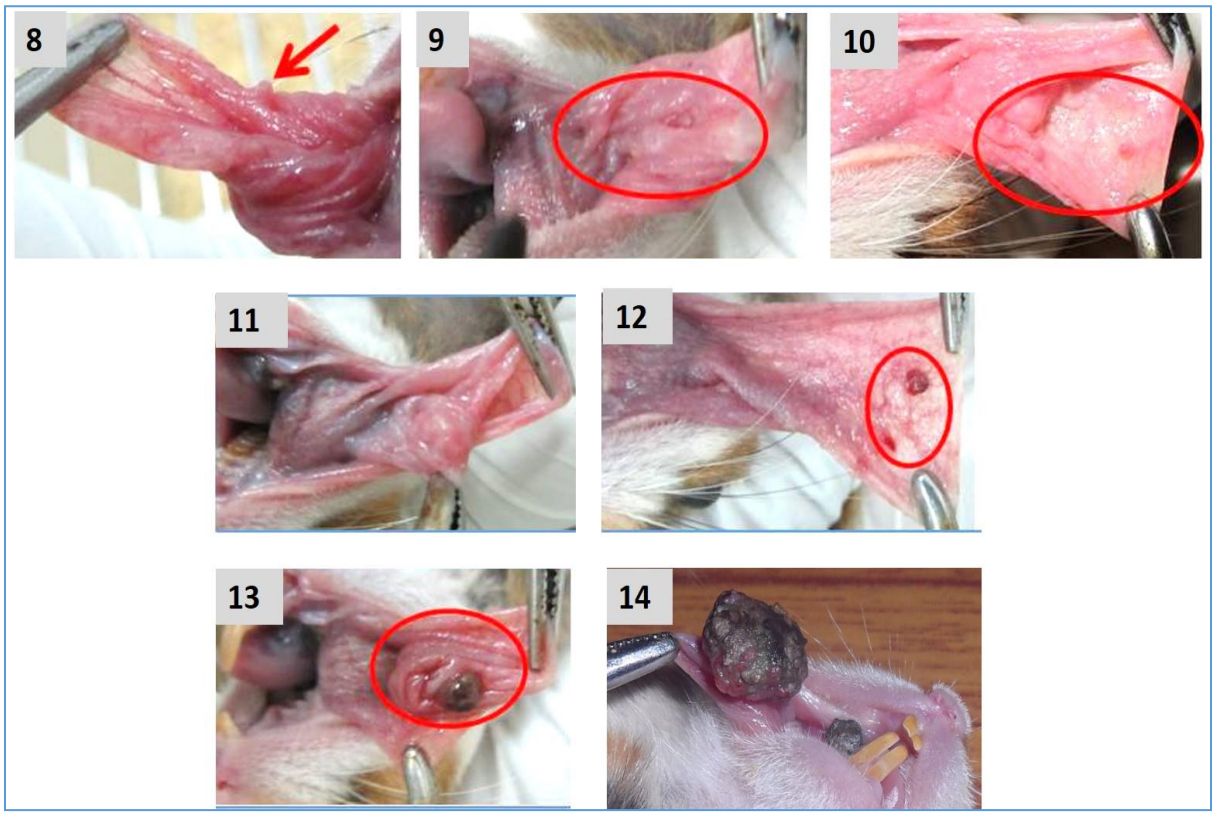

Figure 3.12: Representative photographs showing visual changes in hamster buccal pouch over weeks 8 to 14 in response to application of DMBA. Small papillomas start appearing (indicated by arrow in week 8). Tumours can be observed from week 12 onwards.

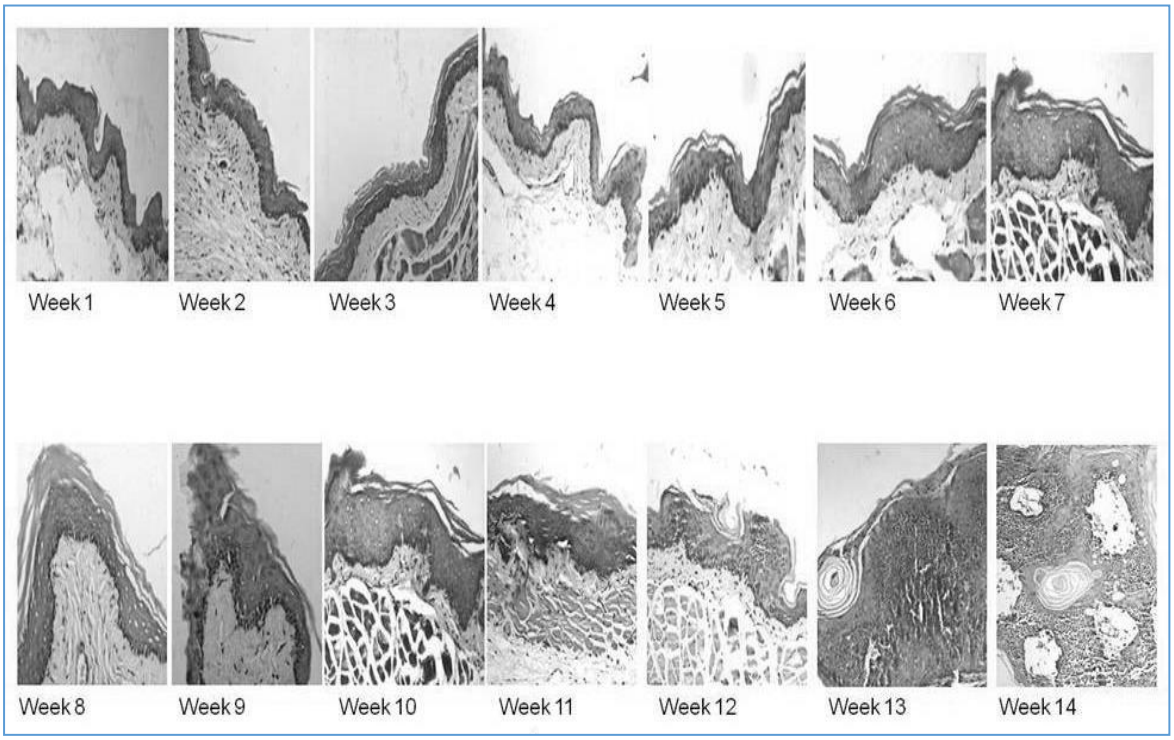

Figure 3.13: Representative histopathology images of hamster buccal pouch over the 14 weeks of DMBA painting. Normal epithelium with all the epithelial layers were observed in the healthy controls and early weeks of DMBA treatment. This was followed by increased cell division and hyperplastic changes (week 3 onwards), dysplastic changes (week 7 onwards) and SCC (week 12 onwards). It should be noted that any tissue section doesn't contain one particular stage exclusively; rather, a given section can have more than two stages. In the present studies, best efforts were made to get assess the histopathological status of the laser probed regions.

3.1.2.6 Misclassifications between treated and controls

Repeated observations of misclassifications of Tx spectra with controls suggested a relook into the analysis. Instead of attributing the observation to tissue heterogeneity in the DMBA painted pouches, it was decided to carefully re-examine the histopathology of control pouches as well. Histopathological analysis of these control tissues have revealed hyperplastic changes in small areas in many age-matched controls and dysplastic changes in small regions in a few control slides. A probable reason for these abnormal changes could be injuries in the pouch due to repeated pulling out of HBP by forceps. Moreover, hamsters store the food pellets in their pouch which may lead to further mechanical irritation, resulting into small areas of abnormalities. Chronic mechanical irritation has also been shown to be a causative factor in oral cancers [20, 21]. Representative abnormal areas in histopathological sections from two different control pouches are shown in Figure 3.14. Another reason for observed misclassification could be due to differences in the Raman probed area (~200 microns) and the sections used for histopathology evaluation. In order to get better histopathological evaluation, three sections of 5 micron were analyzed owing to practical limitations. Thus despite best of efforts, microheterogenity within the 200 micron of probed area cannot be ruled out.

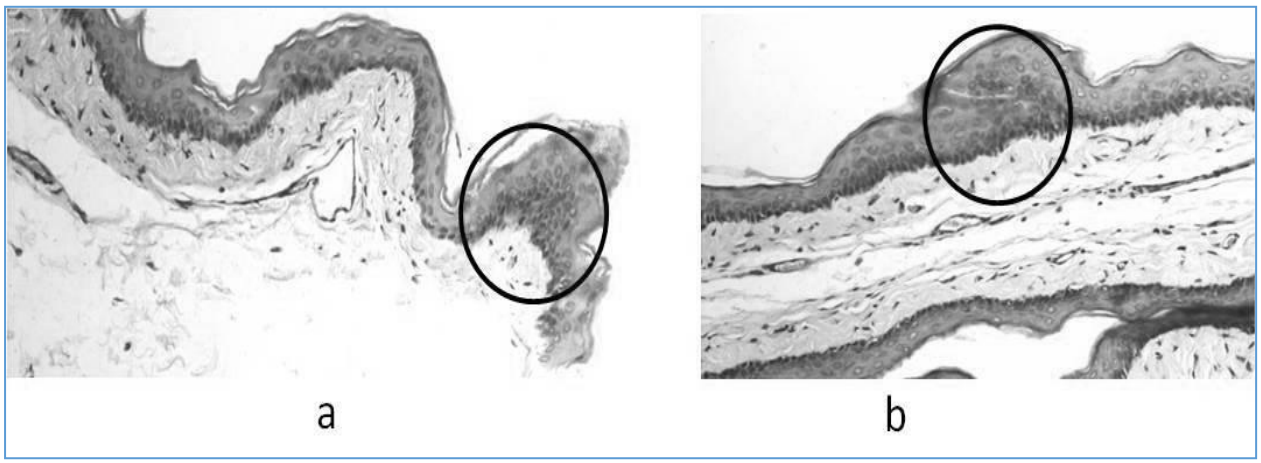

Figure 3.14: Representative images of abnormal areas (in circle) observed in control pouches. As these sections were obtained from vehicle control buccal pouch tissues, they were supposed to be normal. However, certain regions showed higher cell proliferation which could be attributed to repeated mechanical injuries, caused by forceps and food pellets. In the present studies, best efforts were made to assess the histopathological status of the laser probed regions. These control pouches were from the 12^{th} and 14^{th} week of the experiment.

On the basis of observations in this section, the process of carcinogenesis in HBP model can be grouped into three sub-phases- week 0-7, week 8-11 and week 12 to 14. Weeks 0 to 7 show progressive increase in classification efficiency of DMBA treated pouches due to accumulation of hyperplastic and dysplastic changes. Week 8-11 show a similar classification efficiency (plateau phase) suggesting non-appreciable changes during this phase. Histopathology-based evaluation suggests accumulation of hyperplastic and dysplastic changes over these weeks. Various studies on biomarkers like P53, c-Myc, Ki67 have shown culmination of marker co-expression, around 10 weeks of DMBA painting in HBP model [364, 365]. Thus, homogeneity in these conditions could have led to plateauing phase around 8-11 weeks. By 12^{th} week, these changes progress towards SCC with well-defined tumours, and might explain increased classification from 12^{th} to 14^{th} week. Similar trends of classification and misclassification were observed in both, the ex vivo and in vivo approaches. Thus, in vivo diagnosis through RS is quite comparable to ex vivo findings supported by the gold-standard histopathology, giving further proof of RS being a promising non-invasive diagnostic adjunct for screening/diagnosis of oral cancers.

3.1.3 Summary

In this RS study, sequential progression in experimental oral carcinogenesis in the HBP model was explored using three approaches- ex vivo, in vivo sequential and in vivo follow up. In all these studies, spectral changes show lipid dominance in early stages while later stages and tumours showed increased protein to lipid ratio, nucleic acids. On similar lines, early weeks of DMBA treated and control groups showed higher overlap and low classification. Multivariate analysis indicated increasing efficiency of classification with the duration of carcinogen

application. Sensitivity was 70% by week 8, 70 to 80% for week 9 to 11 and 80 to 100% for week 12 to 14. Thus classification increased progressively till 8 weeks, reached a plateau phase between 8 and 12 weeks and subsequently increased upto 100 % by 14 weeks. The misclassifications between treated and control spectra suggested some changes in controls as well, which was confirmed by careful examination of histopathological slides. This suggests RS may be able to identify microheterogeneity which can often go unnoticed in conventional biochemistry wherein tissue extracts are employed, as well as in histopathology. Further, good correlation between both ex vivo and in vivo approaches indicate in vivo diagnosis through RS is quite comparable to ex vivo findings supported by gold-standard, giving further proof of RS being a promising label-free, non-invasive diagnostic adjunct for future clinical applications.

3.2 Comparison of RS vis a vis histopathology and cyclin D1 and investigation of abnormal changes in control tissues

As described in Chapter 3.1, ex vivo and in vivo Raman spectroscopic evaluation of progression of buccal pouch carcinogenesis with respect to vehicle controls was monitored. Further, some control sections suggested abnormalities [191]. In this chapter, standard spectral models were built using spectra corresponding to intermediate stages in carcinogenesis based on histopathological status, i.e. normal, hyperplasia, dysplasia and SCC; and abnormal cell proliferation through IHC of cyclin D1. The models were used to evaluate independent spectra obtained from exclusive set of DMBA treated animals (not used in standard models) and different controls. To investigate abnormal changes in controls tissues, three different types of controls - vehicle controls, DMBA contralateral controls and vehicle contralateral controls, which were exposed to varying period of forceps-handling, were analyzed along with DMBA painted pouches.

3.2.1 Spectral Acquisition

A total of 115 six to eight weeks old Golden Syrian male hamsters (*Mesocricetus auratus*) were used in the study. 70 HBP were painted with DMBA (test group) while 45 were oil painted (vehicle control) using protocol [191, 333, 366] described in Chapter 2. The schematic of experimental protocol is shown in Figure 3.15. In order to carry out stage wise histopathology and immunohistochemical (IHC) analysis, the study was carried out, ex vivo. 5 test and 3 controls animals were sacrificed each week. Buccal pouches were then excised out and further processed for RS and histopathology, as mentioned in Chapter 2.5.3.

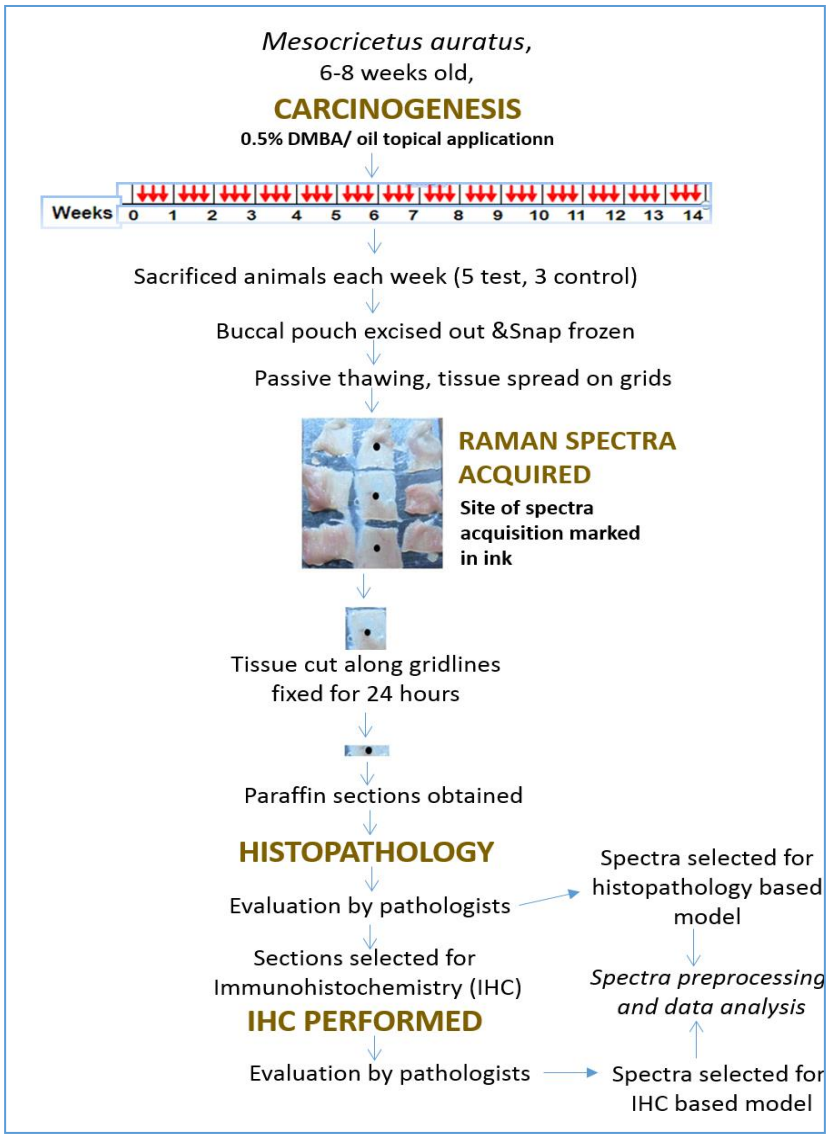

Figure 3.15: Overall schematic of the study. As explained in the text, Raman spectra were acquired ex vivo and were labeled on the basis of the histopathological status of the Raman probed regions. Further, Cyclin D1 expression was studied and another set of labeling was done on basis of Cyclin D1 expression. These two sets of labeled spectra were used for building 2 different models and were evaluated by independent test and control spectra obtained from another set of hamsters.

3.2.2 Findings

PC-LDA models were built using spectra selected with respect to histopathology stages as well as IHC grades; followed by LOOCV and test spectra from exclusive set of DMBA treated animals. In the final step, in order to understand the nature of misclassifications, different types of controls (vehicle control, vehicle contralateral control and DMBA contralateral control) were evaluated against the above developed standard models.

3.2.2.1 Histopathology based spectral model

Bearing in mind that histopathology is the gold-standard, the first standard model was built using histopathologically-certified spectra. Spectra were labeled as per the pathological status- healthy, hyperplasia, dysplasia or SCC of their corresponding tissue sections, and have been referred as 'histopathologically certified spectra'. Thus identified 43, 46, 36 and 37 histopathologically certified spectra from 31 animals for normal, hyperplasia, dysplasia and SCC, respectively were used for model building.

Spectral features:

Mean spectra were calculated from the above mentioned histopathologically certified spectra. Figure 3.16 shows the mean spectra corresponding to 43 healthy, 46 hyperplastic, 36 dysplastic and 37 SCC sections. Healthy spectra showed - 1301 cm^{-1}, 1310 cm^{-1}, δCH_2 (1448 cm^{-1}) and ester bands (1750 cm^{-1}) which indicate dominance of lipid features[367] whereas SCC spectra showed dominance of proteins and nucleic acids with change in features in 1200-1400 cm^{-1} regions, CH_2 (1454 cm^{-1}), 1560 cm^{-1} to 1583 cm^{-1}, and broad Amide I (1651 cm^{-1}). The

pathological tissues, through hyperplastic, dysplastic and SCC spectra showed changes in Amide III and Amide I regions which progressively indicate increased protein dominance. The changes also include broadening of Amide I band. These spectral features corroborate with reports on spectra of human buccal mucosa [336, 337]. A probable explanation for this observation could be changes in expression profile of various proteins during pathological conditions, leading to protein dominating spectra [10]. These findings further corroborate with earlier reports of ex vivo and in vivo RS studies on human subjects as well as hamster models [9, 332, 336, 337]. 1563 cm^{-1} band may be attributed to increased nucleic acids, also observed in prior studies [332]. As per our observations in the pathological HBP, extensive blood vessel network was prominently visible, especially in late weeks. Thus 1583 cm^{-1} band may be assigned to heme proteins abundant on account of angiogenesis- a hallmark of carcinogenesis[23].

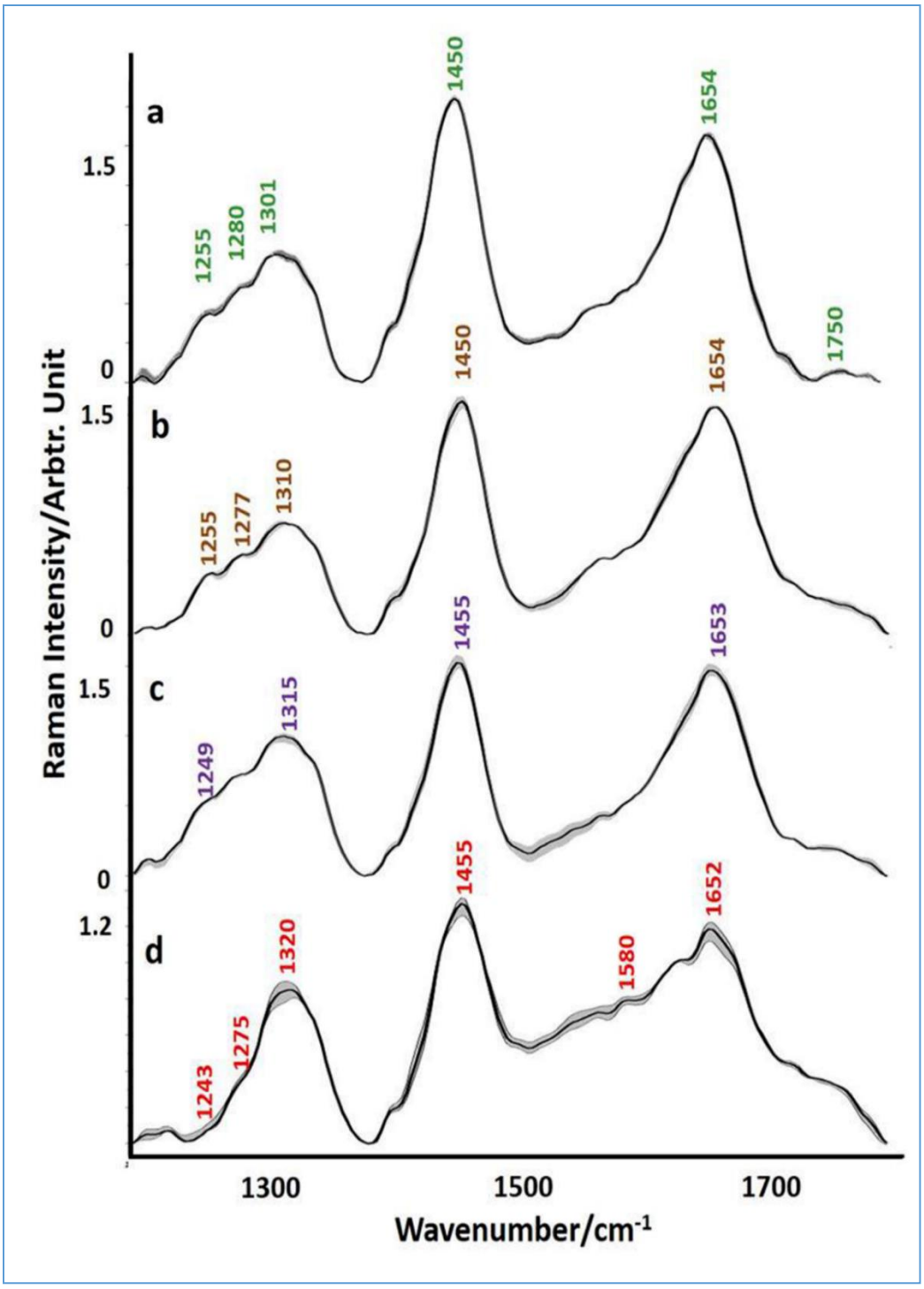

Figure 3.16: Mean spectra of intermediate histopathological stages in experimental oral carcinogenesis. a: control, b: hyperplasia, c: dysplasia, d: SCC.

Unsupervised analysis

Vector normalized first derivatives of the prereprocessed spectra were subjected to unsupervised PCA. Ten factors were explored for trends in classification. Scores of factor 1 was plotted against scores of factor 2 to obtain the scatter plot. The scatter plot reveals tendency of classification for the cancer stages, with healthy controls and SCC spectra forming exclusive clusters. Hyperplasia and dysplastic spectra showed overlap with each other as well as spectra from healthy controls. Loading factors and scatter plots have been shown in Figure 3.17.

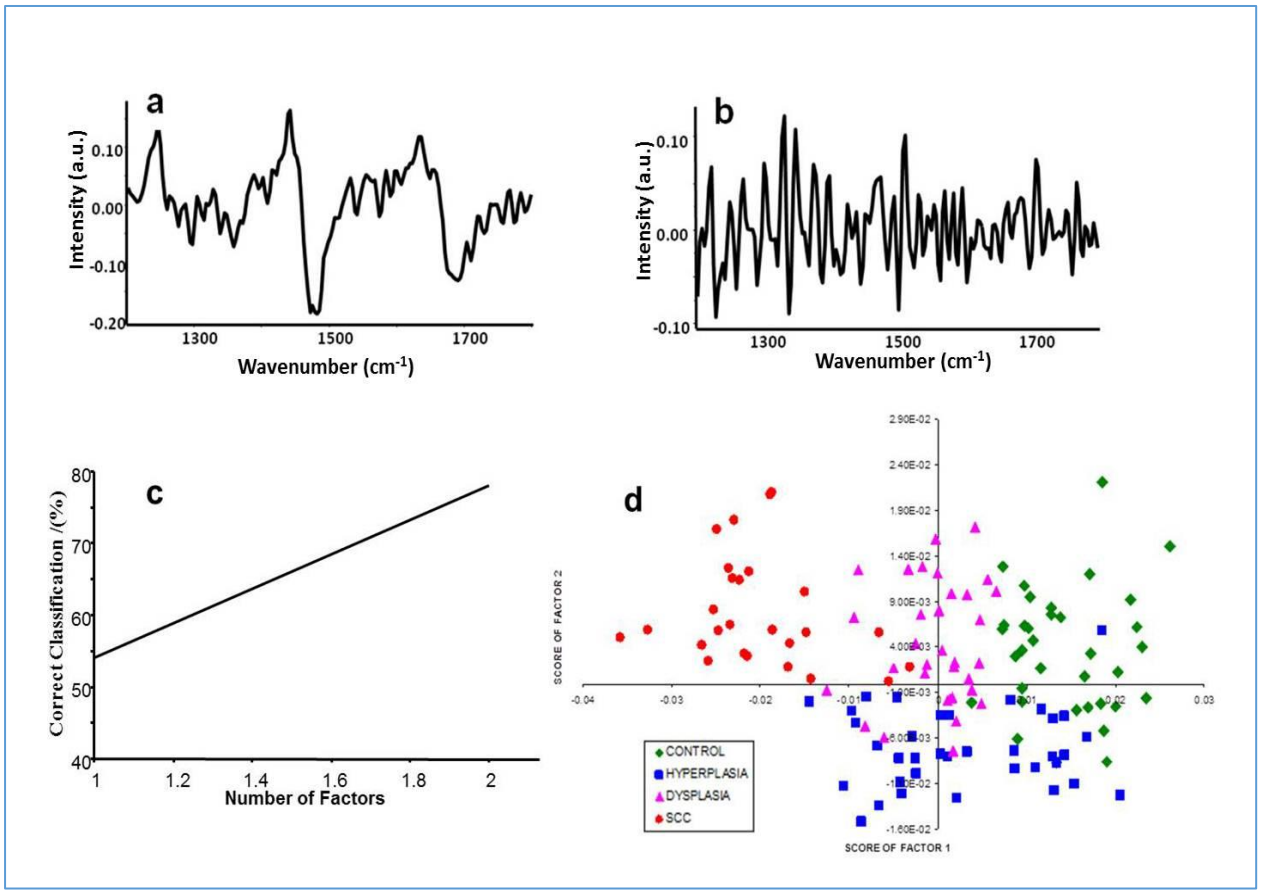

Figure 3.17: Histopathology based model. a and b: Factor loadings for PC1 and PC2; c: PC-LDA scree plot for correct classification; d: PCA scatter plot for factor 1 (X axis) against factor 2 (Y axis).

Supervised analysis

Supervised analysis was used to build the standard model to explore classification as well as evaluation of independently obtained spectra.

Standard model: As mentioned earlier, PC-LDA models were built for normal, hyperplasia, dysplasia and SCC. The classification contributed by 10 factors has been shown as scree plot in Figure 3.17c. First 2 factors accounted for 78% classification were subsequently used for model building. PC-LDA findings were evaluated by LOOCV and results have been presented in Table 3.7 (PC-LDA model) and Table 3.8 (LOOCV data). LOOCV results suggest that out of 43 control spectra, 28 were correctly classified, 11 misclassified with hyperplasia and 4 with dysplasia. In case of hyperplasia, 29 out of 46 spectra were truly classified while 12, 2 and 3 spectra misclassified respectively with control, dysplasia and SCC. Dysplasia showed true classification for 24 out of 36 spectra. Misclassifications with control and hyperplasia were 1 and 10, respectively. For SCC spectra, true classification was observed for 31 out of 37 spectra while 3 spectra each misclassified with hyperplasia and dysplasia.

	Control	Hyperplasia	Dysplasia	SCC	Total
Control	28	11	4	0	43
Hyperplasia	12	29	2	3	46
Dysplasia	1	10	24	1	36
SCC	0	4	3	30	37

Table 3.7: Histopathology based spectral model- confusion matrix for PC-LDA training model (Diagonal elements are true positive predictions while non-diagonal elements represent misclassifications).

	Control	Hyperplasia	Dysplasia	SCC	Total
Control	**28**	11	4	0	43
Hyperplasia	12	**29**	2	3	46
Dysplasia	1	10	**24**	1	36
SCC	0	3	3	**31**	37

Table 3.8: Histopathology based spectral model- confusion matrix after LOOCV. (Diagonal elements, shown in bold, are true positive predictions while non-diagonal elements represent misclassifications).

Evaluation of standard model

The standard model was first evaluated against Tx spectra from DMBA treated pouches. For ease in understanding, the Tx spectra obtained over the period of 14 weeks were subdivided into 4 groups: T1-T3, T4-T7, T8-T11 and T12-T14 spectra. These four groups were created on basis of histopathological observations as majority spectra in these groups consist of healthy, hyperplasia, dysplasia and SCC, respectively. As shown in Table 3.9, for T1 to T3, out of 100 spectra 63, 34 and 3 spectra were predicted as control, hyperplastic and dysplastic, respectively. For T4-T7, out of 164 spectra, 60, 79 and 23 spectra were predicted as control, hyperplastic and dysplastic, respectively. For T8-T11, out of 151 spectra, 24, 40, 61 and 26 spectra were predicted respectively as control, hyperplastic, dysplastic and SCC. Thus the number of spectra being predicted as higher pathologies increased with the duration of DMBA application. In case of T12 to T14, out of 101 spectra, none were predicted as controls while 86 spectra were classified as dysplastic or SCC. As hyperplasia could be due to various reasons like injury and inflammation, it may not necessarily be a precancer stage. Thus, Spectra being predicted as dysplastic or SCC are being considered potentially cancerous. We observe that almost 85% (86 out of 101) spectra from 12 to 14 weeks are predicted as dysplastic/SCC, whereas only 3% (3 out of 100) spectra from week 1 to 3 are classified as dysplastic/SCC or as potentially cancerous. The observations suggest Raman spectroscopy based prediction is in agreement with histopathological observations.

	Control	Hyperplasia	Dysplasia	SCC	Total
T1-T3	63	34	3	0	100
T4-T7	60	79	23	2	164
T8-T11	24	40	61	26	151
T12-T14	0	15	32	54	101

Table 3.9: Evaluation of histopathology based model using exclusive spectra from DMBA painted HBP. The spectra were grouped as T1-T3, T4-T7, T8-T11 and T12-T14. With increase in the duration of DMBA application, the number of spectra being predicted as higher pathologies (dysplastic/SCC) increases. Almost 85% (86 out of 101) spectra from 12 to 14 weeks are predicted as dysplastic/SCC.

3.2.2.2 Cyclin D1 based spectral model

As is well known, biochemical changes precede morphological changes, evaluation based on suitable biomarker expressions can also serve as a reliable additional scrutiny. HBP has shown comparable expression of biomarkers like P53, Bcl2, PCNA and Cyclin D1 with respect to human oral mucosa [83]. Cyclin D1 has a major regulatory role at G1/S checkpoint and is an important biomarker as deregulation of G1 to S phase progression of cell cycle and is a common target in carcinogenesis [368]. Many studies have reported over expression of Cyclin D1 in head and neck, oral, laryngeal and nasopharyngeal carcinoma [17, 369]. Hence, abnormal cell proliferation through cyclin D1 expression was also employed to build standard model and evaluate the independent test set, which included controls. Cyclin D1 expression was graded on scale of 0 to +3 (minimum/healthy to maximum/SCC). In this thesis, 0, +1, +2 and +3 levels of expression have been denoted as G0, G1, G2 and G3 respectively. G0 and G1 grades show zero or minimum expression of the biomarkers, usually observed in controls and early weeks, G2 shows intermediate amount of expression in tissue sections which could be histopathologically severely hyperplastic/dysplastic while G3 involves expression in maximum/entire regions in a tissue section, usually in tumours or later stages of carcinogenesis.

IHC

Following the protocol mentioned in Chapter 2, IHC based models were built from 30 animals after evaluation of sections on the basis of cyclin D1 expression. Standard model was built using 23, 20, 20 and 19 spectra corresponding to G0, G1, G2 and G3 grades, respectively.

Spectral Features: Figure 3.18 shows the mean spectra for G0, G1, G2 and G3. G0 spectra resemble healthy spectra with dominance of lipid features- 1303 cm^{-1}, δCH_2 (1448 cm^{-1}), Amide I (1655 cm^{-1}), and ester bands (1750 cm^{-1}), whereas G3 spectra show dominance of proteins and nucleic acids with change in features in 1200-1400 cm^{-1} regions corresponding to Amide III, CH 2 (1454 cm^{-1}), 1583 cm^{-1}, and broad Amide I (1651 cm^{-1}) similar to SCC spectra. A reason for this similarity with mean spectra of histopathological stages is that G0 expression of cyclin D1 is observed in healthy tissues G1 in hyperplasia and LGD, G2 in various grades of dysplasia, G3 is usually expressed in tissue regions which are histopathologically SCC. Thus features of G0, G1, G2 and G3 mean spectra are comparable to healthy, hyperplasia, dysplasia and SCC mean spectra, respectively.

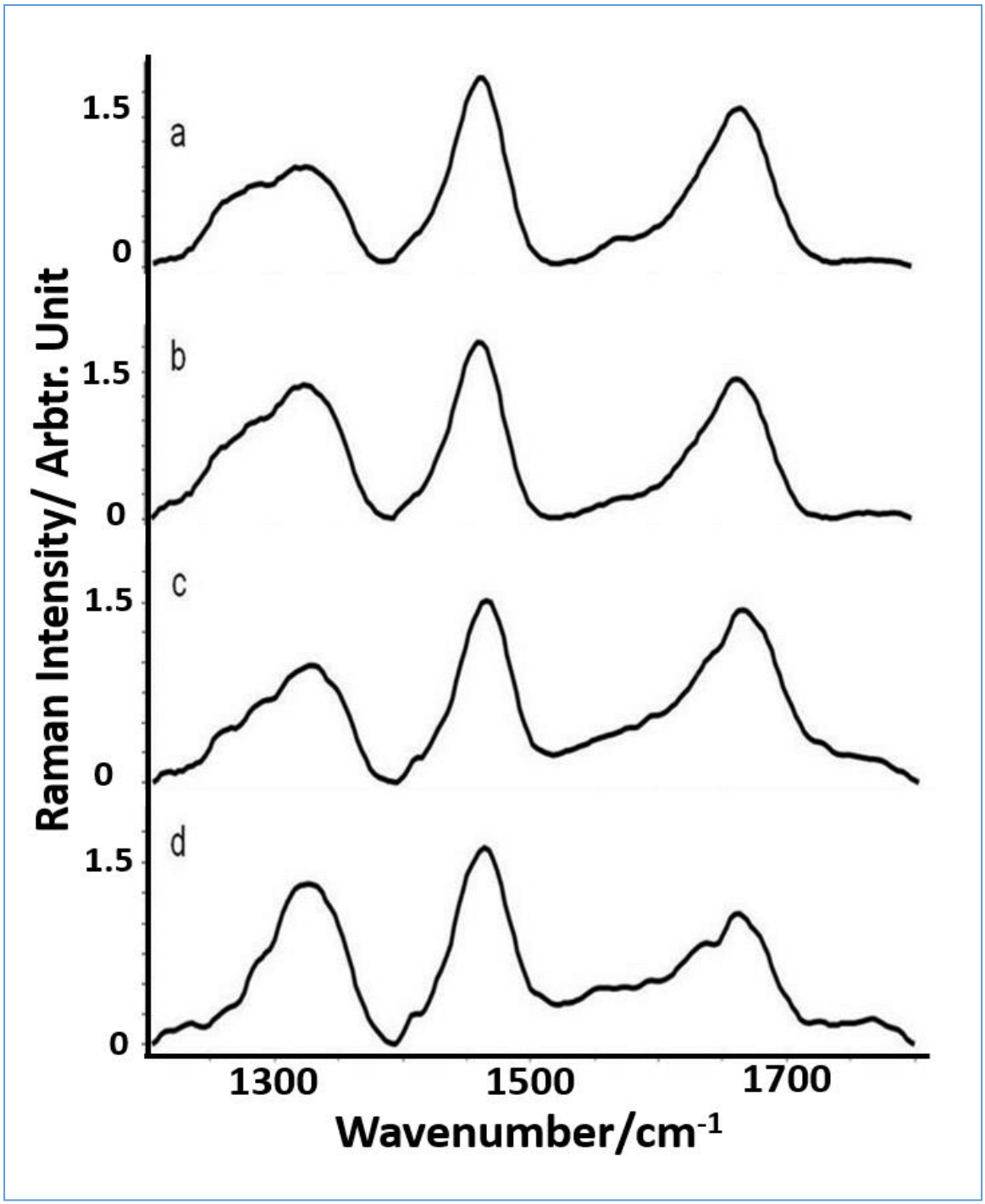

Figure 3.18: Mean spectra - a: G0, b: G1, c: G2, d:G3.

Unsupervised analysis

As in case of spectra evaluated on basis of histopathology, vector normalized first derivatives of the preprocessed spectra were subjected to unsupervised PCA. Ten factors were explored for trends in classification. Scores of factor 1 was plotted against scores of factor 2 to obtain the scatter plot. The scatter plot reveals tendency of classification for the spectra. While G0 and G3 spectra have formed exclusive clusters, G1 and G2 spectra showed overlap with each other as well as with G1 spectra. Loading factors and scatter plots have been shown in Figure 3.19.

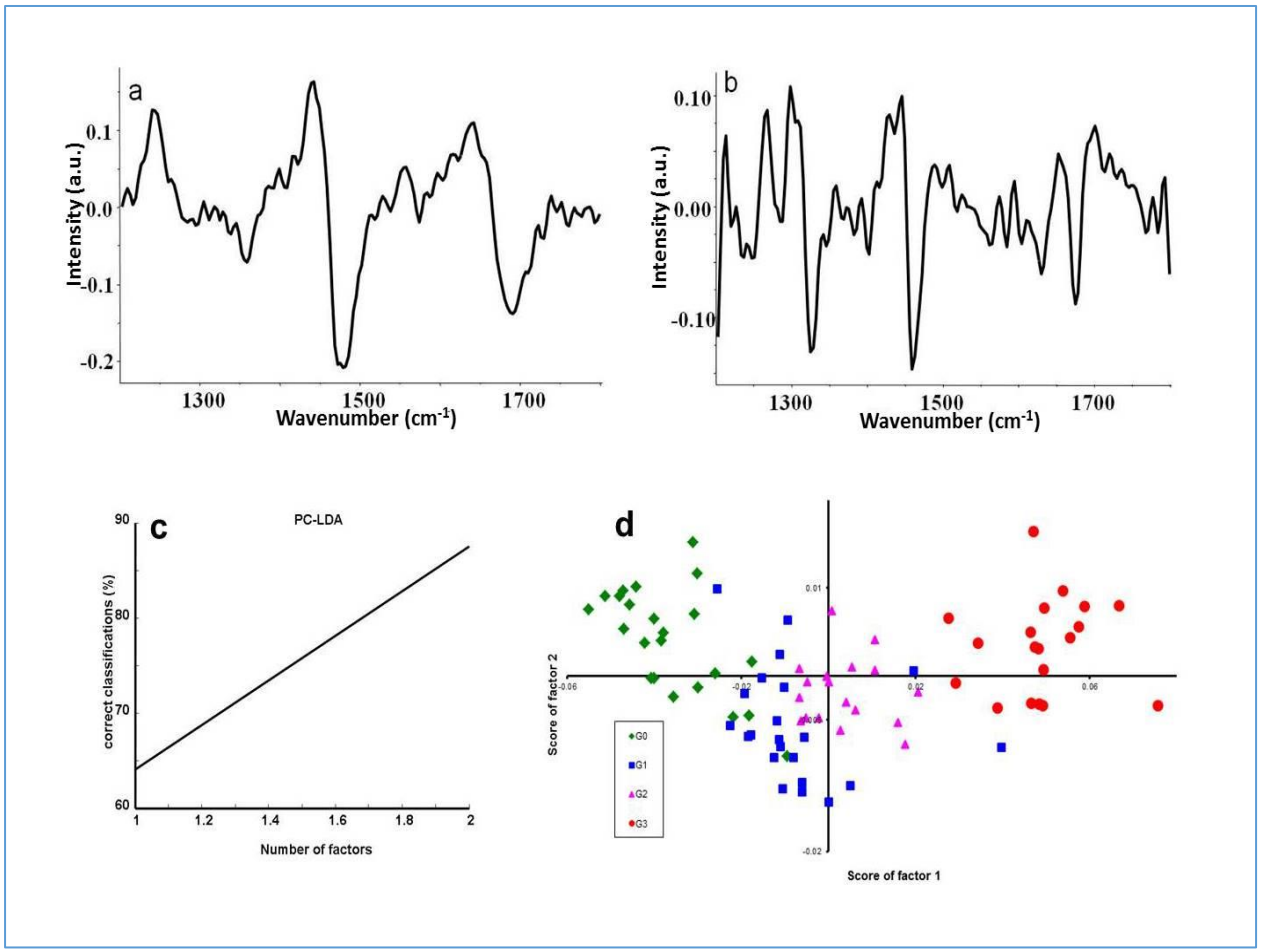

Figure 3.19: Cyclin D1 based model. a and b: Factor loadings for PC1 and PC2; c: PC-LDA scree plot for correct classification; d: PCA scatter plot for factor 1 (X axis) against factor 2 (Y axis).

Supervised analysis

Supervised analysis was used to build the standard model to explore classification as well as evaluation of independently obtained spectra.

Standard model: PC-LDA model (Table 3.10) was trained for spectra belonging to the tissue sections which showed G0, G1, G2 and G3 gradings based on Cyclin D1 biomarker expression. The classification contributed by 10 factors were calculated using MATLAB based software and a scree plot for the same has been shown in Figure 3.19c. First 2 factors were used for model building. The model was further evaluated by LOOCV (Table 3.11). As seen in Table 3.11, for G0 spectra, obtained from 7 animals, 19 spectra were truly classified while 4 spectra misclassified with G1. In case of G1, where 8 animals were used, 15 out of 20 spectra were truly classified while 3, 2 and 0 misclassified respectively with G0, G2 and G3. 20 spectra from 7 animals, graded as G2, showed true classification for 14 spectra. Misclassifications with G0 and G1 were 1 and 5, respectively. For G3 spectra from 8 animals, true classification was observed for 17 out of 19 spectra while 2 spectra misclassified with G2.

	G0	G1	G2	G3
G0	19	4	0	0
G1	3	15	2	0
G2	1	4	15	0
G3	0	0	2	17

Table 3.10: Cyclin D1 based spectral model- Confusion matrix for training model using PC LDA.

	G0	G1	G2	G3
G0	19	4	0	0
G1	3	15	2	0
G2	1	5	14	0
G3	0	0	2	17

Table 3.11: Cyclin D1 based spectral model- LOOCV of training model. (Diagonal elements are true positive predictions while non-diagonal elements represent misclassifications).

Evaluation of standard model

As in case of histopathology based model, the standard model was evaluated against Tx spectra from DMBA treated pouches. For ease in understanding, the Tx spectra obtained over the period of 14 weeks were subdivided into 4 groups: T1-T3, T4-T7, T8-T11 and T12-T14. These four groups were created on basis of histopathological observations as majority spectra in these groups consist of healthy, hyperplasia, dysplasia and SCC respectively. As shown in Table 3.12, for T1-T3, out of 98 spectra, 39, 50, 6 and 3 spectra were classified as G0, G1, G2 and G3, respectively. For T4-T7 out of 171 spectra, 53, 81, 36 and 1 spectra were classified as G0, G1, G2 and G3, respectively. T8-T11 spectra show classification of 48, 49, 56 and 14 spectra with G0, G1, G2 and G3, respectively. For T12 to T14, 52 out of 102 spectra classified as G3, while 37 spectra classified as G2. In concordance with observations in case of histopathology based model, 89 out of 102 (87%) spectra were predicted as higher pathologies, showing moderate to severe expression of cyclin D1 and thus abnormal proliferation.

	G0	G1	G2	G3	Total
T1-T3	39	50	6	3	98
T4-T7	53	81	36	1	171
T8-T11	48	49	56	14	167
T12-T14	0	13	37	52	102

Table 3.12: Evaluation of Cyclin D1 based model using exclusive spectra from DMBA painted HBP. The spectra were grouped as T1-T3, T4-T7, T8-T11 and T12-T14. With increase in the duration of DMBA application, the number of spectra being predicted as higher pathologies (G2/G3) increases. Almost 89% (89 out of 102) spectra from 12 to 14 weeks are predicted as G2/G3.

3.2.2.3 Investigation of abnormal changes in controls: evaluation against standard models

As observed during evaluation of spectra from DMBA painted HBP against the two standard models, RS based findings were in agreement with histopathological/IHC reports available. In the next step, spectra from the control HBP were evaluated against the 2 standard models with the hypothesis that the control spectra predicted in the pathological groups can indicate changes in their respective tissue, due to repeated mechanical irritations. To explore and understand abnormal change in controls, three different types of controls were employed in this study: (i) vehicle controls- spectra recorded from oil painted right buccal pouches of control animals; (ii) vehicle contralateral- spectra were acquired from the left pouches of vehicle controls and (iii) DMBA contralateral- spectra were acquired from the left pouches of DMBA painted animals.

Evaluation against histopathology based model: As hyperplasia may be caused by injuries and inflammations hence only those spectra which were predicted as dysplasia or SCC have been considered for analysis. As shown in Table 3.13, 4, 36 and 65 vehicle contralateral, vehicle control and DMBA contralateral, were predicted as dysplastic or SCC spectra, respectively. These results also indicate that prediction as dysplasia and SCC were least in case of vehicle contralaterals and highest for DMBA contralateral.

Evaluation against IHC based model: In case of IHC based model, (Table 3.14) 3, 37 and 68 vehicle contralateral, vehicle control and DMBA contralateral were predicted as G2 or G3, respectively. Thus, similar to histopathological findings, predictions as G2 and G3 were least in case of vehicle contralaterals and highest for DMBA contralateral spectra.

	Control	Hyperplasia	Dysplasia	SCC	Total
Vehicle Control	189	110	30	6	335
DMBA Contralateral	149	160	59	9	377
Vehicle Contralateral	41	30	4	0	75

Table 3.13: Evaluation of training models with control spectra from independent animals for histopathology based model. Prediction as dysplasia and SCC were least in case of vehicle contralaterals and highest for DMBA contralateral, suggesting least amount of changes due to repeated irritations in case of vehicle contralaterals. DMBA contralaterals show highest prediction as abnormal pathologies probably because these pouches undergo transformation due to leaching of DMBA in saliva when DMBA is applied on the right buccal pouch of test animals.

	G0	G1	G2	G3	Total
Vehicle Controls	191	107	29	8	335
DMBA Contralateral	146	163	54	14	377
Vehicle Contralateral	51	21	3	0	75

Table 3.14: Evaluation of training models with control spectra from independent animals for cyclin D1 based model. Prediction as G2 and G3 were least in case of vehicle contralaterals and highest for DMBA contralateral, suggesting least amount of changes due to repeated irritations in case of vehicle contralaterals. DMBA contralaterals show highest prediction as abnormal pathologies probably because these pouches undergo transformation due to leaching of DMBA in saliva when DMBA is applied on the right buccal pouch of test animals.

To further confirm if the tissue region, corresponding to spectra which were predicted as abnormal by RS, actually harboured any abnormality, the histopathology sections corresponding to such spectra were re-evaluated by the pathologists. Small foci of dysplasia were observed in 3 such sections while one section showed presence of carcinoma. It is understood that it is a rare observation, not reported so far. IHC of some of these sections showed higher expression of cyclin D1 in the circled areas, (Figure 3.20) compared to other control regions.

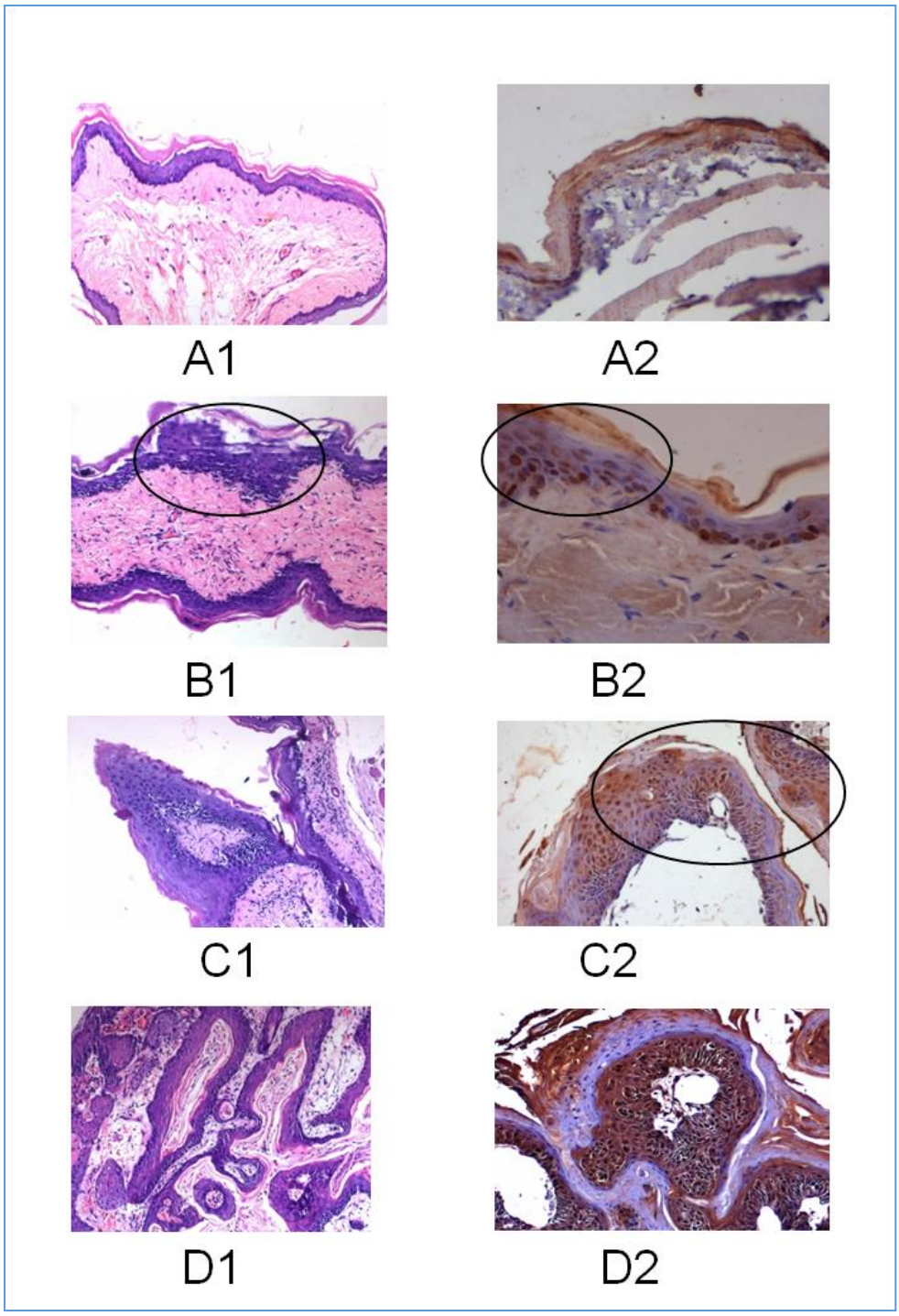

Figure 3.20: Representative images of histopathology (A1 to D1) and IHC (A2 to D2) for (A) vehicle contralateral, (B) vehicle control, (C) DMBA contralateral and (D) DMBA treated pouches.

The prediction of control spectra with treated groups can be attributed to abnormal changes in the mucosa in response to chronic mechanical irritation [370]. Chronic irritation can lead to increased mitotic activity which occurs during repair of the ulcerated tissues and may precede neoplasia [21]. Injuries/wounds resulting from irritations can also elicit inflammatory response leading to neoplasia [371]. Oral cancer incidences are also reported in non-tobacco habitués, especially in women [372]. A probable cause in such cases is chronic physico-mechanical irritations in the oral cavity due to irregular/sharp teeth, poor fillings and improperly fit dentures [20, 21, 370]. In case of HBP carcinogenesis, as a pair of forceps is used to pull out pouches during painting, visual observations and spectral acquisition, forceps induced repeated irritations and injuries cannot be ruled out. In addition, hamsters store food pellets in these pouches, which may further aggravate the irritations/injuries resulting into small areas of abnormalities.

When rate of misclassification/prediction with dysplasia and SCC between the three types of controls- vehicle control, vehicle contralateral and DMBA contralaterals are compared, least misclassifications are observed in case of vehicle contralateral, followed by vehicle controls and DMBA contralaterals. A probable reason for this observation in the vehicle contralateral pouches could be minimal damage to the mucosa as they were not subected to repeated handling, sparing continuous mechanical irritations/injuries. DMBA contralaterals, on the other hand show more misclassification than vehicle contralaterals and controls. This could be due to leaching and mixing of DMBA in saliva, and indirectly, but continuously affecting the contralateral pouches, though all these pouches were visually normal. On further analysis, it was also observed that these animals belonged to 11 to 14 weeks of treatment, indicating that higher duration of handling and associated injuries may be a reason for these abnormal developments. To the best of our knowledge, these observations of higher pathologies has not been reported in control

animals although, cases of tumour development in pet hamsters [18, 373] and in contralateral HBP [19] are reported.

In the present study, though only a small number of control spectra were predicted as higher pathologies, these are important as they could easily be misunderstood as false positives. In our previous in vivo studies on human oral cancers [9, 10, 337], similar misclassifications observed between normal (control) and tumours were attributed mainly to tumour heterogeneity- presence of normal and/or inflammatory islands in the tumours. No histopathological confirmation of normal tissues could be made due to ethical considerations. The use of animal models therefore offered an advantage in this study by facilitatinng histopathological confirmation of the suspected abnormalities in the control tissues. As definite histopathological and biochemical changes could be detected in these control sections, all such misclassifications should be given due consideration as such changes arising from chronic irritations can progress into neoplasms. Such observations in control tissues are usually not observed during experiments. A probable reason for this could be the use of tissue extracts (in case of many biochemical studies) wherein such small abnormalities may get overlooked. Moreover, typical biological experiments may involve many different methods and thus same tissue area may not be available for all the techniques.

Another highlight of this study was the approach used for histopathological corroboration. The usual approach in case of an in vivo approach involves spectra acquisition from the suspected sites under the guidance of a medical practitioner and histopathology is carried out from 1 or 2 sections from surgical excisions/biopsies. As a standard practice, the highest pathology observed in the section is assigned as the histopathological status. Thus, spectral and histopathological

information may not arise from the same tissue regions. Moreover, control tissues from healthy volunteers cannot be made available due to ethical reasons and thus spectra are acquired from cut margins from patients. In the present study, a uniform protocol was adopted for spectral acquisition to avoid any bias and the best efforts were made to carry out spectral acquisition and histopathology from the same tissue regions from carcinogen painted as well as healthy control groups. Overall findings demonstrate that RS can detect clinically invisible micro-changes, which were also corroborated with histopathology and IHC.

3.2.3 Summary

Spectral models were trained on basis of histopathological stages (control, hyperplasia, dysplasia and SCC) and Cyclin D1 expression (G0, G1, G2 and G3), respectively. Evaluation of spectra from DMBA treated tissues showed increasing incidence of higher pathologies with progression of weeks (3% for week 1-3 to 89% for week 12-14). To explore and understand abnormal changes in controls, three different types of controls: vehicle controls, vehicle contralateral controls and DMBA contralateral controls were evaluated against the models. Prediction of control spectra as higher pathologies (dysplasia/SCC/G2/G3) were least in case of vehicle contralaterals and highest for DMBA contralateral. A probable reason for this observation in the vehicle contralateral pouches could be minimal damage to the mucosa as they were not subjected to repeated handling, sparing continuous mechanical irritations/injuries. DMBA contralaterals, showed the most misclassifications probably due to changes induced by indirect exposure to DMBA (present in saliva) which could have leached out from the DMBA painted pouches. All these pouches were visually normal. It was also observed that these animals belonged to 11 to 14 weeks of treatment, indicating that higher duration of handling and associated injuries may be a

reason for these abnormal developments. Small foci of higher pathologies were observed in histopathological sections.

3.3 Combined Raman and Optical Coherence Tomography (OCT) study on hamster buccal pouch model

Recent years have revealed a renewed interest in the simultaneous applications of optical spectroscopy and imaging techniques for disease diagnosis [374] as both morphological and biochemical changes can be explored, leading to a better prognosis. Such studies can be informative in conditions like cancer which involve significant changes in tissue architecture and biochemistry. While, imaging systems can acquire morphological and structural information, the complementary molecular and biochemical information may be obtained through spectroscopy in an objective manner. Thus, their simultaneous application can provide valuable diagnostic information [375] as has been shown in various multimodal approaches.

In the RS based studies described in Chapter 3.2, misclassifications of control spectra with tumour spectra were investigated and changes were observed in some control tissues. In the present study, DMBA painted and control tissues were also subjected to OCT for further corroboration. As already mentioned in Chapter 1.5.3, OCT is an interferometric imaging technique that maps depth-wise reflections. A typical set up for OCT is described in Chapter 2.

3.3.1 Combined RS and OCT

Complementary nature of RS and OCT were demonstrated in a study by Ko *et al* where the two diverse techniques were used to analyze the micro-structural and biochemical features of dental caries [376]. OCT imaging of teeth demonstrated increased light backscattering intensity at sites of carious lesions. OCT imaging was found to be useful for screening carious sites and determining lesion depth, while RS could provide biochemical information of caries. This study suggested the benefit of a single device capable of RS and OCT for complete tissue

characterization. Patil *et al* (2008) reported about a dual-modal device capable of sequential acquisition of RS and OCT along a common optical axis [377]. The device enhanced application of both RS and OCT by guiding RS acquisition with OCT images while also compensating for the lack of molecular specificity in OCT with the biochemical specificity of RS. They acquired NIR RS and OCT data through common sampling optics. Patil *et al* also reported morphological and biochemical characterization of skin cancers to discriminate malignant and non-malignant lesions [378]. Qi *et al* performed experiments on mouse kidneys, livers, and small intestines tissues and observed increased prediction accuracy through support vector machines [379]. Combined RS/OCT could effectively improve tissue classification compared to OCT alone. Zakharov *et al* carried out a comparative analysis of combined RS and OCT method for detection of skin and lung cancers using back scattering, with improved specificity and sensitivity [380].

3.3.2 Combined Raman and OCT study in oral cancers

3.3.2.1 Sample selection and processing

Control and DMBA painted tissues corresponding to week 1 and week 13 (C1, C13, T1 and T13) were employed which included 6 DMBA painted and 8 control tissues.

RS: In vivo Raman spectra were recorded from 2 animals each, at the end of 1 and 13 weeks after anaesthetizing the animals. Approximately 10 spectra were recorded from each tissue integrated for 15 seconds and averaged over 3 accumulations. The HBP from which spectra were acquired were excised out after sacrificing the animals, fixed in NBF for 24 hours and transported to Bhabha Atomic Research Centre, Vishakhapatnam for OCT study.

OCT imaging: The formalin fixed tissues were thoroughly rinsed with saline solution prior to OCT imaging. A schematics of the OCT instrument employed in the study has been shown in Figure 2.12.

3.3.2.2 Findings

Visible and histopathological changes: C1 and T1 tissues were visually normal and showed intact epithelium in the H&E stained histopathological sections. T13 tissue showed presence of tumours and revealed SCC, with presence of keratin pearls in the H&E stained section [191].

RS: In concordance with the mentioned spectral features in the previous sections, Raman spectra showed lipid dominance in the early weeks while later weeks and tumours showed increased protein to lipid ratio (Figure 3.21).

OCT: While OCT images suggested intact epithelial architecture for 6 controls and 4 DMBA treated pouches of early weeks, the entire layer was disrupted in case of tumours from week 13 (n=2). Also, the carcinogen treated tissues appeared to show higher scattering with a total loss of layered architecture by 13 weeks of DMBA application, also reported earlier by Matheny *et al* [187].

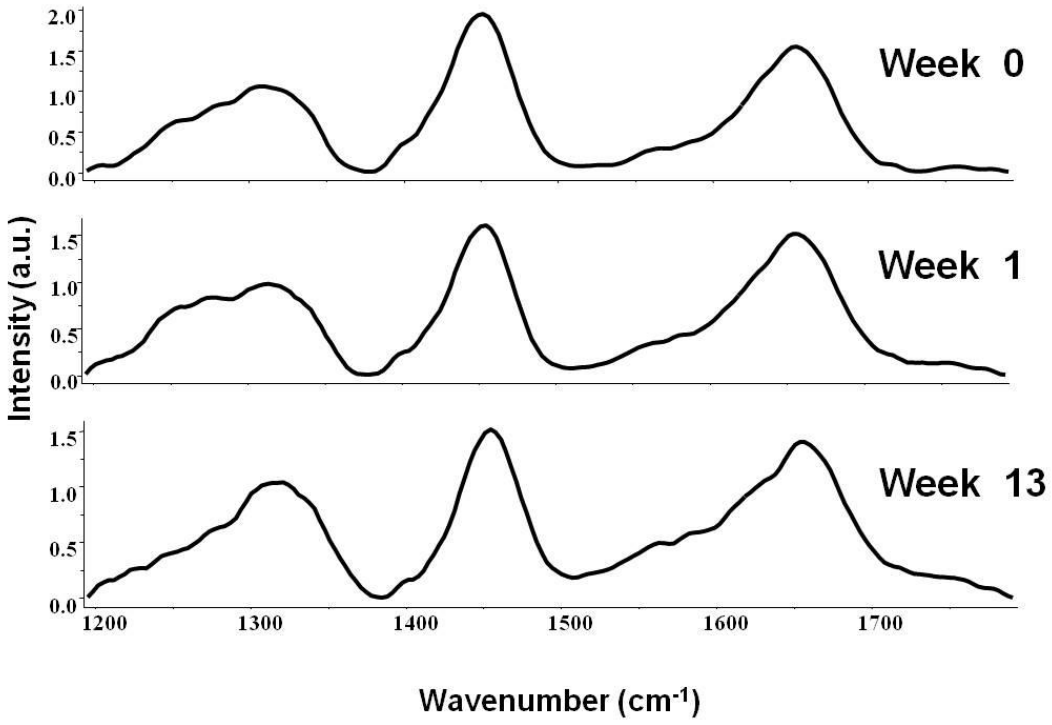

Figure 3.21: Mean spectra reveal loss of lipids and increase in protein contents in carcinogen-treated tumour spectra (week13) as compared to control (week 0) and early week (week 1).

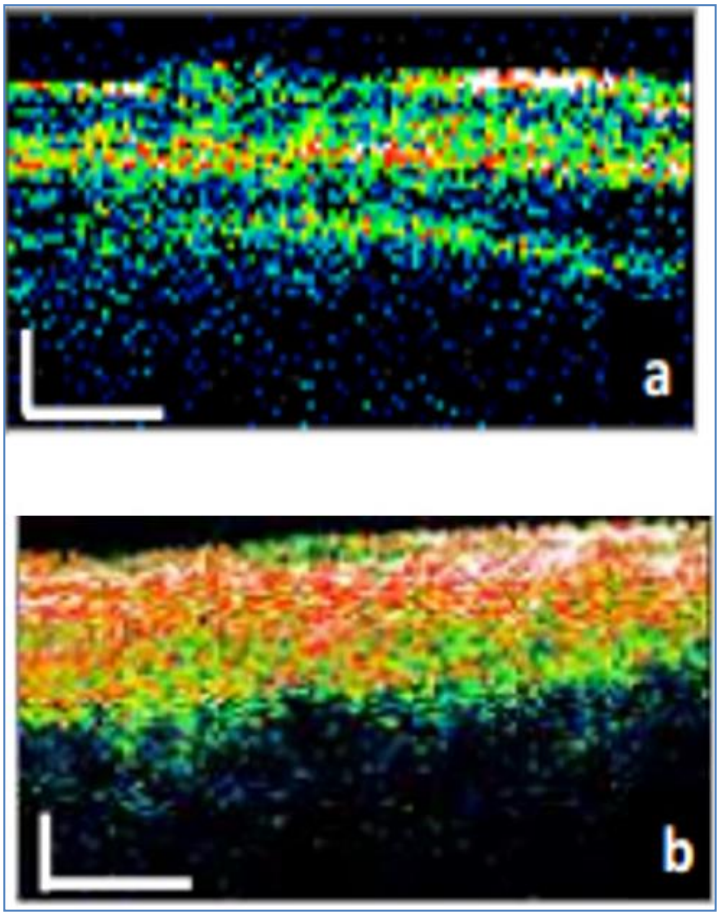

Figure 3.22: OCT images of a: week 1 and b: week 13, showing layered and disrupted architecture of epithelium in control and DMBA treated tissues, respectively. Scale bar is 0.2 mm.

Abnormal changes in control tissues: When the OCT images of control tissues of later weeks were examined, higher scattering was observed in some samples. In 2 vehicle control tissues, epithelial architecture was disrupted in OCT images, suggesting damage to the epithelium of such tissues and in concordance with Raman findings. The OCT images showing disrupted epithelium have been shown in Figure 3.23.

This being a parallel study can lead to a mismatch in the tissue regions investigated by two techniques. A combined RS-OCT instrument with a common integrated clinical probe but independent RS and OCT detectors, will help signal acquisition simultaneously for both the techniques and at the same time to allow better correlation. Such an instrument can be used to study a large cohort. Further improvements in the results can be achieved by advanced analysis of the RS and OCT signal itself [381] and by combining OCT with other modalities such as Raman spectroscopy (RS) [382]. A multi-modal and multi-functional OCT imaging and RS system integrated with the existing clinical modalities may provide high resolution diagnostic images of morphological, biochemical, molecular and functional information for early cancer diagnosis[383]. The use of OCT in combination with other optical techniques can hereby assist in screening and eventually even optically diagnose malignancies non-invasively.

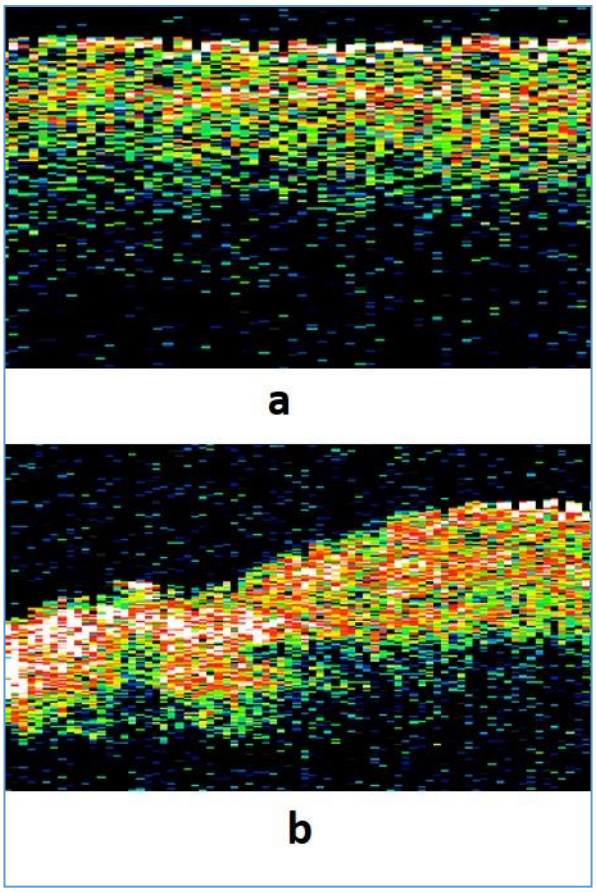

Figure 3.23: OCT images of late week vehicle controls (both a and b) showing disrupted architecture of epithelium. Scale bar is 0.2 mm.

3.3.3 Summary

Both RS and OCT hold the potential to provide functional optical biopsies of cancers. Raman spectroscopy showed efficiency in classifying normal and cancer cases. OCT images showed higher scattering with increasing duration of DMBA application and complete loss of layered architecture in tumour tissues. OCT images of 2 control tissues of later weeks showed disrupted epithelial architecture, suggesting damage to the epithelium of such tissues and in concordance with Raman findings in Chapter 3.1 and 3.2. Further improvements can be achieved by signal acquisition through a common probe for both Raman and OCT and advanced analysis of the RS and OCT signal.

3.4 Effect of discontinuation of carcinogen in experimental oral carcinogenesis: in vivo Raman spectroscopic investigation

In the study on sequential progression of experimental carcinogenesis (Section 3.1) using HBP model, plateauing of classification efficiency was observed from 8 to 11 weeks [191]. Continuous application of DMBA, beyond 8 weeks results into development of tumours (histopathologically SCC) after 12 weeks. Thus, in the present study, the effect of discontinuation of DMBA after 8 weeks was studied to investigate progression to tumours. Such study can be considered analogous to quitting tobacco habits, a major etiological agent, and its effect on cancer progression. However, not many studies have explored cancer risk and progression after cessation of habit. Most such studies are association studies which derive their conclusion retrospectively. An intervention study associated regression of premalignant conditions to discontinued or reduced tobacco habit [384]. In this study, HBP model was used to achieve the objective. A set of hamsters was treated with carcinogen for 14 weeks while another set was treated with carcinogen for 8 weeks only and animals were kept alive after that. Spectra were recorded at the end of 8 and 14 weeks from all animals. Spectra were also recorded from appropriate control animals. Findings are discussed.

3.4.1 Spectra acquisition and model building

Following set of animals were employed. A schematic has been shown in Figure 3.24.

(a) Set 1 (Carcinogen control): DMBA application for 14 weeks (n =5) and then spectra acquired (T14c, 34 spectra).

(b) Set 2 (Discontinuation experiment): DMBA application only for 8 weeks and then discontinued (n =5). Spectra were recorded from these animals at the end of 8 weeks (T8dc, 55 spectra) and 14 weeks (T14dc, 46 spectra).

(c) Set 3 (Vehicle control): Vehicle oil was applied (n =5) for 8 weeks and then discontinued. Spectra were acquired at week 0 (C0, 37 spectra), week 8 (C8dc, 42 spectra) and week 14 (C14dc, 57 spectra).

(d) Set 4 (For model training): DMBA application was carried out for 14 weeks continuously and spectra were recorded at the end of 0, 8 and 14 weeks of treatment. Spectra employed for model building were: week 0 (T0, 32 spectra), week 8 (T8, 37 spectra), week 14 (T14, 28 spectra). The spectra model was used for evaluation of spectra from Set 1 to 3.

All spectra were acquired in vivo using protocols mentioned in the Chapter 2 (Materials and Methods).

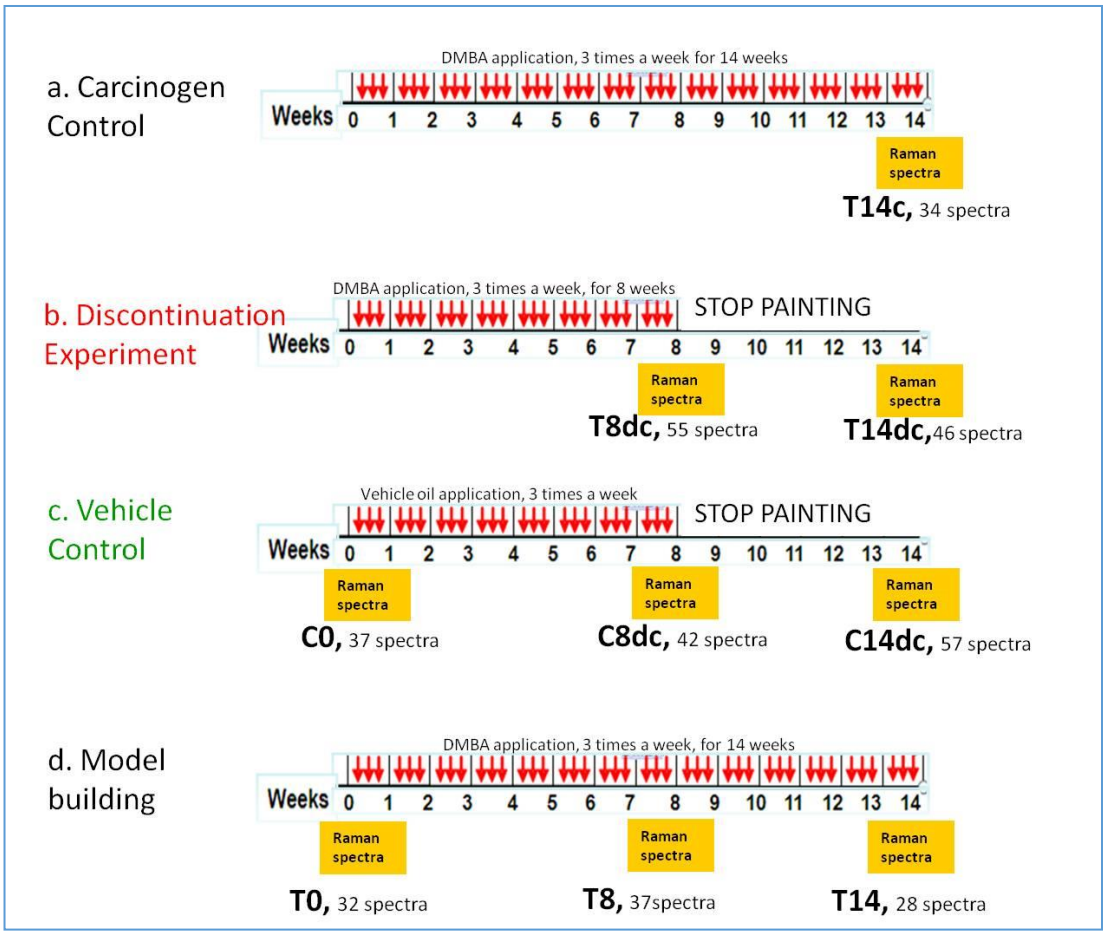

Figure 3.24: Schematics of protocol followed. a: Set 1(Carcinogen control): DMBA was applied for 14 weeks and spectra recorded at the end of 14 weeks. b: Set 2 (Discontinuous experiment): DMBA was applied for 8 weeks. Spectra were recorded at the end of 8 and 14 weeks. c: Set 3 (Vehicle control): Vehicle oil was applied for 8 weeks and spectra were recorded at the end of 0, 8 and 14 weeks. d: Set 4 (For model building). DMBA was applied continuously for 1 weeks, spectra were recorded at week 0, at the end of 8 weeks and at the end of 14 weeks. All spectra were acquired in vivo using protocols mentioned in the Chapter on Materials and Methods.

3.4.2 Findings

Mean spectra: Figure 3.25 (i) shows the in vivo mean spectra of C0, T8dc, T14dc and T14. C0 spectra (Figure 3.25 i a) show lipid rich features with bands at - 1301 cm^{-1}, 1448 cm^{-1}, 1720 cm^{-1} and 1745 cm^{-1} [367]. As T0 and C0 spectra were acquired at week 0 (prior to DMBA application), both have similar features. Mean spectra for T8dc and T14dc show similar features which increasing protein dominance, showing bands at 1324 cm^{-1}, 1454 cm^{-1}, broader Amide I (1651 cm^{-1}) and lack of 1745 cm^{-1} band. T14 spectra show dominance of proteins and nucleic acids with change in features in 1200-1400 cm^{-1} regions, CH_2 (1454 cm^{-1}), 1560 cm^{-1} to 1580 cm^{-1}, and broad Amide I (1651 cm^{-1}). Changes in Amide III and Amide I regions suggest progressively increasing protein dominance. A probable explanation for this observation could be changes in expression profile of proteins such as surface/receptor proteins, enzymes, antigens, and antibodies during pathological conditions [10]. These findings further corroborate earlier reports of ex vivo and in vivo RS studies on human subjects as well as hamster models [191, 332, 337, 385]. 1563 cm^{-1} band may be attributed to increased nucleic acids which has also been observed in prior studies and can be attributed to high concentration of nucleic acids in cancer tissues [332]. As per our previous observations in the pathological HBP [191, 366], 1583 cm^{-1} band may be assigned to heme proteins abundant on account of angiogenesis- a well-known hallmark of carcinogenesis[23].

Difference spectra: Difference spectra were computed to understand subtle differences between two groups of spectra and have been shown in Figure 2 (ii). First, differences between DMBA treated and C0 spectra were explored by subtracting mean C0 spectra from T14, T14dc and T8dc spectra (Figure 3.25 ii a to c). The negative bands were contributed by C0 spectra. As control

spectra have high lipid to protein ratio, difference spectra suggest positive features for proteins (and also nucleic acids) and negative features for lipid bands (Negative bands at 1300, 1440 and 1745 cm^{-1}). Next, differences between the DMBA treated spectra were explored. Differences were similar between T14-T14dc and T14-T8dc spectra, with positive bands for nucleic acids and proteins. Negative bands for lipids were present, suggesting T8dc spectra having features intermediate to C0 and T14 spectra. Difference spectrum between T8dc and T14dc revealed poor features, indicating similarities between the two groups (Figure 3.25 ii f).

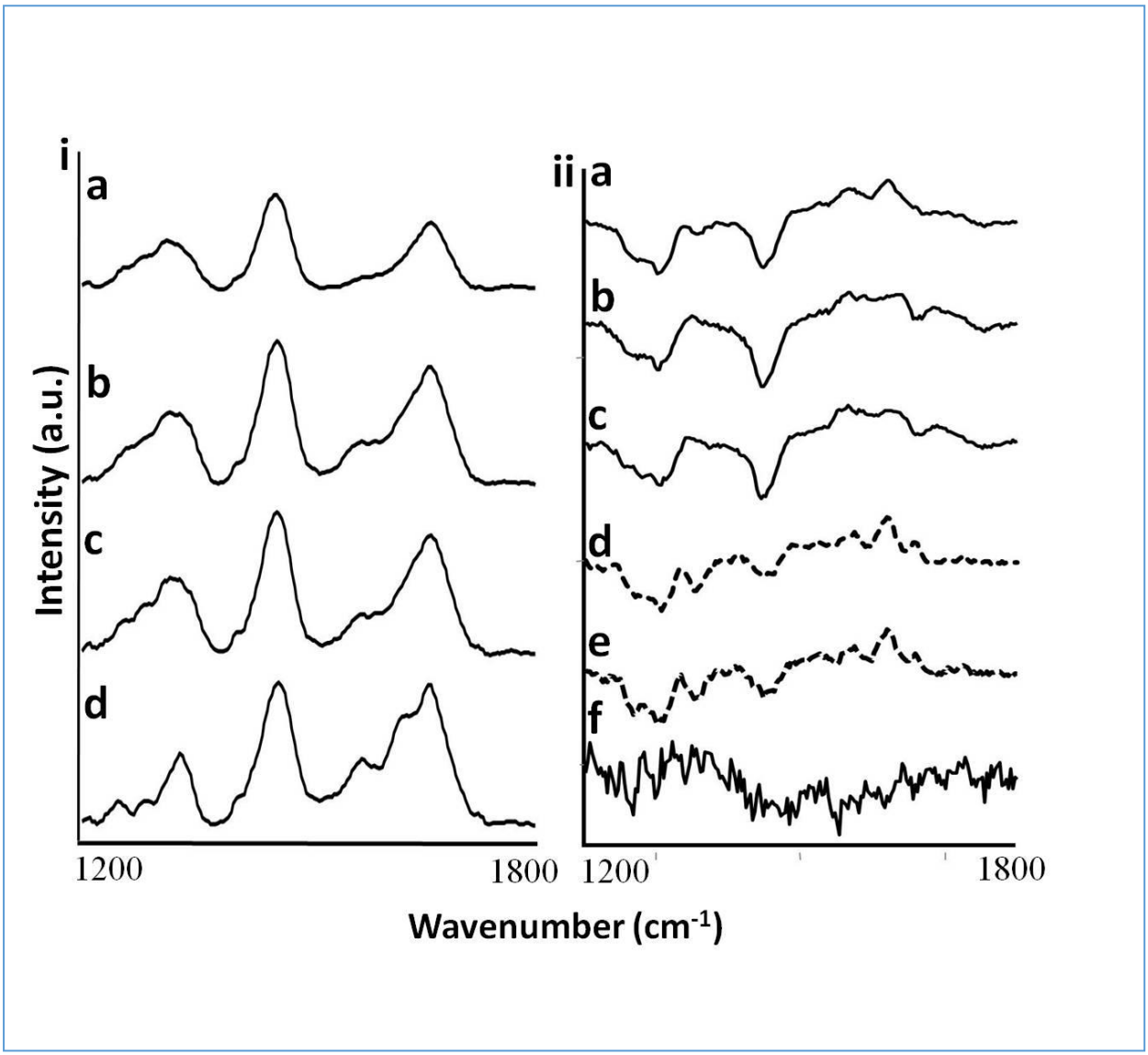

Figure 3.25: (i) Mean spectra a: C0, b: T8dc, c: T14dc and d: T14.

(ii) Difference spectra. a:T14-C0, b: T14dc-C0, c: T8dc-C0, d: T14-T14dc, e: T14-T8dc, f: T14dc-T8dc.

PCA: PCA scatter plot, shown in Figure 3.26: (a) PC1 (b) PC2 and (c) PCA scatter plot. c shows 3 exclusive clusters: 1st for T14 spectra, 2nd for T8 spectra and 3rd consisting of all the vehicle controls (C0, C8dc, C14dc). The spectra of interest, T14dc, were spread across these clusters. As seen in scatter plot, most T14dc spectra overlapped with controls or T8 cluster. Some T14dc spectra (~13; 28%) overlapped with the T14 spectra indicating that some area in mucosa can progress to higher pathologies even after withdrawal of the carcinogenic agents.

PC-LDA: PC-LDA model was trained using C0, T8 and T14 tumour 5 DMBA treated animals. 2 factors contributing 90% classification were employed. LOOCV confusion matrix is shown in Table 3.15a. As shown in the table, 30/32 T0, 29/37 T8 and 22/28 T14 spectra were correctly classified. Misclassifications can be attributed to tissue heterogeneity.

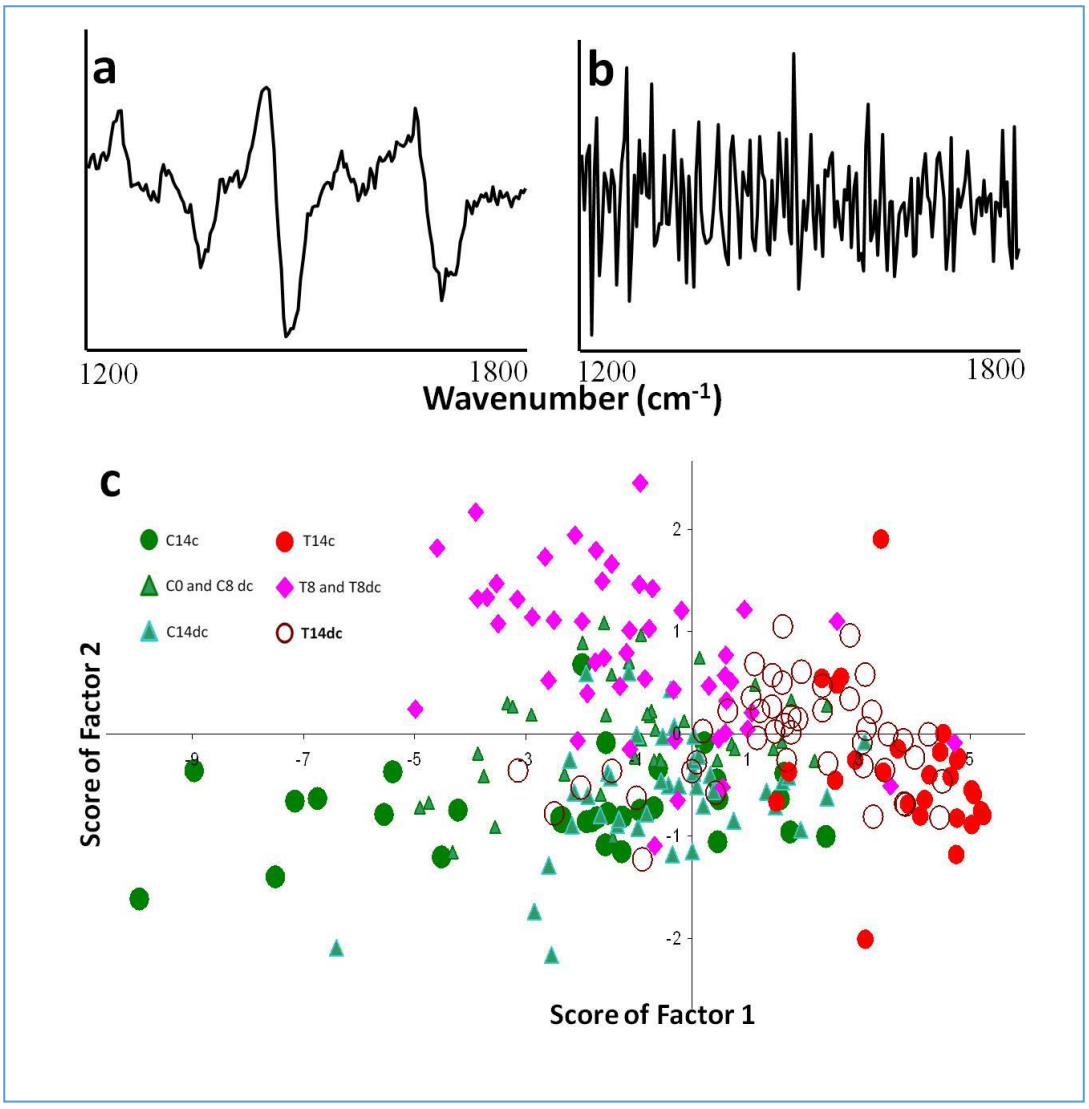

Figure 3.26: (a) PC1 (b) PC2 and (c) PCA scatter plot.

Evaluation of spectra against PC-LDA model: All spectra acquired in the present experiment were evaluated against the training model as shown in Table 3.15b. Most control spectra were correctly predicted as C0 (91/136). The control spectra predicted as T8 can be attributed to tissue heterogeneity in T8. In case of T14c, 22/34 and 10/34 spectra were predicted as tumour and T8 respectively. Though, 14 weeks of DMBA application results into SCC and severe dysplasia in most regions, it should be noted that not all regions get uniformly transformed in the buccal mucosa and small patches of healthy, hyperplasia and mild dysplasia are often observed. This can explain prediction of 2 spectra as T0. In case of T8dc, where DMBA was applied till 8 weeks, majority of spectra were predicted as T0 (13/55) or T8 (34/55) as most regions are normal, hyperplastic or mild dysplastic after 8 weeks. 8/55 spectra were predicted as tumour which could be attributed to development of higher pathologies. T14dc spectra, DMBA application was withdrawn after 8 weeks are the focus of this study. In this case, 9/46 spectra were predicted as T0 while 24/46 spectra were predicted as T8. Thus, 72% of T14dc spectra resembled either T8 or control spectra. 13/46 spectra were predicted as T14 group which suggests that 28% spectra resembled tumour features. As a comparison, 65% spectra (22/34) of 14 weeks of continuous application of DMBA (T14c), were predicted as T14 while in case of 8 weeks of DMBA application, 14% (8/55) spectra were predicted as T14. This observation suggests that discontinuation/withdrawal of carcinogen application may reduce cancer progression vis a vis continuous application. However, interestingly, visual inspection of pouches on which DMBA application was stopped after 8 weeks did not show macroscopic tumour development after 14 weeks, unlike the pouches undergoing continuous application of carcinogen where visible tumours were observed at the end of 14 weeks.

	T0	**T8**	**T14**
T0	**30**	1	1
T8	3	**29**	5
T14	2	4	**22**

(a)

	T0	**T8**	**T14**	Total
T14 dc (Discontinued DMBA painting after 8 weeks, spectra after 14 weeks)	9	24	13	46
T8dc (spectra after DMBA application for 8 weeks)	13	34	8	55
C14dc (Discontinued oil painting after 8 weeks, spectra after 14 weeks)	32	23	2	57
C8 dc (Spectra from vehicle control after oil painting for 8 weeks)	30	11	1	42
C0 (No painting, Spectra from 0 week)	29	8	0	37
T14 c (continuous DMBA treatment for 14 week)	2	10	22	34

Table 3.15: (a) PC-LDA model and (b) Evaluation of independent spectra.

Histopathological evaluation of the T14dc pouches majorly revealed epithelial hyperplasia or mild dysplasia. Also, higher pathologies such a severe dysplasia and carcinoma in situ were observed in some sections of the buccal pouch mucosa indicating cancer progression in spite of carcinogen withdrawal, corroborating classification of T14dc spectra with T14. In case of buccal pouch which were continuously painted for 14 weeks with DMBA, mostly severe dysplasia and SCC were observed. Representative images have been shown in Figure 3.27 .

Histopathologically, the buccal mucosa, after 8 weeks of DMBA application presents hyperplasia, hyperkeratosis and small regions of early and mild dysplastic changes as observed previously and also in phase 1 experiment. Dysplasia is a precancerous condition which can have a malignant transformation rate of 12.1 in 4.3 years in case of human beings [386]. However, risk of progression from dysplasia to higher pathology can be reduced/delayed by withdrawal of carcinogenic insult. Interestingly, such an observation also tows the line of 'cancer prevention of delay' by Lippman and Hong [387]. In the present experiment, delay was induced by discontinuation of DMBA application on HBP after 8 weeks. As per guidelines of IAEC, the animals were sacrificed after 14 weeks of experiment. Till this time, no visible tumours were observed on HBP where DMBA application was discontinued but histopathological evaluation of these pouches revealed higher pathologies including severe dysplasia and carcinoma in situ in some sections of the buccal pouch mucosa. Findings further show that RS has been successful in identification of changes before visual or palpable tumours suggesting RS as a promising label-free, non-invasive candidate tool for screening general population and also monitor disease progression which can often remain unnoticed by conventional screening tools.

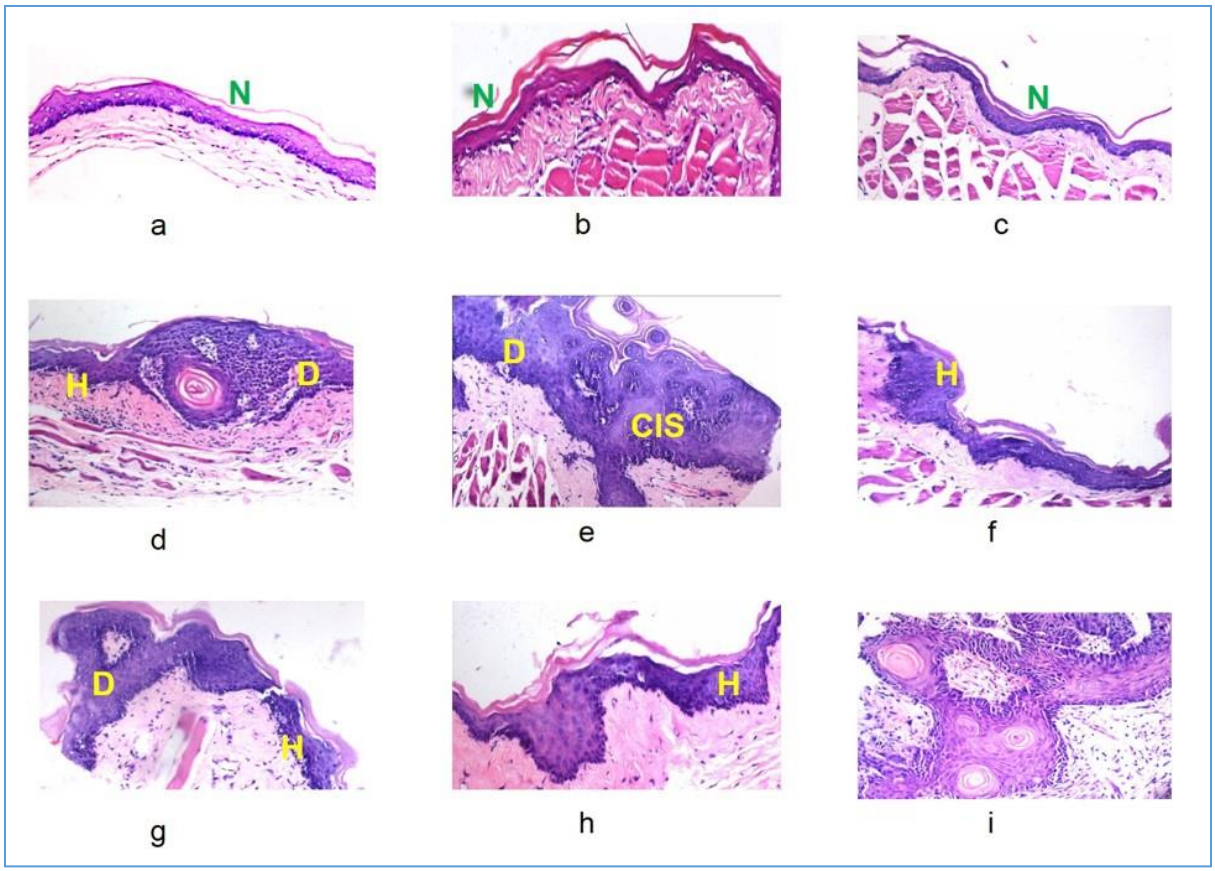

Figure 3.27: Representative hematoxylin and eosin stained histopathology images. (N: normal, H: hyperplasia, D: dysplasia, CIS: carcinoma in situ). a to c: normal images from vehicle control pouches; d to f: images from T14dc tissues showing hyperplasia and severe dysplasia (d), severe dysplasia and carcinoma in situ (e) and hyperplasia (f); g and h: images from week 8 showing hyperplasia and mild to moderate dysplasia (g), and hyperplasia and mild dysplasia (h); i: image from T14 tissue showing carcinoma.

Tobacco is a major etiological agent for oral as well as lungs cancers, supported by many association studies. Cross sectional studies have shown decreased prevalence of oral premalignant disorders (OPMD) such as leukoplakia in non-habitués. Regression of leukoplakia has been attributed to discontinued or reduced tobacco habit [384]. However, such studies, based on conventional oral examinations, do not provide concrete evidence about changes in risk after cessation of tobacco habit. Moreover, such studies, based on human subjects have variabilities in terms of socio economic, dietary and environmental conditions and genetic susceptibility, which varies from individual to individual. Further, quitting tobacco is a difficult task and people who quit may be tempted to expose themselves to tobacco even during intervention experiments [388, 389]. The present study using HBP model of carcinogenesis suggests that 28% spectra (T14dc) were predicted as T14/tumour group when DMBA application was discontinued after 8 weeks; while in case of 14 (T14c) and 8 weeks (T8dc) of continuous application of DMBA, 65% and 14% spectra were predicted as T14/tumour group, respectively. Though the results may not be directly extrapolated to human subjects due to difference in terms of the dosage and duration of carcinogen exposure, the present experiment is indicative of a direct cause and consequence effect between withdrawal of carcinogen and reduced risk of cancers over a defined time period (14 weeks in this case). Tobacco habit is rampant in various forms across the world, exposing the habitués to several potentially carcinogenic compounds. DMBA has been observed in high concentration in the tar fraction of cigarette smoke [341]. Quitting tobacco habit can thus reduce exposure to such carcinogens, however, the feasibility of cancer progression cannot be ruled out as indicated by the 28% spectra which matched with tumours and also showed higher pathology during histopathological evaluation. However, on the brighter side, the progression would be very less compared to those continuing with the habit (28% vs 65%). The present study has

implications in increasing awareness among the general population against the ill effects of tobacco abuse. Further, findings suggest that RS can be used for prospective screening as a label free and noninvasive tool to identify risk prone population.

3.4.3 Summary

Multivariate analysis revealed that when DMBA application was discontinued after 8 weeks (but spectra acquired after 14 weeks), 28% spectra were predicted with tumour group; while in case of 14 and 8 weeks of continuous DMBA application, 65% and 14% spectra were predicted with tumour-group, respectively. The study suggests a cause-and-consequence effect between DMBA-withdrawal and reduced cancer-progression in HBP model in a definite time-period (28% vs 65%), which could be investigated by RS. On similar lines, quitting tobacco can reduce carcinogen-exposure and thus risk of cancer-progression. Findings further suggest RS as a prospective label-free and noninvasive tool to screen risk-prone population.

4 Chapter 4: Conclusion and Outlook

Prelude

This chapter summarizes the thesis and provide an outlook of the work done.

4.1 Conclusion

Oral cancers are a major health concern in the South Asian nations as well as the developed world. Despite advancements in treatment modalities, oral cancers still suffer from a poor 5-year survival rate of ~50%. Studies have shown that early detection improves prognosis and 5-year survival rate [2, 3]. Moreover, cancer treatment is a costly affair and poses huge financial burden to the families affected. Thus, prevention and early detection are the most viable and practical solution for successful management of oral cancers. The currently practiced diagnostic gold-standard, biopsy followed by histopathology, is invasive (and painful), prone to subjective errors and not convenient for repeated sampling during screening and therapeutic monitoring. Hence, Raman spectroscopy (RS), a rapid, objective, non-invasive technique which is sensitive to tissue biochemistry could be more effective in early diagnosis, as biochemical changes precede visible morphological alterations during carcinogenesis. RS has shown promising results in the diagnosis of several cancers, [5] including oral cancers wherein classification of pathological conditions and detection of factors such as cancer field effects, demonstrates efficiency of the technique. These studies have relied on clinical examination and histopathology for pathological status. However, as mentioned earlier, histopathology suffers from limitations; and biopsy is carried out only after clinically apparent premalignant/cancerous conditions develop in oral mucosa. It would be imperative to that biochemical changes preceding malignant conditions be explored and verified vis a vis gold standard histopathology. Hence, the present study was undertaken on the widely used hamster buccal pouch (HBP) model of oral carcinogenesis for RS based investigation of sequential changes in oral carcinogenesis, from healthy condition to tumour condition, along with suitable age-matched controls. A summary of the findings presented in the thesis have been mentioned in the following sub sections.

4.1.1 Sequential cancer progression in hamster buccal pouch model

In this objective, sequential progression in experimental oral carcinogenesis in the HBP model was monitored using three approaches- ex vivo, in vivo sequential and in vivo follow up. Ex vivo study employed ex vivo tissues while in vivo studies employed anaesthetized animals for spectral acquisition. In case of in vivo sequential study, animals were sacrificed each week after spectral acquisition while in vivo follow up study was used to follow up the same animals throughout the study. In all these studies, spectral changes showed lipid dominance in early stages while later stages and tumours showed increased protein to lipid ratio and nucleic acids. On similar lines, early weeks of DMBA painted and control groups showed higher overlap and low classification. Multivariate analysis indicated increasing efficiency of classification with the duration of carcinogen application. Sensitivity was 70% by week 8, 70 to 80% for week 9 to 11 and 80 to 100% for week 12 to 14. Thus classification increased progressively till 8 weeks, reached a plateau phase between 8 and 12 weeks and finally increased up to 100 % by 14 weeks. Various studies have shown culmination of expression of biomarkers such as P53, C-myc, and Ki67 around 10 weeks, justifying the observation. Few misclassifications between carcinogen painted and control spectra suggested some abnormalities in controls as well, which were subsequently corroborated by careful examination of histopathological slides. In vivo findings, quite comparable to gold-standard supported ex vivo findings, give further proof of RS being a promising diagnostic adjunct for future clinical applications.

4.1.2 Comparison of RS with histopathology and biomarker and investigation of abnormal changes in control tissues

This study was carried out to further explore the abnormal observations in control pouches by employing spectral models based on pathological stages in oral carcinogenesis. Spectral models were trained on basis of histopathological stages (control, hyperplasia, dysplasia and SCC) and Cyclin D1 expression (G0, G1, G2 and G3), respectively. These models were evaluated by spectra from DMBA treated tissues. Results showed increasing incidence of higher pathologies (dysplasia/SCC/G2, G3) with progression of weeks (3% for week 1-3 to 89% for week 12-14). To explore and understand abnormal changes in control tissues, three different types of controls: vehicle controls, vehicle contralateral controls and DMBA contralateral controls were evaluated against the models. Prediction of control spectra as higher pathologies (dysplasia/SCC/G2/G3) were least in case of vehicle contralaterals and highest for DMBA contralateral. A probable reason for this observation in the vehicle contralateral pouches could be minimal damage to the mucosa as they were not exposed to repeated handling, sparing continuous mechanical irritations/injuries. DMBA contralaterals, on the other hand, showed the maximum misclassifications, possibly due to changes induced by indirect exposure to DMBA which could have leached out from the DMBA treated pouches. All these pouches were visually normal. It was also observed that these animals belonged to 11 to 14 weeks of treatment, indicating that higher duration of handling and associated injuries and longer exposure to DMBA may be a reason for these abnormal developments. Small foci of higher pathologies were observed in histopathological sections indicating RS could identify abnormalities at microscopic level. Raman mapping of tissue sections from various time points in the HBP carcinogenesis may lead to elucidation of changes at the cellular and sub-cellular level. These changes can be further

explored through complementary biological studies to gain additional insights. Overall, observations demonstrate that clinically invisible micro-changes may be detected using RS, which were also corroborated by gold standard histopathology and IHC studies, further supporting the role of RS as a screening tool for both high risk (habitués) and general populations.

4.1.3 Combined Raman and Optical Coherence Tomography (OCT) study

This study was carried out to verify abnormal changes mentioned above using complementary techniques such as OCT which provide structural information. Raman spectra were acquired from limited early and late week DMBA treated and control buccal pouches followed by OCT imaging of the same regions. OCT images showed higher scattering with increasing duration of DMBA application and complete loss of layered architecture in tumor tissues. OCT images of control tissues of later weeks also showed disrupted epithelial architecture, suggesting damage to the epithelium of such tissues and in concordance with Raman findings in Chapter 3.1 and 3.2. Further improvements can be achieved by signal acquisition through a common probe for both Raman and OCT and advanced analysis of the RS and OCT signal. Observations suggest potential of multimodal application of spectroscopic and imaging techniques in identification of abnormalities.

4.1.4 Effect of discontinuation of carcinogen in experimental oral carcinogenesis

The effect of discontinuation of DMBA was also investigated to study the cause and consequences between withdrawal of carcinogen and reduced risk of cancers in a defined time period. DMBA application was carried out only for 8 weeks but spectra were recorded at the end 8 and 14 weeks. Multivariate analysis revealed that when DMBA application was discontinued

after 8 weeks (but spectra acquired after 14 weeks), 28% spectra were predicted with tumor group; while in case of 14 and 8 weeks of continuous DMBA application, 65% and 14% spectra were predicted with tumour-group, respectively. Thus, withdrawal of carcinogen may not rule out cancer progression but can prevent/delay further damage (28% vs 65%). The preliminary finding suggests cause and consequences between exposure to carcinogen and tumours. Further studies on carcinogen withdrawal at different weeks/stages may help assess the regression/progression rate of risk prone sites and also provide first experimental evidence to assist public awareness programmes against the ill effects of well-known etiological agents such as tobacco.

4.2 Outlook

A metaphorical war is ongoing against cancer to raise public awareness and strengthen scientific and clinical resources [390]. However, in spite of developments in the field, we are yet to achieve a vantage point to understand cancers. With increasing incidence, at present, early detection poses a feasible solution to decrease mortality rates and provide a better quality life to the survivors. Amidst the diagnostic adjuncts being extensively explored, techniques such as RS hold the potential to translate to clinics and mass screening programmes. While the present study was carried out on animal models using both ex vivo and in vivo approaches, several groups, including ours, have also been simultaneously exploring the avenue of RS based diagnosis/detection on human subjects and volunteers over the last few years. Rapid developments in technology can enhance Raman applications [391] and further reduce spectra acquisition times to enable quicker diagnosis and general screening in a clinical scenario.

In the present study, for the first time, RS based investigation of sequential changes in oral carcinogenesis was carried out from absolutely healthy condition to tumour condition, along with suitable age matched controls. The study included both in vivo and ex vivo approaches supported by gold standard, with a sufficiently large sample size. Spectral models were trained using gold standard histopathology and IHC. It should be noted that cancer progression in tissues/organs is not uniform, especially during intermediate stages. Thus, heterogeneity within the Raman probed region cannot be ruled out and despite best efforts, pose a hurdle to develop pure models for intermediate stages such as hyperplasia and mild dysplasia. Another major outcome of the present study has been Raman spectroscopic identification of abnormal changes in apparently normal control mucosa, subsequently corroborated by gold standard and IHC. These abnormal changes, which may often be wrongly concluded as 'false positives', have revealed small foci of higher pathologies and also showed higher expression of cyclin D1 with respect to histopathologically normal regions. These observations strengthen the applicability of RS as a candidate tool for screening due to the sensitivity of the technique in detecting abnormal changes at microscopic level. Various in vivo clinical studies further indicate that mass screening campaigns can be carried out, starting with the high risk populations. In the next step, such screening can identify low risk populations and educate them about dental care as irregular/sharp dentures may also lead to cancer after years of repeated irritations of the adjacent oral mucosa. Such campaigns will facilitate translation of RS as a screening tool and reduce workload on clinicians and pathologists, especially in the highly populated developing nations.

Overall, findings suggest potential of RS in monitoring progression during carcinogenesis and in identifying abnormal changes and microheterogenity in buccal pouch which may often go unnoticed in clinical examinations and conventional studies wherein tissue extracts/homogenates

are employed. Over all, results provide further proof of RS being a potential adjunct for prospective non-invasive, label-free, online applications for screening in general, vis a vis conventional screening which is shown to be effective in high risk groups.

5 References

1. Jemal A, Siegel R, Xu J, Ward E: **Cancer statistics, 2010**. *CA Cancer J Clin* 2010, **60**(5):277-300.
2. Mehrotra R, Gupta DK: **Exciting new advances in oral cancer diagnosis: avenues to early detection**. *Head Neck Oncol* 2011, **3**(1):33.
3. Sankaranarayanan R, Ramadas K, Thomas G, Muwonge R, Thara S, Mathew B, Rajan B, Trivandrum Oral Cancer Screening Study G: **Effect of screening on oral cancer mortality in Kerala, India: a cluster-randomised controlled trial**. *Lancet* 2005, **365**(9475):1927-1933.
4. Raman CV, Krishnan KS: **A new type of secondary radiation**. *Nature* 1928, **121**(3048):501-502.
5. Pence I, Mahadevan-Jansen A: **Clinical instrumentation and applications of Raman spectroscopy**. *Chemical Society Reviews* 2016, **45**(7):1958-1979.
6. Venkatakrishna K, Kurien J, Pai KM, Valiathan M, Kumar NN, Murali Krishna C, Ullas G, Kartha V: **Optical pathology of oral tissue: a Raman spectroscopy diagnostic method**. *Current science* 2001, **80**(5):665-669.
7. Guze K, Short M, Sonis S, Karimbux N, Chan J, Zeng H: **Parameters defining the potential applicability of Raman spectroscopy as a diagnostic tool for oral disease**. *Journal of biomedical optics* 2009, **14**(1):014016-014016-014019.
8. Bergholt MS, Zheng W, Huang Z: **Characterizing variability in in vivo Raman spectroscopic properties of different anatomical sites of normal tissue in the oral cavity**. *Journal of Raman Spectroscopy* 2012, **43**(2):255-262.
9. Singh SP, Deshmukh A, Chaturvedi P, Murali Krishna C: **In vivo Raman spectroscopic identification of premalignant lesions in oral buccal mucosa**. *J Biomed Opt* 2012, **17**(10):105002.
10. Singh S, Sahu A, Deshmukh A, Chaturvedi P, Krishna CM: **In vivo Raman spectroscopy of oral buccal mucosa: a study on malignancy associated changes (MAC)/cancer field effects (CFE)**. *Analyst* 2013, **138**(14):4175-4182.
11. Sahu A, Deshmukh A, Hole AR, Chaturvedi P, Krishna CM: **In vivo subsite classification and diagnosis of oral cancers using Raman spectroscopy**. *Journal of Innovative Optical Health Sciences* 2016:1650017.
12. Salley JJ: **Experimental carcinogenesis in the cheek pouch of the Syrian hamster**. *J Dent Res* 1954, **33**(2):253-262.
13. Gimenez-Conti IB, Slaga TJ: **The hamster cheek pouch carcinogenesis model**. *Journal of Cellular Biochemistry* 1993, **53**(S17F):83-90.
14. Ghanate AD, Kothiwale S, Singh SP, Bertrand D, Krishna CM: **Comparative evaluation of spectroscopic models using different multivariate statistical tools in a multicancer scenario**. *J Biomed Opt* 2011, **16**(2):025003.
15. Hall M, Peters G: **Genetic alterations of cyclins, cyclin-dependent kinases, and Cdk inhibitors in human cancer**. *Adv Cancer Res* 1996, **68**:67-108.
16. Staibano S, Lo Muzio L, Pannone G, Mezza E, Argenziano G, Vetrani A, Lucariello A, Franco R, Errico ME, De Rosa G *et al*: **DNA ploidy and cyclin D1 expression in basal cell carcinoma of the head and neck**. *Am J Clin Pathol* 2001, **115**(6):805-813.
17. Xu J, Gimenez-Conti IB, Cunningham JE, Collet AM, Luna MA, Lanfranchi HE, Spitz MR, Conti CJ: **Alterations of p53, cyclin D1, rb, and H-ras in human oral carcinomas related to tobacco use**. *Cancer* 1998, **83**(2):204-212.

18. Selk Ghaffari M, Moayer F, Dezfoulian O: **Spontaneous differentiated squamous cell carcinoma of cheek pouch in a Syrian hamster**. *Iranian Journal of Veterinary Research* 2009, **10**(1):84-86.
19. Dachi SF, Sanders JE, Urie EM: **Effects of dimethyl sulfoxide on dimethylbenzanthracene-induced carcinogenesis in the hamster cheek pouch**. *Cancer research* 1967, **27**(7):1183-1185.
20. Piemonte ED, Lazos JP, Brunotto M: **Relationship between chronic trauma of the oral mucosa, oral potentially malignant disorders and oral cancer**. *Journal of oral pathology & medicine* 2010, **39**(7):513-517.
21. Preston-Martin S, Pike MC, Ross RK, Jones PA, Henderson BE: **Increased Cell Division as a Cause of Human Cancer**. *Cancer Research* 1990, **50**(23):7415-7421.
22. Huang D, Swanson EA, Lin CP, Schuman JS, Stinson WG, Chang W, Hee MR, Flotte T, Gregory K, Puliafito CA *et al*: **Optical coherence tomography**. *Science* 1991, **254**(5035):1178-1181.
23. Hanahan D, Weinberg RA: **Hallmarks of cancer: the next generation**. *Cell* 2011, **144**(5):646-674.
24. Sontheimer H: **Diseases of the Nervous System**: Academic Press; 2015.
25. Wagener DJT: **The History of Oncology**: Bohn Stafleu Van Loghum; 2009.
26. Hajdu SI: **Greco-Roman thought about cancer**. *Cancer* 2004, **100**(10):2048-2051.
27. Papavramidou N, Papavramidis T, Demetriou T: **Ancient Greek and Greco–Roman Methods in Modern Surgical Treatment of Cancer**. *Annals of Surgical Oncology* 2010, **17**(3):665-667.
28. DeVita VT, Rosenberg SA: **Two Hundred Years of Cancer Research**. *New England Journal of Medicine* 2012, **366**(23):2207-2214.
29. **Stat Bite: Death Rates From Heart Disease and Cancer in People Younger Than 85**. *Journal of the National Cancer Institute* 2005, **97**(5):330.
30. Twombly R: **Cancer Surpasses Heart Disease as Leading Cause of Death for All But the Very Elderly**. *Journal of the National Cancer Institute* 2005, **97**(5):330-331.
31. Murray C, Lopez A: **Global Health status in developing countries: Global burden of Diseases and Injuries in SEARO**. *Harvard School of Public Health* 1996, **1**.
32. **Global Adult Tobacco Survey, India, Fact sheet**. In. India: WHO; 2010.
33. Rajaraman P, Anderson BO, Basu P, Belinson JL, D'Cruz A, Dhillon PK, Gupta P, Jawahar TS, Joshi N, Kailash U: **Recommendations for screening and early detection of common cancers in India**. *The Lancet Oncology* 2015, **16**(7):e352-e361.
34. Sankaranarayanan R, Swaminathan R, Brenner H, Chen K, Chia KS, Chen JG, Law SC, Ahn Y-O, Xiang YB, Yeole BB: **Cancer survival in Africa, Asia, and Central America: a population-based study**. *The lancet oncology* 2010, **11**(2):165-173.
35. Muwonge R, Ramadas K, Sankila R, Thara S, Thomas G, Vinoda J, Sankaranarayanan R: **Role of tobacco smoking, chewing and alcohol drinking in the risk of oral cancer in Trivandrum, India: a nested case-control design using incident cancer cases**. *Oral oncology* 2008, **44**(5):446-454.
36. Radoï L, Luce D: **A review of risk factors for oral cavity cancer: the importance of a standardized case definition**. *Community dentistry and oral epidemiology* 2013, **41**(2):97-109.
37. Neville BW, Day TA: **Oral cancer and precancerous lesions**. *CA: a cancer journal for clinicians* 2002, **52**(4):195-215.
38. Marshall JR, Graham S, Haughey BP, Shedd D, O'Shea R, Brasure J, Wilkinson GS, West D: **Smoking, alcohol, dentition and diet in the epidemiology of oral cancer**. *European Journal of Cancer Part B: Oral Oncology* 1992, **28**(1):9-15.
39. Hecht SS: **Tobacco carcinogens, their biomarkers and tobacco-induced cancer**. *Nat Rev Cancer* 2003, **3**(10):733-744.
40. Johnson N: **Tobacco use and oral cancer: a global perspective**. *Journal of Dental Education* 2001, **65**(4):328-339.

41. Jayalekshmi PA, Gangadharan P, Akiba S, Koriyama C, Nair RRK: **Oral cavity cancer risk in relation to tobacco chewing and bidi smoking among men in Karunagappally, Kerala, India: Karunagappally cohort study**. *Cancer science* 2011, **102**(2):460-467.
42. Madani A, Dikshit M, Bhaduri D: **Risk for oral cancer associated to smoking, smokeless and oral dip products**. *Indian journal of public health* 2012, **56**(1):57.
43. Jayalekshmi P, Gangadharan P, Akiba S, Nair R, Tsuji M, Rajan B: **Tobacco chewing and female oral cavity cancer risk in Karunagappally cohort, India**. *British journal of cancer* 2009, **100**(5):848-852.
44. Alwan A: **Global status report on noncommunicable diseases 2010**: World Health Organization; 2011.
45. Guha N, Warnakulasuriya S, Vlaanderen J, Straif K: **Betel quid chewing and the risk of oral and oropharyngeal cancers: A meta-analysis with implications for cancer control**. *International Journal of Cancer* 2014, **135**(6):1433-1443.
46. Znaor A, Brennan P, Gajalakshmi V, Mathew A, Shanta V, Varghese C, Boffetta P: **Independent and combined effects of tobacco smoking, chewing and alcohol drinking on the risk of oral, pharyngeal and esophageal cancers in Indian men**. *International journal of cancer* 2003, **105**(5):681-686.
47. Balaram P, Sridhar H, Rajkumar T, Vaccarella S, Herrero R, Nandakumar A, Ravichandran K, Ramdas K, Sankaranarayanan R, Gajalakshmi V: **Oral cancer in southern India: The influence of smoking, drinking, paan-chewing and oral hygiene**. *International journal of cancer* 2002, **98**(3):440-445.
48. Scully C: **Oral cancer aetiopathogenesis; past, present and future aspects**. *Med Oral Patol Oral Cir Bucal* 2011, **16**(3):e306-e311.
49. Mashberg A, Boffetta P, Winkelman R, Garfinkel L: **Tobacco smoking, alcohol drinking, and cancer of the oral cavity and oropharynx among US veterans**. *Cancer* 1993, **72**(4):1369-1375.
50. Jovanovic A, Schulten EA, Kostense PJ, Snow GB, Waal I: **Tobacco and alcohol related to the anatomical site of oral squamous cell carcinoma**. *Journal of oral pathology & medicine* 1993, **22**(10):459-462.
51. Andre K, Schraub S, Mercier M, Bontemps P: **Role of alcohol and tobacco in the aetiology of head and neck cancer: a case-control study in the Doubs region of France**. *European Journal of Cancer Part B: Oral Oncology* 1995, **31**(5):301-309.
52. Blot WJ, McLaughlin JK, Winn DM, Austin DF, Greenberg RS, Preston-Martin S, Bernstein L, Schoenberg JB, Stemhagen A, Fraumeni JF: **Smoking and drinking in relation to oral and pharyngeal cancer**. *Cancer research* 1988, **48**(11):3282-3287.
53. Lewin F, Norell SE, Johansson H, Gustavsson P, Wennerberg J, Biörklund A, Rutqvist LE: **Smoking tobacco, oral snuff, and alcohol in the etiology of squamous cell carcinoma of the head and neck**. *Cancer* 1998, **82**(7):1367-1375.
54. Moreno-Lopez L, Esparza-Gomez G, Gonzalez-Navarro A, Cerero-Lapiedra R, Gonzalez-Hernandez M, Domınguez-Rojas V: **Risk of oral cancer associated with tobacco smoking, alcohol consumption and oral hygiene: a case-control study in Madrid, Spain**. *Oral oncology* 2000, **36**(2):170-174.
55. Ko YC, Huang YL, Lee CH, Chen MJ, Lin LM, Tsai CC: **Betel quid chewing, cigarette smoking and alcohol consumption related to oral cancer in Taiwan**. *Journal of oral pathology & medicine* 1995, **24**(10):450-453.
56. Combes J-D, Franceschi S: **Role of human papillomavirus in non-oropharyngeal head and neck cancers**. *Oral oncology* 2014, **50**(5):370-379.

57. Sugerman P, Shillitoe E: **The high risk human papillomaviruses and oral cancer: evidence for and against a causal relationship**. *Oral diseases* 1997, **3**(3):130-147.
58. Gupta K, Metgud R: **Evidences suggesting involvement of viruses in oral squamous cell carcinoma**. *Pathology research international* 2013, **2013**.
59. Park N-H, Li S-L, Xie J-F, Cherrick HM: **In vitro and animal studies of the role of viruses in oral carcinogenesis**. *European Journal of Cancer Part B: Oral Oncology* 1992, **28**(2):145-152.
60. Sand L, Jalouli J: **Viruses and oral cancer. Is there a link?** *Microbes and infection* 2014, **16**(5):371-378.
61. Maden C, Beckmann AM, Thomas DB, McKnight B, Sherman KJ, Ashley RL, Corey L, Daling JR: **Human papillomaviruses, herpes simplex viruses, and the risk of oral cancer in men**. *American journal of epidemiology* 1992, **135**(10):1093-1102.
62. Ankathil R, Mathew A, Joseph F, Nair M: **Is oral cancer susceptibility inherited? Report of five oral cancer families**. *European Journal of Cancer Part B: Oral Oncology* 1996, **32**(1):63-67.
63. Pogoda JM, Preston-Martin S: **Solar radiation, lip protection, and lip cancer risk in Los Angeles County women (California, United States)**. *Cancer Causes & Control* 1996, **7**(4):458-463.
64. Winn DM: **Diet and nutrition in the etiology of oral cancer**. *The American journal of clinical nutrition* 1995, **61**(2):437S-445S.
65. Winn DM, Ziegler RG, Pickle LW, Gridley G, Blot WJ, Hoover RN: **Diet in the etiology of oral and pharyngeal cancer among women from the southern United States**. *Cancer research* 1984, **44**(3):1216-1222.
66. Potter JD, Steinmetz K: **Vegetables, fruit and phytoestrogens as preventive agents**. *IARC scientific publications* 1995(139):61-90.
67. Block G, Patterson B, Subar A: **Fruit, vegetables, and cancer prevention: a review of the epidemiological evidence**. *Nutrition and cancer* 1992, **18**(1):1-29.
68. Pitot HC: **The molecular biology of carcinogenesis**. *Cancer* 1993, **72**(S3):962-970.
69. Hau J: **Animal Models for Human Diseases**. In: *Sourcebook of Models for Biomedical Research.* Edited by Conn PM: Humana Press; 2008: 3-8.
70. Steidler N, Reade P: **Experimental induction of oral squamous cell carcinomas in mice with 4-nitroquinolone-1-oxide**. *Oral surgery, oral medicine, oral pathology* 1984, **57**(5):524-531.
71. Wong P, Wilson D: **4 Nitroquinoline 1-oxide-induced carcinogenesis in the rat palate**. *Journal of Oral Pathology & Medicine* 1983, **12**(5):375-384.
72. Steidler N, Rich A, Reade P: **Experimental induction of preneoplastic and neoplastic changes in the lingual mucosa of rats**. *Journal de biologie buccale* 1985, **13**(4):339-346.
73. Tang X-H, Knudsen B, Bemis D, Tickoo S, Gudas LJ: **Oral cavity and esophageal carcinogenesis modeled in carcinogen-treated mice**. *Clinical Cancer Research* 2004, **10**(1):301-313.
74. Sakaki T, Tamura I, Kadota H, Kakudo K: **Changing expression of E-and P-cadherin during rat tongue carcinogenesis induced by 4-nitroquinoline 1-oxide**. *Journal of oral pathology & medicine* 2003, **32**(9):530-537.
75. Vered M, Yarom N, Dayan D: **4NQO oral carcinogenesis: animal models, molecular markers and future expectations**. *Oral oncology* 2005, **41**(4):337-339.
76. Chen Y-K, Lin L-M: **DMBA-induced hamster buccal pouch carcinoma and VX2-induced rabbit cancer as a model for human oral carcinogenesis**. *Expert review of anticancer therapy* 2010, **10**(9):1485-1496.
77. Lin L-M, Chen Y-K, Chen C-H, Chen Y-W, Huang AH-C, Wang W-C: **VX2-induced rabbit buccal carcinoma: a potential cancer model for human buccal mucosa squamous cell carcinoma**. *Oral oncology* 2009, **45**(11):e196-e203.

78. van Es RJ, Dullens HF, van der Bilt A, Koole R, Slootweg PJ: **Evaluation of the VX2 rabbit auricle carcinoma as a model for head and neck cancer in humans**. *Journal of Cranio-Maxillofacial Surgery* 2000, **28**(5):300-307.
79. Keyes PH, Dale PP: **A preliminary survey of the pouches and dentition of the Syrian hamster**. *Journal of Dental Research* 1944, **23**(6):427-438.
80. Morris AL: **Factors influencing experimental carcinogenesis in the hamster cheek pouch**. *Journal of dental research* 1961, **40**(1):3-15.
81. Shklar G: **Experimental oral pathology in the Syrian hamster**. 1972.
82. Balasenthil S, Saroja M, Ramachandran C, Nagini S: **Of humans and hamsters: comparative analysis of lipid peroxidation, glutathione, and glutathione-dependent enzymes during oral carcinogenesis**. *British Journal of Oral and Maxillofacial Surgery* 2000, **38**(4):267-270.
83. Nagini S, Letchoumy PV, Thangavelu A, Ramachandran C: **Of humans and hamsters: a comparative evaluation of carcinogen activation, DNA damage, cell proliferation, apoptosis, invasion, and angiogenesis in oral cancer patients and hamster buccal pouch carcinomas**. *Oral oncology* 2009, **45**(6):e31-e37.
84. Ambatipudi S, Bhosale PG, Heath E, Pandey M, Kumar G, Kane S, Patil A, Maru GB, Desai RS, Watt FM: **Downregulation of keratin 76 expression during oral carcinogenesis of human, hamster and mouse**. *PloS one* 2013, **8**:e70688.
85. Gimenez-Conti IB, Bianchi AB, Stockman SL, Conti CJ, Slaga TJ: **Activating mutation of the Ha-ras gene in chemically induced tumors of the hamster cheek pouch**. *Molecular carcinogenesis* 1992, **5**(4):259-263.
86. Gimenez-Conti IB, LaBate M, Liu F, Osterndorff E: **p53 alterations in chemically induced hamster cheek-pouch lesions**. *Molecular carcinogenesis* 1996, **16**(4):197-202.
87. Husain Z, Fei Y, Roy S, Solt DB, Polverini PJ, Biswas DK: **Sequential expression and cooperative interaction of c-Ha-ras and c-erbB genes in in vivo chemical carcinogenesis**. *Proceedings of the National Academy of Sciences* 1989, **86**(4):1264-1268.
88. Suda D, Schwartz J, Shklar G: **GGT reduction in beta carotene-inhibition of hamster buccal pouch carcinogenesis**. *European Journal of Cancer and Clinical Oncology* 1987, **23**(1):43-46.
89. Solt DB: **Localization of gamma-glutamyl transpeptidase in hamster buccal pouch epithelium treated with 7, 12-dimethylbenz [a] anthracene**. *Journal of the National Cancer Institute* 1981, **67**(1):193-200.
90. Schwartz JL, Shklar G: **Glutathione inhibits experimental oral carcinogenesis, p53 expression, and angiogenesis**. 1996.
91. Shklar G, Schwartz J: **Vitamin E inhibits experimental carcinogenesis and tumour angiogenesis**. *European Journal of Cancer Part B: Oral Oncology* 1996, **32**(2):114-119.
92. Suda D, Schwartz J, Shklar G: **Inhibition of experimental oral carcinogenesis by topical beta carotene**. *Carcinogenesis* 1986, **7**(5):711-715.
93. Shklar G: **Inhibition of oral mucosal carcinogenesis by vitamin E**. *J Natl Cancer Inst* 1982, **68**:791-797.
94. Walker F, Carter J, Crawford G, Laird H, Lessells A, Pollet J: **Hamster cheek pouch mucosubstances and immunological privilege**. *British journal of experimental pathology* 1970, **51**(4):379.
95. MacDonald DG: **Comparison of epithelial dysplasia in hamster cheek pouch carcinogenesis and human oral mucosa**. *Journal of Oral Pathology & Medicine* 1981, **10**(3):186-191.
96. Nauta J, Roodenburg J, Nikkels P, Witjes M, Vermey A: **Comparison of epithelial dysplasia—the 4NQO rat palate model and human oral mucosa**. *International journal of oral and maxillofacial surgery* 1995, **24**(1):53-58.

97. Lingen MW, Kalmar JR, Karrison T, Speight PM: **Critical evaluation of diagnostic aids for the detection of oral cancer**. *Oral oncology* 2008, **44**(1):10-22.
98. Fedele S: **Diagnostic aids in the screening of oral cancer**. *Head & neck oncology* 2009, **1**(1):5.
99. Epstein J, Silverman S, Epstein J, Lonky S, Bride M: **Analysis of oral lesion biopsies identified and evaluated by visual examination, chemiluminescence and toluidine blue**. *Oral oncology* 2008, **44**(6):538-544.
100. Epstein JB, Güneri P, Boyacioglu H, Abt E: **The limitations of the clinical oral examination in detecting dysplastic oral lesions and oral squamous cell carcinoma**. *The Journal of the American Dental Association* 2012, **143**(12):1332-1342.
101. Torras CC, Escoda CG: **Techniques for early diagnosis of oral squamous cell carcinoma: systematic review**. *Medicina oral, patología oral y cirugía bucal Ed inglesa* 2015, **20**(3):17.
102. Sankaranarayanan R, Ramadas K, Thomas G, Muwonge R, Thara S, Mathew B, Rajan B: **Effect of screening on oral cancer mortality in Kerala, India: a cluster-randomised controlled trial**. *The Lancet*, **365**(9475):1927-1933.
103. Eisen D, Frist S: **The relevance of the high positive predictive value of the oral brush biopsy**. *Oral oncology* 2005, **41**(7):753-755.
104. Poate T, Buchanan J, Hodgson T, Speight P, Barrett A, Moles D, Scully C, Porter S: **An audit of the efficacy of the oral brush biopsy technique in a specialist Oral Medicine unit**. *Oral oncology* 2004, **40**(8):829-834.
105. Potter TJ, Summerlin D-J, Campbell JH: **Oral malignancies associated with negative transepithelial brush biopsy**. *Journal of oral and maxillofacial surgery* 2003, **61**(6):674-677.
106. Rick GM, Slater L: **Oral brush biopsy: the problem of false positives**. *Oral Surgery, Oral Medicine, Oral Pathology, Oral Radiology, and Endodontology* 2003, **96**(3):252.
107. Scheifele C, Schmidt-Westhausen A-M, Dietrich T, Reichart PA: **The sensitivity and specificity of the OralCDx technique: evaluation of 103 cases**. *Oral oncology* 2004, **40**(8):824-828.
108. Epstein JB, Scully C, Spinelli J: **Toluidine blue and Lugol's iodine application in the assessment of oral malignant disease and lesions at risk of malignancy**. *Journal of oral pathology & medicine* 1992, **21**(4):160-163.
109. Du Gf, Li Cz, Chen Hz, Chen Xm, Xiao Q, Cao Zg, Shang Sh, Cai X: **Rose bengal staining in detection of oral precancerous and malignant lesions with colorimetric evaluation: a pilot study**. *International journal of cancer* 2007, **120**(9):1958-1963.
110. Gandolfo S, Pentenero M, Broccoletti R, Pagano M, Carrozzo M, Scully C: **Toluidine blue uptake in potentially malignant oral lesions in vivo: clinical and histological assessment**. *Oral oncology* 2006, **42**(1):88-94.
111. Martin I, Kerawala C, Reed M: **The application of toluidine blue as a diagnostic adjunct in the detection of epithelial dysplasia**. *Oral Surgery, Oral Medicine, Oral Pathology, Oral Radiology, and Endodontology* 1998, **85**(4):444-446.
112. Warnakulasuriya K, Johnson NW: **Sensitivity and specificity of OraScan® toluidine blue mouthrinse in the detection of oral cancer and precancer**. *Journal of oral pathology & medicine* 1996, **25**(3):97-103.
113. Chen Y-W, Lin J-S, Wu C-H, Lui M-T, Kao S-Y, Fong Y: **Application of in vivo stain of methylene blue as a diagnostic aid in the early detection and screening of oral squamous cell carcinoma and precancer lesions**. *Journal of the Chinese Medical Association* 2007, **70**(11):497-503.
114. Peng G, Long Q, Wu Y, Zhao J, Chen L, Li X: **Evaluation of double vital staining with lugol's iodine and methylene blue in diagnosing superficial esophageal lesions**. *Scandinavian journal of gastroenterology* 2011, **46**(4):406-413.

115. Lingen M, Kalmar J, Karrison T, Speight P: **Critical evaluation of diagnostic aids for the detection of oral cancer**. *Oral Oncol* 2008, **44**:10 - 22.
116. Patton L, Epstein J, Kerr A: **Adjunctive techniques for oral cancer examination and lesion diagnosis: a systematic review of the literature**. *J Am Dent Assoc* 2008, **139**:896 - 905.
117. Ram S, Siar C: **Chemiluminescence as a diagnostic aid in the detection of oral cancer and potentially malignant epithelial lesions**. *Int J Oral Maxillofac Surg* 2005, **34**:521 - 527.
118. Epstein J, Gorsky M, Lonky S, Silverman S, Epstein J, Bride M: **The efficacy of oral lumenoscopy (ViziLite) in visualizing oral mucosal lesions**. *Spec Care Dentist* 2006, **26**:171 - 174.
119. Farah C, McCullough M: **A pilot case control study on the efficacy of acetic acid wash and chemiluminescent illumination (ViziLitetrade mark) in the visualisation of oral mucosal white lesions**. *Oral Oncol* 2007, **43**:820 - 824.
120. Oh E, Laskin D: **Efficacy of the ViziLite system in the identification of oral lesions**. *J Oral Maxillofac Surg* 2007, **65**:424 - 426.
121. Epstein J, Silverman S, Epstein J, Lonky S, Bride M: **Analysis of oral lesion biopsies identified and evaluated by visual examination, chemiluminescence and toluidine blue**. *Oral Oncol* 2008, **44**:538 - 544.
122. Khanna SS, Karjodkar FR: **Circulating immune complexes and trace elements (Copper, Iron and Selenium) as markers in oral precancer and cancer: a randomised, controlled clinical trial**. *Head Face Med* 2006, **2**:33.
123. Nagler RM, Barak M, Peled M, Ben-Aryeh H, Filatov M, Laufer D: **Early diagnosis and treatment monitoring roles of tumor markers Cyfra 21-1 and TPS in oral squamous cell carcinoma**. *Cancer* 1999, **85**(5):1018-1025.
124. Faria PCB, Sena AAS, Nascimento R, Carvalho WJ, Loyola AM, Silva SJ, Durighetto AF, Oliveira AD, Oliani SM, Goulart LR: **Expression of annexin A1 mRNA in peripheral blood from oral squamous cell carcinoma patients**. *Oral oncology* 2010, **46**(1):25-30.
125. Shpitzer T, Bahar G, Feinmesser R, Nagler RM: **A comprehensive salivary analysis for oral cancer diagnosis**. *Journal of cancer research and clinical oncology* 2007, **133**(9):613-617.
126. Nagler RM, Lischinsky S, Diamond E, Klein I, Reznick AZ: **New insights into salivary lactate dehydrogenase of human subjects**. *Journal of Laboratory and Clinical Medicine* 2001, **137**(5):363-369.
127. Sanjay P, Hallikeri K, Shivashankara A: **Evaluation of salivary sialic acid, total protein, and total sugar in oral cancer: a preliminary report**. *Indian Journal of Dental Research* 2008, **19**(4):288.
128. Park NJ, Zhou H, Elashoff D, Henson BS, Kastratovic DA, Abemayor E, Wong DT: **Salivary microRNA: discovery, characterization, and clinical utility for oral cancer detection**. *Clinical Cancer Research* 2009, **15**(17):5473-5477.
129. Masters BR: **The development of fluorescence microscopy**. *eLS* 2010.
130. Stokes GG: **On the change of refrangibility of light**. *Philosophical Transactions of the Royal Society of London* 1852:463-562.
131. Wagnieres GA, Star WM, Wilson BC: **In vivo fluorescence spectroscopy and imaging for oncological applications**. *Photochemistry and photobiology* 1998, **68**(5):603-632.
132. Pottier R: **In vitro and in vivo fluorescence monitoring of photosensitizers**. *Journal of Photochemistry and Photobiology B: Biology* 1990, **6**(1):103-109.
133. Nilsson H, Johansson J, Svanberg K, Svanberg S, Jori G, Reddi E, Segalla A, Gust D, Moore A, Moore TA: **Laser-induced fluorescence in malignant and normal tissue in mice injected with two different carotenoporphyrins**. *British journal of cancer* 1994, **70**(5):873.
134. Ramanujam N: **Fluorescence spectroscopy in vivo**. *Encyclopedia of analytical chemistry* 2000.

135. Neves V, Heister E, Costa S, Tilmaciu C, Flahaut E, Soula B, Coley HM, McFadden J, Silva SR: **Design of double-walled carbon nanotubes for biomedical applications**. *Nanotechnology*, **23**(36):365102.
136. De Veld D, Witjes M, Sterenborg H, Roodenburg J: **The status of in vivo autofluorescence spectroscopy and imaging for oral oncology**. *Oral Oncol* 2005, **41**:117 - 131.
137. Inaguma M, Hashimoto K: **Porphyrin-like fluorescence in oral cancer: In vivo fluorescence spectral characterization of lesions by use of a near-ultraviolet excited autofluorescence diagnosis system and separation of fluorescent extracts by capillary electrophoresis**. *Cancer* 1999, **86**:2201 - 2211.
138. Chen CT, Chiang HK, Chow SN, Wang CY, Lee YS, Tsai JC, Chiang CP: **Autofluorescence in normal and malignant human oral tissues and in DMBA-induced hamster buccal pouch carcinogenesis**. *Journal of oral pathology & medicine* 1998, **27**(10):470-474.
139. Wang CY, Tsai T, Chen HC, Chang SC, Chen CT, Chiang CP: **Autofluorescence spectroscopy for in vivo diagnosis of DMBA-induced hamster buccal pouch pre-cancers and cancers**. *J Oral Pathol Med* 2003, **32**(1):18-24.
140. Heintzelman DL, Utzinger U, Fuchs H, Zuluaga A, Gossage K, Gillenwater AM, Jacob R, Kemp B, Richards-Kortum RR: **Optimal excitation wavelengths for in vivo detection of oral neoplasia using fluorescence spectroscopy**. *Photochemistry and Photobiology* 2000, **72**(1):103-113.
141. Gillenwater A, Jacob R, Ganeshappa R, Kemp B, El-Naggar AK, Palmer JL, Clayman G, Mitchell MF, Richards-Kortum R: **Noninvasive diagnosis of oral neoplasia based on fluorescence spectroscopy and native tissue autofluorescence**. *Archives of Otolaryngology–Head & Neck Surgery* 1998, **124**(11):1251-1258.
142. Braichotte DR, Wagnieres GA, Bays R, Monnier P, Bergh HEvd: **Clinical pharmacokinetic studies of photofrin by fluorescence spectroscopy in the oral cavity, the esophagus, and the bronchi**. *CANCER-PHILADELPHIA*- 1995, **75**:2768-2768.
143. Ebenezar J, Ganesan S, Aruna P, Muralinaidu R, Renganathan K, Saraswathy TR: **Noninvasive fluorescence excitation spectroscopy for the diagnosis of oral neoplasia in vivo**. *BIOMEDO* 2012, **17**(9):0970071-0970078.
144. Müller MG, Valdez TA, Georgakoudi I, Backman V, Fuentes C, Kabani S, Laver N, Wang Z, Boone CW, Dasari RR: **Spectroscopic detection and evaluation of morphologic and biochemical changes in early human oral carcinoma**. *Cancer* 2003, **97**(7):1681-1692.
145. Venugopal C, Nazeer SS, Balan A, Jayasree R: **Autofluorescence spectroscopy augmented by multivariate analysis as a potential noninvasive tool for early diagnosis of oral cavity disorders**. *Photomedicine and laser surgery* 2013, **31**(12):605-612.
146. Haris P, Balan A, Jayasree R, Gupta A: **Autofluorescence spectroscopy for the in vivo evaluation of oral submucous fibrosis**. *Photomedicine and laser surgery* 2009, **27**(5):757-761.
147. Jayanthi J, Mallia RJ, Shiny ST, Baiju KV, Mathews A, Kumar R, Sebastian P, Madhavan J, Aparna G, Subhash N: **Discriminant analysis of autofluorescence spectra for classification of oral lesions in vivo**. *Lasers in surgery and medicine* 2009, **41**(5):345-352.
148. Shaiju SN, Ariya S, Asish R, Haris PS, Anita B, Kumar GA, Jayasree RS: **Habits with killer instincts: in vivo analysis on the severity of oral mucosal alterations using autofluorescence spectroscopy**. *BIOMEDO* 2011, **16**(8):087006-087006-087013.
149. Nazeer SS, Asish R, Venugopal C, Anita B, Gupta AK, Jayasree RS: **Noninvasive assessment of the risk of tobacco abuse in oral mucosa using fluorescence spectroscopy: a clinical approach**. *BIOMEDO* 2014, **19**(5):057013-057013.

150. A'Amar O, Liou L, Rodriguez-Diaz E, De las Morenas A, Bigio I: **Comparison of elastic scattering spectroscopy with histology in ex vivo prostate glands: potential application for optically guided biopsy and directed treatment**. *Lasers in medical science* 2013, **28**(5):1323-1329.
151. Jerjes W, Swinson B, Pickard D, Thomas G, Hopper C: **Detection of cervical intranodal metastasis in oral cancer using elastic scattering spectroscopy**. *Oral oncology* 2004, **40**(7):673-678.
152. Jerjes W, Swinson B, Johnson K, Thomas G, Hopper C: **Assessment of bony resection margins in oral cancer using elastic scattering spectroscopy: a study on archival material**. *Archives of oral biology* 2005, **50**(3):361-366.
153. Sharwani A, Jerjes W, Salih V, Swinson B, Bigio I, El-Maaytah M, Hopper C: **Assessment of oral premalignancy using elastic scattering spectroscopy**. *Oral oncology* 2006, **42**(4):343-349.
154. Kubelka P: **New Contributions to the Optics of Intensely Light-Scattering Materials. Part II: Nonhomogeneous Layers***. *JOSA* 1954, **44**(4):330-335.
155. De Veld DC, Skurichina M, Witjes MJ, Duin RP, Sterenborg HJ, Roodenburg JL: **Autofluorescence and diffuse reflectance spectroscopy for oral oncology**. *Lasers in surgery and medicine* 2005, **36**(5):356-364.
156. Subhash N, Mallia J, Thomas SS, Mathews A, Sebastian P, Madhavan J: **Oral cancer detection using diffuse reflectance spectral ratio R540⁄ R575 of oxygenated hemoglobin bands**. *BIOMEDO* 2006, **11**(1):014018-014018-014016.
157. Jayanthi J, Nisha G, Manju S, Philip E, Jeemon P, Baiju K, Beena V, Subhash N: **Diffuse reflectance spectroscopy: diagnostic accuracy of a non-invasive screening technique for early detection of malignant changes in the oral cavity**. *BMJ open* 2011, **1**(1):e000071.
158. Mallia R, Thomas SS, Mathews A, Kumar R, Sebastian P, Madhavan J, Subhash N: **Oxygenated hemoglobin diffuse reflectance ratio for in vivo detection of oral pre-cancer**. *BIOMEDO* 2008, **13**(4):041306-041306-041310.
159. Stephen MM, Jayanthi JL, Unni NG, Kolady PE, Beena VT, Jeemon P, Subhash N: **Diagnostic accuracy of diffuse reflectance imaging for early detection of pre-malignant and malignant changes in the oral cavity: a feasibility study**. *BMC cancer* 2013, **13**(1):278.
160. Skala MC, Palmer GM, Vrotsos KM, Gendron-Fitzpatrick A, Ramanujam N: **Comparison of a physical model and principal component analysis for the diagnosis of epithelial neoplasias in vivo using diffuse reflectance spectroscopy**. *Optics express* 2007, **15**(12):7863-7875.
161. Chen Y-W, Liaw Y-K, Hung H-R, Chung P-C, Tseng S-H: **Differentiating Early Oral Cancer from Normal Oral Tissue Using Diffuse Reflectance Spectroscopy**. In: *Asia Communications and Photonics Conference: 2013*. Optical Society of America: AF4I. 3.
162. Einstein G, Udayakumar K, Aruna PR, Koteeswaran D, Ganesan S: **Diffuse reflectance spectroscopy for monitoring physiological and morphological changes in oral cancer**. *Optik-International Journal for Light and Electron Optics* 2016, **127**(3):1479-1485.
163. Bezerra HG, Costa MA, Guagliumi G, Rollins AM, Simon DI: **Intracoronary Optical Coherence Tomography: A Comprehensive ReviewClinical and Research Applications**. *JACC: Cardiovascular Interventions* 2009, **2**(11):1035-1046.
164. Drexler W, Morgner U, Ghanta RK, Kärtner FX, Schuman JS, Fujimoto JG: **Ultrahigh-resolution ophthalmic optical coherence tomography**. *Nature medicine* 2001, **7**(4):502-507.
165. An L, Wang RK: **In vivo volumetric imaging of vascular perfusion within human retina and choroids with optical micro-angiography**. *Optics Express* 2008, **16**(15):11438-11452.
166. Boppart SA, Luo W, Marks DL, Singletary KW: **Optical coherence tomography: feasibility for basic research and image-guided surgery of breast cancer**. *Breast Cancer Res Treat* 2004, **84**(2):85-97.

167. Vakoc BJ, Fukumura D, Jain RK, Bouma BE: **Cancer imaging by optical coherence tomography: preclinical progress and clinical potential**. *Nature Reviews Cancer* 2012, **12**(5):363-368.
168. Wessels R, De Bruin D, Faber D, Van Leeuwen T, Van Beurden M, Ruers T: **Optical biopsy of epithelial cancers by optical coherence tomography (OCT)**. *Lasers in medical science* 2014, **29**(3):1297-1305.
169. Bezerra HG, Costa MA, Guagliumi G, Rollins AM, Simon DI: **Intracoronary optical coherence tomography: a comprehensive review clinical and research applications**. *JACC Cardiovascular interventions* 2009, **2**(11):1035-1046.
170. Larina IV, Ivers S, Syed S, Dickinson ME, Larin KV: **Hemodynamic measurements from individual blood cells in early mammalian embryos with Doppler swept source OCT**. *Optics letters* 2009, **34**(7):986-988.
171. Böhringer H, Boller D, Leppert J, Knopp U, Lankenau E, Reusche E, Hüttmann G, Giese A: **Time-domain and spectral-domain optical coherence tomography in the analysis of brain tumor tissue**. *Lasers in surgery and medicine* 2006, **38**(6):588-597.
172. Assayag O, Grieve K, Devaux B, Harms F, Pallud J, Chretien F, Boccara C, Varlet P: **Imaging of non-tumorous and tumorous human brain tissues with full-field optical coherence tomography**. *NeuroImage: Clinical* 2013, **2**:549-557.
173. Olmedo JM, Warschaw KE, Schmitt JM, Swanson DL: **Optical coherence tomography for the characterization of basal cell carcinoma in vivo: a pilot study**. *J Am Acad Dermatol* 2006, **55**(3):408-412.
174. Mogensen M, Joergensen TM, Nurnberg BM, Morsy HA, Thomsen JB, Thrane L, Jemec GB: **Assessment of optical coherence tomography imaging in the diagnosis of non-melanoma skin cancer and benign lesions versus normal skin: observer-blinded evaluation by dermatologists and pathologists**. *Dermatologic surgery : official publication for American Society for Dermatologic Surgery [et al]* 2009, **35**(6):965-972.
175. Jørgensen TM, Tycho A, Mogensen M, Bjerring P, Jemec GB: **Machine-learning classification of non-melanoma skin cancers from image features obtained by optical coherence tomography**. *Skin Research and Technology* 2008, **14**(3):364-369.
176. Wong BJ, Jackson RP, Guo S, Ridgway JM, Mahmood U, Su J, Shibuya TY, Crumley RL, Gu M, Armstrong WB *et al*: **In vivo optical coherence tomography of the human larynx: normative and benign pathology in 82 patients**. *Laryngoscope* 2005, **115**(11):1904-1911.
177. Çilesiz I, Fockens P, Kerindongo R, Faber D, Tytgat G, ten Kate F, van Leeuwen T: **Comparative optical coherence tomography imaging of human esophagus: How accurate is localization of the muscularis mucosae?** *Gastrointestinal endoscopy* 2002, **56**(6):852-857.
178. Cobb MJ, Hwang JH, Upton MP, Chen Y, Oelschlager BK, Wood DE, Kimmey MB, Li X: **Imaging of subsquamous Barrett's epithelium with ultrahigh-resolution optical coherence tomography: a histologic correlation study**. *Gastrointestinal endoscopy* 2010, **71**(2):223-230.
179. Pitris C, Jesser C, Boppart SA, Stamper D, Brezinski ME, Fujimoto JG: **Feasibility of optical coherence tomography for high-resolution imaging of human gastrointestinal tract malignancies**. *Journal of gastroenterology* 2000, **35**(2):87-92.
180. Poneros JM, Brand S, Bouma BE, Tearney GJ, Compton CC, Nishioka NS: **Diagnosis of specialized intestinal metaplasia by optical coherence tomography**. *Gastroenterology* 2001, **120**(1):7-12.
181. Kut C, Chaichana KL, Xi J, Raza SM, Ye X, McVeigh ER, Rodriguez FJ, Quiñones-Hinojosa A, Li X: **Detection of human brain cancer infiltration ex vivo and in vivo using quantitative optical coherence tomography**. *Science translational medicine* 2015, **7**(292):292ra100-292ra100.
182. Escobar PF, Belinson JL, White A, Shakhova NM, Feldchtein FI, Kareta MV, Gladkova ND: **Diagnostic efficacy of optical coherence tomography in the management of preinvasive and**

invasive cancer of uterine cervix and vulva. *International journal of gynecological cancer : official journal of the International Gynecological Cancer Society* 2004, **14**(3):470-474.
183. Tearney G, Brezinski M, Southern J, Bouma B, Boppart S, Fujimoto J: **Optical biopsy in human urologic tissue using optical coherence tomography**. *The Journal of urology* 1997, **157**(5):1915-1919.
184. Prestin S, Rothschild SI, Betz CS, Kraft M: **Measurement of epithelial thickness within the oral cavity using optical coherence tomography**. *Head & neck* 2012, **34**(12):1777-1781.
185. Wilder-Smith P, Lee K, Guo S, Zhang J, Osann K, Chen Z, Messadi D: **In vivo diagnosis of oral dysplasia and malignancy using optical coherence tomography: preliminary studies in 50 patients**. *Lasers in surgery and medicine* 2009, **41**(5):353-357.
186. Tsai M-T, Lee C-K, Lee H-C, Chen H-M, Chiang C-P, Wang Y-M, Yang C-C: **Differentiating oral lesions in different carcinogenesis stages with optical coherence tomography**. *BIOMEDO* 2009, **14**(4):044028-044028-044027.
187. Matheny ES, Hanna NM, Jung WG, Chen Z, Wilder-Smith P, Mina-Araghi R, Brenner M: **Optical coherence tomography of malignancy in hamster cheek pouches**. *J Biomed Opt* 2004, **9**(5):978-981.
188. Hanna NM, Waite W, Taylor K, Jung WG, Mukai D, Matheny E, Kreuter K, Wilder-Smith P, Brenner M, Chen Z: **Feasibility of three-dimensional optical coherence tomography and optical Doppler tomography of malignancy in hamster cheek pouches**. *Photomed Laser Surg* 2006, **24**(3):402-409.
189. Graf RN, Robles FE, Chen X, Wax A: **Detecting precancerous lesions in the hamster cheek pouch using spectroscopic white-light optical coherence tomography to assess nuclear morphology via spectral oscillations**. *BIOMEDO* 2009, **14**(6):064030-064030-064038.
190. Pande P, Shrestha S, Park J, Serafino MJ, Gimenez-Conti I, Brandon J, Cheng Y-S, Applegate BE, Jo JA: **Automated classification of optical coherence tomography images for the diagnosis of oral malignancy in the hamster cheek pouch**. *BIOMEDO* 2014, **19**(8):086022-086022.
191. Kumar P, Bhattacharjee T, Ingle A, Maru G, Krishna CM: **Raman Spectroscopy of Experimental Oral Carcinogenesis: Study on Sequential Cancer Progression in Hamster Buccal Pouch Model**. *Technol Cancer Res Treat* 2015.
192. Rigas B, Morgello S, Goldman IS, Wong P: **Human colorectal cancers display abnormal Fourier-transform infrared spectra**. *Proceedings of the National Academy of Sciences* 1990, **87**(20):8140-8144.
193. Jackson M, Kim K, Tetteh J, Mansfield JR, Dolenko B, Somorjai RL, Orr FW, Watson PH, Mantsch HH: **Cancer diagnosis by infrared spectroscopy: methodological aspects**. In: *BiOS'98 International Biomedical Optics Symposium: 1998*. International Society for Optics and Photonics: 24-34.
194. Fukuyama Y, Yoshida S, Yanagisawa S, Shimizu M: **A study on the differences between oral squamous cell carcinomas and normal oral mucosas measured by Fourier transform infrared spectroscopy**. *Biospectroscopy* 1999, **5**(2):117-126.
195. Banerjee S, Pal M, Chakrabarty J, Petibois C, Paul RR, Giri A, Chatterjee J: **Fourier-transform-infrared-spectroscopy based spectral-biomarker selection towards optimum diagnostic differentiation of oral leukoplakia and cancer**. *Anal Bioanal Chem* 2015, **407**(26):7935-7943.
196. Larkin P: **Infrared and raman spectroscopy : principles and spectral interpretation**. Amsterdam ; Boston: Elsevier; 2011.
197. Parker FS: **Applications of infrared, raman, and resonance raman spectroscopy in biochemistry**. New York: Plenum Press; 1983.

198. Morris MD, Matousek P: **Emerging Raman applications and techniques in biomedical and pharmaceutical fields**. Heidelburg ; New York: Springer; 2010.
199. Colthup NB, Daly LH, Wiberley SE: **Introduction to infrared and Raman spectroscopy**, 3rd edn. Boston: Academic Press; 1990.
200. Cazes J (ed.): **Analytical instrumentation handbook**, 3 edn. Boca Raton, FL: CRC press; 2004.
201. Lewis IR, Edwards HGM: **Handbook of Raman spectroscopy : from the research laboratory to the process line**. New York: Marcel Dekker; 2001.
202. Müller U: **M. Diem: Introduction to modern vibrational spectroscopy, J. Wiley, New York, Chichester, 1993, ISBN 0-471-59584-5, 285 Seiten, Preis:£ 49.50**. *Berichte der Bunsengesellschaft für physikalische Chemie* 1994, **98**(10):1347-1348.
203. Pelletier MJ: **Analytical applications of Raman spectroscopy**: Wiley-Blackwell; 1999.
204. Das RS, Agrawal Y: **Raman spectroscopy: Recent advancements, techniques and applications**. *Vibrational Spectroscopy* 2011, **57**(2):163-176.
205. Kneipp K, Kneipp H, Itzkan I, Dasari RR, Feld MS: **Surface-enhanced Raman scattering and biophysics**. *Journal of Physics: Condensed Matter* 2002, **14**(18):R597.
206. Xie W, Schlücker S: **Medical applications of surface-enhanced Raman scattering**. *Physical Chemistry Chemical Physics* 2013, **15**(15):5329-5344.
207. Tolles WM, Nibler J, McDonald J, Harvey A: **A review of the theory and application of coherent anti-Stokes Raman spectroscopy (CARS)**. *Appl Spectrosc* 1977, **31**(4):253-271.
208. Kudelski A: **Analytical applications of Raman spectroscopy**. *Talanta* 2008, **76**(1):1-8.
209. White JC: **Stimulated raman scattering**. In: *Tunable lasers.* Springer; 1987: 115-207.
210. Yakovlev VV, Petrov GI, Zhang HF, Noojin GD, Denton ML, Thomas RJ, Scully MO: **Stimulated Raman scattering: old physics, new applications**. *Journal of modern optics* 2009, **56**(18-19):1970-1973.
211. Eesley GL: **Coherent Raman Spectroscopy**: Elsevier; 2013.
212. Dingari NC, Horowitz GL, Kang JW, Dasari RR, Barman I: **Raman spectroscopy provides a powerful diagnostic tool for accurate determination of albumin glycation**. *PLoS One* 2012, **7**(2):e32406.
213. Barman I, Dingari NC, Kang JW, Horowitz GL, Dasari RR, Feld MS: **Raman spectroscopy-based sensitive and specific detection of glycated hemoglobin**. *Analytical chemistry* 2012, **84**(5):2474-2482.
214. Filik J, Stone N: **Drop coating deposition Raman spectroscopy of protein mixtures**. *Analyst* 2007, **132**(6):544-550.
215. Matousek P, Clark I, Draper E, Morris M, Goodship A, Everall N, Towrie M, Finney W, Parker A: **Subsurface probing in diffusely scattering media using spatially offset Raman spectroscopy**. *Appl Spectrosc* 2005, **59**(4):393-400.
216. Stone N, Kerssens M, Lloyd GR, Faulds K, Graham D, Matousek P: **Surface enhanced spatially offset Raman spectroscopic (SESORS) imaging–the next dimension**. *Chemical Science* 2011, **2**(4):776-780.
217. Sharma B, Ma K, Glucksberg MR, Van Duyne RP: **Seeing through bone with surface-enhanced spatially offset Raman spectroscopy**. *Journal of the American Chemical Society* 2013, **135**(46):17290-17293.
218. Lepot L, De Wael K, Gason F, Gilbert B: **Application of Raman spectroscopy to forensic fibre cases**. *Science & Justice* 2008, **48**(3):109-117.
219. Mogilevsky G, Borland L, Brickhouse M, Fountain III AW: **Raman spectroscopy for homeland security applications**. *International Journal of Spectroscopy* 2012, **2012**.

220. Gantner E, Steinert D: **Applications of laser Raman spectrometry in process control, using optical fibers**. *Fresenius' Journal of Analytical Chemistry* 1990, **338**(1):2-8.
221. Schmitt M, Popp J: **Raman spectroscopy at the beginning of the twenty-first century**. *Journal of Raman Spectroscopy* 2006, **37**(1-3):20-28.
222. Herrero AM: **Raman spectroscopy a promising technique for quality assessment of meat and fish: A review**. *Food Chemistry* 2008, **107**(4):1642-1651.
223. Ashton L, Lau K, Winder CL, Goodacre R: **Raman spectroscopy: lighting up the future of microbial identification**. *Future microbiology* 2011, **6**(9):991-997.
224. Virkler K, Lednev IK: **Analysis of body fluids for forensic purposes: from laboratory testing to non-destructive rapid confirmatory identification at a crime scene**. *Forensic Science International* 2009, **188**(1):1-17.
225. Neugebauer U, Trenkmann S, Bocklitz T, Schmerler D, Kiehntopf M, Popp J: **Fast differentiation of SIRS and sepsis from blood plasma of ICU patients using Raman spectroscopy**. *Journal of biophotonics* 2014, **7**(3-4):232-240.
226. Saade J, Pacheco MTT, Rodrigues MR: **Identification of hepatitis C in human blood serum by near-infrared Raman spectroscopy**. *Journal of Spectroscopy* 2008, **22**(5):387-395.
227. Carmona P, Molina M, Calero M, Bermejo-Pareja F, Martínez-Martín P, Toledano A: **Discrimination analysis of blood plasma associated with Alzheimer's disease using vibrational spectroscopy**. *Journal of Alzheimer's Disease* 2013, **34**:911-920.
228. Schipper HM, Kwok CS, Rosendahl SM, Bandilla D, Maes O, Melmed C, Rabinovitch D, Burns DH: **Spectroscopy of human plasma for diagnosis of idiopathic Parkinson's disease**. 2008.
229. Rehman A, Anwar S, Firdous S, Ahmed M, Rasheed R, Nawaz M: **Dengue blood analysis by Raman spectroscopy**. *Laser Physics* 2012, **22**(6):1085-1089.
230. Krishna CM, Sockalingum G, Kurien J, Rao L, Venteo L, Pluot M, Manfait M, Kartha V: **Micro-Raman spectroscopy for optical pathology of oral squamous cell carcinoma**. *Appl Spectrosc* 2004, **58**(9):1128-1135.
231. Sunder N, Rao N, Kartha V, Ullas G, Kurien J: **Laser raman spectroscopy: A novel diagnostic tool for oral cancer**. *Journal of Orofacial Sciences* 2011, **3**(2):15.
232. Başar G, Parlatan U, Şeninak Ş, Günel T, Benian A, Kalelioğlu İ: **Investigation of preeclampsia using raman spectroscopy**. *Journal of Spectroscopy* 2012, **27**(4):239-252.
233. Saleem M, Bilal M, Anwar S, Rehman A, Ahmed M: **Optical diagnosis of dengue virus infection in human blood serum using Raman spectroscopy**. *Laser Physics Letters* 2013, **10**(3):035602.
234. Torres Filho IP, Terner J, Scheider L: **Resonance Raman spectroscopy of human sickle cell hemoglobin from transgenic mice**. *The FASEB Journal* 2009, **23**(1_MeetingAbstracts):768.762.
235. Wood BR, McNaughton D: **Resonance raman spectroscopy of erythrocytes**. *Handbook of Vibrational Spectroscopy* 2008.
236. Motz JT, Fitzmaurice M, Miller A, Gandhi SJ, Haka AS, Galindo LH, Dasari RR, Kramer JR, Feld MS: **In vivo Raman spectral pathology of human atherosclerosis and vulnerable plaque**. *Journal of Biomedical Optics* 2006, **11**(2):021003-021003-021009.
237. De Jong B, Schut TB, Coppens J, Wolffenbuttel K, Kok D, Puppels G: **Raman spectroscopic detection of changes in molecular composition of bladder muscle tissue caused by outlet obstruction**. *Vibrational spectroscopy* 2003, **32**(1):57-65.
238. Maher JR, Takahata M, Awad HA, Berger AJ: **Raman spectroscopy detects deterioration in biomechanical properties of bone in a glucocorticoid-treated mouse model of rheumatoid arthritis**. *Journal of biomedical optics* 2011, **16**(8):087012-087012-087016.

239. Chen T, Kozloff KM, Goldstein SA, Morris MD: **Bone tissue ultrastructural defects in a mouse model for osteogenesis imperfecta: a Raman spectroscopy study**. In: *Biomedical Optics 2004: 2004*. International Society for Optics and Photonics: 85-92.
240. Hanlon E, Manoharan R, Koo TW, Shafer K, Motz J, Fitzmaurice M, Kramer J, Itzkan I, Dasari R, Feld M: **Prospects for in vivo Raman spectroscopy**. *Physics in medicine and biology* 2000, **45**(2):R1.
241. Nijssen A, Koljenović S, Schut TCB, Caspers PJ, Puppels GJ: **Towards oncological application of Raman spectroscopy**. *Journal of biophotonics* 2009, **2**(1-2):29-36.
242. Choo-Smith LP, Edwards H, Endtz HP, Kros J, Heule F, Barr H, Robinson J, Bruining H, Puppels G: **Medical applications of Raman spectroscopy: from proof of principle to clinical implementation**. *Biopolymers* 2002, **67**(1):1-9.
243. Gentleman E, Swain RJ, Evans ND, Boonrungsiman S, Jell G, Ball MD, Shean TAV, Oyen ML, Porter A, Stevens MM: **Comparative materials differences revealed in engineered bone as a function of cell-specific differentiation**. *Nat Mater* 2009, **8**(9):763-770.
244. Malini R, Venkatakrishna K, Kurien J, Pai KM, Rao L, Kartha VB, Krishna CM: **Discrimination of normal, inflammatory, premalignant, and malignant oral tissue: a Raman spectroscopy study**. *Biopolymers* 2006, **81**(3):179-193.
245. Oliveira AP, Bitar RA, Silveira Jr L, Zângaro RA, Martin AA: **Near-infrared Raman spectroscopy for oral carcinoma diagnosis**. *Photomedicine and Laser Therapy* 2006, **24**(3):348-353.
246. Hu Y, Jiang T, Zhao Z: **Discrimination of squamous cell carcinoma of the oral cavity using Raman spectroscopy and chemometric analysis**. In: *Intelligent Networks and Intelligent Systems, 2008 ICINIS'08 First International Conference on: 2008*. IEEE: 633-636.
247. Singh S, Krishna CM: **Raman spectroscopic studies of oral cancers: correlation of spectral and biochemical markers**. *Analytical Methods* 2014, **6**(21):8613-8620.
248. Ryzhikova E, Kazakov O, Halamkova L, Celmins D, Malone P, Molho E, Zimmerman EA, Lednev IK: **Raman spectroscopy of blood serum for Alzheimer's disease diagnostics: specificity relative to other types of dementia**. *Journal of biophotonics* 2014, **9999**.
249. Bueno Filho AC, Silveira Jr L, Yanai ALSA, Fernandes AB: **Raman spectroscopy for a rapid diagnosis of sickle cell disease in human blood samples: a preliminary study**. *Lasers in medical science* 2015, **30**(1):247-253.
250. Sahu A, Dalal K, Naglot S, Aggarwal P, Krishna CM: **Serum based diagnosis of asthma using Raman spectroscopy: an early phase pilot study**. 2013, **8(11)**:e78921.
251. Li X, Jin H: **Raman Spectroscopy of serum for cancer detection**. In: *Engineering in Medicine and Biology Society, 2001 Proceedings of the 23rd Annual International Conference of the IEEE: 2001*. IEEE: 3221-3224.
252. Pichardo-Molina J, Frausto-Reyes C, Barbosa-García O, Huerta-Franco R, González-Trujillo J, Ramírez-Alvarado C, Gutiérrez-Juárez G, Medina-Gutiérrez C: **Raman spectroscopy and multivariate analysis of serum samples from breast cancer patients**. *Lasers in medical science* 2007, **22**(4):229-236.
253. Bhattacharjee T, Khan A, Kumar P, Ingle A, Maru G, Krishna CM: **Raman spectroscopy of serum: A study on 'pre'and 'post'breast adenocarcinoma resection in rat models**. *Journal of biophotonics* 2014, **9999**.
254. Lin D, Feng S, Pan J, Chen Y, Lin J, Chen G, Xie S, Zeng H, Chen R: **Colorectal cancer detection by gold nanoparticle based surface-enhanced Raman spectroscopy of blood serum and statistical analysis**. *Optics express* 2011, **19**(14):13565-13577.

255. Li X, Yang T, Li S: **Discrimination of serum Raman spectroscopy between normal and colorectal cancer using selected parameters and regression-discriminant analysis**. *Applied optics* 2012, **51**(21):5038-5043.
256. Wang G, Lipert RJ, Jain M, Kaur S, Chakraboty S, Torres MP, Batra SK, Brand RE, Porter MD: **Detection of the potential pancreatic cancer marker MUC4 in serum using surface-enhanced Raman scattering**. *Analytical chemistry* 2011, **83**(7):2554-2561.
257. González-Solís JL, Martínez-Espinosa JC, Torres-González LA, Aguilar-Lemarroy A, Jave-Suárez LF, Palomares-Anda P: **Cervical cancer detection based on serum sample Raman spectroscopy**. *Lasers in medical science* 2014, **29**(3):979-985.
258. Owens GL, Gajjar K, Trevisan J, Fogarty SW, Taylor SE, Gama-Rose D, Martin-Hirsch PL, Martin FL: **Vibrational biospectroscopy coupled with multivariate analysis extracts potentially diagnostic features in blood plasma/serum of ovarian cancer patients**. *Journal of biophotonics* 2014, **7**(3-4):200-209.
259. Baker MJ, Hussain SR, Lovergne L, Untereiner V, Hughes C, Lukaszewski RA, Thiéfin G, Sockalingum GD: **Developing and understanding biofluid vibrational spectroscopy: a critical review**. *Chemical Society Reviews* 2016.
260. Harris AT, Lungari A, Needham CJ, Smith SL, Lones MA, Fisher SE, Yang XB, Cooper N, Kirkham J, Smith DA: **Potential for Raman spectroscopy to provide cancer screening using a peripheral blood sample**. *Head & neck oncology* 2009, **1**(1):1-8.
261. Feng S, Chen R, Lin J, Pan J, Chen G, Li Y, Cheng M, Huang Z, Chen J, Zeng H: **Nasopharyngeal cancer detection based on blood plasma surface-enhanced Raman spectroscopy and multivariate analysis**. *Biosensors and Bioelectronics* 2010, **25**(11):2414-2419.
262. Sahu A, Sawant S, Mamgain H, Krishna CM: **Raman spectroscopy of serum: an exploratory study for detection of oral cancers**. *Analyst* 2013, **138**(14):4161-4174.
263. Sahu A, Sawant S, Talathi-Desai S, Murali Krishna C: **Raman spectroscopy of serum: A study on oral cancers**. *Biomedical Spectroscopy and Imaging* 2015, **4**(2):171-187.
264. Sahu AK, Dhoot S, Singh A, Sawant SS, Nandakumar N, Talathi-Desai S, Garud M, Pagare S, Srivastava S, Nair S: **Oral cancer screening: serum Raman spectroscopic approach**. *BIOMEDO* 2015, **20**(11):115006-115006.
265. Sahu A, Nandakumar N, Sawant S, Krishna CM: **Recurrence prediction in oral cancers: a serum Raman spectroscopy study**. *Analyst* 2015, **140**(7):2294-2301.
266. Kho KW, Malini O, Shen ZX, Soo KC: **Surface enhanced Raman spectroscopic (SERS) study of saliva in the early detection of oral cancer**. In: *Biomedical Optics 2005: 2005*. International Society for Optics and Photonics: 84-91.
267. Rekha P, Aruna P, Daniel A, Prasanna SW, Udayakumar K, Ganesan S, Bharanidharan G, David B: **Raman spectroscopic characterization of blood plasma of oral cancer**. In: *Photonics (ICP), 2013 IEEE 4th International Conference on: 2013*. IEEE: 135-137.
268. Elumalai B, Prakasarao A, Ganesan B, Dornadula K, Ganesan S: **Raman spectroscopic characterization of urine of normal and oral cancer subjects**. *Journal of Raman Spectroscopy* 2015, **46**(1):84-93.
269. Sahu A, Tawde S, Pai V, Gera P, Chaturvedi P, Nair S, Krishna CM: **Raman spectroscopy and cytopathology of oral exfoliated cells for oral cancer diagnosis**. *Analytical Methods* 2015, **7**(18):7548-7559.
270. Haka AS, Volynskaya Z, Gardecki JA, Nazemi J, Lyons J, Hicks D, Fitzmaurice M, Dasari RR, Crowe JP, Feld MS: **In vivo Margin Assessment during Partial Mastectomy Breast Surgery Using Raman Spectroscopy [? Q1: Running head: Raman Margin Assessment at Partial Mastectomy. Short title OK? Q1]**. *Cancer Research* 2006, **66**(6):3317-3322.

271. Lieber CA, Majumder SK, Ellis DL, Billheimer DD, Mahadevan-Jansen A: **In vivo nonmelanoma skin cancer diagnosis using Raman microspectroscopy**. *Lasers in surgery and medicine* 2008, **40**(7):461-467.
272. Bitar R, Martins M, Ribeiro D, Carvalho C, Santos E, Ramalho L, Ramalho F, Martinho H, Martin A: **In vivo Raman spectroscopy for breast cancer: diagnosis in animal model**. In: *Biomedical Optics (BiOS) 2008: 2008*. International Society for Optics and Photonics: 68530O-68530O-68537.
273. Kirsch M, Schackert G, Salzer R, Krafft C: **Raman spectroscopic imaging for in vivo detection of cerebral brain metastases**. *Anal Bioanal Chem* 2010, **398**(4):1707-1713.
274. Beljebbar A, Dukic S, Amharref N, Manfait M: **Ex vivo and in vivo diagnosis of C6 glioblastoma development by Raman spectroscopy coupled to a microprobe**. *Anal Bioanal Chem* 2010, **398**(1):477-487.
275. Bergholt MS, Zheng W, Lin K, Ho KY, Teh M, Yeoh KG, So JBY, Huang Z: **Raman endoscopy for in vivo differentiation between benign and malignant ulcers in the stomach**. *Analyst* 2010, **135**(12):3162-3168.
276. Bergholt MS, Zheng W, Lin K, Ho KY, Teh M, Yeoh KG, Yan So JB, Huang Z: **In vivo diagnosis of gastric cancer using Raman endoscopy and ant colony optimization techniques**. *International journal of cancer* 2011, **128**(11):2673-2680.
277. Bergholt MS, Zheng W, Ho KY, Teh M, Yeoh KG, So J, Shabbir A, Huang Z: **Fiber-optic Raman spectroscopy probes gastric carcinogenesis in vivo at endoscopy**. *J Biophotonics* 2013, **6**(1):49-59.
278. Huang Z, Bergholt MS, Zheng W, Lin K, Ho KY, Teh M, Yeoh KG: **In vivo early diagnosis of gastric dysplasia using narrow-band image-guided Raman endoscopy**. *BIOMEDO* 2010, **15**(3):037017-037017-037015.
279. Huang Z, Teh SK, Zheng W, Lin K, Ho KY, Teh M, Yeoh KG: **In vivo detection of epithelial neoplasia in the stomach using image-guided Raman endoscopy**. *Biosensors and Bioelectronics* 2010, **26**(2):383-389.
280. Duraipandian S, Bergholt MS, Zheng W, Ho KY, Teh M, Yeoh KG, So JBY, Shabbir A, Huang Z: **Real-time Raman spectroscopy for in vivo, online gastric cancer diagnosis during clinical endoscopic examination**. *BIOMEDO* 2012, **17**(8):081418-081418.
281. Day J, Bennett R, Smith B, Kendall C, Hutchings J, Meaden G, Born C, Yu S, Stone N: **A miniature confocal Raman probe for endoscopic use**. *Physics in medicine and biology* 2009, **54**(23):7077.
282. Robichaux-Viehoever A, Kanter E, Shappell H, Billheimer D, Jones III H, Mahadevan-Jansen A: **Characterization of Raman spectra measured in vivo for the detection of cervical dysplasia**. *Appl Spectrosc* 2007, **61**(9):986-993.
283. Kanter EM, Vargis E, Majumder S, Keller MD, Woeste E, Rao GG, Mahadevan-Jansen A: **Application of Raman spectroscopy for cervical dysplasia diagnosis**. *Journal of biophotonics* 2009, **2**:81.
284. Kanter EM, Majumder S, Vargis E, Robichaux-Viehoever A, Kanter GJ, Shappell H, Jones III HW, Mahadevan-Jansen A: **Multiclass discrimination of cervical precancers using Raman spectroscopy**. *Journal of Raman Spectroscopy* 2009, **40**(2):205-211.
285. Richards-Kortuml R: **Rapid Communication Development of a Fiber Optic Probe to Measure NIR Raman Spectra of Cervical Tissue In Vivo**. *Photochemistry and photobiology* 1998, **68**(3):427-431.
286. Kanter EM, Majumder S, Kanter GJ, Woeste EM, Mahadevan-Jansen A: **Effect of hormonal variation on Raman spectra for cervical disease detection**. *American journal of obstetrics and gynecology* 2009, **200**(5):512. e511-512. e515.

287. Duraipandian S, Zheng W, Ng J, Low JJ, Ilancheran A, Huang Z: **Non-invasive analysis of hormonal variations and effect of postmenopausal Vagifem treatment on women using in vivo high wavenumber confocal Raman spectroscopy**. *Analyst* 2013, **138**(14):4120-4128.
288. Duraipandian S, Zheng W, Ng J, Low JJ, Ilancheran A, Huang Z: **Near-infrared-excited confocal Raman spectroscopy advances in vivo diagnosis of cervical precancer**. *BIOMEDO* 2013, **18**(6):067007-067007.
289. Buckley K, Kerns JG, Gikas PD, Birch HL, Vinton J, Keen R, Parker AW, Matousek P, Goodship AE: **Measurement of abnormal bone composition in vivo using noninvasive Raman spectroscopy**. *IBMS BoneKEy* 2014, **11**.
290. Shaikh R, Dora TK, Chopra S, Maheshwari A, Bharat R, Krishna CM: **In vivo Raman spectroscopy of human uterine cervix: exploring the utility of vagina as an internal control**. *BIOMEDO* 2014, **19**(8):087001-087001.
291. Bergholt MS, Zheng W, Lin K, Wang J, Xu H, Ren J-l, Ho KY, Teh M, Yeoh KG, Huang Z: **Characterizing Variability of In Vivo Raman Spectroscopic Properties of Different Anatomical Sites of Normal Colorectal Tissue towards Cancer Diagnosis at Colonoscopy**. *Analytical chemistry* 2014, **87**(2):960-966.
292. Bergholt MS, Lin K, Wang J, Zheng W, Xu H, Huang Q, Ren Jl, Ho KY, Teh M, Srivastava S: **Simultaneous fingerprint and high-wavenumber fiber-optic Raman spectroscopy enhances real-time in vivo diagnosis of adenomatous polyps during colonoscopy**. *Journal of biophotonics* 2015, **9999**.
293. Jermyn M, Mok K, Mercier J, Desroches J, Pichette J, Saint-Arnaud K, Bernstein L, Guiot M-C, Petrecca K, Leblond F: **Intraoperative brain cancer detection with Raman spectroscopy in humans**. *Science translational medicine* 2015, **7**(274):274ra219-274ra219.
294. Desroches J, Jermyn M, Mok K, Lemieux-Leduc C, Mercier J, St-Arnaud K, Urmey K, Guiot MC, Marple E, Petrecca K *et al*: **Characterization of a Raman spectroscopy probe system for intraoperative brain tissue classification**. *Biomed Opt Express* 2015, **6**(7):2380-2397.
295. Bakker Schut T, Witjes M, Sterenborg H, Speelman O, Roodenburg J, Marple E, Bruining H, Puppels G: **In vivo detection of dysplastic tissue by Raman spectroscopy**. *Analytical chemistry* 2000, **72**(24):6010-6018.
296. Singh S, Deshmukh A, Chaturvedi P, Krishna CM: **Raman spectroscopy in head and neck cancers: Toward oncological applications**. *Journal of cancer research and therapeutics* 2012, **8**(6):126.
297. Singh S, Deshmukh A, Chaturvedi P, Krishna CM: **In vivo Raman spectroscopy for oral cancers diagnosis**. In: *SPIE BiOS: 2012*. International Society for Optics and Photonics: 82190K-82190K-82196.
298. Deshmukh A, Singh S, Chaturvedi P, Krishna CM: **Raman spectroscopy of normal oral buccal mucosa tissues: study on intact and incised biopsies**. *Journal of biomedical optics* 2011, **16**(12):127004-12700410.
299. Krishna H, Majumder SK, Chaturvedi P, Gupta PK: **Anatomical variability of in vivo Raman spectra of normal oral cavity and its effect on oral tissue classification**. *Biomedical Spectroscopy and Imaging* 2013, **2**(3):199-217.
300. Krishna H, Majumder SK, Chaturvedi P, Sidramesh M, Gupta PK: **In vivo Raman spectroscopy for detection of oral neoplasia: A pilot clinical study**. *Journal of biophotonics* 2014, **7**(9):690-702.
301. Sahu A, Deshmukh A, Hole AR, Chaturvedi P, Krishna CM: **In vivo subsite classification and diagnosis of oral cancers using Raman spectroscopy**. *Journal of Innovative Optical Health Sciences*, **0**(0):1650017.
302. Mantsch HH, Shaw RA: **Vibrational spectroscopy and medicine: an alliance in the making**. *Vibrational spectroscopy* 2002, **30**(1):31-41.

303. Motz JT, Gandhi SJ, Scepanovic OR, Haka AS, Kramer JR, Dasari RR, Feld MS: **Real-time Raman system for in vivo disease diagnosis**. *J Biomed Opt* 2005, **10**(3):031113.
304. Krafft C, Popp J: **The many facets of Raman spectroscopy for biomedical analysis**. *Anal Bioanal Chem* 2015, **407**(3):699-717.
305. Chen P, Shen A, Zhou X, Hu J: **Bio-Raman spectroscopy: a potential clinical analytical method assisting in disease diagnosis**. *Analytical Methods* 2011, **3**(6):1257-1269.
306. Mizuno A, Nozawa H, Yaginuma T, Matsuzaki H, Ozaki Y, Iriyama K: **Effect of aldose reductase inhibitor on experimental diabetic cataract monitored by laser Raman spectroscopy**. *Exp Eye Res* 1987, **45**(1):185-186.
307. Mizuno A, Toshima S, Mori Y: **Confirmation of lens hydration by Raman spectroscopy**. *Exp Eye Res* 1990, **50**(6):647-649.
308. Nozawa H, Yaginuma T, Mizuno A: **Raman spectroscopic study of the effect of aldose reductase inhibitor on experimental diabetic cataract**. *Nippon Ganka Gakkai zasshi* 1988, **92**(1):194-201.
309. Mizuno A, Kanematsu EH, Suzuki H, Ihara N: **Laser Raman spectroscopic study of hereditary cataractous lenses in ICR/f-strain rat**. *Jpn J Ophthalmol* 1988, **32**(3):281-287.
310. Wang C, Wang Y, Huffman NT, Cui C, Yao X, Midura S, Midura RJ, Gorski JP: **Confocal laser Raman microspectroscopy of biomineralization foci in UMR 106 osteoblastic cultures reveals temporally synchronized protein changes preceding and accompanying mineral crystal deposition**. *J Biol Chem* 2009, **284**(11):7100-7113.
311. Ohsaki K, Shibata A, Yamashita S, Oe M, Wang KQ, Cui PC, Ye Q: **Demonstrations of de-and remineralization mechanism as revealed in synthetic auditory ossicle (Apaceram) of rats by laser-Raman spectrometry**. *Cell Mol Biol (Noisy-le-grand)* 1995, **41**(8):1155-1167.
312. Bakker Schut TC, Witjes MJ, Sterenborg HJ, Speelman OC, Roodenburg JL, Marple ET, Bruining HA, Puppels GJ: **In vivo detection of dysplastic tissue by Raman spectroscopy**. *Anal Chem* 2000, **72**(24):6010-6018.
313. A. ME: **Oesophagal Cancer**. In: *World Cancer Report 2014 (International Agency for Research on Cancer).* vol. 3: World Health Organization; 2014: 528-543.
314. Boere IA, Bakker Schut TC, van den Boogert J, de Bruin RWF, Puppels GJ: **Use of fibre optic probes for detection of Barrett's epithelium in the rat oesophagus by Raman spectroscopy**. *Vibrational Spectroscopy* 2003, **32**(1):47-55.
315. Hattori Y, Komachi Y, Asakura T, Shimosegawa T, Kanai G-I, Tashiro H, Sato H: **In Vivo Raman Study of the Living Rat Esophagus and Stomach Using a Micro-Raman Probe Under an Endoscope**. *Appl Spectrosc* 2007, **61**(6):579-584.
316. Abramczyk H, Brozek-Pluska B: **Raman imaging in biochemical and biomedical applications. Diagnosis and treatment of breast cancer**. *Chem Rev* 2013, **113**(8):5766-5781.
317. Hirosawa N, Sakamoto Y, Katayama H, Tonooka S, Yano K: **In Vivo Investigation of Progressive Alterations in Rat Mammary Gland Tumors by Near-Infrared Spectroscopy**. *Analytical Biochemistry* 2002, **305**(2):156-165.
318. Kast RE, Serhatkulu GK, Cao A, Pandya AK, Dai H, Thakur JS, Naik VM, Naik R, Klein MD, Auner GW *et al*: **Raman spectroscopy can differentiate malignant tumors from normal breast tissue and detect early neoplastic changes in a mouse model**. *Biopolymers* 2008, **89**(3):235-241.
319. Bitar RA, Ribeiro DG, dos Santos EAP, Ramalho LNZ, Ramalho FS, Martin AA, Martinho HS: **In vivo diagnosis of mammary adenocarcinoma using Raman spectroscopy: an animal model study**. In*: 2010*. 756005-756005-756006.
320. Bhattacharjee T, Kumar P, Maru G, Ingle A, Krishna CM: **Swiss bare mice: a suitable model for transcutaneous in vivo Raman spectroscopic studies of breast cancer**. *Lasers Med Sci* 2014, **29**(1):325-333.

321. Bhattacharjee T, Maru G, Ingle A, Krishna CM: **Transcutaneous in vivo Raman spectroscopy: Detection of age-related changes in mouse breast**. *Vibrational Spectroscopy* 2013, **67**:80-86.
322. Bhattacharjee T, Maru G, Ingle A, Krishna CM: **Transcutaneous in vivo Raman spectroscopic studies in a mouse model: evaluation of changes in the breast associated with pregnancy and lactation**. *J Biomed Opt* 2013, **18**(4):047004.
323. Amharref N, Beljebbar A, Dukic S, Venteo L, Schneider L, Pluot M, Manfait M: **Discriminating healthy from tumor and necrosis tissue in rat brain tissue samples by Raman spectral imaging**. *Biochimica et Biophysica Acta (BBA) - Biomembranes* 2007, **1768**(10):2605-2615.
324. Krafft C, Kirsch M, Beleites C, Schackert G, Salzer R: **Methodology for fiber-optic Raman mapping and FTIR imaging of metastases in mouse brains**. *Anal Bioanal Chem* 2007, **389**(4):1133-1142.
325. Uckermann O, Galli R, Tamosaityte S, Leipnitz E, Geiger KD, Schackert G, Koch E, Steiner G, Kirsch M: **Label-free delineation of brain tumors by coherent anti-Stokes Raman scattering microscopy in an orthotopic mouse model and human glioblastoma**. *PLoS One*, **9**(9):e107115.
326. Wang H, Huang N, Zhao J, Lui H, Korbelik M, Zeng H: **Depth-resolved in vivo micro-Raman spectroscopy of a murine skin tumor model reveals cancer-specific spectral biomarkers**. *Journal of Raman Spectroscopy* 2011, **42**(2):160-166.
327. Pandya AK, Serhatkulu GK, Cao A, Kast RE, Dai H, Rabah R, Poulik J, Banerjee S, Naik R, Adsay V *et al*: **Evaluation of pancreatic cancer with Raman spectroscopy in a mouse model**. *Pancreas* 2008, **36**(2):e1-8.
328. O'Brien CM, Vargis E, Paria BC, Bennett KA, Mahadevan-Jansen A, Reese J: **Raman spectroscopy provides a noninvasive approach for determining biochemical composition of the pregnant cervix in vivo**. *Acta Paediatr* 2014, **103**(7):715-721.
329. Shen A, Liao Z, Wang H, Goan I, Wu Y, Wang X, Yu Z, Hu J: **Study on the in vitro and in vivo activation of rat hepatic stellate cells by Raman spectroscopy**. *J Biomed Opt* 2007, **12**(3):034003.
330. Duarte J, Hage R, Silveira JL, Silveira F, Pacheco MTT, Munin E, Plapler H: **Analysis of colon tumors in rats by near-infrared Raman spectroscopy**. In*: 2007*. 642714-642714-642716.
331. Mognetti B, Di Carlo F, Berta GN: **Animal models in oral cancer research**. *Oral Oncol* 2006, **42**(5):448-460.
332. Oliveira AP, Bitar RA, Silveira L, Zangaro RA, Martin AA: **Near-infrared Raman spectroscopy for oral carcinoma diagnosis**. *Photomed Laser Surg* 2006, **24**(3):348-353.
333. Ghanate AD, Kumar G, Talathi S, Maru GB, Krishna CM: **Raman spectroscopic detection of early stages in DMBA-induced tumor evolution in hamster buccal pouch model: an exploratory study**. In*: 2010*. 817303-817303-817307.
334. Singh SP, Sahu A, Deshmukh A, Chaturvedi P, Krishna CM: **In vivo Raman spectroscopy of oral buccal mucosa: a study on malignancy associated changes (MAC)/cancer field effects (CFE)**. *Analyst* 2013, **138**(14):4175-4182.
335. Singh SP, Deshmukh A, Chaturvedi P, Krishna CM: **Raman spectroscopy in head and neck cancers: toward oncological applications**. *J Cancer Res Ther* 2012, **8 Suppl 1**:S126-132.
336. Deshmukh A, Singh SP, Chaturvedi P, Krishna CM: **Raman spectroscopy of normal oral buccal mucosa tissues: study on intact and incised biopsies**. *J Biomed Opt* 2011, **16**(12):127004.
337. Sahu A, Deshmukh A, Ghanate AD, Singh SP, Chaturvedi P, Krishna CM: **Raman spectroscopy of oral buccal mucosa: a study on age-related physiological changes and tobacco-related pathological changes**. *Technol Cancer Res Treat* 2012, **11**(6):529-541.
338. Yigit N, Kryštufek B: **Mesocricetus auratus**. In.: IUCN; 2008.

339. Gattermann R, Fritzsche P, Neumann K, Al-Hussein I, Kayser A, Abiad M, Yakti R: **Notes on the current distribution and the ecology of wild golden hamsters (Mesocricetus auratus)**. *Journal of Zoology* 2001, **254**(03):359-365.
340. **DMBA, SID=24893738, (accessed Dec 21, 2015).** In. National Center for Biotechnology Information.
341. Lee LL, Lee JSC, Waldman SD, Casper RF, Grynpas MD: **Polycyclic aromatic hydrocarbons present in cigarette smoke cause bone loss in an ovariectomized rat model**. *Bone* 2002, **30**(6):917-923.
342. Frenkel K, Wei L, Wei H: **7, 12-dimethylbenz [a] anthracene induces oxidative DNA modification in vivo**. *Free Radical Biology and Medicine* 1995, **19**(3):373-380.
343. Takada K, Yokohama I, Chida K, Noda J: **New measurement system for fault location in optical waveguide devices based on an interferometric technique**. *Applied optics* 1987, **26**(9):1603-1606.
344. Fujimoto JG, Pitris C, Boppart SA, Brezinski ME: **Optical coherence tomography: an emerging technology for biomedical imaging and optical biopsy**. *Neoplasia* 2000, **2**(1):9-25.
345. Zysk AM, Nguyen FT, Oldenburg AL, Marks DL, Boppart SA: **Optical coherence tomography: a review of clinical development from bench to bedside**. *Journal of biomedical optics* 2007, **12**(5):051403-051403-051421.
346. Gobinet C, Vrabie V, Manfait M, Piot O: **Preprocessing methods of Raman spectra for source extraction on biomedical samples: application on paraffin-embedded skin biopsies**. *Biomedical Engineering, IEEE Transactions on* 2009, **56**(5):1371-1382.
347. Nijssen A, Koljenovic S, Bakker Schut TC, Caspers PJ, Puppels GJ: **Towards oncological application of Raman spectroscopy**. *J Biophotonics* 2009, **2**(1-2):29-36.
348. Abdi H, Williams LJ: **Principal component analysis**. *Wiley Interdisciplinary Reviews: Computational Statistics* 2010, **2**(4):433-459.
349. Varmuza K, Filzmoser P: **Introduction to multivariate statistical analysis in chemometrics**: CRC press; 2009.
350. Jain AK, Murty MN, Flynn PJ: **Data clustering: a review**. *ACM computing surveys (CSUR)* 1999, **31**(3):264-323.
351. Chatfied C, Collins AJ: **Introduction to multivariate analysis**: Springer; 2013.
352. Pena D: **Multivariate data analisis**. *McGraw Hill-Interamericana de Espana SAU* 2002.
353. Schervish MJ: **A review of multivariate analysis**. *Statistical Science* 1987:396-413.
354. Seal H: **Multivariate statistical analysis for biologists**. *Methuen* 1964.
355. Tabachnick BG, Fidell LS: **Using multivariate statistics**. 2001.
356. Kelly JG, Trevisan J, Scott AD, Carmichael PL, Pollock HM, Martin-Hirsch PL, Martin FL: **Biospectroscopy to metabolically profile biomolecular structure: a multistage approach linking computational analysis with biomarkers**. *Journal of proteome research* 2011, **10**(4):1437-1448.
357. Ghanate AD, Kothiwale S, Singh SP, Bertrand D, Krishna CM: **Comparative evaluation of spectroscopic models using different multivariate statistical tools in a multicancer scenario**. *J Biomed Opt*, **16**(2):025003.
358. Kemsley E: **Discriminant analysis of high-dimensional data: a comparison of principal components analysis and partial least squares data reduction methods**. *Chemometrics and intelligent laboratory systems* 1996, **33**(1):47-61.
359. Korenius T, Laurikkala J, Juhola M: **On principal component analysis, cosine and Euclidean measures in information retrieval**. *Information Sciences* 2007, **177**(22):4893-4905.
360. Balakrishnama S, Ganapathiraju A, Picone J: **Linear discriminant analysis for signal processing problems**. In: *Southeastcon'99 Proceedings IEEE: 1999*. IEEE: 78-81.

361. Harris A, Rennie A, Waqar-Uddin H, Wheatley S, Ghosh S, Martin-Hirsch D, Fisher S, High A, Kirkham J, Upile T: **Raman spectroscopy in head and neck cancer**. *Head & Neck Oncology* 2010, **2**(1):26.
362. Bergner N, Romeike BF, Reichart R, Kalff R, Krafft C, Popp J: **Tumor margin identification and prediction of the primary tumor from brain metastases using FTIR imaging and support vector machines**. *Analyst* 2013, **138**(14):3983-3990.
363. Francisco-Fernández M, Tarrío-Saavedra J, Mallik A, Naya S: **A comprehensive classification of wood from thermogravimetric curves**. *Chemometrics and Intelligent Laboratory Systems* 2012, **118**:159-172.
364. Derka S, Vairaktaris E, Papakosta V, Vassiliou S, Acil Y, Vylliotis A, Spyridonidou S, Lazaris A, Mourouzis C, Kokkori A: **Cell proliferation and apoptosis culminate in early stages of oral oncogenesis**. *Oral oncology* 2006, **42**(5):540-550.
365. Papakosta V, Vairaktaris E, Vylliotis A, Derka S, Nkenke E, Vassiliou S, Lazaris A, Mourouzis C, Rallis G, Spyridonidou S: **The co-expression of c-myc and p53 increases and reaches a plateau early in oral oncogenesis**. *Anticancer research* 2006, **26**(4B):2957-2962.
366. Kumar P, Bhattacharjee T, Pandey M, Hole AR, Ingle A, Murali Krishna C: **Raman spectroscopy in experimental oral carcinogenesis: investigation of abnormal changes in control tissues**. *J Raman Spectrosc* 2016, **In Press**.
367. Parker FS: **Applications of infrared, Raman, and resonance Raman spectroscopy in biochemistry**: Springer Science & Business Media; 1983.
368. Hall M, Peters G: **Genetic alterations of cyclins, cyclin-dependent kinases, and Cdk inhibitors in human cancer**. *Advances in cancer research* 1996, **68**:67-108.
369. Lamb J, Ewen ME: **Cyclin D1 and molecular chaperones: implications for tumorigenesis**. *Cell Cycle* 2003, **2**(6):525-527.
370. Thumfart W, Weidenbecher M, Waller G, Pesch H-J: **Chronic mechanical trauma in the aetiology of oro-pharyngeal carcinoma**. *Journal of maxillofacial surgery* 1978, **6**:217-221.
371. Grivennikov SI, Greten FR, Karin M: **Immunity, Inflammation, and Cancer**. *Cell* 2010, **140**(6):883-899.
372. Wey PD, Lotz MJ, Triedman LJ: **Oral cancer in women nonusers of tobacco and alcohol**. *Cancer* 1987, **60**(7):1644-1650.
373. Martorell J, Fondevila D, Ramis A: **Spontaneous squamous cell carcinoma of the cheek pouch in two dwarf hamsters (Phodopus sungorus)**. *Veterinary Record* 2005, **156**(20):650-651.
374. Popp J, Tuchin VV, Chiou A, Heinemann SH: **Handbook of biophotonics**, vol. 2: John Wiley & Sons; 2011.
375. Liu C-H, Qi J, Lu J, Wang S, Wu C, Shih W-C, Larin KV: **Improvement of tissue analysis and classification using optical coherence tomography combined with Raman spectroscopy**. *Journal of Innovative Optical Health Sciences* 2015, **08**(04):1550006.
376. Ko AC-T, Hewko M, Leonardi L, Sowa MG, Dong CC, Williams P, Cleghorn B: **Ex vivo detection and characterization of early dental caries by optical coherence tomography and Raman spectroscopy**. *Journal of biomedical optics* 2005, **10**(3):031118-03111816.
377. Patil CA, Bosschaart N, Keller MD, van Leeuwen TG, Mahadevan-Jansen A: **Combined Raman spectroscopy and optical coherence tomography device for tissue characterization**. *Optics letters* 2008, **33**(10):1135-1137.
378. Patil CA, Krishnamoorthi H, Ellis DL, van Leeuwen TG, Mahadevan-Jansen A: **A clinical probe for combined Raman spectroscopy-optical coherence tomography (RS-OCT) of the skin cancers**. In*: 2010*. 75480L-75480L-75486.

379. Qi J, Sudheendran N, Liu C-H, Santos GM, Young ED, Lazar AJ, Lev DC, Pollock RE, Larin KV, Shih W-C: **Raman spectroscopy complements optical coherent tomography in tissue classification and cancer detection**. In*: 2015*. 931807-931807-931805.
380. Zakharov VP, Bratchenko IA, Artemyev DN, Myakinin OO, Kornilin DV, Kozlov SV, Moryatov AA: **Comparative analysis of combined spectral and optical tomography methods for detection of skin and lung cancers**. *Journal of Biomedical Optics* 2015, **20**(2):025003-025003.
381. Faber D, van der Meer F, Aalders M, van Leeuwen T: **Quantitative measurement of attenuation coefficients of weakly scattering media using optical coherence tomography**. *Optics express* 2004, **12**(19):4353-4365.
382. Patil CA, Kalkman J, Faber DJ, Nyman JS, van Leeuwen TG, Mahadevan-Jansen A: **Integrated system for combined Raman spectroscopy–spectral domain optical coherence tomography**. *Journal of biomedical optics* 2011, **16**(1):011007-011007-011010.
383. Divakar Rao K, Sahoo N, Krishna CM: **Perspectives of optical coherence tomography imaging and Raman spectroscopy in cancer diagnosis**. *Biomedical Spectroscopy and Imaging* 2015, **4**(1).
384. Murti P, Bhonslel R, Mehta F, Pindhorg J: **Effect of cessation of tobacco use on the incidence of oral mucosal lesions in a I0-yr follow-up study of I2 212 users**. *Oral diseases* 1995, **2**:54-53.
385. Singh S, Deshmukh A, Chaturvedi P, Krishna CM: **In vivo Raman spectroscopic identification of premalignant lesions in oral buccal mucosa**. *BIOMEDO* 2012, **17**(10):1050021-1050029.
386. Mehanna HM, Rattay T, Smith J, McConkey CC: **Treatment and follow-up of oral dysplasia - a systematic review and meta-analysis**. *Head Neck* 2009, **31**(12):1600-1609.
387. Lippman SM, Hong WK: **Cancer Prevention by Delay Commentary re: JA O'Shaughnessy et al., Treatment and Prevention of Intraepithelial Neoplasia: An Important Target for Accelerated New Agent Development. Clin. Cancer Res., 8: 314–346, 2002**. *Clinical cancer research* 2002, **8**(2):305-313.
388. D'Argenzio A, D'Argenio P, Ferrante G, Minardi V, Possenti V, Quarchioni E, Baldissera S, Salmaso S, Gruppo TP: **40% of smokers try to stop smoking, only 8% succeed in**. *Epidemiologia e prevenzione* 2011, **35**(5-6):362.
389. Control CfD, Prevention: **Quitting smoking among adults--United States, 2001-2010**. *MMWR Morbidity and mortality weekly report* 2011, **60**(44):1513.
390. Hanahan D: **Rethinking the war on cancer**. *The Lancet* 2014, **383**(9916):558-563.
391. Schmälzlin E, Moralejo B, Rutowska M, Monreal-Ibero A, Sandin C, Tarcea N, Popp J, Roth MM: **Raman Imaging with a Fiber-Coupled Multichannel Spectrograph**. *Sensors* 2014, **14**(11):21968-21980.

Appendix 1: Highlights and limitations of various oral cancer diagnostic adjuncts.

Sl No.	Technique/tool	Highlights	Limitations
1. Common Diagnostic adjunct	Cytology	Ease in collection and transportation of sample; almost non invasive	Time consuming, subjective, low accuracy in low-risk population
	Vital staining	Aids clinical identification and demarcation of oral premalignant disorders	Poor sensitivity and accuracy for dysplasia and lower pathologies, subjective
2. Chemilumines cence-based	Vizilite plus/ Microlux DL	Commercially available, Aids clinical identification of oral premalignant disorders	Scope of improvement, more studies needed, especially in low risk population
3. Biomarker based	Body-fluid based assays	Specific identification; Samples can be obtained using invasive (biopsy sections), minimum invasive (blood/serum) and non invasive approaches (saliva, urine)	Efficient markers still not available; Time consuming
4. Optical Techniques	Fluorescence spectroscopy	High sensitivity, advancements	Fluorophore- (and thus) wavelength-dependent
	OCT	Optical analogue of ultrasonography	More advancement needed
	FTIR	Based on absorption, advanced instrumentations, good for section imaging	Bands affected by presence of water, limited in vivo application
	Raman spectroscopy	Based on inelastic scattering, bands not affected by water, in vivo adaptations	Weak phenomenon, Imaging is time consuming; still evolving

Publications and Reprints

Prelude

This section contains reprints of publications arising out of the thesis.

Technology in Cancer Research & Treatment
2016, Vol. 15(5) NP60–NP72

DOI: 10.1177/1533034615598622
tct.sagepub.com
SAGE

Raman Spectroscopy of Experimental Oral Carcinogenesis: Study on Sequential Cancer Progression in Hamster Buccal Pouch Model

Piyush Kumar, MSc[1], Tanmoy Bhattacharjee, MSc[1], Arvind Ingle, MVSc, PhD[1], Girish Maru, PhD[1], and C. Murali Krishna, PhD[1]

Abstract

Oral cancers suffer from poor 5-year survival rates, owing to late detection of the disease. Current diagnostic/screening tools need to be upgraded in view of disadvantages like invasiveness, tedious sample preparation, long output times, and interobserver variances. Raman spectroscopy has been shown to identify many disease conditions, including oral cancers, from healthy conditions. Further studies in exploring sequential changes in oral carcinogenesis are warranted. In this Raman spectroscopy study, sequential progression in experimental oral carcinogenesis in Hamster buccal pouch model was investigated using 3 approaches—*ex vivo*, *in vivo* sequential, and *in vivo* follow-up. In all these studies, spectral changes show lipid dominance in early stages while later stages and tumors showed increased protein to lipid ratio and nucleic acids. On similar lines, early weeks of 7,12-dimethylbenz(a)anthracene-treated and control groups showed higher overlap and low classification. The classification efficiency increased progressively, reached a plateau phase and subsequently increased up to 100% by 14 weeks. The misclassifications between treated and control spectra suggested some changes in controls as well, which was confirmed by a careful reexamination of histopathological slides. These findings suggests Raman spectroscopy may be able to identify microheterogeneity, which may often go unnoticed in conventional biochemistry wherein tissue extracts are employed, as well as in histopathology. *In vivo* findings, quite comparable to gold-standard supported *ex vivo* findings, give further proof of Raman spectroscopy being a promising label-free, noninvasive diagnostic adjunct for future clinical applications.

Keywords

Raman spectroscopy, PCA, PC-LDA, Hamster buccal pouch, sequential oral carcinogenesis, DMBA

Abbreviations

ACTREC, Advanced Centre for Treatment, Research and Education in Cancer; CCD, charge-coupled device; DMBA, 7,12-dimethylbenz(a)anthracene; HBP, Hamster buccal pouch; LGD, low-grade dysplasia; LOOCV, leave-one-out cross-validation; PCA, principal component analysis; PC-LDA, principal component-based linear discriminant analysis; RS, Raman spectroscopy; SCC, squamous cell carcinoma

Received: January 8, 2015; Revised: March 31, 2015; Accepted: July 1, 2015.

Introduction

Oral cancer is the most common cancer in Indian males with a poor 5-year survival rate,[1,2] ascribed to late detection of the disease and recurrences. Early detection of oral cancers is important as it leads to better prognosis and increased 5-year survival rate up to 90%.[3-5] Currently practiced screening/diagnostic tools suffer from several disadvantages like tedious sample preparation, long output times, and interobserver

[1] Advanced Centre for Treatment, Research and Education in Cancer, Tata Memorial Centre, Navi Mumbai, India

Corresponding Author:
C. Murali Krishna, PhD, Chilakapati Laboratory, Advanced Centre for Treatment, Research and Education in Cancer (ACTREC), Tata Memorial Centre (TMC), Kharghar, Sector '22', Navi Mumbai 410210, India.
Email: mchilakapati@actrec.gov.in; pittu1043@gmail.com

variances.[6,7] Biopsy followed by histopathology, the current gold standard, is not only invasive but also depends on selection of appropriate region. Further, it may not be very convenient for screening and therapeutic monitoring which require repeated sampling. Rapid, objective, and preferably noninvasive alternatives as screening/diagnostic techniques are hence being extensively explored.[8]

Raman spectroscopy (RS) is one such tool, which has found applicability in discriminating many diseases from healthy conditions.[9] The RS, which can provide chemical fingerprint/biochemical profile, has shown promising results in the diagnosis of several cancers,[8,10-15] including oral cancers.[16-25] Both *ex vivo* and *in vivo* RS studies in oral cancers have shown classification of pathological conditions along with detection of confounding factors like age-related changes and early events like cancer field effects in oral cancer,[16,17,21-25] demonstrating efficiency of the technique. Still, further studies in exploring sequential changes in oral carcinogenesis are warranted. As such studies are not feasible in humans due to practical considerations, experimental carcinogenesis is the ideal approach. Hamster buccal pouch (HBP) is a widely used model for experimental oral carcinogenesis,[26-28] owing to attributes such as cancer progression through stages similar to human oral carcinogenesis and 100% incidence of tumors in 14 weeks on treatment with 7,12-dimethylbenz(a)anthracene (DMBA).[29,30] In fact, feasibility of RS-based classification of frank tumors[31] as well as carcinogen-induced variations in HBP[32] on a limited sample size has already been reported.

The current study aims for sequential Raman spectroscopic evaluation of DMBA-induced buccal pouch carcinogenesis with respect to vehicle-treated age-matched controls. The following 3 approaches were adopted in this study: (1) *Ex vivo*—RS of excised snap frozen buccal pouches from hamsters 0 to 14 weeks postcarcinogen treatment, (2) *In vivo*—*In vivo* RS of buccal pouch 0 to 14 weeks posttreatment, and (3) follow-up approach—*In vivo* RS of buccal pouch of the same animals for 0 to 14 weeks posttreatment. Multivariate analyses were carried out to evaluate sequential changes associated with progression of cancer. Findings of the study are reported in the manuscript.

Materials and Methods

Ethics Approval

The study was approved by the Institutional Animal Ethics Committee, Advanced Centre for Treatment, Research and Education in Cancer (ACTREC), endorsed by the Committee for the Purpose of Control and Supervision of Experiments on Animals, Government of India: approval no. 12/2009, ACTREC.

Animal Model

A total of 181 six- to eight-week-old Golden Syrian male hamsters (*Mesocricetus auratus*) were used in the study. Oral carcinogenesis was induced in 103 HBPs (treated group) using standard DMBA carcinogenesis protocols.[33] Briefly, 0.5% DMBA (Sigma-Aldrich, purity 95%, MO, USA) dissolved in groundnut oil (Dhara, Mumbai, India) was topically applied using a paint-brush (Camlin, no. 4, Mumbai, India) on the right buccal pouch thrice a week for 14 weeks. Seventy-eight HBPs were treated with only oil (vehicle control group). All animals were housed under standard laboratory conditions, fed a diet of in-house-prepared pellets, and provided with water ad libitum. The schematics of experimental protocol are shown in Figure 1A.

The study was carried out using the following 3 approaches:

1. *Ex vivo* study: 5 test and 3 control animals were killed every week postcarcinogen treatment for 14 weeks. Buccal pouch were then excised out of the sacrificed hamsters, snap frozen in liquid nitrogen, and stored at −80°C. Spectra were recorded from these tissues after passive thawing on ice and spreading over aluminum grids (3 × 3). One spectrum was recorded from each grid, tissues were cut along gridlines and processed for histopathology (Figure 1B).
2. *In vivo* study: *In vivo* Raman spectra were acquired from 2 test and 2 control HBPs of anaesthetized animals (150 mg ketamine and 10 mg xylazine/kg body weight) every week for 14 weeks. After spectra acquisition, the animals were killed, pouches excised out, and processed for histopathology.
3. Follow-up study: *In vivo* Raman spectra were acquired from buccal pouch of the same hamsters (3 test and 3 controls) postanaesthetization for 14 weeks without sacrifice.

The buccal pouches were also photographed (Canon SX220HS, Tokyo, Japan) every week. The total number of animals used in various approaches are shown in Table 1.

Raman Spectroscopy

Spectra were recorded with HE-785 commercial Raman spectrometer (Horiba Jobin Yvon, France), details of which have been described elsewhere.[22,23] Briefly, this system consists of a diode laser (PI-ECL-785-300-FC; Process Instruments, Utah, USA) of 785 nm wavelength as excitation source and HE 785 spectrograph coupled with a charge-coupled device (CCD; Synapse, France) as dispersion and detection elements. The spectrograph is equipped with a fixed 950 gr/mm grating. Spectral resolution, as specified by the manufacturer, is $\sim 4\ cm^{-1}$. The excitation source and the detection system were coupled by commercially available fiber-optic Ramanprobe (Model: RPS 785/ 12-5; InPhotonics Inc, Downy St, USA) consisting of 105 μm excitation fiber and 200 μm collection fiber (NA 0.40). As per manufacturer's specifications, theoretical spot size and depth of penetration of the Raman probe are 105 μm and 1 mm, respectively. Typically, laser power −70 mW was used for excitation. Spectra were integrated for 15 seconds and averaged over 3 accumulations. Approximately 9 spectra were recorded from each pouch in *ex vivo* study, 1 spectrum from

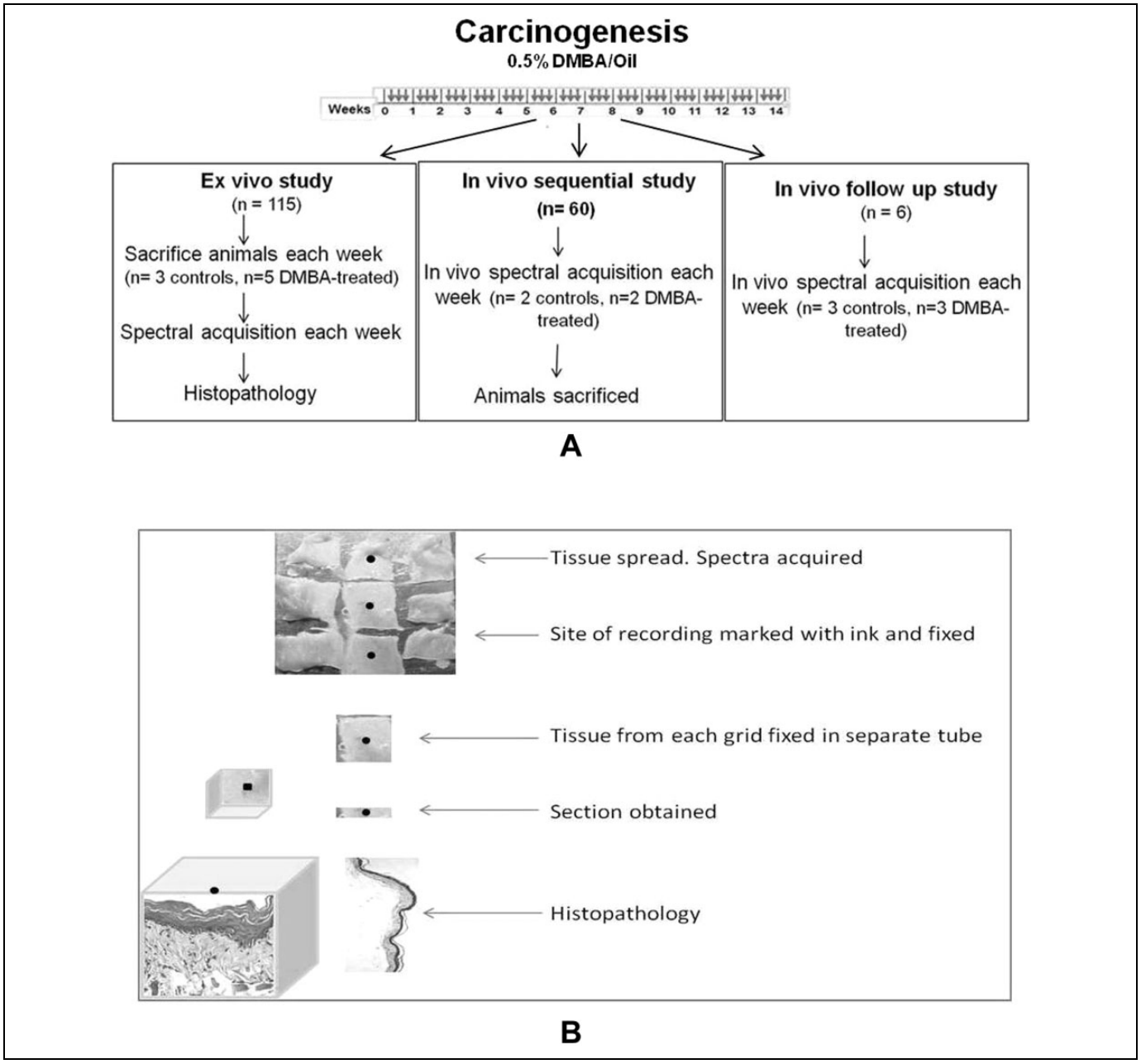

Figure 1. Schematics of protocols followed: (A) DMBA application regime (thrice weekly application for 14 weeks, small arrows indicate application of oil/DMBA) and protocol for *ex vivo*, *in vivo* sequential, and *in vivo* follow-up study. (B) Protocol for obtaining sections for histopathology. DMBA indicates 7,12-dimethylbenz(a)anthracene.

each aluminum grid, as shown in Figure 1B. In case of *in vivo* sequential study, 15 spectra were recorded from selected sites and 10 to 15 spectra were recorded from each pouch for *in vivo* follow-up study.

In this manuscript, control and DMBA-treated groups have been designated as C and T, respectively, while the number succeeding C (Cx) or T (Tx) denotes the number of weeks of treatment with DMBA or oil. Thus, C0, C1, and C14 indicate control of 0, 1, and 14 weeks of oil treatment and T0, T1, and T14 indicate DMBA treatment for 0, 1, and 14 weeks, respectively.

Data Analysis

Spectral preprocessing. Raw Raman spectra were corrected for CCD response using a National Institute of Standards and Technology certified SRM 2241 material, followed by subtraction of spectral contribution from optical elements.[34] To remove interference of slow moving background, first derivatives of spectra (Savitzky-Golay method; window size 3) were computed.[35,36] Spectra were interpolated in the 1200 to 1800 cm^{-1} region as our previous studies on oral cancer have already demonstrated the efficacy of this region in classification.

Table 1. Number of Animals Used Per Week.

Weeks	0	1	2	3	4	5	6	7	8	9	10	11	12	13	14	Total
Ex vivo																
Control	3	3	3	3	3	3	3	3	3	3	3	3	3	3	3	45
Treated	–	5	5	5	5	5	5	5	5	5	5	5	5	5	5	75
Total	3	8	8	8	8	8	8	8	8	8	8	8	8	8	8	115
In vivo																
Control	2	2	2	2	2	2	2	2	2	2	2	2	2	2	2	30
Treated	2	2	2	2	2	2	2	2	2	2	2	2	2	2	2	30
Total	4	4	4	4	4	4	4	4	4	4	4	4	4	4	4	60
Follow-up																
Control	3	3	3	3	3	3	3	3	3	3	3	3	3	3	3	3
Treated	3	3	3	3	3	3	3	3	3	3	3	3	3	3	3	3
Total	6	6	6	6	6	6	6	6	6	6	6	6	6	6	6	6

Moreover, this region is free from interference of fiber signals. Interpolated spectra were vector normalized to remove intensity-related variations and subjected to multivariate analysis.

Computation of mean spectra. Average or mean spectra were computed from the background-corrected spectra for each class and baseline corrected by fitting a fifth order polynomial function using LabSpec 4.18 (Horiba Jobin Yvon). These baseline-corrected spectra followed by area normalization were used for obtaining mean for spectral comparison across different groups.

Multivariate analysis. Preprocessed spectra were subjected to unsupervised principal component analysis (PCA), as well as supervised principal component-based linear discriminant analysis (PC-LDA) using algorithms implemented in MATLAB-based in-house software.[37] The PCA is the most frequently applied method for computing linear latent variables, which allows visual inspection of clustering of objects or variables through unsupervised classification.[38] The main aim of PCA is dimension reduction by which it explains maximum variability with few principal components/factors. First few PCs contribute to maximum variance. Scatter plots are often used to visualize/represent multivariate data by plotting score of PCs against each other.

Linear discriminant analysis (LDA), a supervised classification method, maximizes interclass separation and reduces intraclass separation to bring out discrimination.[39] For data with high dimensionality, dimension reduction may be achieved by application of PC-LDA: PCA followed by LDA, using PCA scores, instead of original variables. Classification efficiency of standard models is evaluated by leave-one-out cross-validation (LOOCV), which is based on a hypothetical validation set used in absence of an explicit validation set. Leave-one-out involves using a single observation from the original sample as the validation data and the remaining observations as training data. This is repeated such that each observation in the sample is used once as the validation data and averaged over the rounds.

Results and Discussion

The study aims to evaluate ability of RS to distinguish DMBA-induced sequential cancer progression in HBP. The HBP model is well characterized for experimental oral carcinogenesis and is shown to progress through precancer stages, that is, hyperplasia, dysplasia, carcinoma in situ, and squamous cell carcinoma (SCC), as observed in human oral cancers. As per histopathological reports in literature, HBPs, during weeks 0 to 4 of DMBA-induced carcinogenesis, are mostly healthy/normal, with some inflammatory and hyperplastic changes observed around second week. Weeks 5 to 11 show varying grades of dysplasia, along with hyperplastic and normal areas. Weeks 12 to 14 are mostly SCC along with other precancer stages.

Three approaches were used in the study—*ex vivo*, *in vivo* sequential, and *in vivo* follow-up. In all the approaches, a 3-model system involving week 0 controls (C0) along with DMBA-treated HBP (Tx) and age-matched controls (Cx) were used (eg, C0 vs C1 vs T1, C0 vs C2 vs T2, C0 vs C3 vs T3, and so on up to C0 vs C14 vs T14) for data analysis. This is expected to make the model more robust as compared to a 2-model system where only treated and age-matched controls were used (eg, C1 vs T1). Our RS studies on human oral mucosa have already demonstrated feasibility of classifying early and late physiological age of healthy volunteers which is shown to have no bearing on classification of normal and abnormal conditions.[24] No age-related physiological changes have been reported so far in hamsters. A 3-model system (C0 vs Cx vs Tx) also highlights any possible age-related changes, which could affect classification.

1. *Ex vivo* study: "*Ex vivo*" study involved RS of HBPs excised every week postcarcinogen treatment followed by histopathological examination of the same regions. Spectral features of week 0 control (C0) and DMBA-treated buccal pouches (T1-T14) have been shown in Figure 2. C0 and T0 spectra show dominance of lipid features—1303 cm^{-1}, δCH_2 (1448 cm^{-1}), amide I (1655 cm^{-1}), and ester bands (1750 cm^{-1}), whereas T14 (frank tumors) spectra show dominance of proteins and nucleic acids with change in features in 1200 to 1400 cm^{-1} regions corresponding to amide III, CH_2 (1454 cm^{-1}), 1583 cm^{-1}, and broad amide I (1651 cm^{-1}). The spectra from T2 to T13 also show changes in amide III and amide I regions which progressively indicate increased protein dominance. These spectral features correlate well with human buccal mucosa, featuring similar bands.[16,17] A probable reason for loss of lipids and increased dominance of proteins in tumors or other pathological conditions could be the loss in the architectural arrangement of epithelial layers, indicating loss of lipid features. Moreover, cells under pathological conditions undergo changes in the amounts of surface and receptor proteins, enzymes, antigens, and antibodies, which may give rise to a protein dominated spectrum.[19]

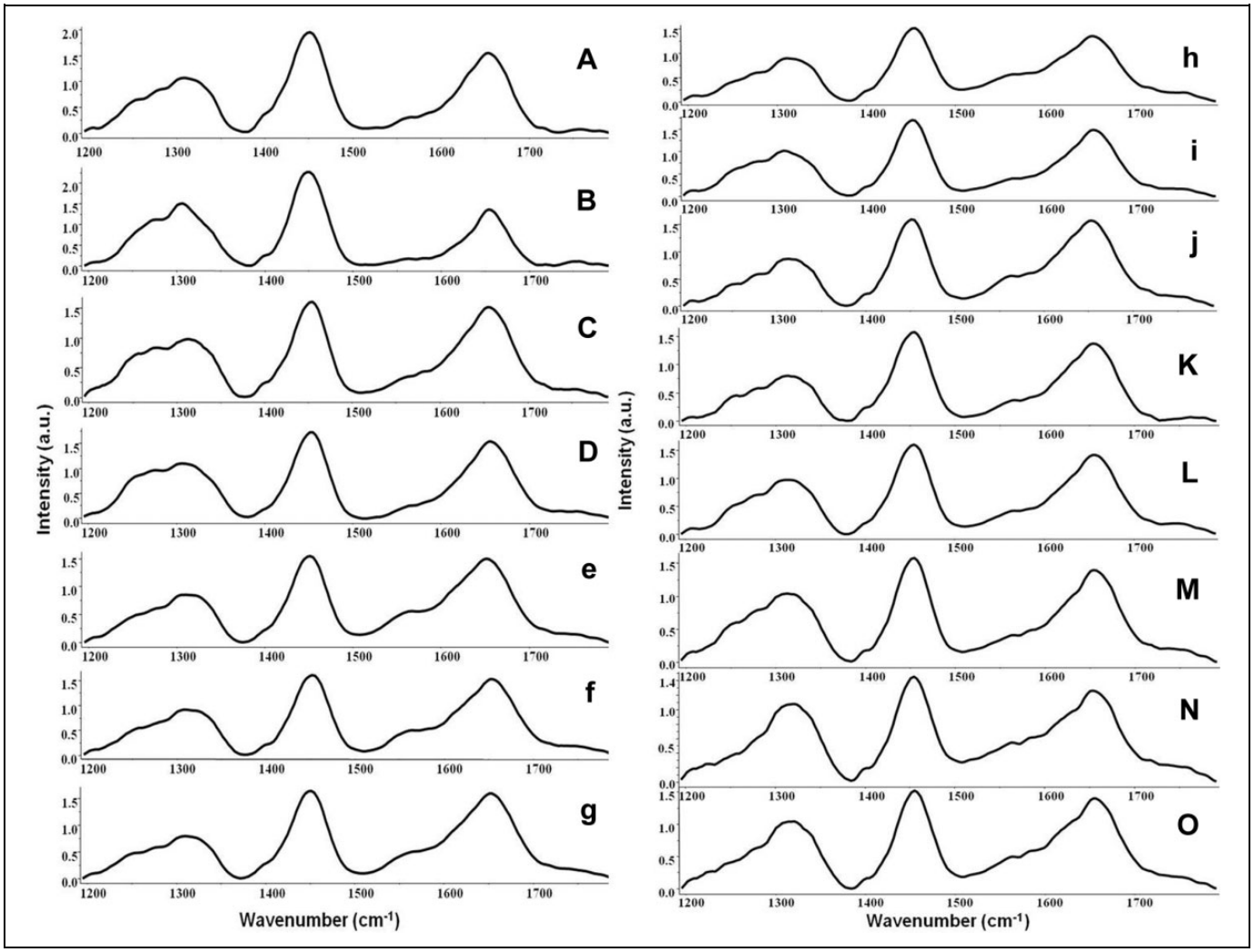

Figure 2. Mean spectra of 7,12-dimethylbenz(a)anthracene (DMBA)-treated Hamster buccal pouch. (A) week 0, (B) week 1, (C) week 2, (D) week 3, (E) week 4, (F) week 5, (G) week 6, (H) week 7, (I) week 8, (J) week 9, (K) week 10, (L) week 11, (M) week 12, (N) week 13, and (O) week 14.

These findings further corroborate earlier reports of *ex vivo* and *in vivo* RS studies on humans.[16-21,40] The 1583 cm^{-1} band, attributed to heme proteins and prominently observed in DMBA-treated pouches of later weeks, could be due to angiogenesis—a well-known hallmark of carcinogenesis.

Multivariate analysis was carried out using both unsupervised PCA and supervised PC-LDA followed by LOOCV.

Principal Component Analysis

Principal component analysis scatter plots for all 14 weeks using scores of factor 1 versus factor 2 are shown in Figure 3. These plots exhibit overlapping clusters for all the 3 groups in the initial weeks, that is, from 0 to 4 weeks. An increased classification of treated pouch spectra was observed from fifth week onward, attributable to DMBA-induced changes. Plateauing of classification was observed for weeks 8 to 11 while exclusive clusters were observed from 12th week onward showing the best classification between treated and control spectra during these later weeks. Poor classification was observed between C0 and age-matched controls, suggesting lack of appreciable age-related changes in the 14-week period of carcinogenesis.

Principal Component-Based Linear Discriminant Analysis

As PCA is an overview tool used to visualize trends in the data and not a classification tool, PC-LDA was carried out to explore feasibility of classification through supervised analysis between C0, Cx, and Tx. To avoid overfitting of the models, 2 to 4 factors were used. Efficiency of models was evaluated by LOOCV. Week-wise LOOCV findings are presented in the form of confusion matrices in Table 2. On the basis of PC-LDA findings, 14 weeks can be subdivided into 3 phases—weeks 0 to 7, weeks 8 to 11, and weeks 12 to 14. T0 to T7 showed progressive increase in classification, up to 70%. T8

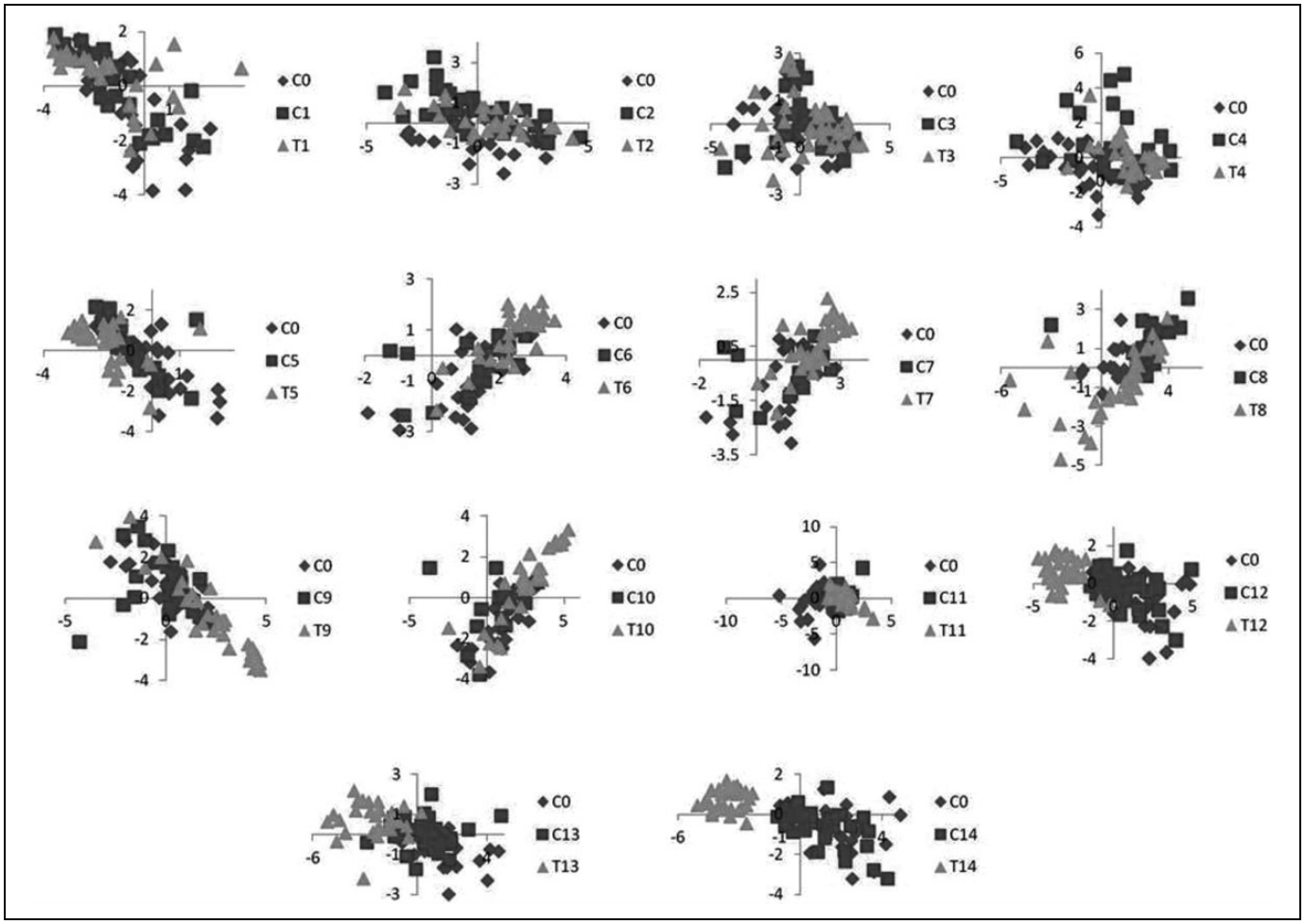

Figure 3. Scatter plots of principal component analysis (PCA) over the period of 14 weeks of DMBA-induced carcinogenesis in Hamster buccal pouch (X-axis: score of factor 1, Y-axis: score of factor 2). C0 indicates week zero-untreated controls; Cx, age-matched controls for a given week; Tx, 7,12-dimethylbenz(a)anthracene (DMBA)-treated spectra of a given week.

Table 2:. LOOCV Confusion Matrix for *Ex Vivo* Study.[a]

	Week 1				Week 2				Week 3				Week 4				Week 5				Week 6				Week 7			
	C0	CX	TX	Tot	C0	CX	TX	Tot	C0	CX	TX	Tot	C0	CX	TX	Tot	C0	CX	TX	Tot	C0	CX	TX	Tot	C0	CX	TX	Tot
C0	23	6	2	31	19	6	6	31	27	2	2	31	26	3	2	31	25	5	1	31	21	4	6	31	24	3	4	31
CX	5	12	16	33	5	17	10	32	3	16	14	33	1	14	12	27	2	29	5	36	1	25	4	30	0	17	13	30
TX	2	14	17	33	3	6	24	33	0	13	27	40	3	10	23	36	0	7	25	32	4	4	24	32	0	11	31	42
	Week 8				Week 9				Week 10				Week 11				Week 12				Week 13				Week 14			
	C0	CX	TX	Tot	C0	CX	TX	Tot	C0	CX	TX	Tot	C0	CX	TX	Tot	C0	CX	TX	Tot	C0	CX	TX	Tot	C0	CX	TX	Tot
C0	24	4	3	31	21	8	2	31	25	3	3	31	25	3	3	31	29	2	0	31	24	6	1	31	26	5	0	31
CX	7	9	11	27	5	22	4	31	1	21	8	30	5	48	15	68	3	31	0	34	4	27	3	34	5	29	0	34
TX	2	3	33	38	2	5	26	33	0	8	23	31	3	13	27	43	0	7	25	32	1	5	25	31	0	0	33	33

Abbreviations: C0, week zero controls; CX, age-matched controls for a given week; TX, 7,12-dimethylbenz(a)anthracene-treated spectra of a given week; Tot, total; LOOCV, leave-one-out cross-validation.

[a]Diagonal elements are true-positive predictions while nondiagonal elements represent misclassifications.

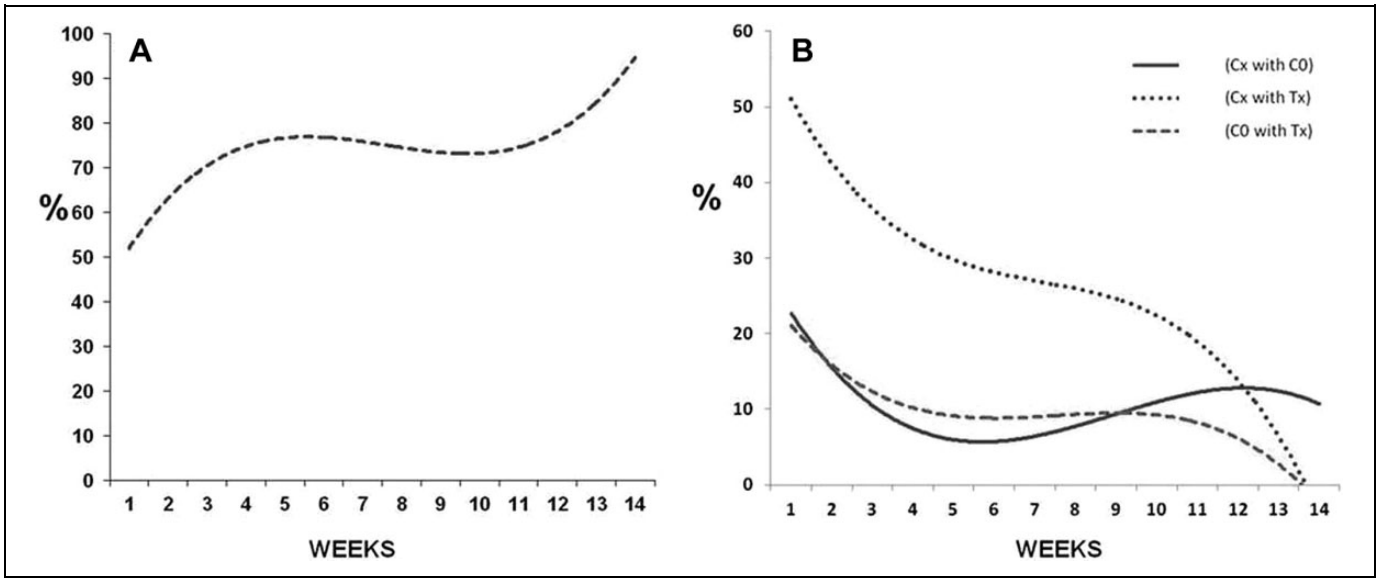

Figure 4. (A) Week-wise true percentage classification of Tx; (B) week-wise percentage misclassification of Cx with C0, Cx with Tx, and C0 with Tx for *ex vivo* study for the period of 14 weeks (X-axis—weeks; Y-axis—percentage of classification). C0 indicates week zero-untreated controls; Cx, age-matched controls for a given week; Tx, 7,12-dimethylbenz(a)anthracene (DMBA)-treated spectra of a given week.

to T11 showed a plateauing phase where classification efficiency remained around 70%, while T12 to T14 showed classification up to 100%. Thus an overall sequential increase in classification efficiency was observed over 14-week carcinogenesis regimen.

For better understanding of the above-mentioned trends in the data, the LOOCV confusion matrices are also presented graphically (Figure 4). It is noteworthy that true classification is indicative of differences between the groups while misclassifications between groups suggest homogeneity and similarity in biochemical properties.[41-43] First, to understand true classification of Tx over 14 weeks, percentage of correct classification for treated group (Tx) was plotted against each week (Figure 4A). Second, to understand behavior of misclassified spectra during carcinogenesis, misclassifications were plotted—percentage of misclassification for Cx with C0, Tx with C0, and Tx with Cx and are shown in Figure 4B. Cx vs C0 would suggest age-related changes, if any between controls while Tx versus Cx/C0 would be indicative of changes due to DMBA-induced carcinogenesis.

Percentage of correct classification for Tx (Figure 4A) increases from about 50% in week 1 to ~70% by the 7th week, remains similar between 8 and 11 weeks, then increases to >90% by 14th week. The trend for misclassifications are shown in Figure 4B. Misclassification of C0 controls with Tx spectra (broken line) and Cx controls with Tx spectra (dotted line) decreased as weeks progressed, suggesting lesser similarities between DMBA-treated pouches and controls. Misclassification of C0 with Cx controls remained almost same throughout 14 weeks, indicating lack of significant changes and hence similarities between controls.

Thus the *ex vivo* study demonstrates feasibility of studying sequential changes during DMBA-induced carcinogenesis. However, this approach is invasive. It is known that noninvasive, *in vivo* approach is always desirable in a clinical set-up, especially for screening and therapeutic monitoring. Hence *in vivo* studies were carried out to ascertain above-described findings of the *ex vivo* study.

2. *In vivo* sequential study: *In vivo* study also exhibits changes similar to *ex vivo* study. Similar spectral features and trends of PCA classification like the *ex vivo* study were observed in this approach (data not shown). To demonstrate these similarities, PC-LDA data are shown in Table 3 and Figure 5. Percentage of correct classification for Tx (Figure 5A) increased from about 50% in week 1 to more than 60% by the 7th week, remained similar between 8 and 11 weeks, then increased to more than 90% by 14th week. Misclassification (Figure 5B) between C0 and Cx (continuous line) remained constant while C0 versus Tx (broken line) and Cx versus Tx (dotted line) decreased over the period of 14 weeks. Thus, trends were similar in *ex vivo* and *in vivo* sequential studies.
3. *In vivo* follow-up study: Follow-up studies allow monitoring of changes *in vivo* in the same animals, avoiding interanimal variations and require fewer animals. Thus *in vivo* follow-up approach was also employed. In this case too, spectral features and PCA results were found to be similar to *ex vivo* and sequential *in vivo* studies (data not shown). Even LOOCV results for each week show similarities between this and the other two approaches as shown in Table 4 and graphically presented in Figure 6. The classification trends observed in this study was comparable to the *in vivo* sequential and *ex vivo* study. True classification (Figure 6A) increased from 0 to 7 weeks, plateaued around 8 to 11 weeks, and then increased

Table 3. LOOCV Confusion Matrix for *in vivo* Sequential Study.[a]

	Week 1				Week 2				Week 3				Week 4				Week 5				Week 6				Week 7			
	C0	CX	TX	Tot	C0	CX	TX	Tot	C0	CX	TX	Tot	C0	CX	TX	Tot	C0	CX	TX	Tot	C0	CX	TX	Tot	C0	CX	TX	Tot
C0	19	5	5	29	19	9	1	29	20	7	2	29	26	2	1	29	19	5	5	29	6	13	10	29	23	4	2	29
CX	3	17	8	28	4	18	3	25	4	26	2	32	4	33	12	49	3	17	8	28	13	16	4	33	2	24	8	34
TX	5	7	20	32	5	9	10	24	2	5	17	24	0	10	20	30	5	7	20	32	9	1	20	30	3	3	21	27

	Week 8				Week 9				Week 10				Week 11				Week 12				Week 13				Week 14			
	C0	CX	TX	Tot	C0	CX	TX	Tot	C0	CX	TX	Tot	C0	CX	TX	Tot	C0	CX	TX	Tot	C0	CX	TX	Tot	C0	CX	TX	Tot
C0	19	7	3	29	21	8	2	31	17	1	11	29	15	12	2	29	24	4	1	29	22	5	2	29	24	5	0	29
CX	1	29	17	47	5	22	4	31	5	26	2	33	7	29	2	38	5	30	19	54	9	16	5	30	7	25	0	32
TX	0	19	35	54	2	5	26	33	10	2	24	36	6	4	22	32	3	5	47	55	6	1	23	30	1	3	26	30

Abbreviations: C0, week zero controls; CX, age-matched controls for a given week; TX, 7,12-dimethylbenz(a)anthracene-treated spectra of a given week; Tot, total; LOOCV, leave-one-out cross-validation; .

[a]Diagonal elements are true-positive predictions while nondiagonal elements represent misclassifications.

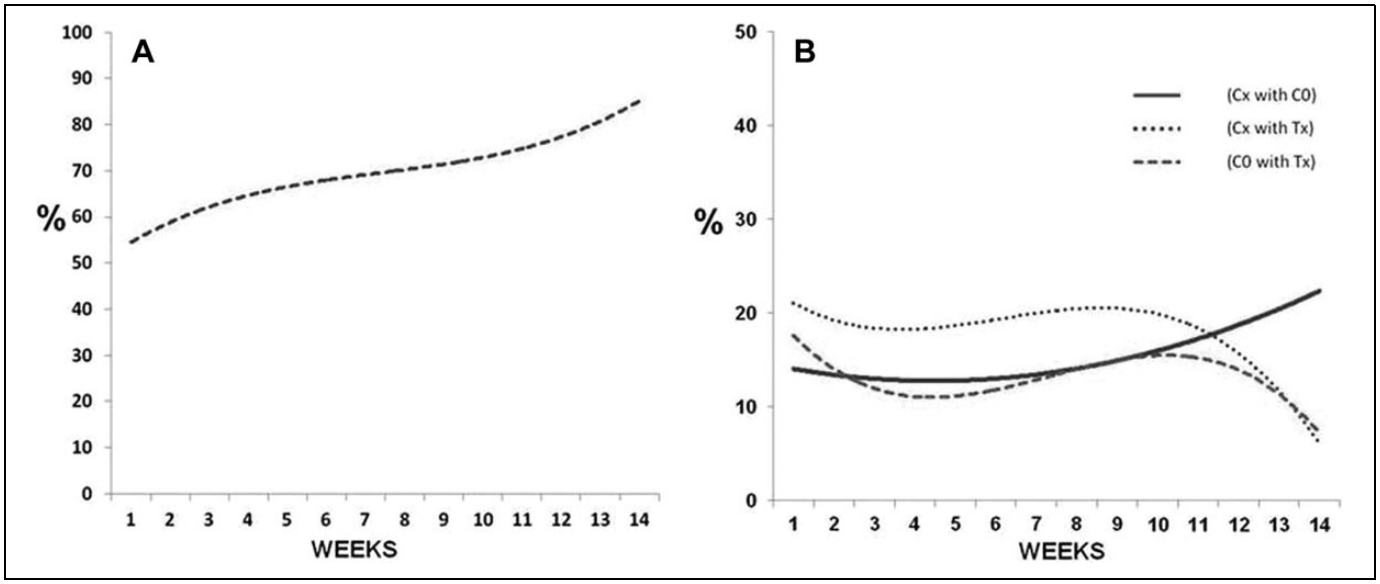

Figure 5. (A) Week-wise true percentage classification of Tx; (B) week-wise percentage misclassification of Cx with C0, Cx with Tx, and C0 with Tx for *in vivo* sequential study for the period of 14 weeks (X-axis—weeks; Y-axis—percentage of classification). C0 indicates week zero-untreated controls; Cx, age-matched controls for a given week; Tx, 7,12-dimethylbenz(a)anthracene (DMBA)-treated spectra of a given week.

beyond 80% by 14th week, whereas misclassifications between C0 and Tx, Cx, and Tx decreased and C0 and Cx remained almost similar (Figure 6B).

A Note on Classifications and Misclassification

True classification is indicative of differences between the groups while misclassifications between groups suggest homogeneity and similarity in biochemical properties. Hence, both true classifications and misclassifications have been used to draw inference in this study (Figures 4-6). In case of the DMBA-treated pouches (Figures 4A, 5A, and 6A), true classification of DMBA-treated pouches shows progressive increase from ~50% in week 1 to ~100% in week 14, indicating potential of RS in identifying sequential changes. But, true classification may not be the complete picture in case of biochemically similar groups. For example, since week 0 and age-matched controls are of similar nature, they are expected to misclassify and thus lead to poorer classifications. Thus logically, if there were age-related differences, misclassifications between week 0 and age-matched controls should have decreased by 14 weeks leading to better classification. No change in misclassification between C0 and Cx might suggest homogeneity[41-43] due to possible lack of appreciable age-related changes. On the contrary, higher misclassifications between Tx and Cx/C0 during the early weeks indicate similarity. The similarities decrease with progression of

Table 4. LOOCV Confusion Matrix for *in vivo* Follow-Up Study.[a]

	Week 1				Week 2				Week 4				Week 5				Week 6				Week 8			
	C0	CX	TX	Tot	C0	CX	TX	Tot	C0	CX	TX	Tot	C0	CX	TX	Tot	C0	CX	TX	Tot	C0	CX	TX	Tot
C0	19	5	5	29	19	5	5	29	25	13	7	45	38	2	5	45	28	11	6	45	35	7	3	45
CX	10	21	8	39	6	21	3	30	5	22	4	31	1	23	8	32	9	10	14	33	8	18	11	37
TX	8	7	26	41	4	5	16	25	1	8	19	28	5	9	21	35	1	10	36	47	4	9	42	55

	Week 9				Week 10				Week 12				Week 13				Week 14			
	C0	CX	TX	Tot	C0	CX	TX	Tot	C0	CX	TX	Tot	C0	CX	TX	Tot	C0	CX	TX	Tot
C0	25	11	8	44	33	10	2	45	39	6	0	45	43	2	0	45	35	3	7	45
CX	8	27	4	39	10	25	8	43	8	29	10	47	1	25	8	34	5	32	10	47
TX	5	9	37	51	5	10	26	41	4	7	36	47	0	8	28	36	0	4	38	42

Abbreviations: C0, week zero controls; CX, age-matched controls for a given week; TX, 7,12-dimethylbenz(a)anthracene-treated spectra of a given week; Tot, total; LOOCV, leave-one-out cross-validation.
[a]Diagonal elements are true-positive predictions while nondiagonal elements represent misclassifications.

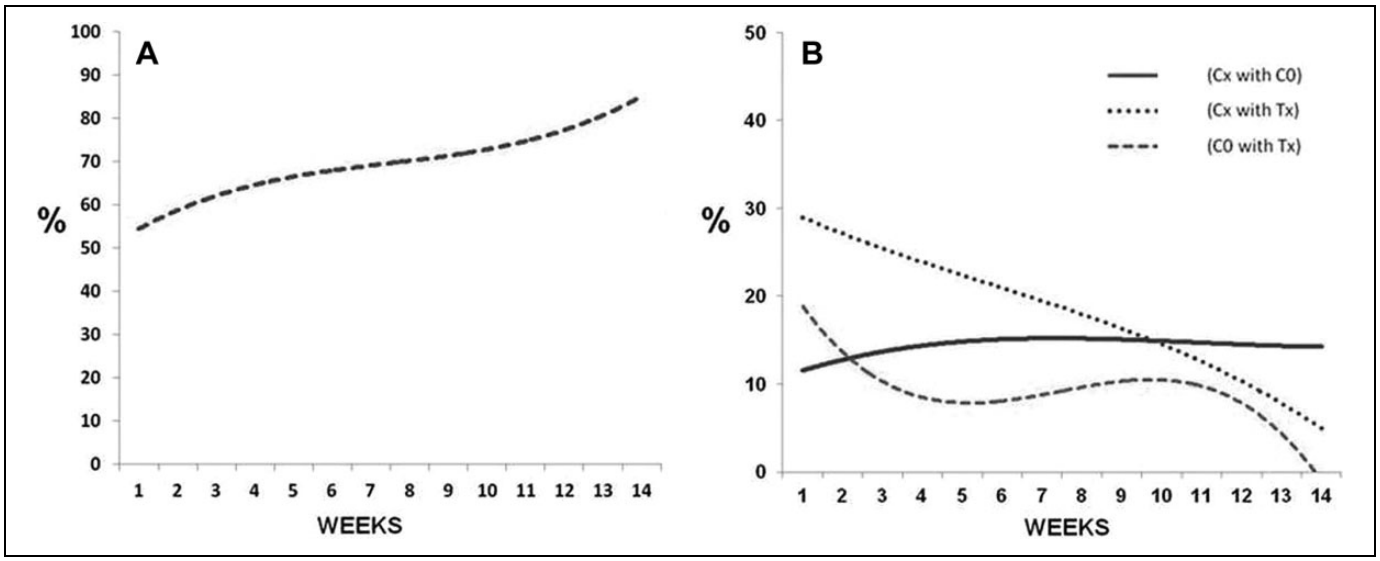

Figure 6. (A) Week-wise true percentage classification of Tx; (B) week-wise percentage misclassification of Cx with C0, Cx with Tx, and C0 with Tx for *in vivo* follow-up study for the period of 14 weeks (X-axis—weeks; Y-axis—percentage of classification). C0 indicates week zero-untreated controls; Cx, age-matched controls for a given week; Tx, 7,12-dimethylbenz(a)anthracene (DMBA)-treated spectra of a given week.

carcinogenesis during later weeks leading to decreased misclassification and as expected, reaches to a minimum by 14 weeks of DMBA treatment.

Visual and Histopathological Support

As shown in Figure 7, the following changes were observed in buccal pouches of hamsters: (1) visibly and histopathologically normal—0 and 1 weeks postcarcinogen treatment; (2) inflammatory and ulcerative changes in response to DMBA toxicity are observed 2 and 3 weeks postcarcinogen treatment (histopathologically hyperplastic); (3) visually normal/ablation of inflammation (attributable to mucosal recovery) is observed 3 to 6/7 weeks posttreatment, histopathologically these tissues show hyperplasia and a few low-grade dysplasia (LGD) regions; (4) visible reddening of mucosa (erythema) appears 7 weeks post-DMBA application, histopathologically these tissues present hyperplasia, LGD, and high-grade dysplasia; (5) mucosal roughening and small papillomas are observed 9 weeks onward, while (6) frank tumors that are pathologically characterized as moderate to well differentiated SCC are seen 12 to 14 weeks postcarcinogen application. Most vehicle-treated HBPs were visibly and histopathologically normal throughout the duration of the study.

Misclassifications Between Treated and Controls

A few misclassifications of treated groups with age-matched controls suggested a reassessment. Histopathological analysis of these control tissues has revealed hyperplastic changes in

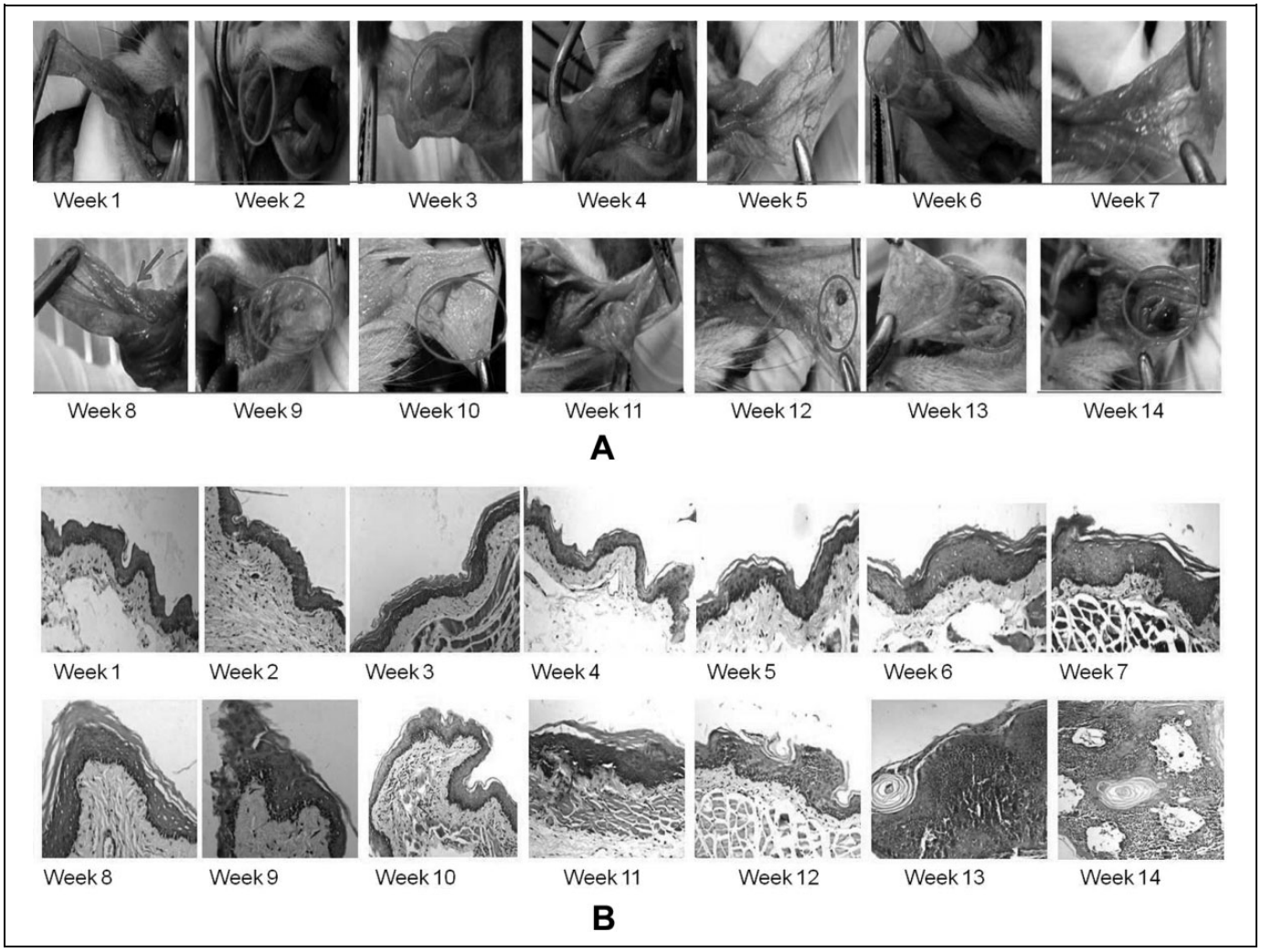

Figure 7. (A) Visual changes over the period of carcinogenesis in hamster buccal pouch (B) representative histopathology images during carcinogenesis in hamster buccal pouch.

small areas in many age-matched controls and dysplastic changes in small regions in a few control slides. A probable reason for these abnormal changes could be tissue injuries in the pouch due to repeated pulling out of HBP by forceps. Moreover, hamsters store the food pellets in their pouch, which may lead to further mechanical irritation, resulting into small areas of abnormalities. Chronic mechanical irritation has also been shown to be a causative factor in oral cancers.[44,45] Representative abnormal areas in histopathological sections from 2 different control pouches are shown in Figure 8. Another reason for observed misclassification could be due to differences in the laser probed area ($\sim$200 μm) and the sections used for histopathology evaluation. In order to get better histopathological evaluation, 3 sections of 5 μm were analyzed owing to practical limitations. Thus despite best of efforts, microheterogenity within the 200 μm of probed area cannot be ruled out.

On the basis of our findings, the process of carcinogenesis in HBP model can be grouped into 3 subphases—weeks 0 to 7, weeks 8 to 11, and weeks 12 to 14. Weeks 0 to 7 show progressive increase in classification efficiency of DMBA-treated pouches due to accumulation of hyperplastic and dysplastic changes. Weeks 8 to 11 show a similar classification efficiency (plateau phase), suggesting nonappreciable changes during this phase. Histopathology-based evaluation suggests accumulation of hyperplastic and dysplastic changes over these weeks. Various studies on biomarkers like P53, C-myc, and Ki67 have shown culmination of marker coexpression, around 10 weeks of DMBA treatment in HBP.[46,47] Thus, homogeneity in these conditions may have lead to plateauing phase around 8 to 11 weeks. By 12th week, these changes progress toward SCC with well-defined tumors and might explain increased classification from 12th to 14th weeks. Similar trends of classification and misclassification were observed in both *ex vivo* and *in vivo* approaches. Thus, *in vivo* diagnosis through RS is quite comparable to *ex vivo* findings supported by the gold-standard histopathology, giving further proof of RS being a promising noninvasive diagnostic adjunct for screening/diagnosis of oral cancers.

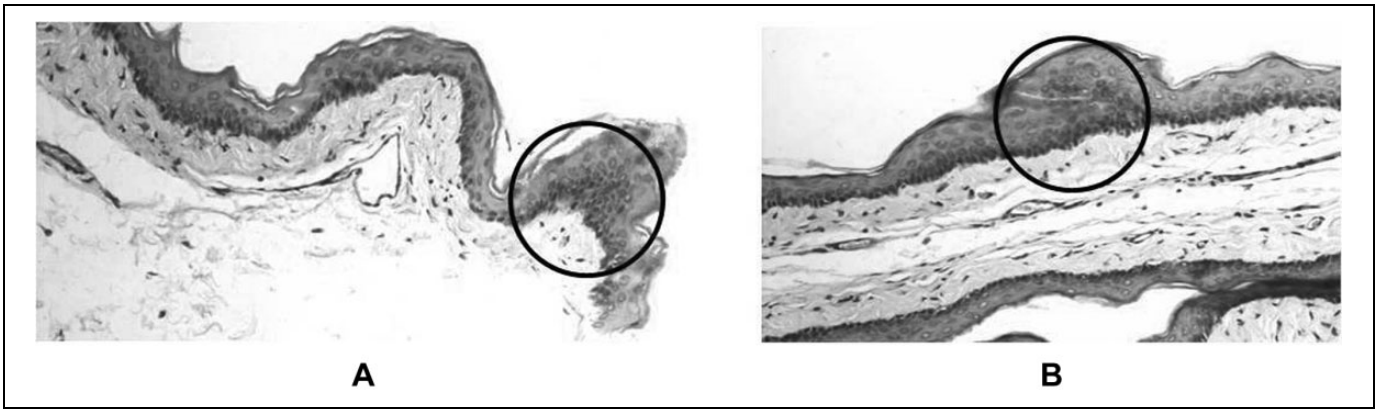

Figure 8. Representative images of abnormal areas (in circle) observed in control pouches.

Conclusion

In this RS study, sequential progression in experimental oral carcinogenesis in HBP model was explored using 3 approaches—*ex vivo*, *in vivo* sequential, and *in vivo* follow-up. In all these studies, spectral changes show lipid dominance in early stages while later stages and tumors showed increased protein to lipid ratio and nucleic acids. On similar lines, early weeks of DMBA-treated and control groups showed higher overlap and low classification. This classification further increased progressively, reached a plateau phase, and subsequently increased up to 100% by 14 weeks. The classifications between treated and control spectra suggested some changes in controls as well, which was confirmed by careful examination of histopathological slides. This suggests RS may be able to identify microheterogeneity, which may often go unnoticed in conventional biochemistry wherein tissue extracts are employed, as well as in histopathology. Further, good correlation between both *ex vivo* and *in vivo* approaches indicates *in vivo* diagnosis through RS is quite comparable to *ex vivo* findings supported by gold standard, giving further proof of RS being a promising label-free, noninvasive diagnostic adjunct for future clinical applications.

Acknowledgements

One of the authors (PK) would like to thank CSIR, New Delhi, for fellowship. The authors would like to thank Dr Lekha Kukreja for histopathological analysis and Mr Pramod Tawde, Mrs Arti Hole, and Miss Aditi Sahu for assistance in animal experiments.

Authors' Note

This work has been done under the project entitled "Comparative evaluation of diagnostic efficacy of laser Raman Spectroscopy and histopathology in oral carcinogenesis: Sequential animal model study" (CSIR Sanction No. 27(0231)/10/EMR-II). The Raman spectrometer employed in the study was procured from DBT project BT/PRI11282/MED/32/83/2008 (Development of *in vivo* laser Raman spectroscopy methods for diagnosis of oral precancerous and cancerous conditions), Department of Biotechnology, Government of India.

Declaration of Conflicting Interests

The author(s) declared no potential conflicts of interest with respect to the research, authorship, and/or publication of this article.

Funding

The author(s) received no financial support for the research, authorship, and/or publication of this article.

References

1. Ferlay J, Soerjomataram I, Ervik M, et al. *GLOBOCAN 2012 v1.0, Cancer Incidence and Mortality Worldwide: IARC CancerBase No. 11* [Internet]. Lyon, France: International Agency for Research on Cancer; 2013. Website. http://globocan.iarc.fr. Accessed July 28, 2015.
2. Jemal A, Siegel R, Xu J, Ward E. Cancer statistics. *C A Cancer J Clin*. 2007;57(1):43-66.
3. Mehrotra R, Gupta DK. Exciting new advances in oral cancer diagnosis: avenues to early detection. *Head Neck Oncol*. 2011; 3:33.
4. Sankaranarayanan R, Ramadas K, Thomas G, et al. Effect of screening on oral cancer mortality in Kerala, India: a cluster-randomised controlled trial. *Lancet*. 2005;365(9475): 1927-1933.
5. Baker SR.Malignant neoplasms of the oral cavity. In Otolaryngology. *Head Neck Surg*. 1993:1281-1343.
6. Abbey LM, Kaugars G., Gunsolley JC, et al. Intraexaminer and interexaminer reliability in the diagnosis of oral epithelial dysplasia. *Oral Surg Oral Med Oral Pathol Oral Radiol Endod*. 1995; 80(2):188-191.
7. Seethalakshmi C. Early detection of oral squamous cell carcinoma (OSCC)—role of genetics: a literature review. *J Clin Diagn Res*. 2013;7(8):1824-1826.
8. Evers DJ, Hendriks B, Lucassen G, Ruers T. Optical spectroscopy: current advances and future applications in cancer diagnostics and therapy. *Future Oncol*. 2012;8(3):307-320.
9. Mahadevan-Jansen A, Mitchell MF, Ramanujam N, Utzinger U, Richards-Kortum R. Development of a fiber optic probe to measure NIR Raman spectra of cervical tissue in vivo. *Photochem Photobiol*. 1998;68(3):427-431.

10. DaCosta RS, Wilson BC, Marcon NE. Optical techniques for the endoscopic detection of dysplastic colonic lesions. *Curr Opin Gastroenterol*. 2005;21(1):70-79.
11. Gniadecka M, Philipsen PA, Sigurdsson S, et al. Melanoma diagnosis by Raman spectroscopy and neural networks: structure alterations in proteins and lipids in intact cancer tissue. *J Invest Dermatol*. 2004;122(2):443-449.
12. Frank CJ, McCreery RL, Redd DC. Raman spectroscopy of normal and diseased human breast tissues. *Anal Chem*. 1995;67(5): 777-783.
13. Kendall C, Day J, Hutchings J, et al. Evaluation of Raman probe for oesophageal cancer diagnostics. *Analyst*. 2010;135(12): 3038-3041.
14. Molckovsky A, Song LM, Shim MG, Marcon NE, Wilson BC. Diagnostic potential of near-infrared Raman spectroscopy in the colon: differentiating adenomatous from hyperplastic polyps. *Gastrointest Endosc*. 2003;57(3):396-402.
15. Crow P, Molckovsky A, Stone N, et al. Assessment of fiberoptic near-infrared Raman spectroscopy for diagnosis of bladder and prostate cancer. *Urology*. 2005;65(6):1126-1130.
16. Venkatakrishna K, Kurien J, Pai KM, et al. Optical pathology of oral tissue: a Raman spectroscopy diagnostic method. *Curr Sci*. 2001;80(1):665-669.
17. Malini R, Venkatakrishna K, Kurien J, et al. Discrimination of normal, inflammatory, premalignant, and malignant oral tissue: a Raman spectroscopy study. *Biopolymers*. 2006;81(3):179-193.
18. Hu Y, Jiang T, Zhao Z. Discrimination of squamous cell carcinoma of the oral cavity using Raman spectroscopy and chemometric analysis. *Intell Netw Intell Syst ICINIS*. 2008;08: 633-636.
19. Guze K, Short M, Sonis S, Karimbux N, Chan J, Zeng H. Parameters defining the potential applicability of Raman spectroscopy as a diagnostic tool for oral disease. *J Biomed Opt*. 2009;14(1): 014016.
20. Bergholt MS, Zheng W, Huang Z. Characterizing variability in in vivo Raman spectroscopic properties of different anatomical sites of normal tissue in the oral cavity. *J Raman Spectrosc*. 2012; 43(2):255-262.
21. Singh SP, Deshmukh A, Chaturvedi P, Krishna CM. In vivo Raman spectroscopy for oral cancers diagnosis. *Proc SPIE*. 2012;8219, 82190K. (February 9); doi:10.1117/12.905453.
22. Singh SP, Deshmukh A, Chaturvedi P, Krishna CM. Raman spectroscopy in head and neck cancers: toward oncological applications. *J Cancer Res Ther*. 2012;8(6):126-132.
23. Singh SP, Deshmukh A, Chaturvedi P, Krishna CM. In vivo Raman spectroscopic identification of premalignant lesions in oral buccal mucosa. *J Biomed Opt*. 2012;17(10):105002.
24. Sahu A, Dalal K, Naglot S, Aggarwal P, Krishna CM. Serum based diagnosis of asthma using Raman spectroscopy: an early phase pilot study. *PLoS One*. 2013;8(11):e78921.
25. Singh SP, Sahu A, Deshmukh A, Chaturvedi P, Krishna CM. In vivo Raman spectroscopy of oral buccal mucosa: a study on malignancy associated changes (MAC)/cancer field effects (CFE). *Analyst*. 2013;138(14):4175-4182.
26. Salley JJ. Experimental carcinogenesis in the cheek pouch of the Syrian hamster. *J Dent Res*. 1954;33(2):253-262.
27. Santis H, Shklar G, Cchauncey HH. Histochemistry of experimentally induced leukoplakia and carcinoma of the hamster buccal pouch. *Oral Surg Med Oral Pathol*. 1964; 17:207-218.
28. Vairaktaris E, Spyridonidou S, Papakosta V, et al. The hamster model of sequential oral oncogenesis. *Oral Oncology*. 2008; 44(4):315-324.
29. Gimenez-Conti IB, Slaga TJ. The hamster cheek pouch carcinogenesis model. *J Cell Biochem*. 1993;53(17F):83-90.
30. Balasenthil S, Saroja M, Ramachandran CR, Nagini S. Of humans and hamsters: comparative analysis of lipid peroxidation, glutathione, and glutathione-dependent enzymes during oral carcinogenesis. *Br J Oral Maxillofac Surg*. 2000;38(4):267-270.
31. Oliveira AP, Bitar RA, Silveira L, Zângaro RA, Martin AA. Near-infrared Raman spectroscopy for oral carcinoma diagnosis. *Photomed Laser Surg*. 2006;24(3):348-353.
32. Ghanate AD, Kumar G, Talathi S, Maru GB, Krishna CM. Raman spectroscopic detection of early stages in DMBA-induced tumor evolution in hamster buccal pouch model: an exploratory study. *Proc SPIE*. 2010:8173.
33. Ambatipudi S, Bhosale PG, Heath E, et al. Downregulation of keratin 76 expression during oral carcinogenesis of human, hamster and mouse. *PLoS One*. 2013;8(7):e70688.
34. Gobinet C, Vrabie V, Manfait M, Piot O. Preprocessing methods of Raman spectra for source extraction on biomedical samples: application on paraffin-embedded skin biopsies. *IEEE Trans Biomed Eng*. 2009;56(5):1371-1382.
35. Nijssen A, Koljenovic S, Schut TCB, Caspers PJ, Pupples GJ. Towards oncological application of Raman spectroscopy. *J Biophoton*. 2009;2(1-2):29-36.
36. Koljenovic S, Choo-Smith LP, Schut TCB, et al. Discriminating vital tumor from necrotic tissue in human glioblastoma tissue samples by Raman spectroscopy. *Lab Invest*. 2002;82(10): 1265-1277.
37. Ghanate AD, Kothiwale S, Singh SP, Bertrand D, Krishna CM. Comparative evaluation of spectroscopic models using different multivariate statistical tools in a multicancer scenario. *J Biomed Opt*. 2011;16(2):025003.
38. Varmuza K, Filzmoser P. *Introduction to Multivariate Statistical Analysis in Chemometrics*. Boca Raton, FL: CRC Press (Taylor & Francis); 2009.
39. Balakrishnama S, Ganapathiraju A, Picone J. Linear discriminant analysis for signal processing problems. *Southeastcon IEEE*. 1999:78-81. doi:10.1109/SECON.1999.766096.
40. Harris AT, Rennie A, Waqar-Uddin H, et al. Raman spectroscopy in head and neck cancer. *Head Neck Oncol*. 2010;2:26.
41. Bergner N, Bocklitz T, Romeike BFM, et al. Identification of primary tumors of brain metastases by Raman imaging and support vector machines. *Chemom Intell Lab Syst*. 2012; 117(August 1):224-232.
42. Francisco-Fernandez M, Tarrío-Saavedra J, Mallik A, Naya S. A comprehensive classification of wood from thermogravimetric curves. *Chemom Intell Lab Syst*. 2012;118(August 15):159-172.
43. Bhattacharjee T, Maru G, Ingle A, Krishna CM. Transcutaneous in vivo Raman spectroscopy: detection of age-related changes in mouse breast. *Vibrational Spec*. 2013;67:80-86.

44. Piemonte DE, Lazos JP, Brunotto M. Relationship between chronic trauma of the oral mucosa, oral potentially malignant disorders and oral cancer. *J Oral Pathol Med*. 2010;39(7): 513-517.
45. Preston-Martin S, Pike MC, Ross RK, Jones PA, Henderson BE. Increased cell division as a cause of human cancer. *Cancer Res*. 1990;50(23):7415-7421.
46. Derka S, Vairaktaris E, Papakosta V, et al. Cell proliferation and apoptosis culminate in early stages of oral oncogenesis. *Oral Oncology*. 2006;42(5):540-550.
47. Papakosta V, Vairaktaris E, Vylliotis A, Derka S, Nkenke E. The co-expression of c-myc and p53 increases and reaches a plateau early in oral oncogenesis. *Anticancer Res*. 2006;26(4B): 2957-2962.

Research article

Journal of RAMAN SPECTROSCOPY

Received: 11 August 2015 Revised: 28 May 2016 Accepted: 3 June 2016 Published online in Wiley Online Library

(wileyonlinelibrary.com) DOI 10.1002/jrs.4977

Raman spectroscopy in experimental oral carcinogenesis: investigation of abnormal changes in control tissues

Piyush Kumar, Tanmoy Bhattacharjee, Manishkumar Pandey, Arti Hole, Arvind Ingle and C. Murali Krishna*

Oral cancer is a major cause of mortality in South Asian men owing to rampant tobacco abuse. Cancers are also reported in non-tobacco habitués, especially women, attributed to chronic irritations from irregular/sharp teeth, improper fillings, and poorly fit dentures. Conventional screening approaches are shown to be effective for high-risk groups (tobacco/alcohol habitués). Raman spectroscopy (RS) is being extensively explored as an alternate/adjunct tool for diagnosis and management of oral cancers. In a previous Raman study on sequential oral carcinogenesis using hamster buccal pouch model, misclassifications between spectra from control and carcinogen [7,12-dimethylbenz(*a*)anthracene (DMBA)]-treated tissues were observed. Histopathology of some control tissues suggested pathological changes, attributable to repeated forceps-induced irritations/trauma during animal handling. To explore these changes, in the present study, we recorded spectra from three different types of controls – vehicle control ($n = 45$), vehicle contralateral ($n = 45$), and DMBA contralateral ($n = 70$) – exposed to varying degree of forceps handling, along with DMBA-treated pouches ($n = 70$) using a 14-week carcinogenesis protocol. Spectra certified on the basis of histopathology and abnormal cell proliferation (cyclin D1 expression) were used to build models that were evaluated by independent test spectra from an exclusive set of DMBA-treated and control animals. Many DMBA-contralateral, vehicle-control, and vehicle-contralateral spectra were identified as higher pathologies, which subsequently corroborated with histopathology/cyclin D1 expression. Repeated forceps-mediated injuries/irritations, during painting and animal handling, may elicit inflammatory responses, leading to neoplasm. The findings of the study suggest that RS could identify micro-changes. Further, RS-based *in vivo* imaging can serve as a promising label-free tool for screening even in the non-habitué population where conventional screening is shown to be not effective. Copyright © 2016 John Wiley & Sons, Ltd.

Additional supporting information may be found in the online version of this article at the publisher's web site.

Keywords: Raman spectroscopy; hamster buccal pouch; experimental oral carcinogenesis; chronic irritation; DMBA

Introduction

Oral cancer is the most common cancer among Indian men,[1] with tobacco being the major etiological agent in the high-risk groups. Cancers are also reported in the non-tobacco habitués, especially women, which could be due to chronic irritations from irregular/sharp teeth, improper fillings, and poorly fit dentures. Despite advancements in treatment modalities, a 5-year survival rate remains a meager 50%. Poor prognosis has been attributed to late detection of the disease, indicating the importance of early diagnosis.[2–4] The currently practiced screening/diagnosis using visual inspection and biopsy of suspected lesions, followed by histopathology, is prone to subjective errors, relying heavily on expertise of the pathologist and the site selected for biopsy. Being an invasive technique, it may not be the method of choice for screening, and repeated biopsies are never convenient to the patients. Moreover, a study by Sankaranarayanan *et al.* suggested that conventional oral visual screening was effective in the high-risk groups.[5] Hence, rapid, objective, and non-invasive techniques, which are sensitive to tissue biochemistry, could be more effective across various groups in general population for early diagnosis, as biochemical changes often precede visible morphological alterations.

The change in biochemical properties is also reflected in the optical properties, and thus, spectroscopic techniques like Raman spectroscopy[6] (RS) may have an advantage over conventional diagnosis. RS is a rapid, non-invasive, and label-free technique being extensively explored in disease diagnosis[7,8] and has shown promising results in the diagnosis of several cancers[9–17] including oral cancers.[18–27] Further studies exploring early changes during oral cancers using hamster buccal pouch (HBP) experimental carcinogenesis[28–30] are also reported.[30,31]

In a recent study,[30] *ex vivo* and *in vivo* Raman spectroscopic evaluations of progression of 7,12-dimethylbenz(*a*)anthracene (DMBA)-induced buccal pouch carcinogenesis with respect to vehicle-treated age-matched controls were carried out. In this study, not only early sequential changes during progression but also misclassifications between treated and control spectra were observed.

* *Correspondence to: Chilakapati Murali Krishna, Chilakapati Laboratory, Advanced Centre for Treatment, Research and Education in Cancer (ACTREC), Tata Memorial Centre (TMC), Kharghar, Sector '22', Navi Mumbai 410210, India.*
E-mail: mchilakapati@actrec.gov.in; pittu1043@gmail.com

ACTREC, Tata Memorial Centre, Kharghar, Sector '22', Navi Mumbai 410210, India

Misclassifications on similar lines, when observed in human studies, are often attributed to heterogeneity on account of patches of healthy regions in the pathological tissues. However, in the mentioned study, histopathological examination of some of the control tissues suggested small foci of abnormal changes, indicating contributions by factors besides heterogeneity to such misclassifications.[30] One such factor responsible for observed abnormalities could be repeated irritations/trauma induced by forceps handling and food pellets. Chronic irritation is an accepted etiological agent in cancers.[32]

In order to understand the nature of aforementioned misclassifications, we carried out the present study, involving 70 animals treated with DMBA and 45 animals used as controls. To investigate changes in controls tissues, three different types of controls – vehicle controls, DMBA-contralateral controls, and vehicle-contralateral controls – which were exposed to varying degree of forceps handling, were analyzed along with DMBA-treated pouches. Standard models were built using spectra corresponding to intermediate stages based on histopathological status – i.e. normal, hyperplasia, dysplasia, and squamous cell carcinoma (SCC) – and expression of cell proliferation marker cyclin D1 through immunohistochemical evaluation. These models were then evaluated using leave-one-out cross-validation (LOOCV) and with independent spectra obtained from an exclusive set of DMBA-treated animals (not used in standard models) and the different types of controls.

Material and methods

Ethics approval

The study was approved by the Institutional Animal Ethics Committee, Advanced Centre for Treatment, Research and Education in Cancer (ACTREC), endorsed by the Committee for the Purpose of Control and Supervision of Experiments on Animals, Government of India (approval no. 12/2009, ACTREC).

Carcinogenesis

A total of 115 six- to eight-week-old Golden Syrian male hamsters (*Mesocricetus auratus*) were used in the study. Oral carcinogenesis was induced in 70 HBP (treated group) using standard DMBA carcinogenesis protocols.[30,33] Briefly, 0.5% DMBA (Sigma-Aldrich, purity 95%) dissolved in groundnut oil (Dhara, India) was topically applied using a paintbrush (Camlin, no. 4) on the right buccal pouch thrice a week for 14 weeks; 45 HBP were treated with only oil (vehicle-control group). All animals were housed under standard laboratory conditions, fed a diet of in-house-prepared pellets, and provided with water *ad libitum*. The schematics of experimental protocol are shown in Fig. 1. The buccal pouches were also photographed (Canon SX220HS) every week.

In order to carry out stage-wise histopathology and immunohistochemistry (IHC), we carried out the study in an *ex vivo* manner. Five test and three control animals were sacrificed every week after carcinogen treatment for 14 weeks. Buccal pouches were then excised out of the sacrificed hamsters, washed in normal saline to get rid of food particles and blood, snap frozen in liquid nitrogen, and stored at −80 °C. Prior to spectra recording, the tissues were passively thawed on ice and washed in normal saline again to remove any possibility of blood (Fig. 1a). From each tissue sample, nine spectra were recorded after spreading the tissues on an aluminum grid (3 × 3). The grid was placed on a sample holder fitted on an XYZ stage, with the fiber optic probe fixed within the apparatus. One spectrum was recorded from the center of each grid, as shown in Fig. 1a.

Raman spectroscopy

Spectra were recorded with HE-785 commercial Raman spectrometer (Horiba Jobin Yvon, France), the details of which have been described elsewhere.[23,25,34] Briefly, this system consists of a diode laser (Process Instruments, USA) of 785 nm wavelength as excitation source and HE 785 spectrograph coupled with a CCD as dispersion and detection elements. The spectrograph is equipped with a fixed 950-g/mm grating. Spectral resolution, as specified by the manufacturer, is ~4 cm^{-1}. The excitation source and the detection system were coupled by commercially available fiber optic Raman probe (InPhotonics Inc., Downy St., USA) consisting of 105 μm excitation fiber and 200 μm collection fiber. As per manufacturer's specifications, theoretical spot size and depth of penetration of the Raman probe are 105 μm and 1 mm, respectively. Typically, laser power of −70 mW was used for excitation. Spectra were integrated for 15 s and averaged over three accumulations. Approximately nine spectra were recorded from each pouch, with one spectrum acquired from each grid.

Histopathology

To identify the sites of spectral acquisition for further studies, they were marked in waterproof India ink, and tissues were cut along gridlines and formalin-fixed (Fig. 1a). The formalin-fixed tissues were embedded in paraffin blocks. To obtain a more precise and practical histopathological evaluation for the laser-probed area, we took three 5 μm parallel sections from the paraffin-embedded tissues. These sections were stained with hematoxylin and eosin dyes and were evaluated by trained pathologists blinded to Raman findings. Based on the histopathological assessment of all the parallel sections by the pathologists, the corresponding spectra were labeled as per their pathological status – healthy, hyperplasia, dysplasia, or SCC – which are the commonly observed major stages in oral carcinogenesis. A flowchart of the schematics is shown in Fig. 1b. The spectra corresponding to the evaluated tissue sections have been referred to as 'histopathologically certified spectra' in this manuscript. Thus, identified 43, 46, 36, and 37 histopathologically certified spectra from 31 animals for normal, hyperplasia, dysplasia, and SCC, respectively, were used to build histopathology-based Raman model and to also obtain mean spectra. Ten factors were explored for principal component analysis (PCA), out of which two factors contributing 78% correct classification were used for building the model (described in the Section on Multivariate Analysis). Loading factors, scree, and scatter plots are shown in Figure S1.

Immunohistochemistry

IHC-based models were built from 30 animals after evaluation of sections on the basis of cyclin D1 expression on a commonly employed scale of 0 to +3. An expression of grade 0 signified minimum or baseline level of expression of cyclin D1 in the tissue sections being investigated. Grades +1, +2, and +3 signified low, medium, and high amounts of expression of cyclin D1, respectively. In this manuscript, grades 0, +1, +2, and +3 have been denoted as G0, G1, G2, and G3, respectively. Standard model was built using 23, 20, 20, and 19 spectra corresponding to G0, G1, G2, and G3 grades,

Journal of RAMAN SPECTROSCOPY

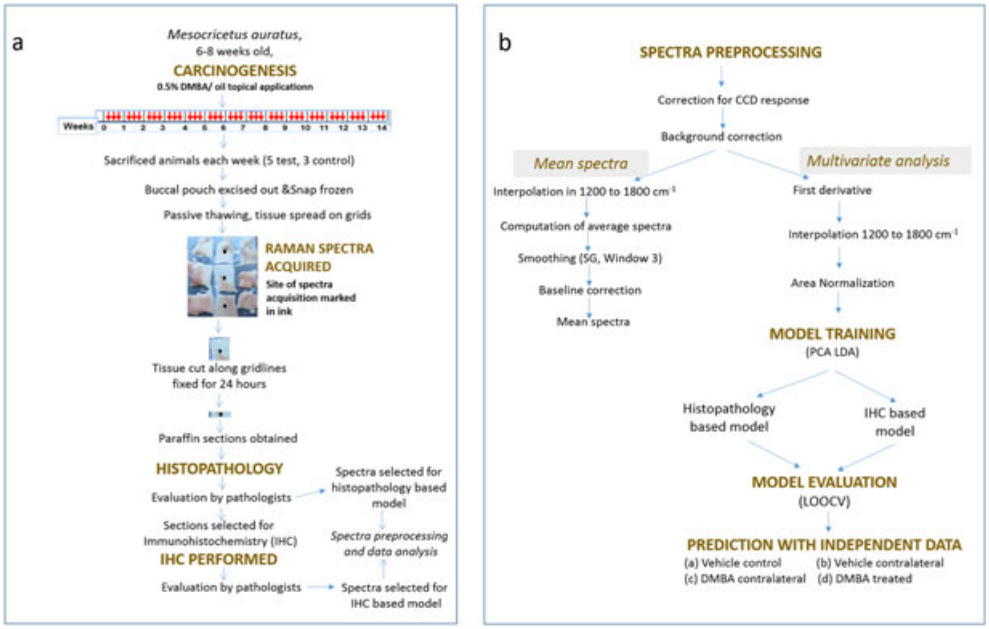

Figure 1. Schematics of protocols followed for (a) carcinogenesis and spectral acquisition and (b) spectral preprocessing and data analysis.

respectively. As shown in Figure S2 and described in the Section on Multivariate Analysis, out of ten factors explored, two factors contributing to 87% classification were selected for model training.

For IHC, two 5 μm tissue sections were taken on poly-L-lysine-coated (Sigma-Aldrich) glass slides. They were deparaffinized with xylene and rehydrated with sequential ethanol washes. To quench the endogenous peroxidase activity, we incubated sections with 2% hydrogen peroxide (Sigma-Aldrich) in methanol for 30 min in the dark. After heat-based antigen retrieval with sodium citrate buffer (pH = 5.8), sections were incubated with normal horse serum (Vector Laboratories, USA) at room temperature. Next, the sections were incubated overnight with rabbit polyclonal anti-human cyclin D1 antibody (1:100, Santa Cruz Biotechnology, USA) at 4 °C for 16 h. Sections were then incubated with biotinylated Universal secondary antibody solution for 30 min followed by incubation with Vectastain Universal ABC (Vector Laboratories, USA) reagent for the same duration. The immunoreaction in tissue sections was visualized using 3,3′-diaminobenzidine tetrahydrochloridehydrate (Sigma-Aldrich). The slides were finally counterstained with hematoxylin, evaluated by pathologists, and assigned with grades of expression.

Data analysis

Spectral preprocessing

Raw Raman spectra were corrected for CCD response using a National Institute of Standards and Technology-certified SRM 2241 material followed by subtraction of spectral contribution from optical elements.[35] To remove interference of slow moving background, we computed first derivatives of spectra.[36] Spectra were interpolated in the 1200–1800 cm^{-1} region as our previous studies on oral cancer have already demonstrated the efficacy of this region in classification.[23,24,27] Moreover, this region is free from interference of fiber signals, which are generated owing to fused silica fibers.[36] Interpolated spectra were area normalized to remove intensity-related variations and subjected to multivariate analysis. The preprocessing steps are outlined in Fig. 1b.

Computation of mean spectra

Average or mean spectra were computed from the background-corrected spectra for each class and baseline corrected by fitting a fifth-order polynomial function using LABSPEC 4.18 (Horiba Jobin Yvon, France). These baseline-corrected spectra were smoothed using Savitzky–Golay filter (window size 3). This was followed by area normalization to obtain mean for spectral comparison across different groups. The number of spectra used to obtain mean spectra for healthy control, hyperplasia, dysplasia, and SCC was 43, 46, 36, and 37, respectively. The number of spectra used to calculate mean for G0, G1, G2, and G3 was 23, 20, 20, and 19, respectively.

Multivariate analysis

Preprocessed spectra were subjected to PCA-based linear discriminant analysis (PC-LDA) using algorithms implemented in MATLAB-based in-house software.[37] PCA is the most frequently applied method for computing linear latent variables, which allows visual inspection of clustering of objects or variables through unsupervised classification. The main aim of PCA is dimension reduction by which it explains maximum variability with few PCs/factors.[38] It has been shown that 99% of variance can be captured by the first ten PCs,[39] contributing to maximum variance.[39,40] LDA, a supervised classification method, maximizes inter-class separation and reduces intra-class separation to bring out discrimination.[41] For data with high dimensionality, dimension reduction may be achieved by application of PC-LDA, PCA followed by LDA, using PCA scores, instead of original variables. Further, for classification methods like LDA, the first few factors/PCs may account for more than 90% classification when PC-LDA is carried out.[40] Thus, in this study, ten factors were explored during PCA. Further, during the LDA step, after analyzing results for the first ten factors, the first two factors were selected, which accounted for classification of 78% and 87% for histopathology- and cyclin D1-based models

through PC-LDA, respectively. The loading factors, scree plot, and scatter plots are shown in Figures S1 and S2 for histopathology- and cyclin D1-based models, respectively. Classification efficiency of standard models was evaluated by LOOCV which is based on a hypothetical validation set used in absence of an explicit validation set. Leave-one-out involves using a single observation from the original sample as the validation data and the remaining observations as training data. This is iterated such that each observation in the sample is used once as the validation data and averaged over the rounds.

Results and discussion

HBP is a commonly used model in experimental oral carcinogenesis owing to attributes like comparable histological similarity with human buccal mucosa and stage-wise progression to cancer through stages like hyperplasia, dysplasia, and SCC on application of DMBA. In a typical DMBA-induced cancer progression, the following changes are often observed: visibly and histopathologically normal mucosa after 1 week of carcinogen treatment, and inflammation, in response to DMBA toxicity, is observed during the second and third weeks of carcinogen treatment (histopathologically hyperplastic). Visually normal mucosa (due to ablation of inflammation) is observed 3–7 weeks after DMBA treatment. Histopathologically, hyperplasia and small regions of low-grade dysplasia (LGD) are observed during this period. Visible reddening of mucosa (erythema) appears 7 weeks after DMBA application; histopathologically, these tissues present hyperplasia, LGD, and high-grade dysplasia. Mucosal roughening along with small papillomas are observed 9 weeks onwards, while frank tumors, pathologically characterized as moderate to well-differentiated SCC, are seen 12–14 weeks after carcinogen application. The first standard model was built using histopathologically certified spectra for control, hyperplasia, dysplasia, and SCC.

As is well known, biochemical changes precede morphological changes, and evaluation based on suitable biomarker expressions can also serve as a reliable additional scrutiny. HBP has shown comparable expression of biomarkers like P53, BCL2, PCNA, and cyclin D1 with respect to human oral mucosa.[42] Cyclin D1 has a major regulatory role at G1/S checkpoint and is an important biomarker as deregulation of G1 to S phase progression of cell cycle and is a common target in carcinogenesis.[43] Many studies have reported overexpression of cyclin D1 in head and neck, oral, laryngeal, and nasopharyngeal carcinomas.[44,45] Hence, abnormal cell proliferation through cyclin D1 expression was also employed to build the second standard model. Cyclin D1 expression was graded on scale of 0 to +3. In this manuscript 0, +1, +2, and +3 levels of expression have been denoted as G0, G1, G2, and G3, respectively. G0 and G1 grades show zero or minimum expression of the biomarkers, usually observed in controls and early weeks; G2 shows intermediate amount of expression in tissue sections, which could be histopathologically severely hyperplastic/dysplastic; and G3 involves expression in maximum/entire regions in a tissue section, usually in tumors or later stages of carcinogenesis.

To train models, we carried out spectral comparison to histopathology stages as well as IHC grades using multivariate tool PC-LDA, followed by LOOCV and evaluation with test spectra from an exclusive set of DMBA-treated animals. In the final step, in order to understand the nature of misclassifications in control tissues, different types of controls (vehicle control, vehicle-contralateral control, and DMBA-contralateral control) were evaluated against the histopathology- and IHC-based models.

Histopathology-based spectral model

Spectral features

Figure 2 shows the mean spectra of healthy, hyperplastic, dysplastic, and SCC spectra. Healthy spectra (Fig. 2a) show 1301 cm^{-1}, 1310 cm^{-1}, δCH_2 (1448 cm^{-1}), and ester band (1750 cm^{-1}), which indicated dominance of lipid features,[46] whereas SCC spectra show dominance of proteins and nucleic acids with change in features in 1200–1400 cm^{-1} regions, CH_2 (1454 cm^{-1}), 1560–1583 cm^{-1}, and broad amide I (1651 cm^{-1}). The pathological tissues, through hyperplastic, dysplastic, and SCC spectra, show changes in amide III and amide I regions, which progressively indicate increased protein dominance. The changes also include broadening of amide I band. Moreover, changes in amide III reveal increasing nucleic acid contents. These spectral features corroborate with reports on spectra of human buccal mucosa.[27,47] A probable explanation for this observation could be changes in expression profile of proteins such as surface/receptor proteins, enzymes, antigens, and antibodies during pathological conditions, leading to protein-rich spectra.[26] These findings further corroborate earlier reports of *ex vivo* and *in vivo* RS studies on human subjects as well as hamster models.[25,27,31,47] A 1563-cm^{-1} band

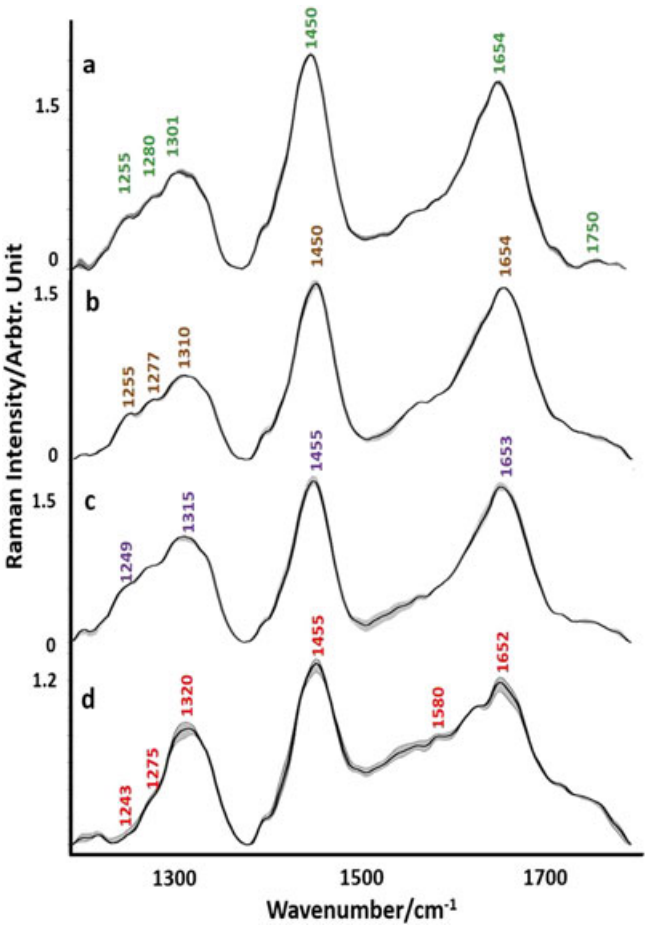

Figure 2. Mean spectra of intermediate histopathological stages in experimental oral carcinogenesis. (a) Control, (b) hyperplasia, (c) dysplasia, (d) SCC (shaded region shows the standard deviation).

may be attributed to increased nucleic acids, which has also been observed in prior studies and can be interpreted with regard to a higher concentration of nucleic acids in cancer tissues.[31] A 1583-cm^{-1} band is contributed by amino acids as well as heme proteins. As per our observations in the pathological HBP, extensive blood vessel network was prominently visible, especially in severe pathological state like SCC. Thus, a 1583-cm^{-1} band may be assigned to heme proteins abundant on account of angiogenesis – a well-known hallmark of carcinogenesis.[48]

Standard model

PC-LDA model (Table 1a) was built for normal, hyperplasia, dysplasia, and SCC. Two factors contributing 78% classification were used for analysis. Findings were evaluated by LOOCV, and results are presented in Table 1b. Out of 43 control spectra (eight animals), 28 were correctly classified, and 11 misclassified with hyperplasia and four with dysplasia. In case of hyperplasia, 29 out of 46 spectra (nine animals) were truly classified, while 12, 2, and 3 spectra misclassified, respectively, with control, dysplasia, and SCC. Dysplasia (seven animals) showed true classification for 24 out of 36 spectra. Misclassifications with control and hyperplasia were one and ten, respectively. For SCC spectra (seven animals), true classification was observed for 31 out of 37 spectra, while three spectra each misclassified with hyperplasia and dysplasia.

Evaluation with DMBA-treated spectra

As shown in Table 1c, for weeks 1–3, out of 100 spectra, 34 and three were predicted as hyperplastic and dysplastic, respectively. For weeks 4–7, out of 164 spectra, 60, 79, and 23 spectra were predicted as control, hyperplastic, and dysplastic, respectively. In case of weeks 8–11, out of 151 spectra, 24, 40, and 61 spectra were predicted as control, hyperplasia, and dysplasia, respectively. Twenty-six spectra were predicted as SCC. Thus, predictions with higher pathologies increase with the duration of carcinogenesis. In case of week 12–14 spectra, out of 101 spectra, 15 spectra were predicted as hyperplasia, while 32 and 54 spectra were predicted as higher pathologies dysplasia and SCC, respectively. As hyperplasia could be due to various reasons like injury and inflammation, only those spectra that were predicted as dysplastic or SCC are being considered potentially cancerous. Thus, almost 85% (86 out of 101) spectra from 12 to 14 weeks are already potentially cancerous/cancerous, whereas only 3% (three out of 100) spectra from week 1 to 3 are classified as potentially cancerous.

Table 1. Histopathology-based spectral model – confusion matrix for training model

	Control	Hyperplasia	Dysplasia	SCC	Total
		1a			
Control	28	11	4	0	43
Hyperplasia	12	29	2	3	46
Dysplasia	1	10	24	1	36
SCC	0	4	3	30	37
		1b			
Control	**28 (65%)**	11	4	0	43
Hyperplasia	12	**29 (63%)**	2	3	46
Dysplasia	1	10	**24 (67%)**	1	36
SCC	0	3	3	**31 (84%)**	37
		1c			
DMBA weeks 1–3	63	34	3	0	100
DMBA weeks 4–7	60	79	23	2	164
DMBA weeks 8–11	24	40	61	26	151
DMBA weeks 12–14	0	15	32	54	101

1a, PC-LDA; 1b, LOOCV (diagonal elements are true positive predictions, while non-diagonal elements represent misclassifications); 1c, evaluation of histopathology-based model using exclusive DMBA-treated animals.

Cyclin D1-based spectral model

Spectral features

Figure 3 shows the mean spectra for G0, G1, G2, and G3. G0 spectra resemble healthy spectra with dominance of lipid features – 1303 cm^{-1}, δCH_2 (1448 cm^{-1}), amide I (1655 cm^{-1}), and ester bands (1750 cm^{-1}) – whereas G3 spectra show dominance of proteins and nucleic acids with change in features in 1200–1400 cm^{-1} regions corresponding to amide III, CH_2 (1454 cm^{-1}), 1583 cm^{-1}, and broad amide I (1651 cm^{-1}) similar to SCC spectra. A reason for this similarity with mean spectra of histopathological stages is that G0 expression of cyclin D1 is observed in healthy tissues G1 in hyperplasia and LGD, and G2 in various grades of dysplasia, and G3 is usually expressed in tissue regions that are histopathologically SCC. Thus, features of G0, G1, G2, and G3 mean spectra are comparable with healthy, hyperplasia, dysplasia, and SCC mean spectra, respectively.

Standard model

PC-LDA model (Table 2a) was trained for G0, G1, G2, and G3 grading based on cyclin D1 expression using two factors and evaluated

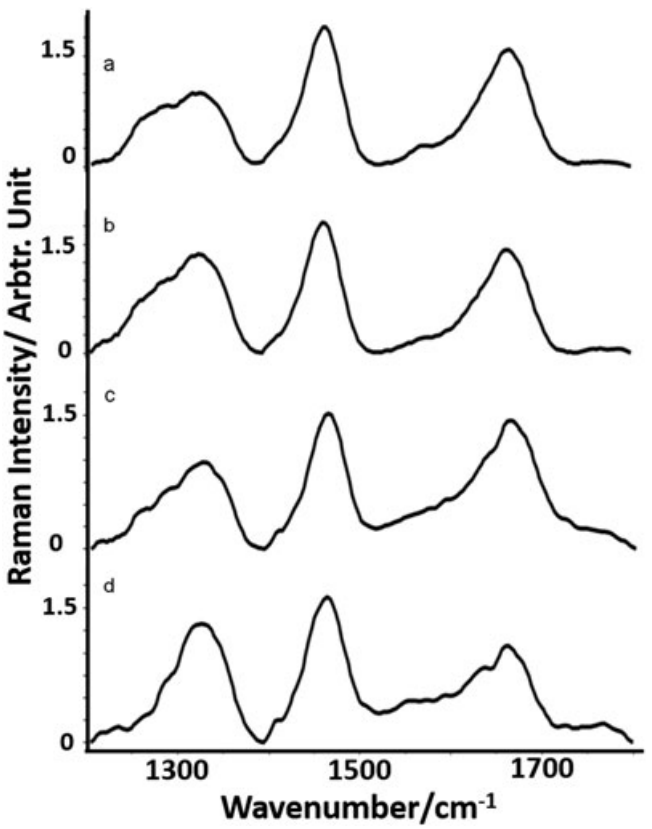

Figure 3. Mean spectra of intermediate stages based on grades of cyclin D1 expression evaluation on a scale of 0 to +3. (a) G0, (b) G1, (c) G2, and (d) G3.

Table 2. Cyclin D1-based spectral model – confusion matrix for training model

	G0	G1	G2	G3	Total
		2a			
G0	19	4	0	0	23
G1	3	15	2	0	20
G2	1	4	15	0	20
G3	0	0	2	17	19
		2b			
G0	**19 (83%)**	4	0	0	23
G1	3	**15 (75%)**	2	0	20
G2	1	5	**14 (70%)**	0	20
G3	0	0	2	**17 (89%)**	19
		2c			
DMBA weeks 1–3	39	50	6	3	98
DMBA weeks 4–7	53	81	36	1	171
DMBA weeks 8–11	48	49	56	14	167
DMBA weeks 12–14	0	13	37	52	102

2a, PC-LDA; 2b, LOOCV (diagonal elements are true positive predictions, while non-diagonal elements represent misclassifications); 2c, evaluation of cyclin D1-based model using exclusive DMBA-treated animals.

Table 3. Evaluation of training models with control spectra from independent animals for (a) histopathology-based model and (b) cyclin D1-based model

	3a				
	Control	Hyperplasia	Dysplasia	SCC	Total
Vehicle control	189	110	30	6	335
DMBA contralateral	149	160	59	9	377
Vehicle contralateral	41	30	4	0	75
	3b				
	G0	G1	G2	G3	Total
Vehicle controls	191	107	29	8	335
DMBA contralateral	146	163	54	14	377
Vehicle contralateral	51	21	3	0	75

using LOOCV (Table 2b). For G0 spectra, obtained from seven animals, 19 spectra were truly classified while four spectra misclassified with G1. In case of G1, where eight animals were used, 15 out of 20 spectra were truly classified, while three, two, and zero misclassified, respectively, with G0, G2, and G3. Twenty spectra from seven animals, graded as G2, showed true classification for 14 spectra. Misclassifications with G0 and G1 were one and five, respectively. For G3 spectra from eight animals, true classification was observed for 17 out of 19 spectra, while two spectra misclassified with G2.

Evaluation with DMBA-treated spectra

In line with histopathology-based models, spectra being predicted as G2 or G3 are being considered potentially cancerous. As shown in Table 2c, for weeks 1 to 3, out of 98 spectra, 39, 50, 6, and 3 spectra were classified as G0, G1, G2, and G3, respectively. For weeks 4–7, out of 171 spectra, 53, 81, 36, and 1 spectra were classified as G0, G1, G2, and G3, respectively. Week 8–11 spectra show classification of 48, 49, 56, and 14 spectra with G0, G1, G2, and G3, respectively. For weeks 12–14, 52 out of 102 spectra classified as G3, while 37 spectra classified as G2. Thus, 89 out of 102 (87%) spectra indicated moderate to severe expression of cyclin D1 and thus abnormal proliferation. Thirteen spectra classified as G1, while none classified as G0.

Evaluation of standard models using independent set of control spectra

To explore and understand any abnormal change in controls, we employed three different types of controls in this study: (1) vehicle-control spectra acquired from oil-treated right buccal pouches of control animals; (2) vehicle-contralateral spectra were acquired from the untreated left pouches of vehicle controls; and (3) DMBA-contralateral spectra were acquired from the untreated left pouch of DMBA-treated animals. As shown in Table 3a, 4, 36, and 68 vehicle contralateral, vehicle control, and DMBA contralateral misclassified with dysplastic or SCC spectra, respectively. These results indicate that misclassifications with dysplasia and SCC were least in case of vehicle contralaterals and highest for DMBA contralaterals. In case of IHC-based model (Table 3b), 3, 37, and 68 vehicle-contralateral, vehicle-control, and DMBA-contralateral spectra, respectively, misclassified with G2 or G3. Thus, similar to histopathological findings, misclassifications with G2 and G3 were least in case of vehicle contralaterals and highest for DMBA-contralateral spectra. Histopathological analyses of these control tissues have even revealed small foci of dysplasia and SCC as shown in the encircled regions in Fig. 4. IHC of these sections showed higher expression of cyclin D1 in these areas (Fig. 4) compared with those of other control regions.

The prediction of control spectra with treated groups may be attributed to abnormal changes in the mucosa in response to chronic mechanical irritation.[32] Chronic irritation may lead to increase in mitotic activity, which occurs during repair of the ulcerated tissues and may precede neoplasia.[49] Injuries/wounds resulting from irritations may also elicit inflammatory response, which may lead to neoplasia.[50] Oral cancer incidences are also observed in non-tobacco habitués, especially in women.[51] A probable cause in such cases is chronic physico-mechanical irritations in the oral cavity due to irregular/sharp teeth, poor fillings, and improperly fit dentures.[32,49,52] In case of HBP carcinogenesis, as a pair of forceps is used to pull out pouches during painting, visual observations, and spectral acquisition, forceps-induced repeated irritations and injuries cannot be ruled out. In addition, hamsters store food pellets in these pouches, which may further aggravate the irritations/injuries resulting into small areas of abnormalities.

When rate of misclassification/prediction with dysplasia and SCC between the three types of controls – vehicle control, vehicle contralateral, and DMBA contralaterals – are compared, least misclassifications are observed in case of vehicle contralateral, followed by vehicle controls and DMBA contralaterals. A probable reason for this observation in the vehicle-contralateral pouches could be minimal damage to the mucosa as they were not exposed to repeated handling, sparing continuous mechanical irritations/injuries. DMBA contralaterals, on the other hand, show more misclassification than vehicle contralaterals and controls. This could be due to leaching and mixing of DMBA in saliva and, indirectly, but continuously affecting the contralateral pouches, although all these pouches were visually normal. On further analysis, it was also observed that these animals belonged to 11–14 weeks of treatment, indicating that higher duration of handling and associated injuries may be

Journal of RAMAN SPECTROSCOPY

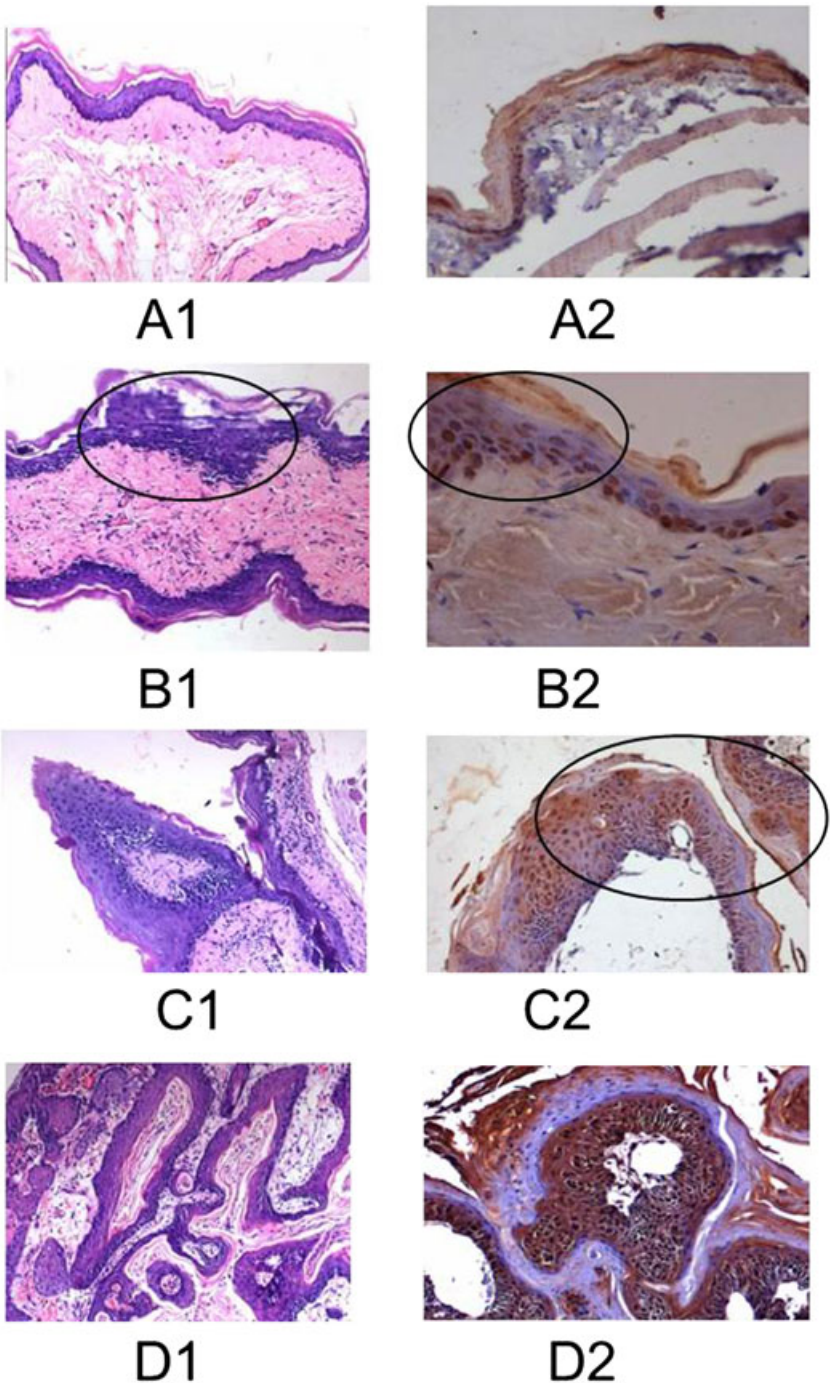

Figure 4. Representative images of histopathology (A1 to D1) and IHC (A2 to D2) for (A) vehicle-contralateral, (B) vehicle-control, (C) DMBA-contralateral, and (D) DMBA-treated pouches. The encircled regions show abnormal areas in an otherwise healthy section.

reasons for these abnormal developments. To the best of our knowledge, these observations of carcinoma/higher pathologies has not been reported in control animals, although cases of tumor development in pet hamsters[53,54] and in contralateral HBP[55] are reported.

In the present study, a small number of control spectra were predicted as higher pathologies. However, these are important as they could easily be misunderstood as false positives. In our previous *in vivo* studies on human oral cancers,[25–27] similar misclassifications observed between normal (control) and tumors were attributed mainly to tumor heterogeneity – presence of normal and/or inflammatory islands in the tumors. No histopathological confirmation of normal tissues could be made owing to ethical considerations. The use of animal models therefore offered an advantage in this study as this facilitated histopathological confirmation of the abnormalities in the control tissues. As definite histopathological and biochemical changes could be detected in these control sections, all such misclassifications should be given due consideration as such changes arising from chronic irritations may eventually progress into neoplasms. Such observations in control tissues are usually not observed. A probable reason for this could be the use of tissue extracts (in case of many biochemical studies) wherein

such small abnormalities may get masked. Moreover, typical biological experiments may involve many different methods, and thus, the same tissue area may not be available for all the techniques.

Another highlight of this study was the approach used for histopathological corroboration. The usual approach in case of an *in vivo* approach involves spectra acquisition from the suspected sites under the guidance of a medical practitioner, and histopathology is carried out from one or two sections from surgical excisions/biopsies. As a standard practice, the highest pathology observed in the section is assigned as the histopathological status. Thus, spectral and histopathological information may not arise from the same tissue regions. Moreover, pure healthy tissues are not available, and thus, spectra are acquired from cut margins. In the present study, a uniform protocol was adopted for spectral acquisition to avoid any bias, and the best efforts were made to carry out spectral acquisition and histopathology from the same tissue regions from carcinogen-treated as well as healthy control groups. Overall findings demonstrate that clinically invisible micro-changes may be detected using RS, which were also corroborated by histopathology and IHC studies.

Conclusion

The major outcome of the present RS-based study has been identification of abnormal changes in apparently normal control mucosa, as confirmed by gold standard. These abnormal changes, which may be wrongly concluded as 'false positives', have revealed small foci of higher pathologies and also showed higher expression of cyclin D1 with respect to histopathologically normal regions. Findings of the study show that RS has been successful in identification of micro-changes in small regions of tissues. Further advancements in RS involving imaging rather than point spectroscopy of entire oral cavity can be carried out in few recordings to enhance screening potentials. Findings suggest RS as a promising, label-free, non-invasive candidate tool for screening even in the non-habitué general population, which may not be feasible by conventional screening tools.

Acknowledgements

This work has been carried out under the project entitled 'Comparative evaluation of diagnostic efficacy of laser Raman spectroscopy and histopathology in oral carcinogenesis: Sequential animal model study' (CSIR Sanction No. 27(0231)/10/EMR-II). One of the authors (P. K.) would like to thank CSIR, New Delhi, for fellowship. The Raman spectrometer employed in the study was procured from DBT project BT/PRI11282/MED/32/83/2008 (Development of *in vivo* laser Raman spectroscopy methods for diagnosis of oral precancerous and cancerous conditions), Department of Biotechnology, Government of India. The authors would like to thank Dr. Lekha Kukreja and Dr. Poonam Gera for histopathological analysis, Mr. Pramod Tawde for assistance in animal experiments, and Miss Aditi Sahu for editorial makeover.

References

[1] A. Jemal, R. Siegel, J. Xu, E. Ward, *CA Cancer J. Clin.* **2010**, *60*, 277.
[2] R. Mehrotra, D. K. Gupta, *Head Neck Oncol.* **2011**, *3*, 33.
[3] R. Sankaranarayanan, K. Ramadas, G. Thomas, R. Muwonge, S. Thara, B. Mathew, B. Rajan, G. Trivandrum, *Lancet* **2005**, *365*, 1927.
[4] S. R. Baker, *Otolaryngol Head Neck Surg.* **1993**, *2*, 1281.
[5] R. Sankaranarayanan, K. Ramadas, G. Thomas, R. Muwonge, S. Thara, B. Mathew, B. Rajan, *Lancet*, **1927** p, 365.
[6] C. V. Raman, K. S. Krishnan, *Nature* **1928**, *121*, 501.
[7] D. Evers, B. Hendriks, G. Lucassen, T. Ruers, *Future Oncol.* **2012**, *8*, 307.
[8] D. I. Ellis, R. Goodacre, *Analyst* **2006**, *131*, 875.
[9] H. H. Kim, *Biomed Res Int* **2015**, *2015*, 670121.
[10] J. Schleusener, P. Gluszczynska, C. Reble, I. Gersonde, J. Helfmann, J. W. Fluhr, J. Lademann, J. Rowert-Huber, M. C. Meinke, *Exp Dermatol*, **2015**.
[11] M. S. Bergholt, K. Lin, J. Wang, W. Zheng, H. Xu, Q. Huang, J. L. Ren, K. Y. Ho, M. Teh, S. Srivastava, B. Wong, K. G. Yeoh, Z. Huang, *J. Biophotonics* **2015**, 9999.
[12] S. Jin, H. Mao, *Nan Fang Yi Ke Da Xue Xue Bao* **2014**, *34*, 391.
[13] C. Kallaway, L. M. Almond, H. Barr, J. Wood, J. Hutchings, C. Kendall, N. Stone, *Photodiagnosis Photodyn. Ther.* **2013**, *10*, 207.
[14] L. M. Almond, J. Hutchings, G. Lloyd, H. Barr, N. Shepherd, J. Day, O. Stevens, S. Sanders, M. Wadley, N. Stone, C. Kendall, *Gastrointest. Endosc.* **2014**, *79*, 37.
[15] S. K. Teh, W. Zheng, K. Y. Ho, M. Teh, K. G. Yeoh, Z. Huang, *Br. J. Surg.* **2010**, *97*, 550.
[16] N. Stone, C. Kendall, J. Smith, P. Crow, H. Barr, *Faraday Discuss.* **2004**, *126*, 141.
[17] E. M. Kanter, S. Majumder, E. Vargis, A. Robichaux-Viehoever, G. J. Kanter, H. Shappell, H. W. Jones 3rd, A. Mahadevan-Jansen, *J Raman Spectrosc* **2009**, *40*, 205.
[18] K. Venkatakrishna, J. Kurien, K. M. Pai, M. Valiathan, N. N. Kumar, C. Murali Krishna, G. Ullas, V. Kartha, *Curr. Sci.* **2001**, *80*, 665.
[19] R. Malini, K. Venkatakrishna, J. Kurien, K. M. Pai, L. Rao, V. Kartha, C. M. Krishna, *Biopolymers* **2006**, *81*, 179.
[20] Y. Hu, T. Jiang, Z. Zhao, in Intelligent Networks and Intelligent Systems, 2008. ICINIS'08. First International Conference on, IEEE, **2008**, pp. 633.
[21] K. Guze, M. Short, S. Sonis, N. Karimbux, J. Chan, H. Zeng, *J. Biomed. Opt.* **2009**, 14, 014016.
[22] M. S. Bergholt, W. Zheng, Z. Huang, *J Raman Spectrosc* **2012**, *43*, 255.
[23] S. Singh, A. Deshmukh, P. Chaturvedi, C. M. Krishna, in *SPIE BiOS*, International Society for Optics and Photonics, **2012**, pp. 82190K.
[24] S. Singh, A. Deshmukh, P. Chaturvedi, C. M. Krishna, *J. Cancer Res. Ther* **2012**, *8*, 126.
[25] S. Singh, A. Deshmukh, P. Chaturvedi, C. M. Krishna, *J. Biomed. Opt.* **2012**, 17.
[26] S. Singh, A. Sahu, A. Deshmukh, P. Chaturvedi, C. M. Krishna, *Analyst* **2013**, *138*, 4175.
[27] A. Sahu, A. Deshmukh, A. D. Ghanate, S. P. Singh, P. Chaturvedi, C. M. Krishna, *Technol. Cancer Res. Treat.* **2012**, *11*, 529.
[28] I. B. Gimenez-Conti, T. J. Slaga, *J. Cell. Biochem.* **1993**, *53*, 83.
[29] J. J. Salley, *J. Dent. Res.* **1954**, *33*, 253.
[30] P. Kumar, T. Bhattacharjee, A. Ingle, G. Maru, C. M. Krishna, *Technol Cancer Res Treat*, **2015**.
[31] A. P. Oliveira, R. A. Bitar, L. Silveira, R. A. Zangaro, A. A. Martin, *Photomed. Laser Surg.* **2006**, *24*, 348.
[32] W. Thumfart, M. Weidenbecher, G. Waller, H.-J. Pesch, *J. Maxillofac. Surg.* **1978**, *6*, 217.
[33] A. D. Ghanate, G. Kumar, S. Talathi, G. B. Maru, C. M. Krishna, *Proc. SPIE* **2010**, *8173*, pp. 817303.
[34] T. Bhattacharjee, P. Kumar, G. Maru, A. Ingle, C. M. Krishna, *Lasers Med. Sci.* **2014**, *29*, 325.
[35] C. Gobinet, V. Vrabie, M. Manfait, O. Piot, *IEEE T Bio-Med Eng* **2009**, *56*, 1371.
[36] A. Nijssen, S. Koljenovic, T. C. Bakker Schut, P. J. Caspers, G. J. Puppels, *J. Biophotonics* **2009**, *2*, 29.
[37] A. D. Ghanate, S. Kothiwale, S. P. Singh, D. Bertrand, C. M. Krishna, *J. Biomed. Opt.*, **2011**, *16*, 025003.
[38] K. Varmuza, P. Filzmoser, *Introduction to Multivariate Statistical Analysis in Chemometrics*, CRC Press, Boca Raton, **2009**.
[39] E. Kemsley, *Chemometr. Intell. Lab.* Elsevier B.V. Registered Office, Amsterdam, The Netherlands **1996**, *33*, 47.
[40] T. Korenius, J. Laurikkala, M. Juhola, *Inform. Sci.* **2007**, *177*, 4893.
[41] S. Balakrishnama, A. Ganapathiraju, J. Picone, in Southeastcon'99. Proceedings. IEEE, IEEE, **1999**, pp. 78.
[42] S. Nagini, P. V. Letchoumy, A. Thangavelu, C. Ramachandran, *Oral Oncol.* **2009**, *45*, e31.
[43] M. Hall, G. Peters, *Adv. Cancer Res.* **1996**, *68*, 67.
[44] J. Xu, I. B. Gimenez-Conti, J. E. Cunningham, A. M. Collet, M. A. Luna, H. E. Lanfranchi, M. R. Spitz, C. J. Conti, *Cancer* **1998**, *83*, 204.
[45] J. Lamb, M. E. Ewen, *Cell Cycle*, Georgetown, Tex. **2003**, *2*, 525.

[46] F. S. Parker, *Applications of Infrared, Raman, and Resonance Raman Spectroscopy in Biochemistry*, Springer Science & Business Media, New York, **1983**.
[47] A. Deshmukh, S. P. Singh, P. Chaturvedi, C. M. Krishna, *J. Biomed. Opt* **2011**, *16*, 127004.
[48] D. Hanahan, R. A. Weinberg, *Cell* **2011**, *144*, 646.
[49] S. Preston-Martin, M. C. Pike, R. K. Ross, P. A. Jones, B. E. Henderson, *Cancer Res.* **1990**, *50*, 7415.
[50] S. I. Grivennikov, F. R. Greten, M. Karin, *Cell* **2010**, *140*, 883.
[51] P. D. Wey, M. J. Lotz, L. J. Triedman, *Cancer* **1987**, *60*, 1644.
[52] E. D. Piemonte, J. P. Lazos, M. Brunotto, *J. Oral Pathol. Med.* **2010**, *39*, 513.
[53] M. Selk Ghaffari, F. Moayer, O. Dezfoulian, *Iran J Vet Res* **2009**, *10*, 84.
[54] J. Martorell, D. Fondevila, A. Ramis, *Veterinary Record* **2005**, *156*, 650.
[55] S. F. Dachi, J. E. Sanders, E. M. Urie, *Cancer Res.* **1967**, *27*, 1183.

Supporting information

Additional supporting information may be found in the online version of this article at the publisher's web site.